Mineralogical and Geochemical Controls on Nutrient Dynamics and Forest Productivity in Managed Northeastern U.S. Forests

Alexandrea Mae Rice
Rockland, PA

B.S. Environmental Science, Allegheny College, 2017
M.S. Forest and Natural Resources Management, SUNY-ESF, 2019

A Dissertation presented to the Graduate Faculty
of the University of Virginia in Candidacy for the Degree of
Doctor of Philosophy

Department of Environmental Sciences

University of Virginia
April 2025

Justin B. Richardson, Advisor
Lauren E. Miller, Committee Member
Charity Nyelele, Committee Member
Patrick J. Drohan, Committee Member
Sean R. Agnew, Committee Member

Abstract

Forests in the northeastern United States are critical for timber, firewood, and woody biofuel production, making sustainable forest management essential for balancing productivity with long-term ecosystem health. Forest productivity depends heavily on the availability of essential nutrients such as calcium (Ca), magnesium (Mg), potassium (K), and phosphorus (P), which are primarily sourced from mineral weathering. Despite the complexities of glacial soils in the northeastern United States, this dissertation investigates how soil parent material mineralogy and nutrient richness influence nutrient cycling and forest productivity across a naturally occurring Ca and Mg gradient in Vermont and New Hampshire. Using integrated mineralogical, geochemical, and isotopic analyses, I quantified nutrient concentrations and pools, rock and soil weathering rates, and nutrient fluxes. Chapter 2 evaluates the sources and weathering of parent material using the glacial till model, Ca and Mg isotopes, and immobile elements. The results indicate that glacial till composition is primarily derived from local bedrock and that soils release more nutrients than rocks when scaled to profile depth. Chapter 3 examines the influence of Ca and Mg bearing minerals on nutrient availability and highlights that mineralogy is a key control on nutrient retention and release rates in soils. Chapter 4 links soil nutrient richness to aboveground biomass, nutrient concentrations in wood and foliage, and merchantable wood value. While nutrient concentrations generally increased with soil nutrient richness, total biomass was highest at the nutrient Poor forest, and merchantable wood volume did not differ significantly across the three forests. These findings highlight the critical role of parent material mineralogy in sustaining nutrient supply and underscore the importance of considering mineralogical and geochemical context when developing adaptive, site-specific management strategies.

Acknowledgements

No journey is without its hardships, but this one will forever be one I cherish, thanks to the incredible people who walked alongside me– often in the rain.

First and foremost, I extend my deepest gratitude to my advisor, Dr. Justin Richardson. Your mentorship has shaped not just my scientific endeavors but also my personal growth. Thank you for your guidance and for making me realize that writing does not have to be as painful as I once thought it was. I am especially grateful for your unwavering support both academic and literal. From insightful edits to sample analysis logistics, to saving me from what could have been a truly unfortunate end…getting locked inside the rock room. Smashing rocks in a soundproof, windowless room seemed like a normal part of geologic research until I realized no one would hear me if I got locked inside. Which in fact I did, and you came to my rescue! So, thank you for rescuing me from what could have been a very geologically ironic demise.

To my collaborators, Tony D'Amato, Nico Perdrial, Victoria Treto, and Grace Smith, thank you for your invaluable insights, and incredible support. From helping establish our field site locations to providing thoughtful feedback on my work, I could not have done this without you. A special thanks to Nico, not just for showing me the ropes of mineral abundance measurements but also for quite literally saving me when my brake pad decided to abandon ship during my visit to run samples in your lab.

To my generous lab mates, Lee Zuniga, Robin Truong, and Nischal Acharya, thank you for your invaluable feedback and support on my presentations and just your amazing selves. I am so grateful to have had such kind and supportive lab mates.

A huge thank you to the incredible undergraduates who fearlessly dove into this research, Marissa Hanley, Rhea Negron, Sydney Carmouche, and Emily Wu. Marissa, from the very first soil samples to our field adventures trying to plug bear-bitten 5-gallon buckets with glue and leaves, your dedication (and friendship) means the world to me. Our journey is extra special to me as I met you on my very first day as a PhD student. Rhea, thank you for braving and entrusting your first field work experience with Marissa and me and for being such a great friend along the way. The countless laughs and just general silliness that would ensue when you were around are truly unforgettable. Sydney, your rock identification skills were nothing short of heroic. I mean there is a whole chapter of this dissertation that your work fully supports! And Emily, your enthusiasm for sorting leaves and tackling a paper of foliar resorption is inspiring. I cannot wait to see where your drive takes you.

To the field crews of 2021- 2024 from UMass and UVM, who helped with soil pits, litter, and water collection, I would probably still be out in the forest digging pits if it were not for you all.

To the departments of UMass and UVA, thank you for the community and encouragement along the way. A special thank you to UVA Environmental Science department for letting me transplant from UMass when Justin moved. I have truly enjoyed my time here.

Finally, to my friends (near and far), family (human and four legged), and Chris (fiancé)- your love and patience through all 10.5 years of my college education have been invaluable. Thank you for the laughs when I needed them most, reminding me what my passions are when I was too deep in research, and most of all, for always believing in me. An extra special thank you goes to Chris who has stuck by my side through, now, two graduate degrees. Your love and support were the reason I felt confident enough to start a PhD and they are also the reason I am actually completing it! I am looking forward to what our next chapter looks like, without schooling involved.

This dissertation is a product not just of my efforts, but of the kindness, brilliance, and generosity of each of you. Thank you for being part of this journey as I will carry your impact with me.

Table of Contents

Chapter 1

Introduction

1.1 The importance of northeastern forests

Northeastern forests play a vital ecological and economic role in the United States. Historically, these forests have undergone drastic changes which started with extensive deforestation and soil degradation during European settlement around the 1600s (Cronon, 1983; Foster and Aber, 2003). Early settlers cleared vast areas of forest for farmland, timber, and fuel which led to widespread deforestation and soil degradation (Beier et al., 2017; Foster et al., 2008). The high economic value of hardwood species such as *Quercus* spp. (oak), *Acer* spp. (maple), and *Fagus* spp. (beech) drove large-scale harvesting for construction and fuel (Rogers et al., 2021). The demand for timber, especially from old-growth forests led to clear-cutting that removed nutrient rich biomass and left soils vulnerable to erosion and degradation (Drummond and Loveland, 2010). Additionally, the introduction of plowing accelerated the breakdown of soil structure further exasperating the loss of soil nutrients. Without modern soil conservation practices such as cover cropping and soil amendments, early agricultural activities contributed to the persistent soil acidification which further decreased the base cation availability to plants (Yesilonis et al., 2016).

Following the widespread abandonment of land in the late 19th and early 20th centuries, northeastern forests started to regenerate, however the legacy effects from severe deforestation continued to influence the soil properties and the forest composition (Foster, 1998). The abandonment of farmland led to natural regeneration of forests which resulted in the dominance of resilient and fast-growing species like *Fagus grandifolia* and *Acer saccharum*. Northern hardwood species like *Fagus grandifolia* can thrive on degraded soil where base cation availability is low, especially calcium (Ca) and magnesium (Mg), unlike *Acer saccharum* which is highly sensitive to soil Ca availability (Flinn and Vellend, 2005; Compton et al., 2007; St. Clair et al., 2008). *Fagus grandifolia* has a competitive advantage in nutrient poor soils as it forms a dense thicket that outcompetes other hardwood species, whereas more commercially valuable hardwood species such as *Acer saccharum* and *Betula alleghaniensis* often struggle to regenerate under such conditions as these species are more dependent on Ca rich soils (Goodale and Aber, 2001; Thompson et al., 2013). The differences in nutrient demands and growth strategies are why studies have found that the position and structure of a forest pre-settlement and post-abandonments differ in composition and structure (Hooker and Compton, 2003; Flinn and Marks, 2007).

Today, in the mid 2020's, northeastern forests are still a key source of timber production for the United States with over 210,000 thousand board feet (MBF) harvested annually from New Hampshire and approximately 520,000 MBF from Vermont (Department of Natural and Cultural Resources, 2020; Vermont Department of Forest, Parks and Recreation, 2022). In addition to sawtimber, firewood remains a critical forest product in the region as firewood serves as a primary heating source for many rural households and contributes to local economies and energy independence. With the rise of bioenergy and the transition to renewable resources, there has been increasing interest in sustainably managing forests to meet woody biomass demands for both timber and non-timber products (Goldemberg and Teixeira Coelho, 2004). The Energy Policy Act (1992) initiated the transition and development of renewable resources for fuel such as bioenergy derived from forests. Following that act, the Energy Independence and Security Act (2007) set ambitious targets for biofuel production which included woody biomass and continue to shape forest management practices today.

In addition to timber and firewood, northeastern forests provide a wide range of non-timber forest products, including maple syrup, mushrooms, medicinal plants, and other specialty goods that contribute largely to local economies and cultural heritage. The value of the region’s forests is also contributed to by forest based recreation such as hiking, wildlife habitat, and carbon sequestration (Kramer et al., 2022). The combined demand for timber, firewood, and non-timber resources in the region supports the need for integrated management approaches that maintain forest productivity while supporting the long-term ecosystem health. However, increasing whole-tree removal to meet biomass harvesting needs, especially for firewood and bioenergy, raises concerns about accelerated soil nutrient depletion, reduced soil quality, and diminish forest resilience. The long-term impacts of intensified harvesting practices on soil nutrient cycling and forest sustainability remain understudied and must be considered in future forest policy and ecosystem management frameworks.

1.2 Geologic history of northeastern United States

The Last Glacial Maximum occurred approximately 26,000 years ago and had a profound impact on the landscape of the northeastern United States (Clark et al., 2009). The Laurentide Ice Sheet during the Wisconsinan glaciation dramatically reshaped the landscape through a combination of erosion, sediment deposition, and the formation of glacial soil parent material (Clark and Pollard, 2010; Denny, 1982; Mickelson et al., 1983). During the Last Glacial Maximum, the Laurentide Ice Sheet covered much of the northeastern United States, extending as far south as Long Island, New York and reaching into Pennsylvanian and New Jersey (Dalton et al., 2020; Dyke and Prest, 1987). The movement of the ice sheet scoured the bedrock, transported sediments, and created a diverse range of landforms such as moraines, outwash plains, and proglacial lakes (Balco et al., 2005; Clark et al., 2009; Teng et al., 2024). As the ice sheet began retreating approximately 19,000 years ago, with deglaciation in Vermont and New Hampshire occurring between 6,000 and 9,000 years ago, deposits of glacial till, stratified drift, and lacustrine sediments were left behind. Meltwater from the retreating glacier contributed to the formation of glacial lakes such as Lake Hitchcock, which deposited fine grained sediments that later influenced soil texture and fertility (Ridge, 2003). Additionally, as the ice sheet retreated, the heavily depressed crust began a gradual uplift (isostatic rebound) ultimately reshaping the topography and hydrology of the region (Godbout et al., 2023; Koteff and Larsen, 1989). This process also contributed to changes in sediment distribution throughout the area, which would influence the formation of soil (Peltier, 2004).

1.3 Dominant soil parent materials across Northeastern U.S.

The retreating of the Laurentide Ice Sheet deposited materials throughout the northeast that have since been reworked and form the soils we see today. The soil parent materials of the northeastern United States are largely the results of glacial deposition and the retreating of the ice sheet. One of the most widespread parent materials throughout the region is glacial till. Glacial till is a mixture of sand, silt, clay, gravel, and boulders that was deposited directly by glacial ice (Easterbrook, 1982; Reineck and Singh, 1980). The mineralogical and lithological makeup of the material varies in composition depending on the type of bedrock from which it was derived (Denny, 1982). Generally, it has been found that the material is from local bedrock extending about 1.5 km northwest of the area (Koteff and Pessl, 1981). Another important material is outwash which typically consists of well-sorted and stratified sediments that were transported and deposited by streams formed from glacial meltwater. The deposits are oftentimes found in valley bottoms and tend to be sandy or gravelly textures that are well drained and great for agriculture (Stone and Borns, 1986). Additionally, glacial lake deposits, also known as lacustrine deposits, are often found in lowland areas. These fine-grained silts and clay were deposited by proglacial lakes and tend to retain moisture, resulting in poorly drained yet fertile soils (Ashley et al., 1991). Lastly, a windblown silt referred to as loess can be found in upland areas where the glacier has retreated from (Bettis et al., 2003). Loess deposits are primarily composed of fine clay minerals like illite, chlorite, kaolinite and vermiculite, and have a fine texture that promotes adequate moisture and soil fertility, making them very suitable for agriculture (Liu et al., 2024; Muhs et al., 2004; Smalley, 1966). These deposits known as parent materials for soils across the landscape are the basis for the diverse soil taxonomy across the northeast.

1.4 Dominant soil types and soil formation processes

Following the deposition of sediments and material after the retreat of the Laurentide Ice Sheet, extensive weathering processes transformed these glacial parent materials into distinct soil horizons (Jenny, 1941). The formation and characteristics of soils in the northeastern United States are influenced by unique climatic, geological, and biological factors. This region is characterized by a humid continental climate which is great for biological activity and organic matter accumulation.

A dominant soil order within the northeastern United States is the Spodosol which is characterized by a well-developed podzolization process (Soil Survey Staff, 2022). Spodosols commonly form under coniferous forests where organic acids from decomposing litter mobilize aluminum (Al) and iron (Fe) and translocate these elements from the E horizon (an eluvial layer) to the B horizon (Buol et al., 2011). This process leads to the accumulation of metal-humus complexes in the B horizon which gives the horizon a distinctive dark or reddish brown color while the overlying E horizon appears pale or why due to the depletion of Fe and Al oxides (Lundstrom et al., 2000). Spodosols often develop from coarse textured, sandy parent materials deposited by glacial processes which leads to acidic conditions and low base cation saturation (Schaetzl and Isard, 1996). The acidic environment created by organic acids further promotes the mobilization of Fe and Al in the soil profile and hinders the formation of clay minerals.

In contrast, low-lying areas and floodplains in the region predominantly are Entisols and Inceptisols (Soil Survey Staff, 2022). Entisols are characterized by their minimal horizon development which often appears as a thin soil layer directly over bedrock or parent material. Entisols form primarily from recent alluvial deposits where soil forming processes have not significantly altered the original parent material (Soil Survey Staff, 2022). Entisols are most commonly found in river valleys, coastal plains and flood plains where sediment there is frequent sediment deposition. On the other hand, Inceptisols have undergone moderate weathering and have some, albeit weak, soil horizon development. Inceptisols typically form under more stable environmental conditions where deposition events are less frequent which allows for the accumulation of organic matter and the initial formation of Bw (cambic) horizons which indicates weak structural changes (Buol et al., 2011). Inceptisols typically develop on gentle slopes, terraces, and stable floodplains where organic matter accumulates gradually over time.

1.5 Soil nutrient dynamics

Soil nutrient dynamics in the northeastern United States are influenced by parent material, climate, vegetation, and historical disturbances. The availability of nutrients in these soils varies significantly and is driven by lithological composition, soil mineralogy, and environmental conditions. The most important soil nutrients in forest ecosystems include calcium (Ca), magnesium (Mg), potassium (K), phosphorus (P), iron (Fe), and aluminum (Al). These nutrients are found both within the plant available nutrient pool and the total nutrient pool. Understanding how these elements move between pools and the factors that influence their availability is essential for assessing soil fertility and forest productivity.

In soils there are two important and commonly assessed operationally-defined pools of nutrients, the total nutrient pool and the plant available nutrient pool. The nutrients in the total nutrient pool are primarily bound within minerals and parent material and therefore are not readily available to plants. These nutrients are released through mineral weathering and chemical dissolution over time (Brantley, 2008; Richardson and Zuñiga 2021; Zhang et al., 2019). The plant available nutrient pools consist of nutrients in solution or adsorbed onto clay surfaces and organic matter which plants can readily access. Calcium and Mg are typically adsorbed within the soil matrix and onto clays and organic matter which reduces their mobility but also minimizes leaching (Edmonds, 1987). However, historical acid rain has led to Ca depletion in northeastern forest soils which has led to reduced soil buffering capacity especially on soils from acidic parent materials (Lawrence and Huntington, 1999; Vadeboncoeur et al., 2014). Potassium, being a monovalent cation with large ionic radii, is less adsorbed to clay surfaces compared to Ca and Mg and is highly soluble. As a result, K availability is often higher than Ca and Mg in the northeast but is more prone to being leached from the soil profile especially in sandy soils with low cation exchange capacity or affected by whole tree harvesting (Cornut et al., 2021; Thiffault et al., 2011; Tripler et al., 2006). Phosphorus is often the most limiting nutrient in northeastern forest soils due to the low abundance and slow weathering rates of P-bearing minerals such as apatite (Gress et al., 2007; Nezat et al., 2008). Under acidic conditions, P rapidly forms insoluble compounds with Fe and Al oxides making it unavailable to plants. Iron and Al are primarily associated with oxide and hydroxide compounds in the soil and are mobilized under acidic conditions where these elements form stable mineral complexes.

Clay minerals play a vital role in nutrient retention and soil fertility due to their high surface area and cation exchange capacity (Hodges, 2010; Martel et al., 1978; Parfitt et al., 2008). Soil parent material also controls the retention and availability of base cations in forest soils through inheritance and formation of clay minerals, organic matter, and pH buffering minerals (Havlin, 2020; Helling et al., 1964). Both clay particles and organic matter feature negatively charged surface sites that adsorb base and acid cations which contribute to the capacity of soil to retain plant-essential nutrients, therefore enhancing overall soil fertility (McKenzie et al., 2004). Additionally, the negatively charged sites act as exchange sites for base cations into soil solution, making them available for uptake by plants. The availability of these nutrients is dependent on soil acidity (concentration of soluble and adsorbed H^+), as increased soil acidity lowers the exchange sites occupied by base cations, which increases the solubility of these nutrients (Kaupenjohann et al., 1989). In acidic soils, acidity occupies sorption sites, leading to an increased leaching of nutrients from the soil (Federer and Hornbeck, 1985; Jackson and Meetei, 2018). Carbonate minerals, such as calcite, play a role in buffering soil pH as their dissolution via carbonation consumes soil protons contributing to partially neutralized soil pH (Dijkstra et al., 2003). The formation of carbonate minerals within temperate ecosystems does not occur but the inheritance of carbonate minerals from sedimentary and metamorphic bedrocks is important across the northeastern United States. Therefore, soils derived from carbonate-bearing bedrocks have a high buffering capacity that resists changes in soil pH, promoting the availability of essential nutrients to plants.

1.6 Essential nutrients for forest growth and development

Inorganic nutrients like Ca, Mg, K, and P play essential roles in tree growth and development, each contributing to specific physiological processes vital for maintaining forest health and productivity. Calcium is a fundamental nutrient that supports cell building, structural integrity, and division in plants (White and Broadley, 2003). It is essential for cell wall stabilization and serves as a secondary messenger in various signal transduction pathways, which regulate plant responses to environmental stimuli. Magnesium plays an important role in plant energy as it serves as the central atom of the chlorophyll molecule (Dukic et al., 2023; Wang et al., 2020). Beyond the role in chlorophyll, Mg also activates several enzymatic reactions involved in carbohydrate metabolism and protein synthesis which contribute to the overall vigor and productivity of the plant. Potassium is crucial for plant growth and function, playing a key role in regulating respiration and stomatal control (Kaiser, 1982). Potassium is essential for maintaining osmotic balance, allowing the plant to adapt to drought conditions and control transpiration rates through stomatal opening and closing. Phosphorus is essential for photosynthesis, nutrient uptake, and plant growth as it forms part of adenosine triphosphate (ATP) which fuels energy transfer processes within plant cells (Schachtman et al., 1998). Phosphorus also plays a vital role in nucleic acids and their syntheses by serving as the structural backbone and the formation and structure of cell membranes serving as the hydrophilic ends of the phospholipid bilayer. While much research in the northeastern United States has focused on nitrogen (N) dynamics due to historical N pollution and its greater demand by forests (Finzi and Canham, 2000; Lovett and Mitchell, 2004; Magill et al., 2004), however the controls of parent material mineral composition on the availability and dynamics of inorganic nutrients remain poorly characterized.

1.7 Influence of soil nutrients on tree species and forest compositions

The northern hardwood forests of the northeastern United States are characterized by the dominance of three species: *Acer saccharum* (sugar maple), *Fagus grandifolia* (American beech), and *Betula alleghaniensis* (yellow birch; Eyre, 1980; Halliday, 1937). Additional species commonly found in this region are *Acer rubrum* (red maple), and *Fraxinus americana* (white ash). The species found in this region differ in levels of shade tolerance, hydrologic conditions and availability, sensitivity to soil nutrients, and value of wood products. *Acer saccharum* and *Fagus grandifolia* are highly shade tolerant species whereas *Betula alleghaniensis* is moderately tolerant. In contrast, *Fraxinus americana* and *Acer rubrum* are less tolerant and typically require more sunlight to establish (Bedard et al., 2022; McClure and Lee, 1993). *Acer saccharum* and *Fraxinus americana* thrive on nutrient rich soils, particularly high in Ca and Mg (Long et al., 2009; St. Clair et al., 2008). *Acer rubrum* and *Betula alleghaniensis* are more adaptable and can tolerate a wide range of conditions, while *Fagus grandifolia* often persists on acidic soils where other species struggle (Burns and Honkala, 1990).

Northern hardwood species are valuable to the timber industry. *Acer saccharum* wood is highly valued for hardness and wood density, making it ideal for flooring, furniture, and musical instruments (Betts, 1959). *Fraxinus americana* is cherished for the flexibility and shock resistance of wood, making it suitable for tool handles and baseball bats (USDA NRCS, 2005). *Betula alleghaniensis* produces strong, close-grained wood that is used in cabinetry, veneer, and flooring (Burns and Honkala, 1990). *Acer rubrum*, although softer than *Acer saccharum*, is also used for furniture and veneer, while *Fagus grandifolia* wood is valued for tool handles, furniture, and flooring due to its hardness and fine texture (Burns and Honkala, 1990). Altogether, these species not only shape the ecological landscape of the northeastern forests but also play significant roles in the timber industry.

Understanding nutrient uptake, allocation, and storage in forest ecosystems requires the consideration of tree species-specific characteristics, and soil conditions (Otto and Watmough, 2021). The nutrient concentrations in foliage and woody biomass of trees vary with the size, with smaller trees typically having higher concentrations than larger trees (Achat et al., 2018). Additionally, nutrient uptake and storage vary considerably among tree species, especially those sensitive to soil acidity and nutrient availability. A well-documented example of nutrient sensitivity is with *Acer saccharum* which requires high Ca concentrations and is highly susceptible to declines in soil Ca availability and increases in acidity (Gauthier et al., 2015; Hallett et al., 2006; Hong et al., 2022; Long et al., 2009; Phillips and Watmough, 2012). Soil Ca depletion is often associated with acid deposition and intensive harvesting practices in the northeastern United States and has been linked to reduced growth and health in *Acer saccharum* populations (Moore et al., 2000; Schaberg et al., 2006). Furthermore, recent studies have shown that high levels of soil Mg and P also support growth in *Acer saccharum* which highlights the importance of maintaining balanced nutrient concentrations in the soils (Gradowsi and Thomas, 2008; St. Clair et al., 2008).

In addition to *Acer saccharum*, *Fagus grandifolia* and *Betula alleghaniensis* are also prominent hardwood species within northeastern forests. Following harvesting or canopy disturbances, *Fagus grandifolia* often dominated the understory through dense thickets of shade-tolerant root suckers that out compete less shade tolerant but commercially valuable species such as *Acer saccharum* and *Betula alleghaniensis* (Rogers et al., 2021). The competition is often exacerbated on nutrient poor soils where *Fagus grandifolia* shows higher tolerance to low fertility than other species (Bakken and Cook, 1998; Kobe et al., 1995).

Species competition can be strongly influenced by the nutrient availability of a site. Studies have shown that *Fraxinus* spp. (ash) and *Acer* spp. dominate on nutrient rich soils whereas *Fagus grandifolia* dominates on less fertile sites (Bakken and Cook, 1998). Nutrient rich soils not only support faster growth and larger biomass production but also influence species diversity and succession patterns (Che and Jin, 2025; Richards et al., 2010). In contrast, soils with low Ca and Mg concentrations may impact regeneration of species like *Acer saccharum* which would shift the forest composition towards more nutrient efficient species like *Fagus grandifolia*.

1.8 Impacts of timber harvesting on soil nutrients

Timber harvesting techniques are essential for sustainable forest management, allowing for the extraction of timber and other forest resources while minimizing impacts to ecosystems. The harvesting techniques employed not only meet economic and social demands but also maintain forest health and productivity when properly implemented. The primary methods for timber harvesting include selective logging, shelterwood cutting, seed tree harvesting, and clear-cutting. Each method has a distinct ecological implication and is chosen based on forest type, management objectives, and desired ecological outcomes. When forest stands become dense, selective cutting is often used to increase light attenuation and reduce forest health risks such as pest infestation or disease outbreaks. Selective cutting involves the removal of specific mature or defective trees which leaves behind trees with higher potential for growth and quality. Selective cutting can be a single tree within stands that is chosen for harvesting by a single species, height or diameter class, whereas a group selection harvest cuts a group of trees to create small openings in the canopy to promote the growth of younger trees (Miller et al., 1995). Shelterwood cutting is applied in phases to gradually replace the older stand with a new generation of trees. The first cut removes weak, diseased, and low-quality trees to improve the vigor of the remaining stand and prepare the site for natural regeneration. The second cut strategically removes selected mature trees to open up the canopy which allows sunlight to reach the forest floor and promote the growth of seedlings and saplings. The final cut removes the remaining mature trees once the regenerating cohort is well established, giving the young trees the space and resources needed for optimal growth (Leak et al., 2014; Pourmajidian et al., 2010). This phased approach helps maintain some canopy cover throughout the process, reducing the risks of erosion and nutrient loss. A more intensive harvesting technique than the selective and shelterwood is a seed tree harvest. In this method, most trees within an area are harvested except for a few carefully selected seed-bearing trees left standing to provide a sufficient seed source for natural regeneration (Girona et al., 2018). The residual seed trees are typically chosen based on health, vigor, and genetic quality to maximize the success of future forest stands. The most intensive and disruptive harvesting method is clearcutting which is where all trees within a designated area are harvested at once. This practice is often used in even-aged forest management systems and is commonly used for species that regenerate in full sunlight, such as *Acer rubrum* (Blumroder et al., 2020; Leak and Filip, 1975). Forest managers balance timber production with the long-term health and sustainability of the forest ecosystem by meticulously selecting specific harvesting regimes for the forest.

Although the increase in biofuels as an alternative source of energy has the potential to mitigate climate change, there may be severe environmental impacts from these intensive harvesting practices. To meet these demands for increased woody biomass, forest managers increase components harvested (i.e whole-tree vs conventional) and shorter harvest rotations (Nicholls et al., 2009). Although the removal of any forest resource decreases the nutrient richness of the site, shifting from the conventional stem-only harvest to whole-tree harvesting devastates soil nutrient pools (Siemion et al., 2011; Wall, 2012) and increases the export of nutrients from the soil (Augusto et al., 2015; Garrett et al., 2021; Hornbeck et al., 1990). The removal of whole-tree biomass has been found to decrease site fertility and forest productivity (i.e. tree growth; Cleavitt et al., 2017; Morris et al., 2014; Richardson et al., 2017; Walmsley et al., 2009). More specifically, one study across three biomes (subtropical, temperate, and boreal) found that intensive management practices such as whole-tree harvest significantly decreased tree height, diameter, and biomass as well as soil Ca concentrations (Achat et al., 2015). The depletion of soil nutrients is expedited as whole-tree harvesting frequency increases because nutrients cannot be replaced via mineral weathering within that short period of time (Vadeboncoeur et al., 2014).

Clear-cutting can have profound impacts on nutrient dynamics especially when it involves whole-tree harvesting. In the northeastern United States, whole-tree harvesting at intervals of 35 to 100 years is projected to decrease soil Ca by 350 to 1066 kg/ha, K by 48 to 570 kg/ha, and Mg by 2 to 200 kg/ha over a 100-year period (Vadeboncoeur et al., 2014). Despite these nutrient losses, some studies have found no significant decreases in overall tree productivity following clear-cutting which suggests that site-specific factors such as soil texture, climate, and base cation capacity play a critical role in offsetting the effects of nutrient depletion (Thiffault et al, 2011).

A global review examining the effects of clear-cutting on temperate forest base cations found that while soil and foliar cation concentrations generally decreased, that there was no consistent decline in tree productivity (Thiffault et al., 2011). Additionally, forests dominated by species with high nutrient uptake rates and substantial biomass tend to be the most affected by clear-cutting, particularly when soil fertility is low (Akselsson et al., 2007; Paré et al., 2002). A laboratory study further supported that low fertility soil hinders seedling growth following biomass removal (Roy et al., 2021). While substantial research has been conducted on the impacts of whole-tree harvesting on forest productivity, limited attention has been given to the dynamics between soil parent material and nutrient status in influencing biomass stocks in Ca, Mg, K, and P.

1.9 Research Objectives

This dissertation investigates the complex relationships between soil mineralogy, nutrient availability, and forest productivity in the post glaciated landscapes of the northeastern United States. In these ecosystems, the mineral composition of the parent material plays a critical role in governing soil development, nutrient cycling, and forest growth (White and Blum, 1995; Vadeboncoeur et al., 2014). Specifically, the type and abundance of minerals inherited from glacially derived parent materials control the rates of mineral weathering which is the primary source of essential nutrients long-term (Brantley et al., 2008; Chadwick and Chorover, 2001).

Understanding how parent material influences nutrient availability is essential for evaluating long-term soil fertility, forest ecosystem health, and the sustainability of timber and biomass harvesting (Nave et al., 2010; Vadeboncoeur et al., 2014). Despite the importance of parent material mineralogy, the contribution of specific minerals to soil nutrient release and their linkage to forest productivity remains underexplored in glaciated regions.

This research addresses the question of how glacial till parent material mineralogy influences forest production in managed forests by integrating mineralogical, geochemical, and isotopic (Ca and Mg) techniques to 1) Compare nutrient release rates from soils and rocks to determine dominant sources of bioavailable nutrients, 2) Quantify the influence of parent material mineralogy on soil nutrient concentrations and release rates, and 3) Assess how soil nutrient richness shaped aboveground biomass accumulation and wood economic value. By linking parent material sources and mineral weathering processes to forest function, this dissertation advances our understanding of nutrient dynamics in glaciated hardwood forest ecosystems and provides insights into developing site-specific, sustainable forest management practices.

1.10 Dissertation structure

This dissertation is organized into five chapters, including an introductory chapter (this chapter, three research chapters, and a final synthesis chapter:

Chapter 1 provides an overview of the research context, objectives, and guiding questions. It introduces the key concepts for understanding rock and soil mineralogy and cycling as well as forest productivity in the northeastern United States.

Chapter 2 identifies the sourcing of parent material rocks through the validation of the glacial till model and constrains the sources on inorganic nutrients to soils along the soil nutrient richness gradient using Ca and Mg isotopes and immobile elements.

Chapter 3 characterizes the mineralogical composition of soils across three forests in Vermont and New Hampshire, with a focus on Ca and Mg bearing minerals. I also investigate the influence of mineral presence and abundance on soil nutrient pools.

Chapter 4 explores how soil nutrient richness influences aboveground nutrient concentrations and total nutrient pools in forest biomass. It also assesses how these patterns influence the volume and estimates the economic value of merchantable wood across sites.

Chapter 5 synthesizes the findings from each chapter, discusses methodological and conceptual limitations, and outlines directions for future research that build upon the insights gained in this dissertation.

References

Achat, D. L., Deleuze, C., Landmann, G., Pousse, N., Ranger, J., and Augusto, L. (2015). Quantifying consequences of removing harvesting residues on forest soils and tree growth - A meta-analysis. Forest Ecology and Management, 348, 124–141. https://doi.org/10.1016/j.foreco.2015.03.042

Achat, D. L., Martel, S., Picart, D., Moisy, C., Augusto, L., Bakker, M. R., and Loustau, D. (2018). Modelling the nutrient cost of biomass harvesting under different silvicultural and climate scenarios in production forests. Forest Ecology and Management, 429, 642–653. https://doi.org/10.1016/j.foreco.2018.06.047

Akselsson, A., Westling, O., Sverdrup, H., Holmqvist, J., Thelin, G., Uggla, E., and Malm, G. (2007). Impact of harvest intensity on long-term base cation budgets in Swedish forest soils. *Water, Air, and Soil Pollution, 7,* 201-210.

Ashley, G. M., Boothroyd, J. C., and Borns, H. W. (1991). Sedimentology of late Pleistocene (Laurentide) deglacial-phase deposits, eastern Maine. *Geological Society of America Bulletin*, 103(9), 1308-1330.

Augusto, L., Achat, D. L., Bakker, M. R., Bernier, F., Bert, D., Danjon, F., Khlifa, R., Meredieu, C., and Trichet, P. (2015). Biomass and nutrients in tree root systems-sustainable harvesting of an intensively managed Pinus pinaster (Ait.) planted forest. GCB Bioenergy, 7(2), 231–243. https://doi.org/10.1111/gcbb.12127

Bakken, P.N and Cook, J.E. (1998). Regeneration potential of six habitat types common to north-central Wisconsin. *N. J. Appl. For, 15*, 116–123

Balco, G., Rovey, C.W., and Stone, J.O.H. (2005). The first glacial maximum in North America. *Science* 307, 222. DOI: 10.1126/science.1103406

Bedard, S., Raymond, P., and DeBlois, J. (2022). Northern hardwood regeneration dynamics 10 years after irregular shelterwood and mechanical control of understory American beech. *Forest Ecology and Management*, *511*. https://doi.org/10.1016/j.foreco.2022.120142

Beier, C.M., Caputo, J., Lawrence, G.B., and Sullivan, T.J. (2017). Loss of ecosystem services due to chronic pollution of forests and surface waters in the Adirondack region (USA). *Journal of Environmental Management, 191*, 19-27. https://doi.org/10.1016/j.jenvman.2016.12.069

Bettis III, E.A., Muhs, D.R., Roberts, H.M., and Wintle, A.G. (2003). Last Glacial loess in the conterminous USA. *Quaternary Science Reviews*, *22*(18-19), 1907-1946. https://doi.org/10.1016/S0277-3791(03)00169-0

Betts, H.S. (1959). Maple (*Acer* species). Forest Service, U.S. Department of Agriculture. 1-12.

Blumroder, J.S., Hoffmann, M.T., Ilina, O., Winter, S., Hobson, P.R. and Ibisch, P.L. (2020). Clearcuts and related secondary dieback undermine the ecological effectiveness of FSC certification in a boreal forest. *Ecological Processes, 9*. https://doi.org/10.1186/s13717-020-0214-4

Brantley, S. L. (2008). Kinetics of mineral dissolution. In *Kinetics of water-rock interaction* (pp. 151-210). Springer.

Buol, S. W., Southard, R. J., Graham, R. C., and McDaniel, P. A. (2011). *Soil Genesis and Classification* (6th ed.). John Wiley and Sons. https://doi.org/10.1002/9780470960622

Burns, R.M., and Honkala, B.H. (1990). Silvics of North America: Volume 2, Hardwoods. Forest Service, United States Department of Agriculture.

Chadwick, O.A., and Chorover, J. (2001). The chemistry of pedogenic thresholds. *Geoderma, 100*(3-4), 321-353. https://doi.org/10.1016/S0016-7061(01)00027-1

Che, Y and Jin, G. (2025). Tree mycorrhizal strategies regulate diversity-productivity relationships across forest strata along soil fertility. *Forest Ecosystems, 12*. https://doi.org/10.1016/j.fecs.2024.100289

Clark, P.U., Dyke, A.S., Shakun, J.D., Carlson, A.E., Clark, J., Wohlfarth, B., Mitrovica, J.X., Hostetler, S.W., and McCabe, A.M. (2009). The last glacial maximum. *Science* 325, 710-714.

Clark, P.U., and Pollard, D. (2010). Origin of the middle Pleistocene transition by ice sheet erosion of regolith. *Paleoceanography*, 13, 1-9. https://doi.org/10.1029/97PA02660

Cleavitt, N. L., Battles, J. J., Johnson, C. E., and Fahey, T. J. (2018). Long-term decline of sugar maple following forest harvest, Hubbard Brook Experimental Forest, New Hampshire. Canadian Journal of Forest Research, 48(1), 23–31. https://doi.org/10.1139/cjfr-2017-0233

Compton, J.E., Hooker, T.D., and Perakis, S.S. (2007). Ecosystem N distribution and δ15N during a century of forest regrowth after agricultural abandonment. *Ecosystems, 10*(7), 1197–1210.

Cornut, I., Le Maire, G., Laclau, J.-P., Guillemot, J., Mareschal, L., Nouvellon, Y., and Delpierre, N. (2021). Potassium limitation of wood productivity: A review of elementary processes and ways forward to modelling illustrated by Eucalyptus plantations, Forest Ecol. Manag., 494, 119275, https://doi.org/10.1016/j.foreco.2021.119275

Cronon, W. (1983). Changes in the land: Indians, Colonists, and the Ecology of New England. Douglas and McIntyre Ltd.

Dalton, A. S., Margold, M., Stokes, C. R., Tarasov, L., Dyke, A. S., Adams, R. S., Allard, S., Arends, H. E., Atkinson, N., Attig, J. W., Barnett, P. J., Barnett, R. L., Batterson, M., Bernatchez, P., Borns, H. W., Breckenridge, A., Briner, J. P., Brouard, E., Campbell, J. E., ... Wright, H. E., Jr. (2020). An updated radiocarbon-based ice margin chronology for the last deglaciation of the North American Ice Sheet Complex. *Quaternary Science Reviews, 234*, 106223. https://doi.org/10.1016/j.quascirev.2020.106223

Denny, C. S. (1982). Geomorphology of New England. *USGS Professional Paper* 1208.

Department of Natural and Cultural Resources. (2020). New Hampshire Forest Action Plan-2020. https://www.nhdfl.dncr.nh.gov/forest-action-plan

Drummond, M.A., and Loveland, T.R. (2010). Land-use pressure and a transition to forest-cover loss in the eastern United States. *Bioscience, 60*(4), 286-298. https://doi.org/10.1525/bio.2010.60.4.7

Dijkstra, F.A., Van Breemen, N., Jongmans, A.G., Davies, G.R., and Likens, G.E. (2003). Calcium weathering in forested soils and the effect of different tree species. *Biogeochemistry, 62,* 253-275.

Dukic, E., van Maldegem, K.A., Shaikh, K.M., Fukuda, K., Topel, M., Solymosi, K., Hellsten, J., Hansen, T.H., Husted, S., Higgins, J., Sano, S., Ishijima, S., and Spetea, C. (2023). Chloroplast magnesium transporters play essential but differential roles in maintaining magnesium homeostasis. *Frontiers in Plant Science* 14. https://doi.org/10.3389/fpls.2023.1221436

Dyke, A.S. and Prest, V.K. (1987). Late Wisconsinan and Holocene history of the Laurentide Ice Sheet. *Geographie physique et Quaternaire, 41*(2), 237-263. https://doi.org/10.7202/032681ar

Easterbrook, D.J. (1982). Characteristic features of glacial sediments. In *Sandstone Depositional Environments*, pp. 1-10.

Edmonds, R.L. (1987). Decomposition rates and nutrient dynamics in small-diameter woody litter in four forest ecosystems in Washington, U.S.A. *Canadian Journal of Forest Research, 17,* 499-509.

Eyre, F.H. (1980). Forest cover types. In *Forest cover types of the United States and Canada.* Washington, DC.

Federer, C.A., and Hornbeck, J.W. 1985. The buffer capacity of forest soils in New England. Water Air Soil Pollut. 26: 163–173.

Finzi, A.C., and Canham, C.D. (2000). Sapling growth in response to light and nitrogen availability in a southern New England forest. *Forest Ecology and Management*, 131, 153-165. https://doi.org/10.1016/S0378-1127(99)00206-6

Flinn, K.M., and Marks, P.L. (2007). Agricultural legacies in forest environments: Tree communities, soil properties, and light availability. *Ecological Applications, 17*(5), 1424–1440.

Flinn, K.M., and Vellend, M. (2005). Environmental causes and consequences of forest clearance and agricultural abandonment in central New York, USA. *Journal of Biogeography, 32*(3), 439–452.

Foster, C.H.W. (1998). Stepping back to look forward: A history of the Massachusetts forest. Harvard University Forest.

Foster, D., and Aber, J. (2004). Forest in Time: the environmental consequences of 1,000 years of change in New England. Yale University Press.

Foster, D. R., Donahue, B., Kittredge, D., Motzkin, G., Hall, B., Turner, B., and Chilton, E. (2008). New England’s forest landscape: Ecological legacies and conservation patterns shaped by agrarian history. In C. L. Redman and D. R. Foster (Eds.), *Agrarian landscapes in transition: Comparisons of long-term ecological and cultural change* (pp. 44–88). Oxford University Press.

Garrett, L. G., Smaill, S. J., Beets, P. N., Kimberley, M. O., and Clinton, P. W. (2021). Impacts of forest harvest removal and fertiliser additions on end of rotation biomass, carbon and nutrient stocks of Pinus radiata. Forest Ecology and Management, 493. https://doi.org/10.1016/j.foreco.2021.119161

Gauthier, M.M., Guillemette, F., and Bedard, S. (2015). On the relationship between saplings and ingrowth in northern hardwood stands. Forest ecology and management, 358, 261-271. https://doi.org/10.1016/j.foreco.2015.09.020

Girona, M.M., Lussier, J.M., Morin, H., and Thiffault, N. (2018). Conifer regeneration after experimental shelterwood and seed-tree treatments in boreal forests: Finding silvicultural alternatives. *Frontiers in Plant Science, 9*. https://doi.org/10.3389/fpls.2018.01145

Godbout, P.M., Brouard, E., and Roy, M. (2023). 1-km resolution rebound surfaces and paleotopography of glaciated North America since the Last Glacial Maximum. *Scientific Data, 10.*

Goldemberg, J., and Teixeira Coelho, S. (2004). Renewable energy- traditional biomass vs. modern biomass. *Energy Policy, 32*, 711-714.

Goodale, C.L., and Aber, J.D. (2001). The long-term effects of land-use history on nitrogen cycling in northern hardwood forests. *Ecological Applications, 11*(1), 253–267.

Gradowski, T. and Thomas, S.C. (2008). Responses of *Acer saccharum* canopy trees and saplings to P, K, and lime additions under high N deposition. *Tree Physiology, 28*(2), 173-186.

Gress, S.E., Nichols, T.D., Northcraft, C.C. and Peterjohn, W.T. (2007). Nutrient limitation in soils exhibiting differing nitrogen availabilities: What lies beyond nitrogen saturation? *Ecology ,88*, 119-130. https://doi.org/10.1890/0012-9658(2007)88[119:NLISED]2.0.CO;2

Hallett, R. A., Bailey, S. W., Horsley, S. B., and Long, R. P. (2006). Influence of nutrition and stress on sugar maple at a regional scale. Canadian Journal of Forest Research, 36(9), 2235-2246. https://doi.org/10.1139/x06-120

Halliday, E.D. (1937). A forest classification for Canada. Canada Department of Mines and Resources, Lands, Parks and Forest Branch.

Havlin, J.L. (2020). Soil: Fertility and nutrient management. In *Landscape and land capacity* (pp. 251-265). CRC Press.

Helling, C.S., Chesters, G., and Corey, R.B. (1964). Contribution of organic matter and clay to soil cation-exchange capacity as affected by the pH of the saturating solution. *Soil Science Society of America Journal, 28*(4), 517-520. https://doi.org/10.2136/sssaj1964.03615995002800040020x

Hodges, S.C. (2010). Soil fertility basics. *Soil science extension, North Carolina State University*, 22, 1-75.

Hong, D.S., Gonzales, K.E., Fahey, T.J., and Yanai, R.D. (2022). Foliar nutrient concentrations of six northern hardwood species responded to nitrogen and phosphorus fertilization but did not predict tree growth. Peer J, https://doi.org/10.7717/peerj.13193.

Hornbeck, J. W., Smith, C. T., Martin, C. W., Tritton, L. M., and Pierce, R. S. (1990). Effects of Intensive Harvesting on Nutrient Capitals of Three Forest Types in New England. 30, 55–64.

Hooker, T.D., and Compton, J.E. (2003). Forest ecosystem carbon and nitrogen accumulation during the first century after agricultural abandonment. *Ecological Applications, 13*(2), 299–313.

Jackson, K., and Thomas Meetei, T. (2018). Influence of soil pH on nutrient availability: A Review. Journal of Emerging Technologies and Innovative Research, 5(12), 707–713. www.jetir.org

Jenny, H. (1941). Factors of soil formation: A system of quantitative pedology. Dover Publications, New York, 281 p.

Kaiser, W. M. (1982). Correlation between changes in photosynthetic activity and changes in total protoplast volume in leaf tissue from hygro-, meso- and xerophytes under osmotic stress. Planta, 154, 538-545. https://doi.org/10.1007/BF00402997

Kaupenjohann, M., Zech, W., Hantschel, R., Horn, R., and Schneider, B. U. (1989). Mineral Nutrition of Forest Trees: A Regional Survey. In E.-D. Schulze, O. L. Lange, and R. Oren (Eds.), Forest Decline and Air Pollution (Vol. 77, pp. 282–294). Springer Berlin Heidelberg. https://doi.org/10.1007/978-3-642-61332-6

Kobe, R.K, Pacala, S.W., Silander Jr, J.A. and Canham, C.D. (1995). Juvenile tree survivorship as a component of shade tolerance. Ecol. Appl 5:517–532.

Koteff, C., and Larsen, F.D. (1989). Postglacial uplift in western New England: geologic evidence for delayed rebound. In *Earthquakes at North-Atlantic passive margins: Neotectonics and postglacial rebound.* NATO ASI Series, Vol 266. Springer, Dordrecht.

Koteff, C., and Pessl, F. (1981). Systematic Ice Retreat in New England. In Geological Survey Professional Paper 1179.

Kramer, K., Bouriaud, L., Feindt, R., and van Wassenaer, L. (2022). Roadmap to develop a stress test for forest ecosystem services supply. *One Earth, 5*(1), 25-34. https://doi.org/10.1016/j.oneear.2021.12.009

Lawrence, G.B., and Huntington, T.G. (1999). Soil-calcium depletion linked to acid rain and forest growth in the eastern United States. U.S. Geological Survey Water-Resources Investigations Report 98-4267. https://doi.org/10.3133/wri984267

Leak, W.B. and Filip, S.M. (1975). Uneven-aged management of northern hardwoods in New England. USDA Forest Service Research Paper NE-332.

Leak, W.B., Yamasaki, M., and Holleran, R. (2014). Silvicultural guide for northern hardwoods in the northeast. *USFS General Technical Report NRS-132*.

Liu, Z., Ma, X., Zhou, D., Zhang, H., Bai, Y., and Han, H. (2024). The geological origins and soil properties of loess-like silty clay: a case study in the jinan area. *Scientific Reports, 14*. https://doi.org/10.1038/s41598-024-63394-0

Long, R.P., Horsley, S.B., Hallett, R.A., and Bailey, S.W. (2009). Sugar maple growth in relation to nutrition and stress in the northeastern United States. *Ecological Applications,* 19 (6), 1454-1466. 10.1890/08-1535.1

Lovett, G.M., and Mitchell, M.J. (2004). Sugar maple and nitrogen cycling in the forests of eastern North America. Frontiers in ecology and the Environment, 2 (2), 81-88. https://doi.org/10.1890/1540-9295(2004)002[0081:SMANCI]2.0.CO;2

Lundström, U. S., van Breemen, N., and Bain, D. C. (2000). The podzolization process. A review. *Geoderma*, 94(2-4), 91–107. https://doi.org/10.1016/S0016-7061(99)00036-1

Magill, A.H., Aber, J.D., Currie, W.S., Nadelhoffer, K.J., Martin, M.E., McDowell, W.H., Melillo, J.M., and Steudler, P. (2004). Ecosystem response to 15 years of chronic nitrogen additions at the Harvard Forest LTER, Massachusetts, USA. Forest Ecology and Management, 196, 7-28. https://doi.org/10.1016/j.foreco.2004.03.033

Martel, Y.A., De Kimpe, C.R., and Laverdiere, M.R. (1978). Cation-exchange capacity of clay-rich soils in relation to organic matter, mineral composition, and surface area. *Soil Science Society of America Journal*, *42*(5), 764-767. https://doi.org/10.2136/sssaj1978.03615995004200050023x

McClure, J.W., and Lee, T.D. (1993). Small-scale disturbance in a northern hardwoods forest: effects on tree species abundance and distribution. *Canadian Journal of Forest Research, 23*(7), 1347-1360. https://doi.org/10.1139/x93-172

McKenzie, N. N., Jacquier, D. D., Isbell, R. R., and Brown, K. K. (2004). Australian Soils and Landscapes (pp. 1-433). CSIRO Publishing.

Mickelson, D.M., Clayton, L., Fullerton, D.S., and Borns, H.W. (1983). The Late Wisconsin glacial record of the Laurentide ice sheet in the United States. In *Late Quaternary Environments of the United States*. (pp. 3-39). University of Minnesota Press.

Miller, G.W., Schuler, T.M., and Smith, H.C. (1995) Method for applying groups selection in central Appalachian hardwoods. USFS Research Paper NE-696. U.S. Forest Service.

Morris, D. M., Kwiaton, M. M., and Duckert, D. R. (2014). Black spruce growth response to varying levels of biomass harvest intensity across a range of soil types: 15-year results. Canadian Journal of Forest Research, 44(4), 313–325. https://doi.org/10.1139/cjfr-2013-0359

Moore, J.D., Camite, C., and Ouimet, R., (2000). Effects of liming on the nutrition, vigor, and growth of sugar maple at the Lake Clair Watershed, Quebec, Canada. *Canadian Journal of Forest Research, 30*, 725-735.

Muhs, D. R., Bettis, E. A., and Aleinikoff, J. N. (2004). The origin of loess in the central United States and implications for global dust activity. *Quaternary Science Reviews*, 23(3-4), 263-282.

Nave, L.E., Vance, E.D., Swanston, C.W., and Curtis, P.S. (2010). Harvest impacts on soil carbon storage in temperate forests. *Forest Ecology and Management, 259*, 857-866. https://doi.org/10.1016/j.foreco.2009.12.009

Nezat, C.A., Blum, J.D., Yanai, R.D., and Park, B.B. (2008). Mineral sources of calcium and phosphorus in soils of the Northeastern United States. *Soil Science Society of America Journal, 72*(6), 1786-1794. https://doi.org/10.2136/sssaj2007.0344

Nicholls, D., Monserud, and R.A., Dykstra, D.P. (2009). International bioenergy synthesis-lessons learned and opportunities for the western United States. *Forest Ecology and management, 257*, 1647-1655. https://doi.org/10.1016/j.foreco.2008.11.035

Otto, N.F.J., and Watmough, S.A. (2021). Does forest tree species composition impact modelled soil recovery from acidic deposition? *Canadian Journal of Forest Research, 5*(3), 372-384.https://doi.org/10.1139/cjfr-2021-0170

Pare, D., Rochon, P., and Brais, S. (2002). Assessing the geochemical balance of managed boreal forests. *Ecological Indicators, 1*, 293-311.

Parfitt, R.L., Giltrap, D.J., and Whitton, J.S. (2008). Contribution of organic matter and clay minerals to the cation exchange capacity of soils. *Communications in Soil Science and Plant Analysis, 26*(9-10), 1343-1355. https://doi.org/10.1080/00103629509369376

Peltier, W. R. (2004). Global glacial isostasy and the surface of the ice-age Earth: The ICE-5G (VM2) model and GRACE. *Annual Review of Earth and Planetary Sciences*, 32, 111-149.

Phillips, T., and Watmough, S.A. (2012). A nutrient budget for a selection harvest: implications for long-term sustainability. *Canadian Journal of Forest Research, 42*(12), 2064-2077.

Pourmajidian, M. R., Jalilvand, H., Fallah, A., Hosseini, S. A., Parsakhoo, A., Vosoughian, A., and Rahmani, A. (2010). Effect of shelterwood cutting method on forest regeneration and stand structure in a Hyrcanian forest ecosystem. *Journal of Forestry Research, 21*(3), 265–272.

Reineck, H.E., and Singh, I.B. (1980). Glacial Environment. In *Depositional Sedimentary Environments*, pp. 185-208.

Richards, A.E., Forrester, D.I., and Bauhus, J. (2010). The influence of mixed tree plantations on the nutrition of individual species: a review. *Tree Physiology, 30*(9), 1192-1203.

Richardson, J. B., Petrenko, C. L., and Friedland, A. J. (2017). Base cations and micronutrients in forest soils along three clear-cut chronosequences in the northeastern United States. Nutrient Cycling in Agroecosystems, 109(2), 161–179. https://doi.org/10.1007/s10705-017-9876-4

Richardson, J. B., and Zuñiga, L. X. (2021). Quantifying aluminosilicate manganese release and dissolution rates across organic ligand treatments for rocks, minerals, and soils. Acta Geochim. https://doi.org/10.1007/s11631

Ridge, J. C. (2003). The last deglaciation of the northeastern United States: A combined varve, paleomagnetic, and calibrated radiocarbon chronology. *Quaternary Science Reviews*, 22(7), 733-745.

Rogers, N. S., D'Amato, A. W., and Leak, W. B. (2021). Long-term evolution of composition and structure after repeated group selection over eight decades. Canadian Journal of Forest Research, 51, 1080-1091.

Roy, M. È., Surget-Groba, Y., Delagrange, S., and Rivest, D. (2021). Legacies of forest harvesting on soil properties along a chronosequence in a hardwood temperate forest. Forest Ecology and Management, 496. https://doi.org/10.1016/j.foreco.2021.119437

Schaberg, P. G., Tilley, J. W., Hawley, G. J., DeHayes, D. H., and Bailey, S. W. (2006). Associations of calcium and aluminum with the growth and health of sugar maple trees in Vermont. Forest Ecology and Management, 223(1–3), 159–169. https://doi.org/10.1016/J.FORECO.2005.10.067

Schachtman, D. P., Reid, R. J., and Ayling, S. M. (1998). Update on Phosphorus Uptake Phosphorus Uptake by Plants: From Soil to Cell. Plant Physiology, 116, 447–453. https://academic.oup.com/plphys/article/116/2/447/6085629

Schaetzl, R.J., and Isard, S.A. (1996). Regional-scale relationships between climate and strength of podzolization in the Great Lakes Region, North America. *Catena, 28,* 47-69.

Siemion, J., Burns, D.A., Murdoch, P.S., and Germain, R.H. (2011). The relation of harvesting intensity to changes in soil, soil water, and stream chemistry in a northern hardwood forest, Catskill Mountains, USA. *Forest Ecology and Management, 261*, 1510-1519.

Smalley, I.J. (1966). The properties of glacial loess and the formation of loess deposits. *Journal of Sedimentary Research*, *36*(3), 669-676. https://doi.org/10.1306/74D7153C-2B21-11D7-8648000102C1865D

Soil Survey Staff, 2022. Keys to Soil Taxonomy, 13th edition. USDA Natural Resources Conservation Service.

St. Clair, S. B., Sharpe, W. E., and Lynch, J. P. (2008). Key interactions between nutrient limitation and climatic factors in temperate forests: A synthesis of the sugar maple literature. Canadian Journal of Forest Research, 38(3), 401–414. https://doi.org/10.1139/X07-161

Stone, B. D., and Borns, H. W. (1986). Pleistocene glacial and interglacial stratigraphy of New England. *Quaternary Science Reviews*, 5(1-2), 39-52.

Teng, W., Yu, Q., Mischenko, I.C., Rice, A.M., and Richardson, J.B. (2024). Predicting foliar nutrient concentrations across geologic materials and tree genera in the northeastern United States using spectral reflectance and partial least squares regression models. *Journal of Remote Sensing*, 4. https://doi.org/10.34133/remotesensing.0093

Thiffault, E., Hannam, K.D., Pare, D., Titus, B.D., Hazlett, P.W., Maynard, D.G., and Brais, S. (2011). Effects of forest biomass harvesting on soil productivity in boreal and temperate forests- A review. *Environmental Reviews, 19*, 278-309

Thompson, J.R., Foster, D.R., Scheller, R.M., and Kittredge, D.B. (2011). The influence of land use and climate change on forest biomass and composition in Massachusetts, USA. *Ecological Applications, 21*(7), 2425–2444.

Tripler, C. E., Kaushal, S. S., Likens, G. E., and Walter, M. T. (2006). Patterns in potassium dynamics in forest ecosystems, Ecology Letters, 9, 451–466. https://doi.org/10.1111/j.1461-0248.2006.00891.x

USDA NRCS. (2005). Plant guide for white ash (*Fraxinus americana*). Retrieved March 23, 2025 from https://plants.usda.gov/DocumentLibrary/plantguide/pdf/pg_fram2.pdf

Vadeboncoeur, M. A., Hamburg, S. P., Yanai, R. D., and Blum, J. D. (2014). Rates of sustainable forest harvest depend on rotation length and weathering of soil minerals. Forest Ecology and Management, 318, 194–205. https://doi.org/10.1016/j.foreco.2014.01.012

Vermont Department Forest, Parks and Recreation. Vermont Forest Resources Harvest Summary-2022. https://fpr.vermont.gov/harvest-reports

Wall, A. (2012). Risk analysis of effects of whole-tree harvesting on site productivity. *Forest Ecology and Management*, *282,* 175-184.

Walmsley, J. D., Jones, D. L., Reynolds, B., Price, M. H., and Healey, J. R. (2009). Whole tree harvesting can reduce second rotation forest productivity. Forest Ecology and Management, 257(3), 1104–1111. https://doi.org/10.1016/j.foreco.2008.11.015

Wang, Z., Hassan, M. U., Nadeem, F., Wu, L., Zhang, F., and Li, X. (2020). Magnesium Fertilization Improves Crop Yield in Most Production Systems: A Meta-Analysis. Frontiers in Plant Science, 10(January), 1–10. https://doi.org/10.3389/fpls.2019.01727

White, P. J., and Broadley, M. R. (2003). Calcium in plants. In Annals of Botany (Vol. 92, Issue 4, pp. 487–511). https://doi.org/10.1093/aob/mcg164

Yesilonis, I., Szlavecz, K., and Pouyat, R. (2016). Historical land use and stand age effects on soil properties in the Mid-Atlantic US. *Forest Ecology and Management, 387,* 214-222. https://doi.org/10.1016/j.foreco.2016.03.046

Zhang, Y., Rimstidt, D.J., Huang, Y. and Zhu, C. (2019). Kyanite far from equilibrium dissolution rate at 0-22 ℃ and pH of 3.5-7.5. *Acta Geochimica, 38*(4), 472-480.

Chapter 2

Quantifying nutrient pools and weathering rates in glacial soils of northern New England U.S.: An integration of mineralogy, geochemistry, and Ca and Mg isotopes

---

In preparation for submission in ***Regional Geoderma***

Authors

Alexandrea M. Rice[1,5*], Nicolas Perdrial[2,3], Patrick J. Drohan[4], Anthony W. D'Amato[3], Justin B. Richardson[1,5]

[1]Department of Environmental, Geographic, and Climates Sciences, University of Massachusetts Amherst, Amherst, MA, USA

[2]Department of Geography and Geosciences, University of Vermont, Burlington, VT, USA

[3]Rubenstein School of Environment and Natural Resources, University of Vermont, Burlington, VT, USA

[4]Department of Ecosystem Science and Management, The Pennsylvania State University, University Park, PA, USA

[5]Present address: Department of Environmental Sciences, University of Virginia, VA, USA

*Corresponding Author: utw7wd@virignia.edu

2.0 Abstract

The nutrient availability in glacial soils influences forest productivity particularly in regions where mineral weathering is the primary source of essential elements like calcium and magnesium. This study investigated the nutrient pools and weathering rates of soils and rock in glacial soils at three northern New England forests: Poor forest (Bartlett Experimental Forest, NH), Moderate forest (Dartmouth Second College Grant, NH), and Rich forest (Clement Woodlot, VT). We evaluated the influence of parent material on soil composition and nutrient release rates and focused on rock fragments as potential reservoirs of inorganic nutrients. We found that glacial till composition was predominantly controlled by rock fragments from local bedrock sources matching the underlying rock formations rather than from extended distances from transport by the Laurentide Ice Sheet. The Rich forest had the highest nutrient release rates from rocks due to the abundance of easily weatherable minerals like calcite, while the Poor forest which is dominated by granite had limited nutrient release rates and pools. We compared laboratory weathering rates and found that rocks have higher weathering rates per unit area, but soils have substantially higher surface area in the soil profile and are the dominant source of nutrients in the three forests. Our findings highlight the importance of considering the mineral composition of local geology when developing forest management strategies as nutrient cycling and soil fertility depend on rock and soil weathering processes.

2.1 Introduction

Soils and their underlying parent materials control the sourcing and storage of inorganic nutrients in forest ecosystems. Understanding provenance and availability of inorganic nutrients in soils is essential for the long-term sustainability of forest productivity, including timber production, recruitment of valuable-timber species, woody biomass for biofuel, wildlife habitat, downstream water quality, and many other ecosystem services (Chadwick et al., 1999; Grigal, 2000; Vitousek et al., 2010). Several key studies have demonstrated the critical role of mineral weathering in sustaining nutrient pools within forest ecosystems, particularly regions where atmospheric inputs and recycling aboveground components alone cannot maintain soil fertility (Brantley, 2008; Nezat et al., 2008; Porder and Chadwick, 2009; Vadeboncoeur et al., 2014).

Inorganic nutrients such as calcium (Ca), magnesium (Mg), potassium (K), and phosphorus (P) are primarily sourced from the weathering of minerals within soil and rock parent material (Wilson, 2004). Although precipitation, organic matter decomposition, and lateral flow (surface or subsurface) significantly contribute to nutrient sourcing and cycling, mineral weathering typically serves as the dominant long-term input with soils serving as the largest reservoirs of inorganic nutrients (Chadwick et al., 1999; Hedin et al., 2003). The mineralogical composition of soil parent materials thus plays a fundamental role in determining nutrient availability and soil fertility. In northern New England, parent materials are typically composed of granitic and metamorphic rocks such as mica schists and phyllite (Bennett et al., 2006; Ratcliffe et al., 2011). Within these rocks, minerals that weather easily to moderately include calcite, apatite, and micas which release base cations and nutrients during the weathering process. Conversely, more weather resistant minerals like plagioclase feldspars, hornblende, and quartz contribute minimally to nutrient cycling (Heřmanská et al., 2022; Velbel, 1993; Wilson, 2004; Aoudjit et al., 1996; Taylor and Blum, 1995). Specifically, calcite, apatite, hornblende, plagioclase feldspars, and micas contribute Ca to the soil, while micas and hornblende also contribute Mg. Potassium is primarily sourced from micas and orthoclase, and P mainly from apatite. The weathering of these minerals is not only essential for nutrient supply but also plays a key role in maintaining soil pH, and acid-buffering capacity. The release of base cations helps regulate soil pH which enhances the mobility and availability of nutrients within the ecosystem (Jobbagy and Jackson, 2001; Tardy, 1997).

Evaluating the sourcing of inorganic nutrients in glaciated soils of the northeastern United States is particularly challenging due to the heterogeneity of parent materials shaped by glacial processes. Soils in this region are typically complex and vary spatially due to the deposition of rocks fragments and other materials from the retreat of the Laurentide Ice Sheet (Crowley et al., 2012; Gardner et al., 2023). Among these soils, glacial till is especially heterogeneous and usually is composed of unsorted and unstratified particles sizes from diverse sources (Ciolkosz et al., 1989). This results in a combination of nutrient rich and poor parent materials (Rustad et al., 2020). Glaciofluvial deposits on the other hand are formed from meltwater outwash and often are stratified layers of gravel and sand due to the high energy depositional environment which leads to coarse soil textures (Hobbie et al., 2002). Additionally, the potential of wind blown silt deposits can further complicate identifying nutrient sources in this region since it introduces fine, mineral rich particles on top of glacial till (Smalley, 1966; Muhs, 2013).

During pedogenesis, nutrient-rich minerals are typically depleted in surface horizons due to intense weathering, while deeper horizons, including saprolite, may serve as ongoing nutrient reservoirs during hydrolytic and oxidative weathering processes (Lundstrom et al 2000; Uhlig and Von Blanckenburg, 2019). Despite the recognized importance of mineral weathering in nutrient supply, rock fragments larger than coarse sand (> 2 mm) are generally excluded from standard soil studies. This exclusion may lead to an underestimation of nutrient availability, as these rock fragments may represent a significant and underappreciated reservoir of inorganic nutrients, particularly where the upper mineral soil is rapidly leached of base cations due to acid weathering (Egli et al., 2014; Heckman and Rasmussen, 2011).

Geochemical techniques like trace element analysis and stable isotope ratios (e.g. Ca and Mg) provide valuable methods for quantifying the contributions of different mineral sources to soil nutrient budgets. Isotopic signatures can help distinguish between nutrients derived from mineral weathering, atmospheric inputs, and biological cycling, thereby improving our understanding of nutrient sourcing in forests on glacial till (Bailey et al., 1996; Pett-Ridge et al., 2009). Several studies have successfully used Ca and Mg isotopes to identify mineral provenance and assess the source of nutrients to trees in forest ecosystems (Farkas et al., 2011; Perakis et al., 2006). For instance, Ca isotope ratios have been used to trace the contributions of mineral weathering versus atmospheric deposition in forest soils (Drouet and Herbauts, 2008). Understanding the sources of minerals and soil nutrients is important for predicting the sustainability of forest ecosystems long-term, especially in regions like New England where glacial processes have shaped the landscape and influenced mineral availability (Watmough, 2014; Hynicka and Pett-Ridge, 2016).

Despite previous research, gaps remain in understanding the specific contributions of different parent materials and rock fragments to long-term nutrient availability in glacial soils. Additionally, little work has been done to quantify the role of larger rock fragments in sustaining soil fertility over extended timescales. This study aims to address these gaps by integrating mineralogical, geochemical, and isotopic approaches to constrain nutrient pools and weathering rates in the soils of northern New England forests. Our study had two primary objectives: 1) To evaluate the influence of regional geology on the composition and mineralogy of soil parent materials in northern New England and 2) To quantify the contribution of rock fragments to forest soil nutrient pools.

We hypothesized that rock fragments and overlying soils will be compositionally and mineralogically dominated by the local bedrock formation despite the mixing effects of glaciation. Additionally, we hypothesized that rock fragments can serve as a nutrient reservoir comparable in magnitude to the fine fraction of soil (< 2 mm). By improving our understanding of nutrient pools and weathering processes in these soils, this research will provide insight into the long-term sustainability of forest ecosystems in glaciated regions. Particularly, our results can be used to inform land management strategies aimed at maintaining soil fertility and ecosystem resilience. Our findings may have broader implications for other glaciated regions.

2.2 Methods

2.2.1 Study sites and geologic background

This study was conducted in three forests in northern New England that represent a gradient of Ca and Mg nutrient-richness: “Poor” sites at Bartlett Experimental Forest in Bartlett, NH, “Moderate” sites at Second College Grant in Coos County, NH, and “Rich” sites at Clement Woodlot near Corinth, VT (Rice et al., 2024; Figure 2.1). These sites were selected based on mapped bedrock and parent materials to capture a variation in nutrient availability.

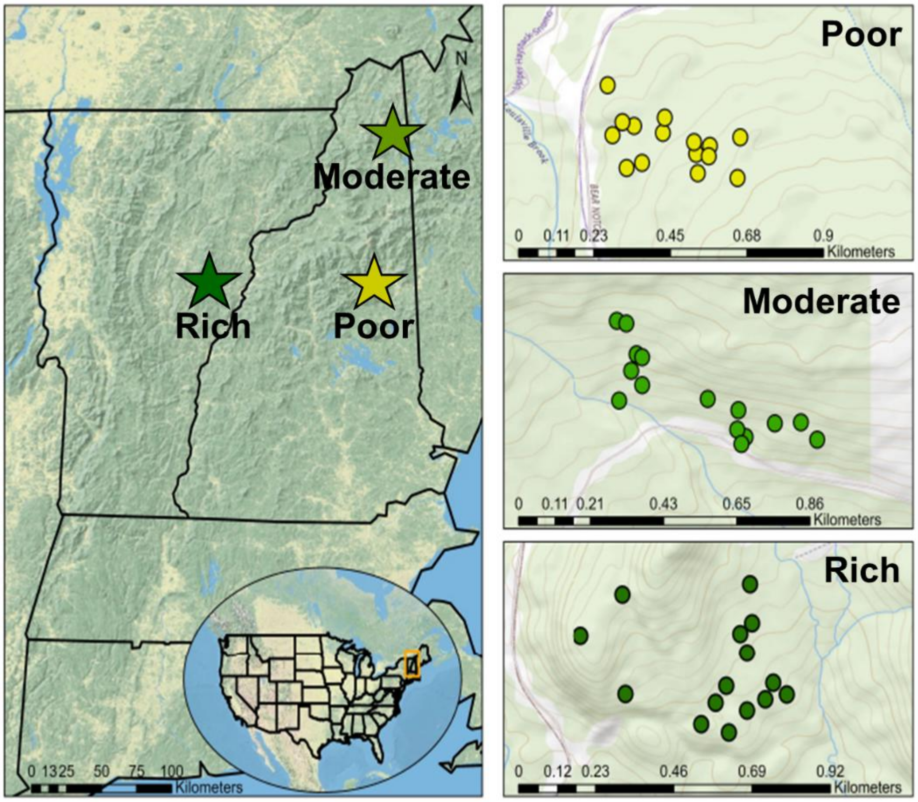

Figure 2.1. Map of the three forests across Vermont and New Hampshire. The distribution of all 15 sampling plots is shown within each forest nutrient richness. Colors correspond to forest nutrient richness and stars are the location of each forest with the circles indicating the location of each plot within a forest. Each topo line represents a 40 m elevation change.

Because this region of the U.S. was glaciated until quite recently (~ 14,000 yrs ago), the soil parent material does not directly correspond to the underlying bedrock but instead reflects a range of neighboring materials carried by the Laurentide Ice Sheet (Likens et al., 1977). The retreat of the Laurentide Ice Sheet left behind a complex of glacial deposits that included till, outwash, and glaciolacustrine sediments that have formed the parent material of soils in the region. In Vermont and New Hampshire, fine silt loess deposits can be found overlying glacial till and outwash sediments which can alter the nutrient availability and dynamics within the ecosystem (Bailey, 2000). Alluvial materials were deposited across the valleys within the landscape which contributed to the heterogeneity of parent material. The level of heterogeneity the deposits have depends on the proximity the area is to sediment sources and the local topography (Jahn, 1947).

The origin of the surficial materials cannot be clearly pinpointed due to the glacial deposits being mixed. However, the reported direction of ice flow and typical transport distances suggest that the parent material at each forest is primarily derived from the local bedrock sources and extend approximately 1.5 km northwest (Koteff and Pessl, 1981). The Rich forest is geologically the most different out of the three forests due to the high abundance of apatite and carbonate minerals within the glacial till. This site is part of the Connecticut Valley Trough, specifically the Waits River Formation which is characterized by limestone and phyllite (Lyons et al., 1997). The limestone is a dark bluish gray color and is mica-rich. The phyllite is dark to silvery gray and contains muscovite, biotite, quartz, and sometimes chlorite (USGS, 2025b). This combination of major rock types contributes to the high Ca and Mg soil nutrients. The Moderate forest is within the Central Main Trough which is primarily composed of the Aziscohos Formation (USGS, 2025a). This formation is composed of metapelitic schists containing coticule laminations, quartz lenses, and feldspathic metatuff (Lyons et al., 1997). These major rock types contribute to the intermediate levels of soil Ca and Mg. The Poor forest geology is characterized by Conway granite, which is a coarse-grained, pink-hued granite composed of biotite, plagioclase, and perthitic feldspar (Liese, 1973). The Poor forest has low soil Ca and Mg due to the acidic and low Ca content nature of granite.

2.2.2 Field sampling

At each of the 45 sampling plots (15 per forest), we excavated one soil pit approximately 0.5 m wide to expose a clean, undisturbed soil profile for sampling and horizon description. The exact dimensions of each pit varied depending on site-specific physical constraints such as the presence of coarse roots, and rocks. Soil pits were dug to a maximum depth of 1 m or until a restrictive layer was encountered which was typically a fragipan or compacted layer that inhibited further excavation. The deepest soils were found at the Rich forest, with 14 out of the 15 pits reaching a depth of 90 cm or more below the surface of the mineral soil. To estimate bulk density throughout the soil profile, we collected two core samples from each soil pit using a metal soil corer (7.30 cm in diameter and 10.8 cm long). One sample was taken from the top of the mineral soil horizon, just below the organic horizon, and the second was collected approximately 50 cm below the surface. There samples were used to determine mineral soil bulk density and calculate nutrient pools.

Soil samples were collected in 5 cm increments from the top of the mineral soil to a depth of 30 cm to capture finer-scale variability in soil properties near the surface. From 30 cm to the base of each pit, soil samples were collected at 10 cm increments to efficiently characterize deeper soil horizons. At the base of each soil pit, a soil core was used to collect soil from the underlying parent material or from beneath any confining layer, when present. In total, 621 soil samples were collected across the 45 plots.

To capture the variability in parent material and rock composition, representative stone and cobbles (50-250 mm in diameter) were collected from each soil pit. A total of 375 rocks were collected across the 45 pits. Care was taken to select cobbles that represented the dominant lithologies observed during excavation with the aim of capturing mineralogical diversity relevant to long-term weathering and nutrient availability.

2.2.3 Soil and rock physical processing

Mineral soil samples were air dried at 70 ℃ until weight remained consistent. Dried soils were passed through a 2 mm sieve and the < 2 mm fine-earth fraction were used for soil analyses. Subsamples of the sieved soils were homogenized using a mortar and pestle to ensure consistency across chemical and physical measurements. The rock fragments (> 2 mm) separated from sieving were weighed separately to determine the rock to soil ratio within each soil horizon, providing an estimate of coarse fragment content throughout the soil profile.

Rocks collected from the soil pits were cleaned and visually classified by general lithology (e.g. granite, schist, sandstone). A total of 375 rocks were collected and identified across the three forests. Each rock was categorized as either locally derived or exogenous (e.g. glacially transported) based on lithologic characteristics and field context. A representative subset of 50 rocks were selected for inorganic nutrient analyses. Each rock was cut in half using either a gravity saw or trim saw depending on the size. One half of each rock sample was crushed to coarse gravel using a hydraulic press. The remaining material was finely powdered (< 0.5 mm) using a tungsten carbide puck mill (ShatterBox) prior to total elemental analysis.

Total elemental concentrations for these soils were previously reported by Rice et al. (2024). To estimate total elemental pools across the soil profile, we calculated the soil mass within each depth increment using measured bulk density and horizon thickness. This mass was then multiplied by the elemental concentration of each increment. Total soil profile pools were calculated by summing the elemental mas across all sampled depths. Coarse rock fragments (> 2 mm) were excluded from these estimates by correcting for measured rock fragment volume and using the fine-earth fraction in bulk density calculations.

2.2.4 Soil particle analysis

To quantify the distribution of particle sizes within the soil across the forest nutrient richness gradient, we selected four plots at varying landscape positions at each forest and used samples from three depth intervals: 5-10 cm, 30-40 cm, and the deepest depth sampled. Organic matter was removed by placing the samples in a hot water bath at 100℃ and gradually adding 15% hydrogen peroxide (H_2O_2) in 1 mL increments until no further reaction occurred for at least one hour (following methods adapted from Lepp et al., 2024). After the complete removal of organic matter, sodium metaphosphate was added to deflocculate clay particles and the mixture was left to sit for at least 48 hours. Grain size distribution was analyzed using a Bettersizer S3 Plus which used laser diffraction technology to measure the frequency of particle sizes in a sample.

2.2.5 Rock nutrient concentrations and pools

To quantify total nutrient concentrations in rocks, powdered samples were digested using a modified version of USEPA Method 3052. Approximately 20 mg of each rock powder was placed into perfluoroalkoxy alkane (PFA) vials and combined with 2.5 mL of 15.6 M HNO_3 and 2.5 mL of 28.9 M HF. The sealed vials were heated at 170℃ for 48 hours to ensure complete dissolution of silicate minerals. Following digestions, the caps were removed and the solutions were evaporated to form a small moist bead. The bead was subsequently rehydrated with 2 mL of 15.6 M HNO_3 and dried down again. This rehydration and evaporation step was repeated once more to remove any remaining HF and promote complete digestion. The final residue was then dissolved in 5 mL of 7.8 M HNO_3 and reheated at 170°C for 24 hours. All digests were diluted to a final volume of 50 mL using 18.2 MΩ·cm deionized water. Each set of 25 samples included a procedural blank and two standard reference materials to ensure analytical accuracy and precision.

The total rock-derived nutrient pools within the soil profile were estimated based on the mass of rock fragments (> 2 mm) present in each soil depth interval. Since coarse rock fragments tend to increase with depth in glaciated soils and sampling depth was limited these estimates represent minimum rock nutrient pools and do not account for coarse fragments below the maximum sampling depth. First, we calculated the mass of coarse fragments in each soil horizon. Then, averaged elemental concentrations from representative rock types at each forest site were multiplied by the rock mass in each sampling interval. Total rock nutrient pools for each plot were calculated by summing nutrient contributions across all sampled depth intervals.

2.2.6 Rock mineral analyses

Bulk rock mineral presence and abundances were determined for 9 powdered rocks, 3 from each forest, by X-ray diffraction (XRD) using a Rigaku MiniFlex II equipped with a Cu K_{α} x-ray source. Approximately 0.50 g of subsample each 50 µm rock powder was mounted on a glass slide and analyzed between 5 and 55° 2θ at 1° per minute at 0.02° resolution. The Rietveld refinement analysis was performed to quantify diffractograms by using the whole profile module in the PDXL2 software (Rigaku corporation 2007-2017; Downs and Hall-Wallace, 2003; Gražulis et al., 2020).

Rock fragments from the unweathered interior from the same subsample of 9 rocks, were used for mineral identification. Minerals were identified using an electron microprobe (Cameca SX-100) and scanning electron microscope energy-dispersive X-ray spectroscopy (SEM-EDS) for elemental mapping of Al, Ca, Fe, K, Mg, Mn, Na, P, S, Si, and Ti (Bailey et al., 2019). ImageJ was used to composite elemental maps and quantify elemental abundances in each rock fragment (Schneider et al., 2012).

2.2.7 Batch reactors for rock weathering rates

We conducted a batch reactor experiment to evaluate the influence pH may have on mineral release rates among the dominant rock types within each nutrient richness. In this laboratory-based experiment, 3.00 (± 0.01) g of each rock sample was weighed into 50 mL centrifuge tubes. The samples were then immersed in a 40 mL solution composed of 0.01 M NaCl, 0.01 M catechol, and 0.01 M citric acid. The pH of solutions were adjusted to 4, 5, or 6 using deionized water and trace metal grade 11.4 M HCl, and 20.6 M NaOH, since the pH of the field soil solution varied from 4.8 to 6.7 among the three forest nutrient richness gradient. The samples were shaken for two-week intervals over a total of 10 weeks. After each two-week period, the solutions were centrifuged at 2600 rpm for 1 hr, and the supernatant was carefully decanted. Subsequently, a new solution of the same pH was added to the tubes. This procedure was repeated every two weeks to minimize precipitation and oversaturation of elements in the solution, ensure discretized replication for the time series, and obtain sufficient sample mass for elemental analyses. Following each weathering interval, the pH of the supernatant was measured to monitor changes in pH after the two-week period of weathering. The supernatant was then acidified with HNO_3 to stabilize the sample and an aliquot was diluted for elemental analysis. This experimental design was also replicated for soil samples collected from each site at three depth intervals (5-10 cm, 30-40 cm, and the deepest sample) as reported in Rice et al. (2024).

Elemental release rates were calculated using area-normalized values derived from surface area measurements of the major rock types, as reported by Richardson and Zuniga (2021) and Richardson et al. (2023). These studies used the BET method for surface area determination which were conducted by Particle Technology Labs which is a commercial laboratory specializing in particle characterization.

To scale weathering rates to the entire soil profile, we first estimated the surface area of each rock and soil sample per unit volume. For soils, we calculated the mass of soil per depth interval and then the weathering rate was multiplied by the surface area and scaled to each depth interval. Then the results were summed across the entire profile. For rocks, we also calculated the mass of rocks per depth interval and then the weathering rate was multiplied by the surface area. First, rock sizes at each soil depth were related to surface area using the published estimates by Cooper and Testa (2001). The weathering rates for the rocks were then multiplied by the estimated surface area of all rocks within the soil profile. Finally, the weathering rates per unit area of each rock were summed across the entire soil profile. We used the average weathering rate of both the soils after 6 weeks had passed to have an equilibrated weathering rate as studies have found accelerated weathering within the first 20 days of a weathering experiment (Vienne et al., 2022).

2.2.8 Elemental concentration analysis

Total digestions and solution nutrient concentrations were analyzed for macroelements (Ca, Mg, K, Fe, Al, P) using an Agilent 5110 Inductively Coupled Plasma-Optical Emission Spectrometer (ICP-OES; Agilent, Santa Clara, CA, USA). Trace elements (Ce, Cr, Hf, Ta, Ti, Zr) were measured using an Agilent 7900 Inductively Coupled Plasma-Mass Spectrometer. Calibrations were made using a nine-point multi-element standard curve. Every 25 samples a Standard Reference Material (SRM) of GSP-2 granodiorite and BHVO-2 basalt was used to ensure accuracy in measurements. Recovery rates for the granodiorite were within 81 - 105 % of the certified values and were within 83 - 112 % for the basalt. The blanks had less than 0.01 mg/L for all elements analyzed.

2.2.9 Ca and Mg isotope procedure

Total digestions of rock and soil samples were analyzed for Ca and Mg isotopes at Princeton University. Each digest was purified from the silicate matrix using a Thermo Dionex 5000+ ion chromatography system (e.g. Higgins et al., 2018; Blattler et al., 2018). Once ions were separated via ion chromatography and purified, a minimum of 5 µg for Ca and 1 µg for Mg from samples was used for analysis. ^{40}Ca, ^{42}Ca, ^{43}Ca, and ^{44}Ca as well as ^{24}Mg and ^{26}Mg isotopes were measured using a Thermo Fisher Scientific Neptune Plus Multi-Collector Inductively Coupled Plasma-Mass Spectrometer (MC-ICP-MS). To avoid ^{38}ArHH^{+} interference, Mg isotope measurements were at low resolution and Ca at medium resolution. When analyzed, samples were bracketed between standard reference materials (either modern sea water, SRM 88b or SRM 915b) to correct for any mass fractionation from the instrument (Galy et al., 2001).

The Ca isotope composition of each sample were reported using delta notation relative to modern seawater using the following equations:

$$\delta^{44/40}Ca = \left(\frac{^{44/40}Ca_{sample}}{^{44/40}Ca_{seawater}} - 1\right) * 1000 \tag{1}$$

$$\delta^{44/42}Ca = \left(\frac{^{44/42}Ca_{sample}}{^{44/42}Ca_{seawater}} - 1\right) * 1000 \tag{2}$$

$$\delta^{44/42}Ca = \left(\frac{^{44/43}Ca_{sample}}{^{44/43}Ca_{seawater}} - 1\right) * 1000 \tag{3}$$

The Mg isotope composition of each sample were reported using delta notation relative to reference material Dead Sea Magnesium using the following equation:

$$\delta^{26/24}Mg = \left(\frac{^{26/24}Mg_{sample}}{^{26/24}Mg_{DSM-3}} - 1\right) * 1000 \tag{4}$$

The $\delta^{44/40}$Ca value for seawater was 0.00 ± 0.11 ‰ and the $\delta^{44/43}$Ca value was 0.16 ± 0.14 ‰. We report external reproducibility for Ca isotope using measured values of Standard Reference Material 915b and our measured $\delta^{44/40}$Ca value relative to modern seawater was 1.23 ± 0.11 ‰ and $\delta^{44/43}$Ca was 0.12 ± 0.09 ‰ which are similar to publish values (Fantle and Tipper, 2014). Similarly, we report Mg isotopes for long-term reproducibility using Mg standard

Cambridge-1 and modern seawater against the Dead Sea Magnesium (DSM-3). Our measured $\delta^{26/24}$Mg for Cambridge-1 was 2.60 ± 0.14 and for modern seawater 0.81 ± 0.03 which are both similar to published values (Young and Galy, 2004).

2.2.10 Glacial till model calculations

To model the estimated makeup of glacial till at each forest, spatial analyses were conducted using ArcMap Pro (version 3.4). A geographic wedge was delineated and extended 32 km northeast from each forest with a bearing of 151 degrees. The wedge was bounded by azimuth of 181 and 121 degrees to encompass the proposed area for the origin of glacial till. The spatial model included calculating the area occupied by each generalized rock type within each wedge. These calculations were based on a geologic base layer obtained from the United States Geological Survey. The base layer provided detailed classifications on lithologies relevant to the study area, including formations.

2.2.11 Statistical Analyses

To assess the significance in Hf, Ti, and Zr concentrations, we used a mixed effects ANOVA (Type III) with forest nutrient richness and depth as fixed effects and plots as random effects. Post hoc analyses were performed using the Tukey Honest Significant Difference (HSD) test to determine pairwise differences between depths as we were not as concerned about the differences among the forests, just within the profile at each forest. All elemental concentrations were log transformed to meet assumptions of an ANOVA test.

We used a mixed effects model to evaluate differences in weathering rates between rocks and soils across the forest nutrient richness gradient. The fixed effects were the material (Rock and soil), and forest nutrient richness and the random effects were plots to account for inherent heterogeneity. All weathering rates were log transformed to ensure the assumptions of normality and equal variances were met. A Tukey HSD post hoc analysis was used to identify pairwise differences between weathering rates among different rock types, and forest nutrient richness. All statistical analyses were performed using R software (version 4.3) with the “lme4” package for mixed effects modelling and “multcomp” package for post hoc comparisons.

2.3 Results and Discussion

2.3.1 Parent Material

2.3.1.1 Glacial till rock composition

The glacial till wedge model predicted distinct rock composition patterns for each forest (Figure 2.2). According to the model, phyllite was expected to be the most abundant rock type at the Rich forest (67.3%), with minor contributions from quartzite (16.2%), granites (12.3%), and other metamorphic rocks (4.1%). In contrast, the Moderate forest was predicted to have the most diverse glacial till composition that is dominated by quartzite rocks (46.7%), followed by schists (13.2%), basalt (13.1%), other metamorphic (11.0%) which include granofels and metatclastic rocks, Tuff (10.4%), phyllite (4.5%), gabbro (1.0%) and minimal granites (0.1%). The Poor forest was predicted to have the highest proportion of granites (70.1%), along with smaller amounts of quartzite (21.4%), other metamorphic rocks (6.4%), schists (1.1%), tuff (0.9%), and gabbro (0.1%).

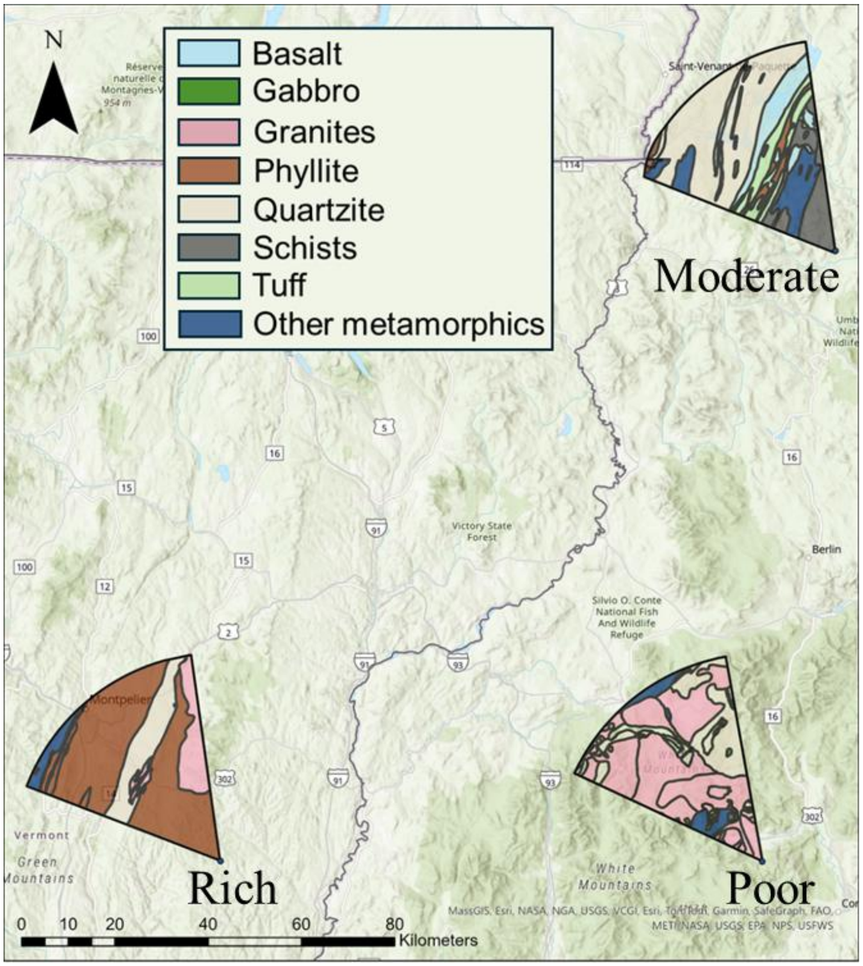

Figure 2.2. Location of the three forests with wedge shaped areas highlighting the expected source of glacial till from the northeast at each forest. The geological data are simplified from Lyons et al., 1997.

When comparing the predicted rock composition to the rocks identified from the soil pits at each forest, we found that the glacial till model captured major trends in dominant rock types but underestimated the diversity of rock compositions at all sites (Figure 2.3). At the Rich forest, the observed rock composition was dominated by quartzite (67.5%), with lesser amounts of schists (18.4%), granites (6.1%), basalt (3.5%), phyllite (2.6%), gabbro (0.9%), and shale (0.9%). This finding contrasts with the model prediction, which identified phyllite as the dominant rock type. Similarly, the Moderate forest had the highest diversity in rock types with quartzite (60.9%) as the most abundant, followed by gneiss (12.7%), phyllite (11.8%), schists (4.5%), basalt (2.7%), shale (2.7%), and gabbro (1.8%). At the Poor forest, as expected, granites dominated (79.3%) the glacial till, followed by basalt (10%), tuff (4.3%), quartzite (3.6%), gabbro (1.4%), gneiss (0.7%), and phyllite (0.7%). Notably, 92% of the rocks in the Moderate forest were derived from local bedrock sources, while the Poor forest had the lowest proportion of local rocks (82%), indicating greater contributions from exogenous sources. The high local bedrock source at the Moderate site may also be attributed to the wide range of rocks present in the Aziscohos formation which ranges from shales and low grade metamorphic rocks to high grade schists while the Conway granite and local areas are dominated by granite, improving the identification of non-locally sourced rocks. Despite this limitation, our results highlight that exogenous sourcing was not the dominant source of glacial till and we provide an estimate from fifteen soil pits. Across all forests, common exogenous rock types included basalt, gabbro, and siltstone with variability depending on the forest.

The discrepancies between the predicted and observed compositions highlight the complexity of glacial till deposition. We found that the glacial till model underestimated the diversity in the rock types found at each forest and these results align with another study using this model (Bailey and Hornbeck, 1992). Specifically, quartzite was a major rock type observed at two of the three forests but was not a dominant rock type in the glacial till model, mainly because it is not a common major rock type but is a common secondary rock type in the bedrock formations (Bennett et al., 2006; Ratcliffe et al., 2011). Our results suggest that while the model is useful for identifying broad compositional trends, site-specific variability is important and the model does not account for secondary rock types which seem to dominate compositionally.

The influence of locally-sourced and exogenous rocks played a key role in shaping the observed glacial till composition. Across all three forests, the predominance of local bedrock derived rocks suggests that glacial till composition at these sites is primarily controlled by local sources, which influences the soil mineralogy and nutrient availability of each site (Grasby et al., 2010). However, the Poor forest which was located the furthest east along the glacial flow path had the highest proportion of exogenous rocks. This pattern supports the idea that glacial movement progressively introduces more distant lithologies, particularly as ice flow extends further from its source areas (Clark, 1987). These results align with previous research that show that glacial till is a heterogeneous mix of rock types that reflects complex depositional histories (Boulton and Paul, 1976; Evans, 2017). Our results suggest that even though glacial transport increases the heterogeneity of the glacial till, the dominant rock types in forest soils are strongly tied to local bedrock formations rather than being dominated by distant, exogenous sources. This reinforces the role of the underlying bedrock, even in post-glaciated regions, as a primary control on soil properties and nutrient availability.

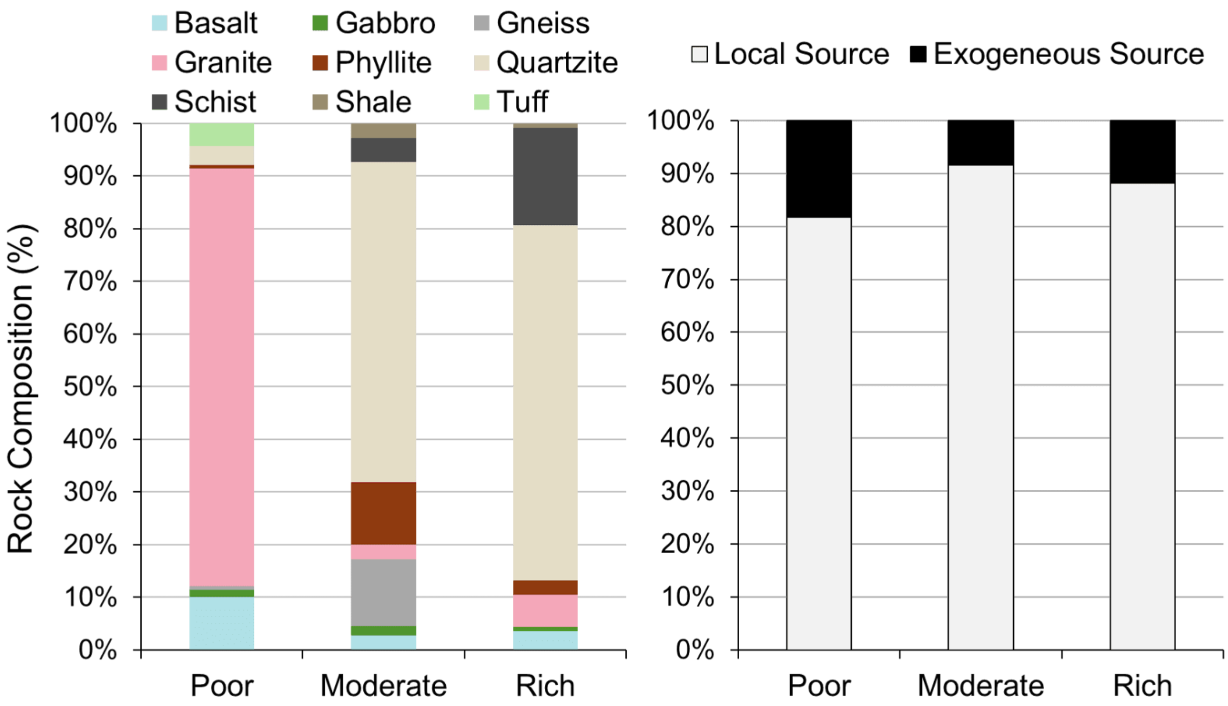

Figure 2.3. Distribution of rock types and source composition across the nutrient richness gradient. Each bar represents the proportion of the total rock count for each rock type.

2.3.1.2 Glaciofluvial and potential loess reworking

Glaciofluvial materials can influence nutrient inputs in forest soils and therefore it is essential to assess their presence when identifying nutrient sources in an ecosystem. To evaluate potential loess deposition, we first analyzed the distribution of particle sizes with depth within soil profiles along the forest nutrient richness gradient (Figure 2.4). We found that silt (2-50 μm) slightly decreased throughout the soil profile at the Rich and Poor forests. The Rich forest had 61% silt near the surface, the middle of the profile 56% and the deepest depth 51%. At the Poor forest, there was also a steady decline in silt content throughout the soil profile from 65% near the surface and 53% at the deepest sample. In contrast, at the Moderate forest silt content was stable (76% at surface to 74% in middle) until it increased at the deepest depth (85%). The distribution of silt content among the three forests is similar to other studies from the region (Norouzi-Moghanjoghi et al., 2025). These results indicate that loess deposition is unlikely to be an important factor influencing soil nutrients at these forests since the percentage remained relatively constant throughout the soil profiles.

The amount of sand (50 µm-2 mm) present within the soil profile provides insights into energy dynamics of sediment deposition and the weathering processes of glaciofluvial parent materials (Figure 2.4). Our results show that sand content varied between surface and deeper horizons at the three forests. At the Rich and Poor forests, sand content was lowest near the surface (39% and 35%, respectively) and increased to the deepest depth (49% and 47%, respectively). This trend suggests that the parent material originally contained more sand, but surface weathering processes, such as mineral dissolution and physical breakdown have reduced sand content over time and increased silt content. The acidic environment of the forest soil through breakdown of organic matter most likely enhanced chemical weathering of silicate minerals, leading to a relative increase in finer particles like silt and clay at the surface (Jobbagy and Jackson, 2001). On the contrary, the Moderate forest sand content decreased from 24% at the surface to 15% at the deepest depth. This pattern suggests that eluviation may have occurred at this forest, where silt and clay were translocated from the near surface horizons to deeper in the profile which would concentrate courses materials near the surface (Phillips, 2007; Warrington et al., 2007). It is also possible that biological activity and soil mixing have brought sand to the surface while redistributing finer particles to deeper horizons which would alter the vertical distribution of soil texture over time and match what we are seeing (Jobbagy and Jackson, 2001). These data and explanations suggest that parent material may be uniform at each forest without the influence of loess deposits.

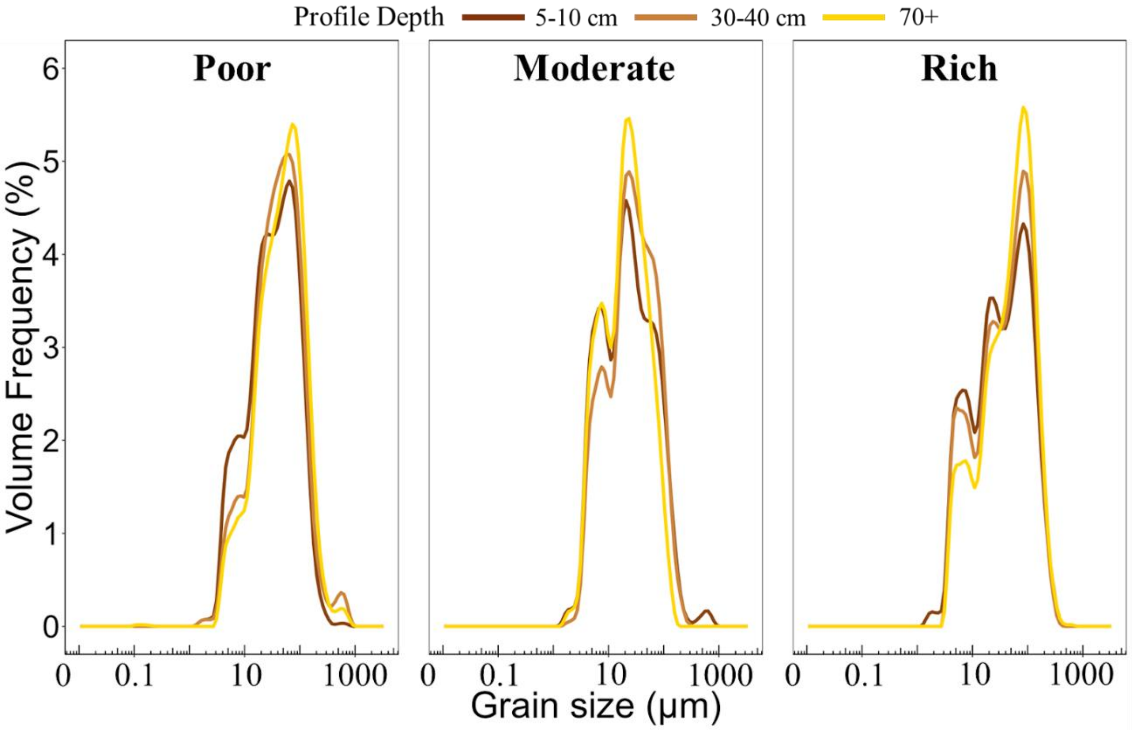

Figure 2.4. Distribution of silt size particles across depths within each forest nutrient richness. The colors are different depths within the soil profile.

To further evaluate the presence of glaciofluvial redeposited/reworked material, we examined the concentrations of immobile elements (Hf, Ti, and Zr) within the soil profiles (Figure 2.5). We found no evidence of silt influence throughout any of the soil profiles across the forest nutrient richness gradient since there were no significant differences with depth ($p > 0.11$). However, the forest nutrient richness had significant differences in elemental concentrations ($p < 0.01$). The Rich forest had the highest concentrations of Hf ($p < 0.01$) and Zr ($p < 0.01$), but the lowest Ti ($p < 0.01$). In contrast, the Poor forest had the lowest Hf ($p < 0.01$) and Zr concentrations ($p < 0.01$), with intermediate Ti concentrations ($p < 0.01$). The range of Ti concentrations for our study fall within the range found in soils across the United States (Burt et al., 2003; Johnson et al., 2004). The range of Hf concentrations are similar to other studies that evaluated several soil profiles (Waroszewski et al., 2019; Kowalska et al., 2022). The range of Zr concentrations is comparable to other studies looking at the distribution of Zr throughout several soil profiles (Braun et al., 2005; Waroszewski et al., 2019). Waroszewski et al. (2019) concluded that decreasing Hf and Zr concentrations corresponding with elevated silt proportions indicated loess deposits. Our results did not show decreasing Hf and Zr concentrations nor higher silt proportions within the upper soil profile, suggesting limited loess deposition. These results further support our conclusion that loess deposits are not contributing to soil nutrient dynamics in these forests.

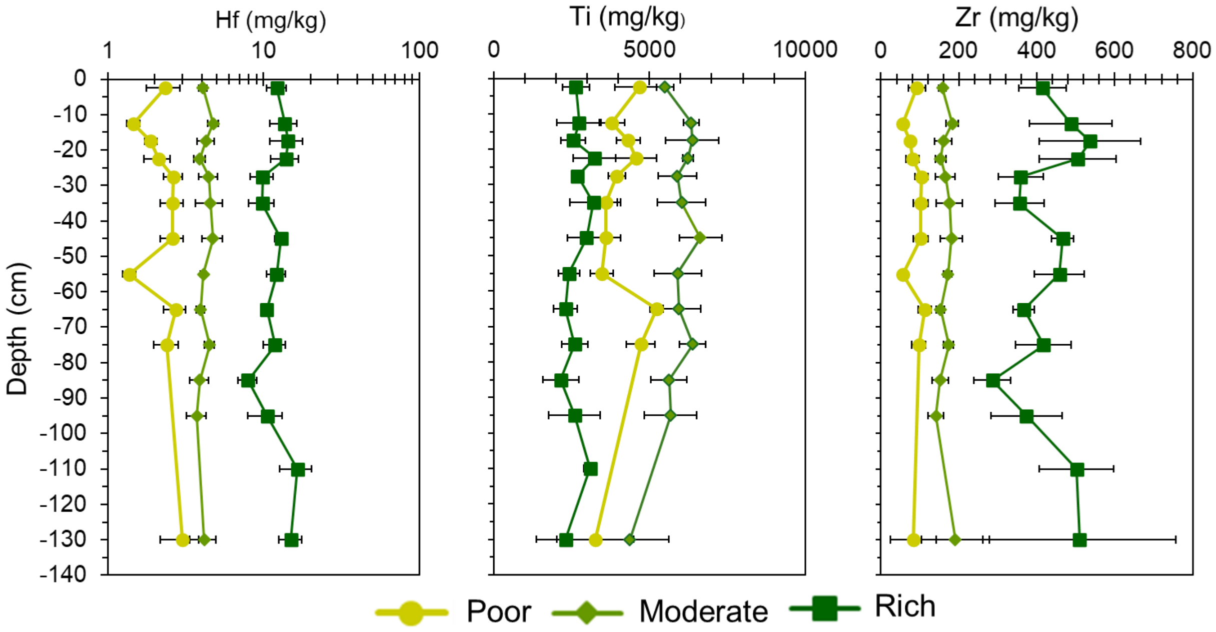

Figure 2.5. Concentrations of immobile elements (Hf, Ti, and Zr) throughout the soil profile of each forest nutrient richness. Each point represents the average for that depth with bars representing standard error.

Next, we examined the geochemistry of the soils using immobile elements (Hf, Ti, Zr) and rare earth elements (Ce, Ta) which can identify different soil materials based upon their elemental composition due to differences in mineralogical composition and extent of chemical weathering (Figure 2.6). The Poor and Moderate forest soils appear to be primarily derived from the glacial till rocks present at these forests. However, in the Poor forest the soils and rocks plotted separately, suggesting a different source contribution. Comparing soil and rock values, we found strong similarities in Ti/Zr and Ce/Ta ratios, with 100% of Moderate and Rich forest soils and 80% of Poor forest soils falling within rock derived values. Soil Ti/Zr ratios ranged from 6.20 to 213 mol/mol and 1.92 to 242 mol/mol in rocks, while Ce/Ta ratios ranged from 10.3 to 143 mol/mol in soils and 1.55 to 175 mol/mol in rocks. The range for Ti/Zr is comparable to other studies in similar climates (Kowalska et al., 2022). The soil was relatively similar to rock values in Cr/Zr and Ta/Zr at the Poor (77%) and Moderate (76%) forests whereas 0% were similar at the Rich forest. Soil Cr/Zr values ranged from 0.03 to 3.10 mol/mol, while rock values ranged from 0.11 to 14.5 mol/mol. Soil Ta/Zr ranged from 2 to 21 mol/mol, and rock values ranged from 2 to 138 mol/mol. The Cr/Zr and Ta/Zr ratios in our study fall in line with similar reports in the northeastern United States (Munroe et al., 2007). The Zr to Hf ratios had the highest soil to rock correlation at the Moderate forest (91%), followed by the Poor forest (34%), while the Rich forest showed no correlation. Soil Zr concentrations ranged from 33.2 to 1135 mg/kg, compared to 4.0 to 449 mg/kg in rocks, whereas soil Hf concentrations ranged from 0.93 to 31.7 mg/kg and rock values ranged from 0.1 to 22.2 mg/kg. The immobile elements and REEs show that soils within the Poor and Moderate sites generally match the glacial till rocks present, with some variation due to soil genesis. However, the immobile elements and REEs for the Rich forest show that the soils strongly contrast from the glacial till which suggests that the soils are not sourced from the weathering of the dominant rock types, but rather from a non-dominant rock type.

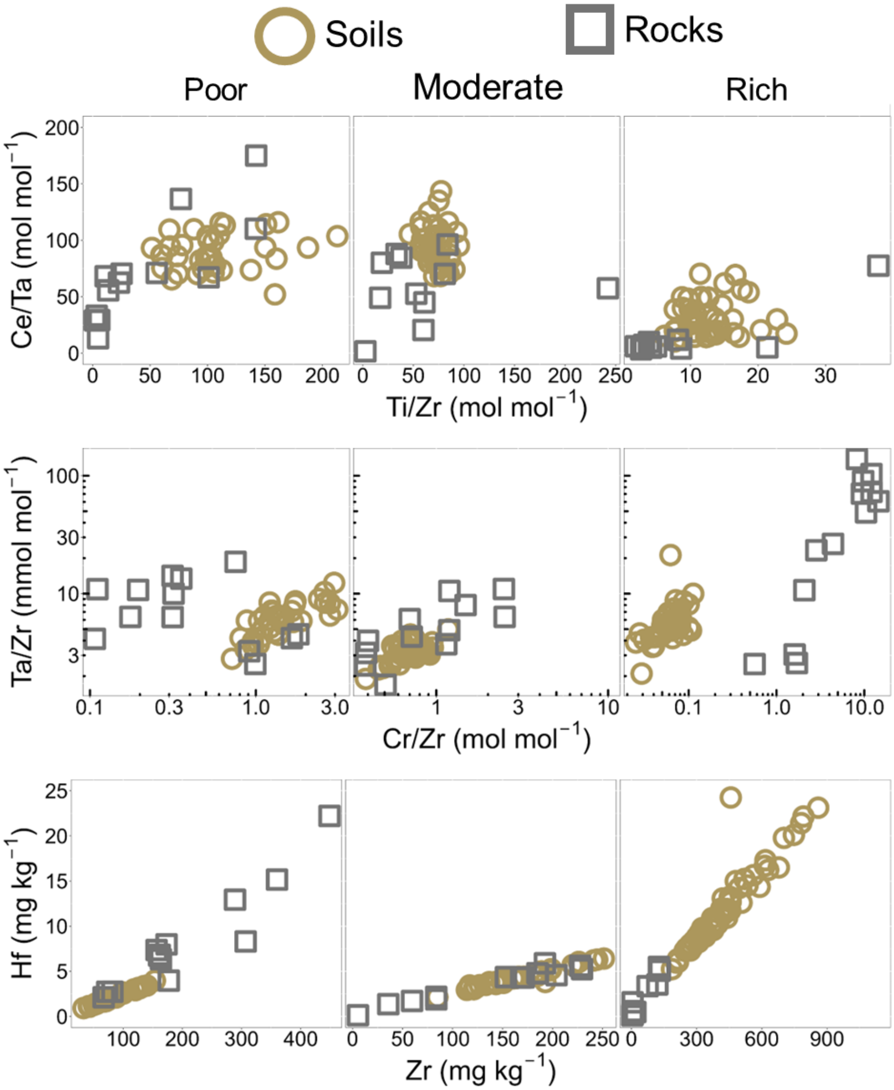

Figure 2.6. Comparison of trace element geochemistry of dominant soil parent material rock with overlying soil at each site. At the Poor forest we analyzed 35 soils and 13 rocks, at the Moderate forest 45 soils and 13 rocks, and at the Rich forest 58 soils and 13 rocks.

We evaluated the $\delta^{44/40}$Ca, $\delta^{44/43}$Ca and $\delta^{26/24}$Mg of the rocks and soil to assess the potential rock sources in glacial till contributing to soil formation across the forest nutrient richness gradient (Figure 2.7). Our isotopic analysis of $\delta^{44/40}$Ca vs $\delta^{26/24}$Mg and $\delta^{44/40}$Ca vs $\delta^{44/42}$Ca indicates that the soil at the Poor and Moderate forests are predominantly derived from the major rock types present in the glacial till, whereas the Rich forest must have additional inputs beyond these local lithologies. Mg isotopes proved to be a stronger tracer of parent material than Ca isotopes, likely due to the abundance of Mg relative to Ca in both the parent material and soils (Rice et al., 2024). At the Poor forest, $\delta^{44/40}$Ca had a wide range in values with the deeper soils plotting closest to the granite. Similarly, $\delta^{26/24}$Mg values in the middle and deep depths are also aligned with granite, suggesting that soil development in this forest is primarily influenced by granite derived material. However, in the 5-10 cm depth, $\delta^{26/24}$Mg deviates from the expected granite signature, suggesting an additional influence such as mixing with another source, differential weathering, or preferential uptake of isotopes by vegetation (Zhao et al., 2020; Ryu et al., 2016). The $\delta^{44/40}$Ca vs $\delta^{44/43}$Ca relationship further supports this, as soils were isotopically similar to the granite. At the Moderate forest, $\delta^{44/40}$Ca values were relatively stable with less variation compared to the Poor forest. The $\delta^{26/24}$Mg values positioned soils between the schist and quartzite, indicate that the soil is derived from a combination of the two rock types. This trend was further supported by the $\delta^{44/40}$Ca vs $\delta^{44/43}$Ca plots, where soils aligned with schist and in some cases plotted between schist and quartzite. Conversely, at the Rich forest, soil isotopic compositions did not match those of the dominant rock types in the glacial till which suggests that there may be another source of Ca and Mg to the soils. Since our analysis was limited to the primary lithologies present at each first, it is possible that a less abundant but geochemically significant rock type contributed to the soil composition but was not captured in our dataset. Additionally, post deposition processes such as weathering and biological cycling can fractionate the isotopes, further altering their signatures from those of the original parent material (Page et al., 2008; Schmitt et al., 2017).

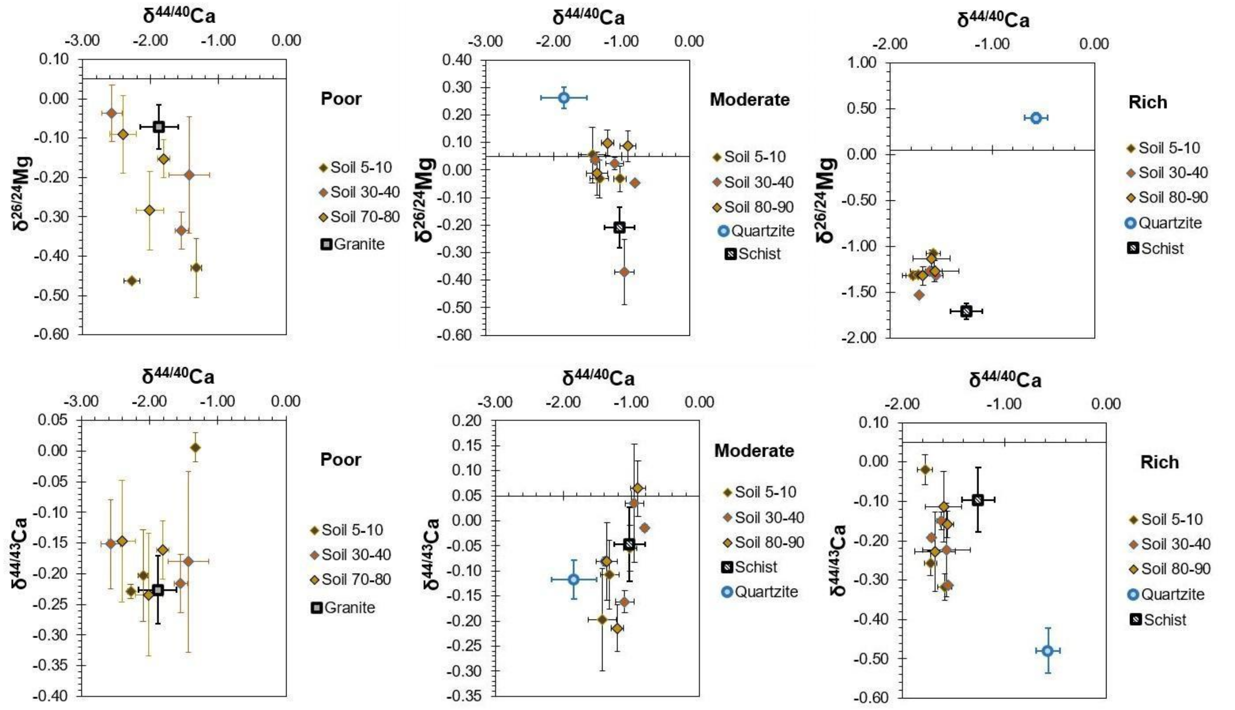

Figure 2.7. Relationship between $\delta^{44/40}$Ca, $\delta 2^{6/24}$Mg (top row), and $\delta^{44/40}$Ca, $\delta^{44/43}$Ca (bottom row) across forest nutrient richness. Symbols represent different soil depths and glacial till rocks. Points represent the mean and bars represent standard error.

Overall, our findings for particle size, immobile elements, REES, Ca isotopes, and Mg isotopes data indicate that loess is not a significant contributor to soil formation across these forests and therefore reinforces the premise that glacial till serves as the dominant parent material. Further supporting this, the soil composition reflects glacial till-derived materials with the Poor and Moderate forests having similar geochemical signatures to the parent material rocks. In contrast, the Rich forest soils had the greatest divergence from rock signatures which indicates that the soils are not derived from the glacial till but rather from glaciofluvial reworking of material and moving them down slope at this forest. With the lack of abundance and stratification of silt within these soil profiles, our results suggest that the soils at the Poor and Moderate forest are derived mainly from the local glacial till sources, whereas the Rich forest has undergone more reworking of the soil and therefore does not correlate to any rock geochemical signature. Collectively these results highlight the sources of Ca and Mg in these while also highlighting the complexity of soil formation processes across the nutrient richness gradient.

2.3.2 Soil and rock nutrient pools

2.3.2.1 glacial till rock and soil bulk reservoirs

Understanding the reservoir of nutrients within the soil is critical for assessing overall nutrient status and identifying where nutrients are stored. We evaluated inorganic nutrients (Ca, Mg, K, Fe, Al, P) pools in both soils and rocks within the top 1 m of the soil profile across a nutrient richness gradient. In our analysis, the soil nutrient pool refers to all nutrients within the < 2 mm fraction while the rock nutrient pools refer to all nutrients within the > 2 mm fraction. Many of these nutrients are within aluminosilicates and unavailable to plant uptake in their current state (Rice et al., 2024).

Soil nutrient pools varied widely across the forests with Ca ranging from 2,650 to 15,600 g/m^2, Mg from 1,350 to 31,900 g/m^2, and K from 5,200 to 13,100 g/m^2 (Figure 2.8). Phosphorus had the smallest pool, ranging from 507 to 1,325 g/m^2. Our soil nutrient pool values are about twice as high as reported nutrient pools in the region (Johnson and Todd, 1998); however, this difference is most likely due to their sampling methods. Johnson and Tood (1998) report Ca, Mg, K, and P pools to a depth of 45 cm, if doubled, their values would be comparable to ours. Our results indicate that, across all forests, soil represented the largest reservoir of inorganic nutrients (Figure 2.8). Surprisingly, the Poor forest had the largest rock associated pools of Ca, Mg, K, and P among the three forests despite the dominant rock type, granite, being relatively poor in these nutrients. In contrast, soil nutrient pools of Mg, Fe, and Al closely followed the nutrient richness gradient with the smallest pool observed at the Poor forest and the largest at the Rich forest.

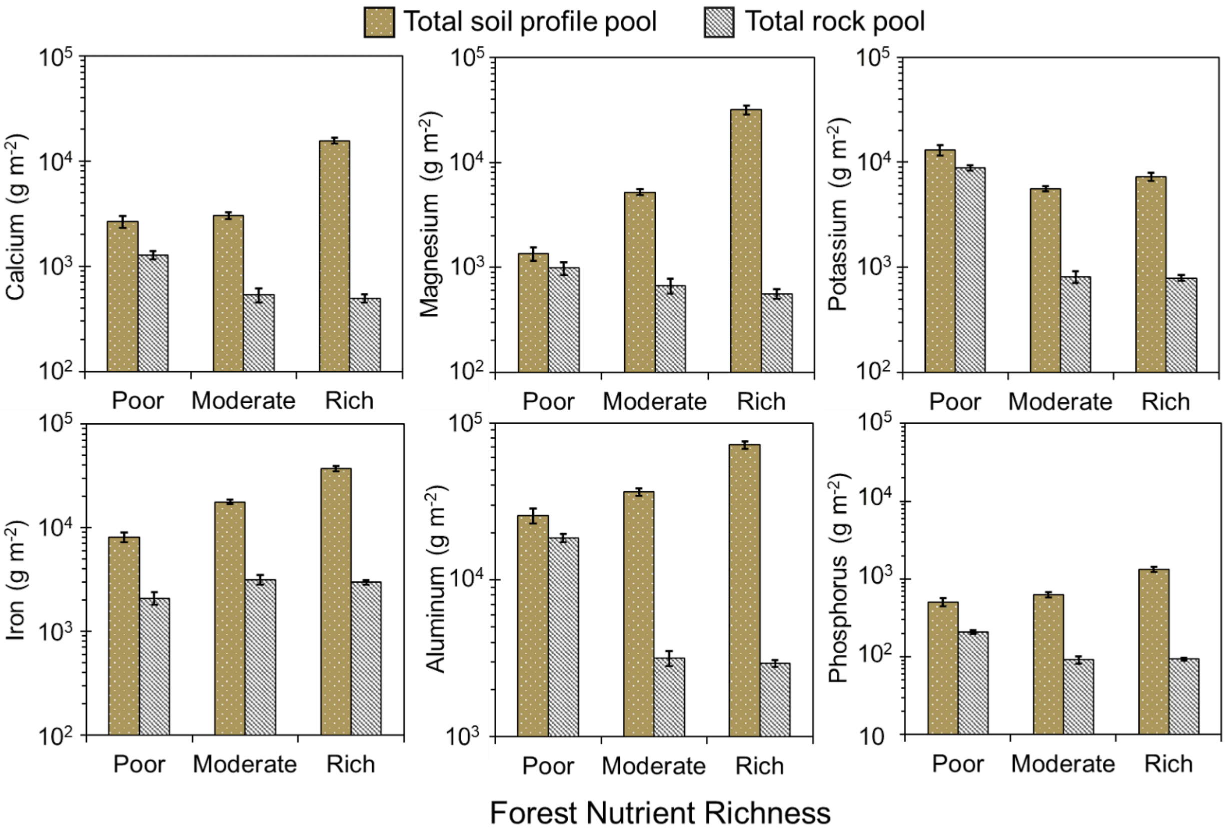

Figure 2.8. Comparison of inorganic nutrients in the total soil profile (everything < 2 mm) and the total rock pool (everything > 2 mm). Bars represent the average weathering rate across the forest nutrient richness gradient and error bars are standard error.

The magnitude of difference between soil and rock nutrient pools was also dependent on soil nutrient richness. The Poor forest had the most similar soil and rock nutrient pools, while the difference between the pools progressively increased from the Moderate forest to the Rich forest. It is possible that we underestimated the rock nutrient pool because these values are calculated for the top 1 m of the soil but does not account for the rock pool in the glacial till parent material that can range from 1 to 100 meters thick depending on location. For this reason, calculating the nutrient pools of rocks in the soil profile is difficult and no other study in the region has reported on these values for comparisons.

Despite the inherently low nutrient content of granite, the Poor forest had the highest pools of Ca, Mg, K, and P in rocks. This may be due to there being more rocks at the Poor forest (0.29 g/cm^3) than the Moderate (0.12 g/cm^3) and Rich (0.09 g/cm^3) forests so when scaled up, the pool is high despite the lack of nutrients in the rock itself. Surprisingly, the large quantity of rocks within the soil profile at the Poor forest did not cause the soil nutrient pools to be vastly smaller than the rock nutrient pools and in fact were comparable for several elements (Mg and K).

2.3.3.2 Rock vs soil release rates

Quantifying weathering rates is essential for understanding nutrient replenishment in soils and their role in sustaining ecosystem productivity. Our laboratory experiments revealed that soils had significantly higher weathering rates for Ca, Mg, K, Fe, Al, and P compared to their respective parent material rocks (Figure 2.9). This suggests that soil formation processes such as mineral dissolution, secondary mineral formations and biological interactions can enhance nutrient release rates beyond what is released from rocks in the area. However, contrary to previous studies, our work demonstrates that the rock weathering releases within the soil profile were not always negligible and could represent up to 18% of the Ca soil weathering rate.

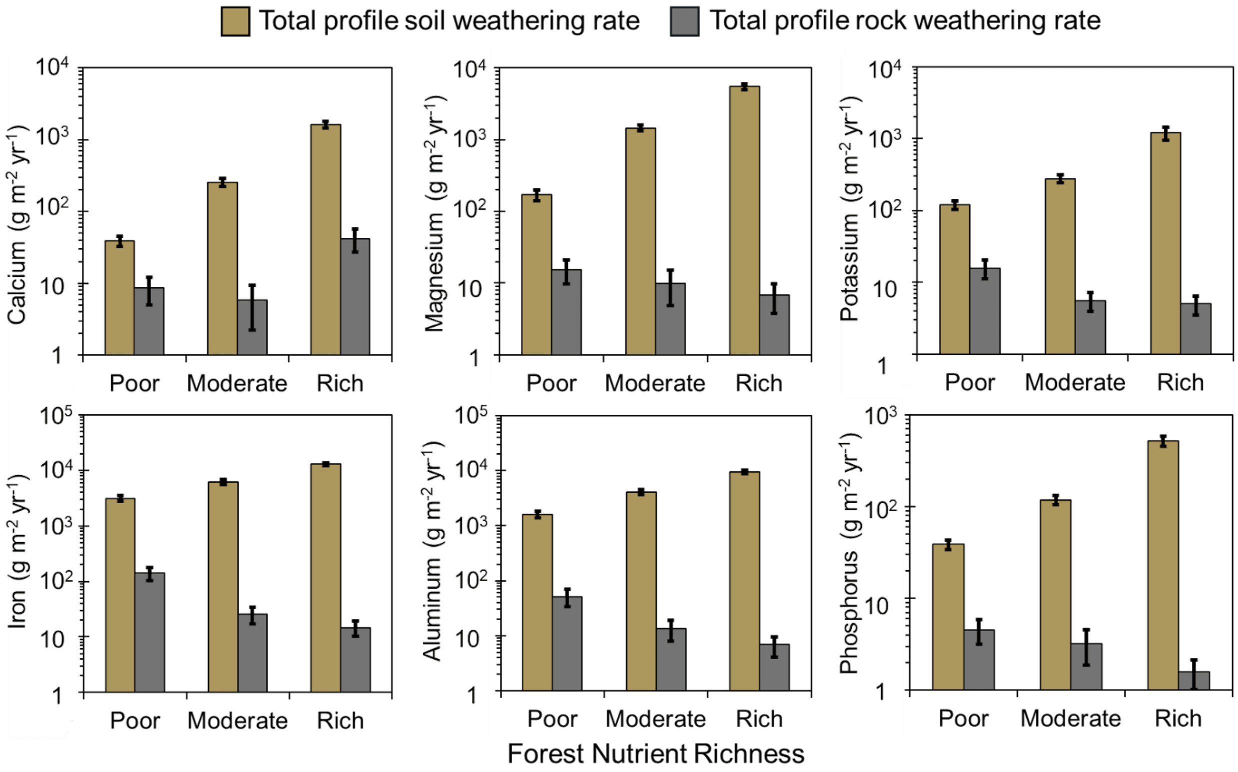

Figure 2.9. The weathering rates of inorganic elements (Ca, Mg, K, Fe, Al, P) from soil and rocks within the soil profile. The units are mass of element, per unit area of the soil profile, scaled per year. Weathering rates are averaged by forest nutrient richness and error bars represent standard error.

Additionally, soil nutrient release rates followed the nutrient richness gradient with the Poor forest having the lowest rates and the Rich forest the highest. This pattern suggests that soils at the Rich forest have undergone greater degrees of weathering likely due to organic acids from decomposition, microbial activity, and root exudates which have accelerated mineral breakdown and nutrient mobilization from the rocks into soil (Landeweert et al., 2001; Vitousek et al., 2003). These results support the idea that soils act as a dynamic system where organic inputs and microbial activity are continuously altering the mineral and nutrient availability in the soil (Berner, 2004).

Rock weathering rates were 1 to 2 orders of magnitude lower and did not follow the nutrient richness gradient unlike soils. Surprisingly, the Rich forest had the lowest rock nutrient weathering rates for all elements except Ca. The elevated Ca weathering rates in the Rich forest rocks suggests the presence of Ca bearing minerals which are more readily weathered in acidic conditions (Brantley, 2008). The rock formations that the rocks at the Rich forest are derived from, the Waites River formation, are composed of Ca rich dolomite, which could be the reason the rocks at this forest have higher Ca weathering rates. The lower weathering rates of other elements in the Rich forest rocks indicate that the parent material consists of more recalcitrant silicate minerals such as quartz and feldspars (Wilson, 2004).

The significant difference between soil and rock weathering rates highlights the role of mineralogy and biotic processes in driving soil development and nutrient availability. While the glacial till composition establishes the initial nutrient supply, our results suggest that pedogenic and biological processes play a significant role in long term soil fertility than parent material alone (Vitousek et al., 2003). The formation of secondary minerals such as clays and hydroxides can influence the retention and availability of nutrients and may be the reason that the weathering rates of soils were higher than the rocks (Brantley, 2008). Similarly, since we added organic acid to the weathering solution, these were to simulate the acids that plants release, which enhance mineral dissolution by chelating metal cations and destabilizing mineral lattices (Hinsinger, 1998; Landeweert et al., 2001).

2.3.3 Rock nutrient abundance and release rates

Quantifying the mineral abundances of rocks allows us to identify the source of inorganic elements to soils. The mineral abundances determined by X-ray diffraction (XRD) revealed distinct compositional differences in dominant rocks among parent materials across the forest nutrient richness gradient (Table 2.1). Quartz content ranged from 5.8 % in rocks at the Poor forest to 27.9% at the Rich forest, increasing progressively from the Poor to Rich forest. This suggests that the more nutrient-rich parent materials at the Poor forest contain a higher proportion of quartz which is resistant to weathering and contributes very little to nutrient availability (Morris and Fletcher, 1987; Wray and Sauro, 2017). The Moderate and Rich forest rocks also contained a large amount of oligoclase and albite whereas oligoclase was absent in the Rich forest rocks. Albite was the dominant feldspar in the Poor forest rocks but was lower in the Moderate and Rich forest rocks. The dominance of albite in the Poor forest rocks combined with the Poor forest having the highest weathering rates for all inorganic elements suggests that feldspars are the main source of these elements despite albite and oligoclase being weather resistant (Chou and Wollast, 1984; Berner et al., 2003). The mineralogical maps further support these compositional differences as these maps show that the Poor forest rocks are dominated by biotite which is a K and Mg bearing mineral (Figure 2.10). The Moderate forest rocks have a more diverse mineralogy, with a large presence of biotite, plagioclase, and hornblende. In contrast, the Rich forest rocks contain high amounts of orthoclase, quartz, and kaolinite which indicate that this site has undergone more advanced weathering.

Table 2.1. Mineral abundances for dominant rock types by X-Ray Diffraction. Three dominant rock types from each forest nutrient class were powdered and analyzed. Standard errors among the three rocks are presented. Totals may be greater than 100% due to variation in mineral composition among rocks. LOQ for XRD is 0.5 to 2% depending on mineral types and peak overlaps.

Mineral Phases	***Bulk Mineral Abundance of Parent Material (%)***		
	Poor	**Moderate**	**Rich**
Quartz	5.8 (0.3)	19.6 (0.4)	27.9 (1.6)
Oligoclase	18.5 (0.6)	27.0 (0.9)	-
Albite	57.7 (0.6)	17.3 (0.7)	19.7 (0.8)
Hornblende	-	25.9 (0.7)	-
Richterite	10.7 (0.6)	-	15.4 (1.3)
Biotite	7.3 (0.5)	4.7 (0.2)	6.7 (0.8)
Chlorite	-	4.5 (0.6)	16.6 (0.5)
Muscovite	-	1.1 (0.1)	-
Kaolinite	-	-	1.3 (10)
Calcite	-	-	11.4 (4)

The rocks at the Moderate forest had a high hornblende content (25.9%), whereas the Poor and Rich forest rocks did not have hornblende. Hornblende is a key source of Ca, Mg, and Fe and is relatively susceptible to weathering (Wallander and Wickman, 1999). The mineral maps confirm this trend (Figure 2.10), showing a widespread distribution of hornblende in the Moderate forest rock with no presence in the rocks of the Poor or Rich forests. The presence of richterite in both the rocks at the Poor (10.7%) and Rich (15.4%) but not in the Moderate forest rocks suggests metamorphic processes have occurred at these forests. Biotite was found in rocks at all three forests, ranging from 4.7% to 7.3%, however, there was no trend in forest nutrient richness. The presence of chlorite followed the nutrient richness gradient, with no presence at the Poor forest, 4.5% at the Moderate forest and 16.6% at the Rich forest. Since chlorite is a secondary mineral commonly derived from the weathering of biotite and followed the nutrient richness gradient, this suggests that there may be a progressive increase in in-situ weathering rates across the gradient, with the most favorable weathering conditions at the Rich forest. Muscovite was only at the Moderate forest rocks and in a low amount (1.1%). The presence of muscovite indicates that either albite and oligoclase have undergone weathering to form these minerals or that metamorphic processes have transformed biotite weathered to form these minerals or that metamorphic processes occurred transforming biotite (Wallander and Wickman, 1999).

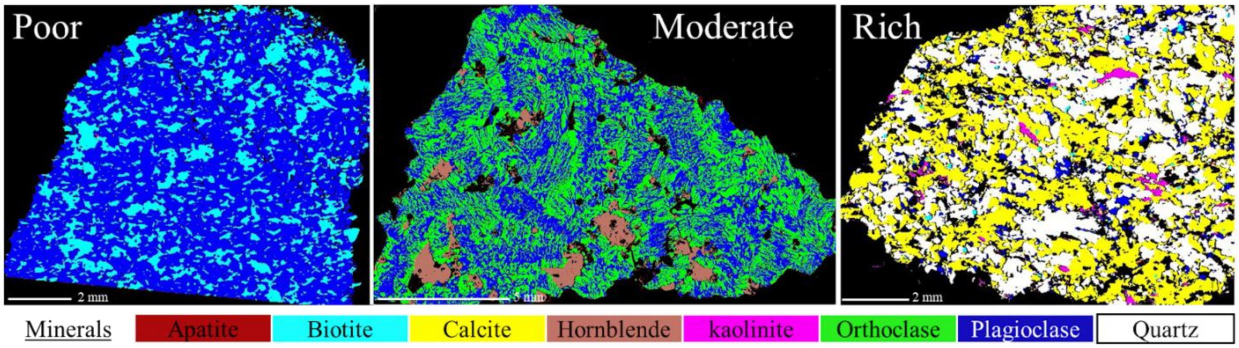

Figure 2.10. Electron microprobe image of mineral assemblage and distribution throughout unweathered pieces of dominant rocks across the forest nutrient richness gradient. Color mineral maps were created for key minerals.

Calcite was only present in rocks at the Rich forest (11.4 %) which indicates that this region had carbonate-bearing lithologies such as limestone or marble. Carbonate rich rocks tend to buffer acidic conditions and enhance the preservation of silicate minerals (Wilson, 2004). The mineralogical maps confirm this by showing a strong presence of calcite in the Rich forest rocks (Figure 2.10). Additionally, kaolinite, which is derived from the weathering of aluminosilicate minerals, was only found in rocks at the Rich forest (1.3%). The presence of kaolinite further supports that there is more advanced weathering in the region of the Rich forest than the other two.

The variations in mineral composition among the three forests provide valuable insight into the potential weathering behavior and contributions to soil mineralogy. The Poor forest was dominated by albite which supports why these soils are nutrient poor since albite is relatively nutrient poor and resistant to weathering (Chou and Wollast, 1984; Wollast and Chou, 1992). The rocks at the Moderate forest were abundant in hornblende and oligoclase which are more susceptible to weathering than albite, making them key sources of Ca and Mg to soils (Zhang et al., 1996). The rocks at the Rich forest had a high abundance of quartz, chlorite, calcite, and kaolinite which likely contribute to the high concentrations of nutrients in the soil at the Rich forest (Rice et al., 2024). The mineralogical maps further support these compositional differences among the three forests and provide spatial context for how different minerals contribute to nutrient availability across the gradient.

Our findings align with previous research defining the influence of parent material rock composition on geochemical cycling and long-term soil development (Jenny, 1941; Chadwick et al., 1999). The presence of calcite and secondary minerals at the Rich forest suggests that this forest may have the greatest capacity for sustaining long-term soil Ca and Mg through weathering. While the dominance of feldspars at the Poor forest may lead to prolonged nutrient release rates, the quantity of nutrient available for plant uptake remains relatively low (Rice et al., 2024).

The weathering rates of inorganic nutrients varied significantly among rock types with distinct differences between soils and parent material rocks. While rocks generally had higher weathering rates, P had an inverse trend suggesting strong biological controls on its mobilization. Specifically, rocks had higher Ca weathering rates than soils ($p < 0.01$). This aligns with prior findings that Ca is more readily weathered from carbonate minerals such as calcite than silicate minerals (White and Blum, 1995; Brantley, 2008; Nezat et al., 2008). However, the weathering rates in the rocks compared to the soils could be due to the rocks being powdered, which increases the surface area available for chemical reaction and exposes minerals typically armored by other minerals in the rock, therefore enhancing the dissolution rate observed in laboratory studies (Power et al., 2025). The high Ca weathering rate in quartzite was unexpected as quartzite is largely composed of silica with minimal Ca-bearing minerals. However, in this region quartzite could be derived from Waits River formation which is a calcareous rich formation composed largely of granulite. During the quartzite intrusion, it is likely that some Ca from the dolomite mixed in which would explain the unexpectedly high Ca weathering rates (Hatch et al., 1988; Stone and Dennis, 1964). The lowest Ca weathering rates were in schist rocks ($p < 0.01$). The Poor and Rich forest soils were significantly different in Ca weathering rates for all rock types ($p < 0.01$) whereas the Moderate forest soils were more similar to schist ($p = 0.86$).

Similar to Ca, Mg weathering rates were significantly higher in rocks than in soils ($p < 0.01$). Gabbro had the highest Mg weathering rate ($p < 0.01$) and granite the lowest ($p < 0.01$). The Moderate forest soils had comparable Mg weathering rates to schist ($p = 1.0$) while the Rich forest soils had comparable weathering rates to gneiss (p = 0.94). The Poor forest soils were more similar to granite (p = 1.0). These results are consistent with studies showing that Mg is primarily released from mafic and intermediate silicate minerals such as biotite and pyroxenes which are abundant in gabbro and gneiss (Dorais et al., 2001). The similarities in weathering rates between soils and specific rock types suggest that local soil formation is primarily derived from in-situ rock weathering rather than influenced by transported exogenous materials.

The weathering rates of K followed the same trend as Ca and Mg, with rocks having higher K weathering rates than soils ($p < 0.01$). Gabbro had the highest K weathering rate ($p < 0.01$) and lowest was in quartzite ($p < 0.01$). Quartzite had comparable K weathering rates as the soil at the Moderate ($p = 0.92$) and Rich forests ($p = 0.10$). Potassium is primarily released from orthoclase and micas which are abundant in granitic and metamorphic rocks. The lower mobility of K in soils is due to its strong retention by clay minerals, and adsorption onto organic matter (Hinsinger, 1998).

Unlike the other elements, Al weathering rates did not differ significantly between soils and rock types (p =0.71) but there were differences among the rock types ($p < 0.01$). Gabbro had the highest Al weathering rates compared to all other rock types ($p < 0.01$), whereas quartzite had the lowest ($p < 0.01$). The low weathering rate for quartzite is expected due to its lack of aluminosilicate minerals. In contrast, Al weathering in gabbro is primarily due to the breakdown of plagioclase and mafic minerals, which contribute to Al rich secondary clays and hydroxides (Brantley, 2008). These clays and hydroxides can act as buffering mechanisms that limit further Al release which potentially explains why Al weathering rates were similar between soils and rocks. This suggests that the primary controls on Al mobility are mineral composition and dissolution kinetics, rather than soil development processes such as organic complexation, microbial activity or changes in soil pH.

Unlike the other inorganic nutrients, P had higher weathering rates in soils compared to rocks ($p < 0.01$). Because soil P weathering rates were much higher than those of rocks, unlike the other elements, the soil P weathering rates do not correlate directly with a specific rock weathering rate. Among the rock types, gabbro had the highest P weathering rates ($p < 0.01$), comparable to gneiss ($p = 0.05$), while quartzite had the lowest ($p < 0.01$). The significantly higher P weathering rates in soil suggest that biological processes such as organic input and root exudation have played a dominant role in mobilizing P over time. These results suggest that P has overtime been influenced in the soil via biological inputs such as roots. Studies have found that mycorrhizal fungi and plant root exudates can enhance dissolution of P bearing minerals by releasing organic acids that chelate metal cations and increase P solubility (Landeweert et al., 2001; Nezat et al., 2007; Hinsinger, 1998).

Overall, our findings emphasize the critical role of parent material mineralogy in governing nutrient release rates. When normalized to mineral surface area, rocks release significantly higher amounts of Ca, Mg, K, Fe, and Al compared to soils along the nutrient richness gradient. However, when weathering rates are scaled to the entire soil profile, soils release orders of magnitudes more elements than rocks (Figure 2.9). This difference arises because soils have a substantially greater surface area throughout the soil profile than rocks, creating higher nutrient release rates despite lower rates per mineral surface area (Figure 2.11). Furthermore, powdered rocks had increased weathering rates due to enhanced reactive surface areas and exposure of previously armored minerals. Our findings align with previous studies that highlight the significance of mineral surface area and soil texture in nutrient weathering rates (Buss et al., 2008; Hartmann et al., 2013). Additionally, other studies have highlighted the critical role of fine particle weathering on long-term soil fertility which reinforces the importance of both mineralogy and soil structure in nutrient dynamics (Brantley and Lebedeva, 2011). Our results suggest that in order to fully understand nutrient cycling and soil fertility within an ecosystem we must consider both soil and rock weathering processes.

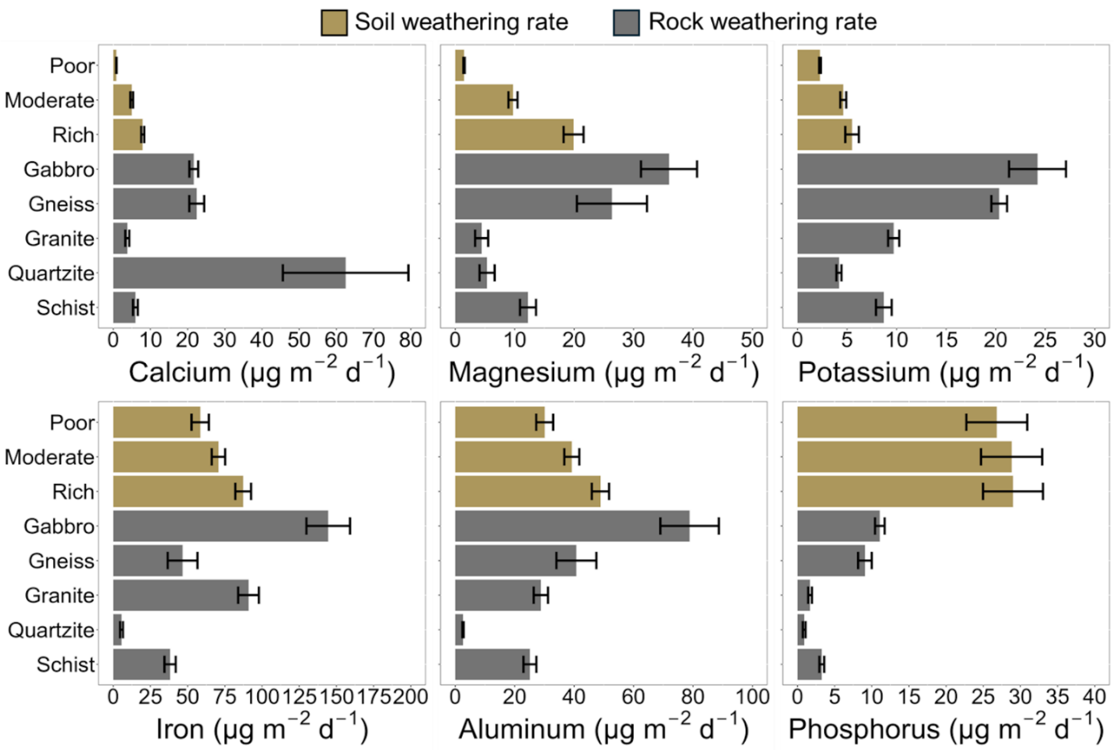

Figure 2.11. Comparison of soil and rock weathering rates of several inorganic elements (Ca, Mg, K, Fe, Al, P). The units are mass of each element, per mineral surface area, and scaled per day of weathering.

2.4 Conclusions

Our results suggest that nutrient availability in glacial soils of northern New England is predominantly governed by the mineralogical composition of the local bedrock, even in areas influenced by glaciation. The Rich forest which was characterized by calcite minerals, had significantly higher nutrient pools and weathering rates than the Poor and Moderate forests which were dominated by granites and schists, respectively. Although rocks had higher weathering rates per mineral surface, the soils released substantially more nutrients when scaled to the entire soil profile. This discrepancy arises from the significantly larger reactive surface area of soils and the influence of pedogenic processes. Our findings highlight the critical role of rock fragments as nutrient reservoirs, which should not be overlooked in studies of soil nutrient dynamics especially in glaciated regions. However, laboratory weathering rates tend to overestimate field rates which further reinforces the importance of soil processes in providing bioavailable nutrients for tree uptake. While rock weathering rates may be lower than the soils, the rocks still remain significant for long-term nutrient release. Therefore, it is essential to consider mineralogical and geochemical characteristics of local bedrock when developing forest management strategies to ensure sustainable soil fertility and ecosystem resilience.

2.5 Acknowledgements

We thank the 2021 soil pit crew for their hard work and dedication in digging the soil pits and collecting rock samples. A special thank you to Wenxiu Teng who physically carried the majority of the rocks from the pits. Thank you to Sydney Carmouche who identified all 375 rocks collected in this study. A special thank you goes to Kevin Evans for his support in locating the field sites, and William Leak, Mariko Yamasaki, and Chris Costello for their dedication to establishing and maintaining several long-term experiments that made this work possible. This research was supported by the USDA National Institute of Food and Agriculture Grant 2021-67019-34250, with additional support from long-term silviculture studies at the Bartlett Experimental Forest that is funded by the USDA Forest Service Northern Research Station.

References

Aoudjit, H., Elsass, F., Righi, D., and Robert, M. (1996). Mica weathering in acidic soils by analytical electron microscopy. *Clay Minerals, 31*, 319-332.

Bailey, S. W. (2000). Geologic and edaphic factors influencing susceptibility of forest soils to environmental change. In *Responses of northern US forests to environmental change* (pp. 27-49). Springer.

Bailey, S. W., and Hornbeck, J. W. (1992). Lithologic composition and rock weathering potential of forested, glacial-till soils (Res. Pap. NE-662). U.S. Department of Agriculture, Forest Service, Northeastern Forest Experiment Station.

Bailey, S. W., Hornbeck, J. W., Driscoll, C. T. and Gaudette, H.E. (1996). *Calcium inputs and transport in a base-poor forest ecosystem as interpreted by Sr isotopes*. Water Resources Research, 32(3), 707–719.

Bailey, S.W., Ross, D.S., Perdrial, N., Jercimovic, M., Webber, J., and Bourgault, R. (2019). Determination of primary mineral content and calcium sources in forest soils using electron probe microanalysis mapping and cluster analysis. *Soil Science Society of America Journal, 83*, 1830-1841.

Bennett, D. S., Wittkop, C. A., and Dicken, C. L. (2006). Bedrock geologic map of New Hampshire: A digital representation of Lyons and others 1997 map and ancillary files (U.S. Geological Survey Data Series 215).

Berner, R. A., Lasaga, A. C., and Garrels, R. M. (2003). The carbonate-silicate geochemical cycle and its effect on atmospheric carbon dioxide over the past 100 million years. *American Journal of Science, 283*(7), 641-683. https://doi.org/10.2475/ajs.283.7.641

Blattler, C. L., Claire, M. W., Prave, A. R., Kirsimäe, K., Higgins, J. A., Medvedev, P. V., and Lepland, A. (2018). Two-billion-year-old evaporites capture Earth's great oxidation. *Science, 360*(6386), 320-323. https://doi.org/10.1126/science.aar2687

Boulton, G.S., and Paul, M.A. (1976). The influence of genetic processes on some geotechnical properties of glacial tills. *Quarterly Journal of Engineering Geology and Hydrogeology, 9*(3), 159-194. https://doi.org/10.1144/gsl.qjeg.1976.009.03.03

Brantley, S.L., and Lebedeva, M. (2011).Learning to read the chemistry of regolith to understand the critical zone. *Annual Review of Earth and Planetary Sciences, 39*, 387-416. https://doi.org/10.1146/annurev-earth-040809-152321

Brantley, S. L. (2008). Kinetics of mineral dissolution. In *Kinetics of water-rock interaction* (pp. 151-210). Springer.

Braun, J.J., Ngoupayou, J.R.N., Viers, J., Dupre, B., Bedimo, J.P.B., Boeglin, J.L., Robain, H., Nyeck, B., Freydier, R., Nkamdjou, L.S., Rouiller, J., and Muller, J.P. (2005). Present weathering rates in a humid tropical watershed: Nsimi, South Cameroon. *Geochimica et Cosmochimica Acta, 69*(2), 357-387. https://doi.org/10.1016/j.gca.2004.06.022

Burt, R., Wilson, M.A., Mays, M.D., and Lee, C.W. (2003). Major and trace elements of selected pedons in the USA. *Journal of Environmental Quality, 32*(6), 2109-2121. https://doi.org/10.2134/jeq2003.2109

Buss, H. L., Sak, P. B., Webb, S. M., and Brantley, S. L. (2008). Weathering of the Rio Blanco Quartz Diorite, Luquillo Mountains, Puerto Rico: Coupling oxidation, dissolution, and fracturing. *Geochimica et Cosmochimica Acta*, *72*(18), 4488-4507. https://doi.org/10.1016/j.gca.2008.06.020

Chadwick, O. A., Derry, L. A., Bern, C. R., and Vitousek, P. M. (1999). Changing sources of nutrients during four million years of ecosystem development. *Nature, 397*(6719), 491-497. https://doi.org/10.1038/17276

Chou, L., and Wollast, R. (1984). Study of the weathering of albite at room temperature and pressure with a fluidized bed reactor. *Geochimica et Cosmochimica Acta, 48*(11), 2205-2217. https://doi.org/10.1016/0016-7037(84)90217-5

Ciolkosz, E.J., Waltman, W.J., Simpson, T.W. and Dobos, R.R. (1989). Distribution and genesis of soils of the northeastern United States. *Geomorphology*, *2*(1-3), 285-302.

Clark, P.U. (1987). Subglacial sediment dispersal and till composition. *The Journal of Geology, 95*(4), 527-541.

Cooper, C.M., and Testa III, S. (2001). A quick method of determining rock surface area for quantification of the invertebrate community. *Hydrobiologia*, *452*, 203-208.

Crowley, K. F., McNeil, B. E., Lovett, G. M., Canham, C. D., Driscoll, C. T., Rustad, L. E., Denny, E., Hallett, R. A., Arthur, M. A., Boggs, J. L., Goodale, C. L., Kahl, J. S., McNulty, S. G., Ollinger, S. V., Pardo, L. H., Schaberg, P. G., Stoddard, J. L., Weand, M. P., and Weathers, K. C. (2012). Do nutrient limitation patterns shift from nitrogen toward phosphorus with increasing nitrogen deposition across the northeastern United States? *Ecosystems*, 15, 940–957. https://doi.org/10.1007/s10021-012-9550-2

Dorais, M. J., Wintsch, R. P., and Becker, H. (2001). The Massabesic Gneiss Complex, New Hampshire: A study of a portion of the Avalon terrane. *American Journal of Science, 301*, 657-682.

Downs, R. T., and Hall-Wallace, M. (2003). The American Mineralogist crystal structure database. *American Mineralogist*, *88*(1), 247–250.

Drouet, T., and Herbauts, J. (2008). Evaluation of the mobility and discrimination of Ca, Sr and Ba in forest ecosystems: Consequence on the use of alkaline-earth element ratios as tracers of Ca. *Plant and Soil*, 302(1-2), 105-121.

Egli, M., Dahms, D., and Norton, K. (2014). "Soil formation rates on silicate parent material in alpine environments: Different approaches–different results?" *Geoderma*, 213, 130-144.

Evans, D.J.A. (2017). Till: A glacial process sedimentology. John Wiley and Sons. https://doi.org/10.1002/9781118652541

Fantle, M.S., and Tipper, E. (2014). Calcium isotopes in the global biogeochemical Ca cycle: Implications for development of a Ca isotope proxy. *Earth-Science Reviews, 129*, 148-177. https://doi.org/10.1016/j.earscirev.2013.10.004

Farkaš, J., Déjeant, A., Novák, M., and Jacobsen, S. B. (2011). Calcium isotope constraints on the uptake and sources of Ca^{2+} in a base-poor forest: A new concept of combining stable ($\delta^{44/42}$Ca) and radiogenic (εCa) signals. *Geochimica et Cosmochimica Acta*, 75(3), 703-719.

Galy, A., Belshaw, N. S., Halicz, L., and O'Nions, R. K. (2001). High-precision measurement of magnesium isotopes by multiple-collector inductively coupled plasma mass spectrometry. *International Journal of Mass Spectrometry, 208*, 89-98. https://doi.org/10.1016/S1387-3806(01)00380-3

Gardner, C.B., Welch, S.A. (2023). Carbonate weathering, phosphate fertilizer, and hydrologic controls on dissolved uranium in rivers in the US Corn Belt. *Science of the Total Environment*, 859, 160219.

Grasby, S.E., Osborn, J., Chen, Z., and Wozniak, P.R.J. (2010). Influence of till provenance on regional groundwater geochemistry. *Chemical Geology, 273*(3-4), 225-237.

Grazulis, S., Merkys, A., and Vaitkus, A. (2020). Crystallography Open Database (COD). In W. Andreoni, S. Yip (eds.) *Handbook of Materials Modeling*, (pp. 1863-1881). Springer Nature Switzerland AG. https://doi.org/10.1007/978-3-319-44677-6_66

Grigal, D. F. (2000). Effects of extensive forest management on soil productivity. *Forest Ecology and Management, 138*(1-3), 167-185. https://doi.org/10.1016/S0378-1127(00)00395-9

Hartmann, J., West, A. J., Renforth, P., Köhler, P., Rocha, C. L. D., Wolf-Gladrow, D. A., Dürr, H. H., and Scheffran, J. (2013). Enhanced chemical weathering as a geoengineering strategy to reduce atmospheric CO_2, supply nutrients, and mitigate ocean acidification. *Reviews of Geophysics*, *51*(2), 113-149. https://doi.org/10.1002/rog.20004

Hatch, N. L., Jr., Robinson, P., and Stanley, R. S. (1988). Stratigraphy of the Connecticut Valley belt. In N. L. Hatch Jr. (Ed.), *Bedrock Geology of Massachusetts* (U.S. Geological Survey Professional Paper 1366-A-D, pp. B1-B34).

Heckman, K., and Rasmussen, C. (2011). "Lithologic controls on regolith weathering and mass flux in forested ecosystems of the southwestern USA." *Geoderma*, 167-168, 248-265. https://doi.org/10.1016/j.geoderma.2011.05.003

Hedin, L.O., Vitousek, P.M., and Matson, P.A. (2003). Nutrient losses over four million years of tropical forest development. *Ecology, 84*(9), 2231-2255. https://doi.org/10.1890/02-4066

Heřmanská, M., Voigt, M. J., Marieni, C., Declercq, J., and Oelkers, E. H. (2022). A comprehensive and internally consistent mineral dissolution rate database: Part I: Primary silicate minerals and glasses. *Chemical Geology, 597,* Article 121782.

Higgins, J.A., Blatter, C.L., Lundstrom, E.A., Santiago-Ramos, D.P., Akhtar, A.A., Cruger Ahm, A.S., Bialik, O., Holmden, C., Bradbury, H., Murray, S.T., and Swart, P.K. (2018). Mineralogy, early marine diagenesis, and the chemistry of shallow-water carbonate sediments. *Geochimica et Cosmochimica Acta, 220*, 512-534. https://doi.org/10.1016/j.gca.2017.09.046

Hinsinger, P. (1998). How do plant roots acquire mineral nutrients? Chemical processes involved in the rhizosphere. *Advances in Agronomy, 64*, 225-265.

Hobbie, S.E., Miley, T.A., and Weiss, M.S. (2002). Carbon and nitrogen cycling in soils from acidic and nonacidic tundra with different glacial histories in northern Alaska. *Ecosystems*, 5(8), 761–776.

Hynicka, J. D., and Pett-Ridge, J. C. (2016). Nitrogen enrichment regulates calcium sources in forests. *Global Change Biology,* 22(10), 3455-3467.

Jahns, R. H. (1947). *Geologic features of the Connecticut Valley, Massachusetts as related to recent floods.* U.S. Geological Survey Water Supply Paper 996.

Jenny, H. (1941). *Factors of Soil Formation: A System of Quantitative Pedology*. Dover Publications, New York, 281 p.

Jobbágy, E. G., and Jackson, R. B. (2001). The distribution of soil nutrients with depth: Global patterns and the imprint of plants. *Biogeochemistry*, 53(1), 51–77.

Johnson, D.W., and Todd, D.E. (1998). Harvesting effects on long-term changes in nutrient pools of mixed oak forest. *Soil Science Society of America Journal, 62,* 1725-1735.

Johnson, C.E., Petras, R.J., April, R.H., and Siccama, T.G. (2004). Post-glacial lead dynamics in a forest soil. *Water, Air, and Soil Pollution: Focus, 4,* 579-590.

Koteff, C., and Pessl, F. (1981). Systematic ice retreat in New England. Geological Survey Professional Paper 1179. U.S. Geological Survey.

Kowalska, J.B., Vogtli, M., Kierczak, J., Egli, M., and Waroszewski, J. (2022). Clay mineralogy fingerprinting of loess-mantled soils on different underlying substrates in the south-western Poland. *Catena, 210*. https://doi.org/10.1016/j.catena.2021.105874

Landeweert, R., Hoffland, E., Finlay, R. D., Kuyper, T. W., and Van Breemen, N. (2001). Linking plants to rocks: Ectomycorrhizal fungi mobilize nutrients from minerals. *Trends in Ecology and Evolution, 16*(5), 248-254. https://doi.org/10.1016/S0169-5347(01)02122-X

Lepp, A.P., Miller, L.E., Anderson, J.B., O'Regan, M., Winsborrow, M.C.M., Smith, J.A., Hillenbrand, C.D., Wellner, J.S., Prothro, L.O., and Podolskiy, E.A. (2024). Insights into glacial processes from micromorphology of silt-sized sediment. *The Cryosphere, 18,* 2297-2319. https://doi.org/10.5194/tc-18-2297-2024

Liese, H. C. (1973). Mineral Composition of the Conway Granite in New Hampshire. GSA Bulletin, 84, 331–334.

Likens, G. E., Bormann, F. H., Pierce, R. S., Eaton, J. S., and Johnson, N. M. (1977). *Biogeochemistry of a Forested Ecosystem*. Springer-Verlag.

Lundström, U. V., Van Breemen, N., and Bain, D. (2000). The podzolization process: A review. *Geoderma*, 94(2–4), 91–107.

Lyons, J. B., Bothner, W. A., Moench, R. H., and Thompson, J. B., Jr. (1997). *Bedrock geologic map of New Hampshire* (U.S. Geological Survey). https://doi.org/10.3133/70211051

Morris, R.C., and Fletcher, A.B. (1987). Increased solubility of quartz following ferrous-ferric iron reactions. *Nature, 330*, 558-561.

Muhs, D.R. (2013). Loess and its geomorphic, stratigraphic, and paleoclimatic significance in the quaternary. USGS Staff-Published Research, University of Nebraska-Lincoln.

Munroe, J.S., Farrugia, G., and Ryan, P.C. (2007). Parent material and chemical weathering in alpine soils on Mt. Mansfield, Vermont, USA. *Catena, 70*, 39-48. https://doi.org/10.1016/j.catena.2006.07.003

Nezat, C. A., Blum, J. D., Yanai, R. D., and Park, B. B. (2008). Mineral sources of calcium and phosphorus in soils of the northeastern United States. *Soil Science Society of America Journal, 72*, 1786-1794. https://doi.org/10.2136/sssaj2007.0344

Nezat, C.A., Blum, J.D., Yanai, R.D., and Hamburg, S.P. (2007). A sequential extraction to determine the distribution of apatite in granitoid soil mineral pools with application to weathering at the Hubbard Brook Experimental Forest, NH, USA. *Applied Geochemistry, 22*(11), 2406-2421. https://doi.org/10.1016/j.apgeochem.2007.06.012

Norouzi-Moghanjoghi, K., Fakhraei, H., Valipour, M., and Driscoll, C.T. (2025). Soil texture-based parameterisation and hydrological insights of a fully coupled surface and subsurface model at the Hubbard Brook Experimental Forest, USA. *Hydrological Processes, 39*. https://doi.org/10.1002/hyp.70045

Page, B.D., Bullen, T.D., and Mitchell, M.J. (2008). Influences of calcium availability and tree species on Ca isotope fractionation in soil and vegetation. *Biogeochemistry, 88*, 1-13.

Perakis, S.S., Maguire, D.A., Bullen, T.D., Cromack, K., Waring, R.H., and Boyle, J.R. (2006). Coupled nitrogen and calcium cycles in forests of the Oregon coast range. *Ecosystems, 9*, 63-74.

Pett-Ridge, J. C., Derry, L. A., and Kurtz, A. C. (2009). *Sr isotopes as a tracer of weathering processes and dust inputs in a tropical granitoid watershed, Luquillo Mountains, Puerto Rico*. Geochimica et Cosmochimica Acta, 73(1), 25-43.

Phillips, J.D. (2007). Development of texture contrast soils by a combination of bioturbation and translocation. *Catena, 70*, 92-104.

Porder, S., and Chadwick, O.A. (2009). Climate and soil-age constraints on nutrient uplift and retention by plants. *Ecology, 90*(3), 623-636. https://doi.org/10.1890/07-1739.1

Power, I.M., Hatten, V.N.J., Guo, M., Schaffer, Z.R., Rausis, K., and Klyn-Hesselink, H. (2025). Are enhanced rock weathering rates overestimates? A few geochemical and mineralogical pitfalls. *Frontiers in Climate, 6*.

Ratcliffe, N. M., Stanley, R. S., Gale, M. H., Thompson, P. J., and Walsh, G. J. (2011). *Bedrock geologic map of Vermont* (U.S. Geological Survey Scientific Investigations Map 3184, p. 3).

Rice, A. R., Perdrial, N., Treto, V., D'Amato, A. W., Smith, G. A., and Richardson, J. B. (2024). Influence of parent material mineralogy on forest soil nutrient release rates across a nutrient richness gradient. Geoderma, 451.

Richardson, J.B., Thrasher, S.A., Saccardi, B., and Clark, E.V. (2023). Sulfidic schist release of As, Cu, and Pb in laboratory experiments and across eleven watersheds in central Massachusetts, USA. https://doi.org/10.1007/s10653-023-01718-1

Richardson, J.B., and Zuniga, L.X. (2021). Quantifying aluminosilicate manganese release and dissolution rates across organic ligand treatments for rocks, minerals, and soils. *Acta Geochimica, 40,* 484-497. https://doi.org/10.1007/s11631-021-00483-1

Rustad, L.E., Knoepp, J., Richter, D.D., and Scott, D.A. (2020). Biogeochemical cycling in forest and rangeland soils of the United States. In Pouyat, R.V., Page-Dumroese, D.S., Patel-Weynand, T., and Geiser, L.H. (eds.) *Forest and rangeland soils of the United States under changing conditions.* Springer, 50-73.

Ryu, J.S., Vigier, N., Decarreau, A., Lee, S.W., Lee, K.S., Song, H., and Petit, S. (2016). Experimental investigation of Mg isotope fractionation during mineral dissolution and clay formation. *Chemical Geology, 445*, 135-145.

Schmitt, A.D., Gangloff, S., Labolle, F., Chabaux, F., and Sille, P. (2017). Calcium biogeochemical cycle at the beech tree-soil solution interface from the Strengbach CZO (NE France): insights from stable Ca and radiogenic Sr isotopes. *Geochimica et Cosmochimica Acta, 213*, 91-109. https://doi.org/10.1016/j.gca.2017.06.039

Schneider, C.A., Rasband, W.S., and Eliceiri, K.W. (2012). NIH image to ImageJ: 25 years of image analysis. *Nature Methods, 9,* 671-675. https://doi.org/10.1038/nmeth.2089

Smalley, I.J. (1966). The properties of glacial loess and the formation of loess deposits. *Journal of Sedimentary Research, 36*(3), 669-676. https://doi.org/10.1306/74D7153C-2B21-11D7-8648000102C1865D

Stone, S. W., and Dennis, J. G. (1964). *The geology of the Milton quadrangle, Vermont* (Vermont Development Department Bulletin No. 26).

Tardy, Y. (1997). Petrology of laterites and tropical soils. *Balkema*, 408.

Taylor, A., and Blum, J. D. (1995). Relation between soil age and silicate weathering rates determined from the chemical evolution of a glacial chronosequence. *Geology, 23*, 979-982.

Uhlig, D., and von Blanckenburg, F. (2019). How slow rock weathering balances nutrient loss during fast forest floor turnover in montane, temperate forest ecosystems. *Frontiers in Earth Science,* 7, 159.

U.S. Geological Survey, Aziscohos Formation, Lower unnamed member at https://mrdata.usgs.gov/geology/state/sgmc-unit.php?unit=NHOCAzl%3B0. (Accessed February 7, 2025a).

U.S. Geological Survey, Waits River Formation- Carbonaceous phyllite and limestone member at https://mrdata.usgs.gov/geology/state/sgmc-unit.php?unit=VTDSw%3B0. (Accessed February 7, 2025b).

Vadeboncoeur, M.A., Hamburg, S.P., Yanai, R.D., and Blum, J.D. (2014). Rates of sustainable forest harvest depend on rotation length and weathering of soil minerals. *Forest Ecology and Management, 318*, 194-205. https://doi.org/10.1016/j.foreco.2014.01.012

Velbel, M. A. (1993). Constancy of silicate-mineral weathering-rate ratios between natural and experimental weathering: Implications for hydrologic control of differences in absolute rates. *Chemical Geology, 105*(1-3), 89–99.

Vienne, A., Poblador, S., Portillo-Estrada, M., Hartmann, J., Ijiehon, S., Wade, P., and Vicca, S. (2022). Enhance weathering using basalt rock powder: Carbon sequestration, co-benefits and risks in a mesocosm study with *Solanum tuberosum*. *Frontiers in Climate, 4*. https://doi.org/10.3389/fclim.2022.869456

Vitousek, P. M., Chadwick, O. A., Crews, T. E., Fownes, J. H., Hendricks, D. M., and Herbert, D. (2003). Soil and ecosystem development across the Hawaiian Islands. *GSA Today, 13*(4), 4-9.

Vitousek, P. M., Porder, S., Houlton, B. Z., and Chadwick, O. A. (2010). Terrestrial phosphorus limitation: Mechanisms, implications, and nitrogen–phosphorus interactions. *Ecological Applications*, 20(1), 5-15. https://doi.org/10.1890/08-0127.1

Wallander, H., and Wickman, T. (1999). Biotite and microcline as potassium sources in ectomycorrhizal and non-mycorrhizal *Pinus sylvestris* seedlings. *Mycorrhiza, 9*, 25-32. https://doi.org/10.1007/s005720050259

Waroszewski, J., Sprafke, T., Kabala, C., Kobierski, M., Kierczak, J., Musztyfaga, E., Loba, A., Mazurek, R., and Labaz, B. (2019). Tracking textural, mineralogical and geochemical signatures in soils developed from basalt-derived materials covered with loess sediments (SW Poland). *Geoderma, 337*, 983-997. https://doi.org/10.1016/j.geoderma.2018.11.008

Warrington, D.N., Goldstein, D., and Levy, G.J. (2007). Clay translocation within the soil profile as affected by intensive irrigation with treated wastewater. *Soil Science, 172*(9), 692-700.

Watmough, S. A. (2014). Calcium, strontium and barium biogeochemistry in a forested catchment and insight into elemental discrimination. *Biogeochemistry*, 122(1), 27–44. https://doi.org/10.1007/s10533-013-9938-x

White, A. F., and Blum, A. E. (1995). Effects of climate on chemical weathering in watersheds. *Geochimica et Cosmochimica Acta, 59*(9), 1729-1747.

Wilson, M. J. (2004). Weathering of the primary rock-forming minerals: processes, products, and rates. *Clay Minerals, 39*(3), 233-266. https://doi.org/10.1180/0009855043930133

Wollast, R., and Chou, L. (1992). Surface reactions during the early stages of weathering of albite. *Geochimica et Cosmochimica Acta, 56*(8), 3113-3121. https://doi.org/10.1016/0016-7037(92)90292-Q

Wray, R.A.L., and Sauro, F. (2017). An updated global review of solutional weathering processes and forms in quartz sandstones and quartzites. *Earth-Science Reviews, 171*, 520-557.

Young, E. D., and Galy, A. (2004). The isotope geochemistry and cosmochemistry of magnesium. *Mineralogy and Geochemistry, 55*, 197-230. https://doi.org/10.2138/gsrmg.55.1.197

Zhang, H., Bloom, P.R., Nater, E.A., and Erich, M.S. (1996). Rates and stoichiometry of hornblende dissolution over 115 days of laboratory weathering at pH 3.6-4.0 and 25°C in 0.01 M lithium acetate. *Geochimica et Cosmochimic Acta*, *60*(6), 941-950. https://doi.org/10.1016/0016-7037(95)00447-5

Zhao, T., Lui, W., and Xu, Z. (2020). Magnesium isotope fractionation during silicate weathering: Constrains from riverine Mg isotopic composition in the southeastern coastal region of China. *Geochemistry, Geophysics, Geosystems, 23*. https://doi.org/10.1029/2021GC010100

Chapter 3

Influence of Parent Material Mineralogy on Forest Soil Nutrient Release Rates across a Nutrient Richness Gradient

---

Published in ***Geoderma (2024)***
DOI: https://doi.org/10.1016/j.geoderma.2024.117081

Authors

Alexandrea M. Rice[1,4*], Nicolas Perdrial[2,3], Victoria Treto[2], Anthony W. D'Amato[3], Grace A. Smith[3], Justin B. Richardson[1,4]

[1]Department of Environmental, Geographic, and Climates Sciences, University of Massachusetts Amherst, Amherst, MA, USA

[2]Department of Geography and Geosciences, University of Vermont, Burlington, VT, USA

[3]Rubenstein School of Environment and Natural Resources, University of Vermont, Burlington, VT, USA

[4]Present address: Department of Environmental Sciences, University of Virginia, VA, USA

*Corresponding Author: utw7wd@virignia.edu

3.0 Abstract

The influence of parent material mineralogy on nutrient release rates in forest wood production remains poorly understood, despite its importance for sustainable forest management. This study investigated how parent material mineralogy impacts soil nutrient abundance and release rates. We studied three forests in Vermont and New Hampshire across a Ca and Mg richness gradient within the soil parent material. We found that both exchangeable and total nutrient concentrations followed the nutrient richness gradient with exchangeable Ca concentrations highest at the rich (758 mg/kg) and lowest at the poor (51.3 mg/kg) sites. Exchangeable Mg concentrations were higher at the rich (41.5 mg/kg) and moderate (42.9 mg/kg) sites relative to the poor (7.04 mg/kg) sites. Total concentrations of Ca were highest at the rich sites (13 mg/g) compared to the moderate (5.73 mg/g) and poor (5.89 mg/g). Total Mg concentrations were higher at the rich (27.3 mg/g) than the moderate (9.47 mg/g) and poor (3.07 mg/g) sites. Using τ values throughout the soil profile compared to the parent material, we found that all three forests were moderate to weakly depleted in Ca, Mg, and K in the upper 30 cm, but P was slightly enriched due to biological uplift. Additionally, we found that calculated field nutrient release rates did not significantly differ among forest nutrient status ($p > 0.05$), indicating the limited effects from across parent materials. We also conducted a follow up batch reactor experiment at varying pH conditions (4, 5, 6) with model organic acids (NaCl, catechol, and citric acid). As expected, pH 4 had the highest Mg release rate (2.19 $mg/m^2/day$) compared to pH 5 (1.27 $mg/m^2/day$), and pH 6 (0.888 $mg/m^2/day$), but surprisingly no effect on Ca release rates, suggesting the more acidic soils of the base cation poor soils results in higher release rates. Our results highlight the dominant contributions of parent material mineralogy has on Ca and Mg release rates, but also that weathering of primary minerals can sustain forest ecosystem productivity.

Keywords: soil nutrient profiles, Ca richness gradient, soil weathering, soil characteristics

3.1 Introduction

The sustainability of timber harvesting in many regions, including northern New England U.S., relies on the nature and abundance of soil minerals as primary factors influencing site nutrient richness (Oursin et al., 2023). Soil mineralogy is key to nutrient sustainability as timber harvesting causes the direct removal of nutrients within woody biomass and also increases the export of nutrients from the soil causing decreases in the nutrient richness of the site (Augusto et al., 2015; Garrett et al., 2021; Hornbeck et al., 1990). The removal of nutrients with whole-tree biomass has been found to decrease site fertility and forest productivity (i.e. tree growth; Cleavitt et al., 2017; Morris et al., 2014; Richard et al., 2022; Richardson et al., 2017; Roy et al., 2021; Walmsley et al., 2009). More specifically, one study across three biomes (subtropical, temperate, and boreal) found that intensive management practices such as whole-tree harvest significantly decreased tree height, diameter, and biomass as well as soil calcium (Ca) concentrations (Achat et al., 2015). Inorganic nutrients (Ca, Mg, K, P, Fe) in soils are vital for plant growth and development. Calcium supports cell development (White and Broadley, 2003), Mg regulates energy storage and photosynthesis (Wang et al., 2020), potassium (K) is involved in driving stomatal pore opening and closing (Kaiser, 1982), and phosphorus (P) is essential for forming genetic, structural, and regulatory molecules (Schachtman et al., 1998). Additionally, iron (Fe) is important in the synthesis of chlorophyll as well as maintaining the function of the chloroplast (Rout and Sahoo, 2015). While not a direct plant essential element, aluminum (Al) in soil does influence the availability of essential nutrients by binding with them especially at low pH (Bojórquez-Quintal et al., 2017). The depletion of soil inorganic nutrients is expedited as whole tree harvesting frequency increases because nutrients cannot be replenished via mineral weathering within that short period of time (Vadeboncoeur et al., 2014). Nevertheless, there is a limited understanding of differences in rates of weathering across diverse forest sites to inform sustainable harvesting guidelines.

Soil parent material is an integral aspect of site index productivity as it governs many aspects from forest species composition (Coile, 1952; Van Breemen et al., 1997), growth rates (St. Clair et al., 2008), and hydrologic dynamics (Adams et al., 2019). In northern New England, parent materials are commonly granitic and metamorphic rocks (e.g. mica schists, greenschist, phyllite) from the Taconic and Alleghanian orogenies. The primary Ca and Mg bearing minerals in granitic and metamorphic rocks include calcite, hydrothermally altered carbonates, plagioclase, chlorite and mica. Additionally, K is primarily sourced from K-orthoclase and P from apatite (Nezat et al., 2004). Therefore, soils rich in aluminosilicate minerals such as K-orthoclase, plagioclase and micas will have lower nutrient concentrations than soils with diverse mineral compositions, especially in Mg and Fe. It is worth noting that dissolution rates of silicate minerals are orders of magnitude lower than those of apatite and carbonates (Heřmanská et al., 2022; Velbel, 1993).

Soil inorganic nutrients are replenished from a combination of aboveground inputs and mineral weathering processes within the soil profile. Despite the importance of aboveground inputs in contributing to soil nutrients, the main contributor to soil nutrient richness is mineral weathering and precipitation (Jenny, 1941; Kelly et al., 1998). The rate of mineral weathering is dependent upon climate conditions, such as precipitation and temperature, and mineral composition within the soil profile, which collectively govern dissolution rates. The stability of minerals is well known, with minerals that were formed under high temperatures and pressures exhibiting greater susceptibility to weathering compared to minerals formed under lower temperatures and pressures (Goldich, 1938; April and Newton, 1992). The dissolution of minerals and their abundances directly regulate the availability of cations and buffering capacity of the soil (Manning, 2022).

Soil parent material also controls the retention and availability of base cations in forest soils through inheritance and formation of clay minerals, organic matter, and pH buffering minerals. Both clay particles and organic matter feature negatively charged surface sites that adsorb base and acid cations which contributes to the capacity of soil to retain plant essential nutrients, therefore enhancing overall soil fertility (McKenzie et al., 2004). Additionally, the negatively charged sites act as exchange sites for base cations into soil solution, making them available for uptake by plants. The availability of these nutrients is dependent on soil acidity, as increased soil acidity lowers the exchange sites occupied by base cations, which increases the solubility of these nutrients (Kaupenjohann et al., 1989). In acidic soils, acidity (H+) occupies sorption sites, leading to an increased leaching of nutrients from the soil (Federer and Hornbeck, 1985; Jackson and Meetei, 2018). Carbonate minerals, such as calcite, play a role in buffering soil pH as their dissolution via carbonation consumes soil protons contributing to partially neutral soil pH (Dijkstra et al., 2003). Therefore, soil with a high buffering capacity resists changes in soil pH, promoting the availability of essential nutrients to plants.

Studies on mineral and rock weathering have employed various approaches, including modeling (Casetou-Gustafson et al., 2019; A. F. White and Brantley, 2003) and in-laboratory batch reactor experiments (Goyne et al., 2006; Richardson and Zuñiga, 2021; Velbel, 1993; Zhang et al., 2019). A comprehensive study examining the dissolution of various minerals, particularly apatite and aluminosilicates, found that apatite was the primary mineral weathered with 1M HNO_3 in granitic-derived parent material (Nezat et al., 2007). Nazet et al. (2007) also indicated that carbonate minerals from soils derived from carbonate rocks were weathered with

1M HNO_3, suggesting that apatite and carbonate minerals weather more rapidly and readily than aluminosilicate minerals. Therefore, the more soluble minerals will be depleted faster than aluminosilicate minerals, leading to nutrient depletion in the upper mineral soils compared to the parent material. Understanding the extent to which the soils are depleted in inorganic nutrients provides a baseline for determining the sustainability of forest management practices.

While other studies have assessed the roles of parent material on soil organic carbon (Pichler et al., 2021), physicochemical properties along a forest productivity gradient (Barnes et al., 2018), and modeled nutrient losses across various harvesting methods (Achat et al., 2018), our study is the one of the first to assess the impact of glacial till parent material, and soil solution chemistry on soil total and available nutrients along a naturally occurring nutrient richness gradient. The overarching goal of the study was to use a nutrient richness gradient to evaluate how parent material mineralogy influences soil nutrient abundance and release. For our first objective, we examined if nutrient rich (e.g. Ca and Mg) parent materials generated soils with greater exchangeable and total nutrients. We hypothesized that the soil of nutrient rich sites would have greater exchangeable and total Ca, K, Mg, and P concentrations because of the high abundance of phyllite and their physicochemical properties promoting nutrient retention. The exchangeable pools are nutrients that are readily available for plant uptake, whereas total nutrients are important for determining longer scale nutrient sustainability of a site. For our second objective, we determined if the enrichment or depletion of soil nutrients throughout the soil profile was influenced by forest nutrient richness. We calculated mass transfer (τ) values and hypothesized that these values would show either more soluble minerals at the rich site and greater depletion of Ca, K, and Mg or that there would be a greater depletion at the nutrient poor site due to the loss of low abundance minerals bearing these nutrients. Further, we hypothesized that the site with lower pH and greater DOC, which promote chemical weathering, would show a greater depletion of nutrients. For our third objective, we tested if parent material and solution chemistry affected nutrient release rates. To meet this objective, we compared dissolution rates with in-situ forest soil leachate and utilized batch reactors across the nutrient-richness gradient. We hypothesized that in-field and batch reactor Ca, K, Mg release rates would be greatest at the nutrient rich site in agreement with solution chemistry composition (e.g. pH).

3.2 Methodology

3.2.1 Study areas

3.2.1.1 Regional characteristics

For this study, we utilized three managed U.S. New England forests with a documented harvest history: Bartlett Experimental Forest in Bartlett, NH, Second College Grant in Coos County, NH, and Clement Woodlot near Corinth, VT (Table 3.1). Overall, the soils are poorly to somewhat excessively drained Spodosols and Inceptisols derived from glacial till. Through the use of Zr/Ti ratios, soil profiles were determined to be derived from uniform parent materials as coefficients of variation within forest nutrient richness were less than 30% (Marsan et al., 1988; Supplemental Table 3.1).

Table 3.1. Site characteristics for each of the three forests used in this study. Soil texture is the dominant texture classification at 30 to 40 cm below the surface of the mineral soil.

Forest	**Nutrient Richness Level‡**	**Lat.**	**Long.**	**Mean elevation (m a.s.l.)**	**Mean Annual Temp. (°C)**	**Mean Annual Precip. (mm)**	**Bedrock Geology**[a]	**Soil Texture**
Bartlett Experimental Forest	Poor	44.048	-71.272	408	6.6	1300	Granite[a]	Sandy loam
Second College Grant	Moderate	44.887	-71.130	550	3.2	1180	Metapelite containing feldspathic metatuff, and quartz[a]	loam
Clement Woodlot	Rich	44.049	-72.311	398	5.3	1100	Carbonaceous phyllite and limestone[b]	Sandy loam

‡ *Nutrient richness is based upon Ca and Mg concentrations within bedrock.*
[a] *Bennett et al., 2006. Bedrock Geologic Map of New Hampshire.*
[b] *Ratcliffe et al., 2011. Bedrock Geologic Map of Vermont.*

In each forest, five circular plots 22.6 m in diameter were established within three developmental stages for a total of 15 plots per forest. This plot area was specifically chosen so that our results can be used in conjunction with or compared to long-term studies in the region (Rogers et al., 2021). The plot developmental stage (young, intermediate, or mature) was determined by the species composition, tree diameter and time since the last recorded harvest. The dominant overstory vegetation is American beech (*Fagus grandifolia*), sugar maple (*Acer saccharum*), and yellow birch (*Betula alleghaniensis*) in mature forest plots. The intermediate plots were partially defined by the additional presence of red maple (*Acer rubrum*), and white ash (*Fraxinus americana*). The presence and prevalence of pin cherry (*Prunus pensylvanica*) and striped maple (*Acer pensylvanicum*) helped define the young forest plots.

3.2.1.2 Natural soil Ca-Mg richness gradient

These three forests represent a natural soil Ca-Mg gradient with Clement Woodlot as the "Rich" site, Second College Grant as the "Moderate" site and Bartlett Experimental Forest as the Ca "Poor" site. This gradient is due to the range in parent material composition (Ratcliffe et al., 2011). Because this region of the U.S. was glaciated until quite recently (ca. 14,000 yrs ago), the soil parent material does not directly correspond to the bedrock but reflects instead a range of neighboring materials carried by the Laurentide ice-sheet. While it is not possible to clearly pinpoint the origin of this surficial material, the direction of low and typical distances covered by the sediments in the region allows us to approximate the parent material as resulting from local bedrock extending about 1.5 km NW of the sites (Koteff and Pessl, 1981). The rich site is the most different of the three forests because of the high abundances of apatite and carbonate in the glacial till parent material. This rich site is part of the Connecticut Valley Trough, specifically the Waits River Formation with limestone and phyllite as the major lithologic constituents (Lyons et al., 1997). The limestone is dark bluish-gray in color and micaceous rich whereas the phyllite is dark to silvery gray with muscovite, biotite and quartz with occasional chlorite (USGS, Waits River Formation). Additionally, while this area is predominantly mapped as Colrain Series, a coarse-loamy, mixed, active, frigid Humic Dystrudept (Soil Survey Staff, 2022), field and laboratory measurements suggest that the sampled site is more accurately classified as an Oxyaquic Eutrudept. The moderate site, Second College Grant, is part of the Central Maine Trough, specifically the Aziscohos Formation with metapelitic schists containing coticule laminations, quartz lenses, and feldspathic metatuff as the major lithological constituents (Lyons et al., 1997; USGS, Aziscohos Formation). Additionally, this area is mapped predominantly as Peru Series which is a coarse-loamy, isotic, frigid Aquic Haplorthod. The poor site, Bartlett Experimental Forest, is predominantly Conway Granite which is a coarse-grained granite with a distinct pink hue. The Conway granite is composed of biotite, plagioclase, and perthic feldspar (Liese, 1973). Additionally, this area is predominantly mapped as Marlow Series which is a Coarse-loamy, isotic, frigid Oxyaquic Haplorthod.

3.2.2 Field sampling

One soil pit (~0.5 m wide) was excavated per plot within each of the three forests for a total of 45 soil pits (Supplemental Figure 3.1). The pits were dug to expose a new, unaltered face for sampling and size varied due to physical restrictions from roots and rocks. The pits were dug to a depth of 1 m, or until a restrictive layer such as a fragipan was encountered. The deepest soils were found at the Ca rich site, with 14 out of the 15 pits reaching a depth of 90 cm or more below the surface of the mineral soil. Additionally, a soil bulk density sample was taken at the top of the mineral soil and ~50 cm deep for two samples per pit using a metal soil corer 7.30 cm in diameter and 10.8 cm long.

Soil samples were collected in 5 cm increments from the surface to 30 cm depth and in 10 cm increments from 30 cm to the base of the soil pit. A core was used to sample the underlying parent material or confining layer. A total of 621 soil samples were collected across the 45 plots. This sampling strategy aimed to capture intra-horizon variability and identify depth-related changes in physicochemical properties, which may be obscured by horizon-based sampling. Depth specific sampling also enables us to use this data in a forest nutrient cycling model (Orton et al., 2016; Sulieman et al., 2018).

Additionally, zero tension lysimeters were installed 50 cm below and parallel to the top of the mineral soil to collect soil water (Jordan, 1968). The lysimeters are 348 cm^2 and drain into a 2 L bottle buried at the bottom of each soil pit. Each spring and fall water was collected from the bottles for elemental analyses and a subsample was frozen for dissolved organic carbon analyses.

3.2.3 Sample processing and inorganic nutrient analysis

3.2.3.1 Parent material mineral abundance

One representative soil sample collected at a depth of 30 cm from each of the three forest sites was selected for in-depth Electron Probe Micro Analysis (EPMA). Samples were prepared commercially by Mineral Opticsso where approximately 5 g of sample was impregnated with epoxy and polished to submicron levels suitable for hyperspectral mapping. Epoxy resin samples were then analyzed using Cameca SX-Five-Tactis electron microprobe located in the University of Massachusetts Amherst Department of Earth, Geographic, and Climate Sciences (Amherst, MA). Five elements (Na, Fe, Ca, Al, Si) were mapped using Kα fluorescence on dedicated wavelength-dispersive spectrometer (WDS) detectors and five elements (Mg, P, K, Ti, Mn) using Kα fluorescence on two electron-dispersive spectrometer (EDS) channels. Column conditions were set at 15keV, 249 nA and dwell time set at 0.02 seconds.

3.2.3.2 Physical processing and characteristics

Mineral soil samples were air dried, passed through a 2 mm sieve and a subsample of the < 2 mm fraction was homogenized using a mortar and pestle. Physical characteristics were determined using the homogenized < 2 mm fraction for analyses of texture, pH, and organic matter content. Particle size distribution of sand (< 2 mm to 63 µm), silt (63 µm to 2 µm), and clay (< 2 µm) was analyzed following Bouyoucos hydrometer method (Gee and Bauder, 1986) where the fraction of each particle size was recorded by mass.

For soil pH, 10 g of 0.01 M $CaCl_2$ was added to about 4 grams of soil and shaken for at least 12 hours. Once settled, the pH of the supernatant was measured using a Fisher Scientific pH meter. Soil organic matter (%) was estimated through loss-on-ignition (LOI) by combusting ~5 g of soil at 550 °C for at least 12 hours. Every 30 samples included a standard reference material and a blank.

For soil dissolved organic carbon, soil water samples were filtered to <0.45µm and acidified to a pH 2 with 10.2 M HCl. Non-particulate dissolved organic carbon was measured using a TOC-L series Shimadzu total carbon analyzer with blanks below detection limits and variability within 2%.

3.2.3.3 Exchangeable soil nutrients

To quantify the exchangeable inorganic nutrients in mineral soils, we followed a modified version of an established extraction procedure (Tessier et al., 1979). In this procedure, 2.0 g of < 2 mm soil were extracted using 30 mL of 0.1 M NH_4Cl and shaken for 24 hrs. The soil slurry was then centrifuged at 2800 rpm for 1 hour and filtered to <0.45 µm. The resulting solution was acidified to 2% HNO_3 to prevent microbial and fungal activity until analyzed.

3.2.3.4 Total soil nutrients

A total digestion of the mineral soil followed a modified version of USEPA Method 3052. Prior to digestion, samples with 8% or higher organic matter underwent combustion at 550 °C to remove organic carbon. To achieve total digestion, 20 mg of sample was placed in a 30 mL perfluoroalkoxy alkane (PFA) vial, along with 2.5 mL of 15.6 M HNO_3 and 2.5 mL of 28.9 M HF. The vials were heated at 170 °C for 48 hrs. After 48 hrs, the mixture was dried down to a moist paste, resuspended with 2 mL of 15.6 M HNO_3, and dried down again. This process was repeated once more before the final paste was resuspended in 5 mL of 7.8 M HNO_3 and heated at 170 °C for 48 hrs. The solution was then diluted to 50 mL using 18.2 MΩ·cm deionized water. A procedure blank, along with two standard reference materials were included with every 25 samples.

3.2.3.5 Elemental concentration analysis

Concentrations of macroelements and nutrients (Al, Fe, Ca, K, Na, Mg, Si, P) in soil exchangeable, total, soil solution, and batch reactor samples were determined using an Agilent 5110 Inductively Coupled Plasma-Optical Emissions Spectrometer (ICP-OES; Agilent, Santa Clara, CA, USA). A nine-point multi-element standard curve was used for calibration. To ensure measurement accuracy, a Standard Reference Material (NIST 2709a San Joaquin Soil) and an in-house Bs horizon soil standard were analyzed every 25 samples. Measured recovery rates for the

San Joaquin soil were within 80-11% of certified values, and in-house Bs concentrations only varied 1-25% of the average in-house value. Elemental concentrations in the blanks were below 0.01 mg/L for all elements analyzed.

3.2.4 Batch reactors for weathering rates

We conducted a batch reactor experiment to determine how mineral release rates may be influenced by pH among the dominant rock types within each nutrient richness. In this laboratory experiment, 3.00 (± 0.01) g of each rock, soil samples from the depth ranges 5 to 10 cm, 30 to 40 cm, and the parent material were immersed in a 40 mL solution composed of 0.01 M NaCl, 0.01 M catechol, and 0.01 M citric acid. The pH of the solutions was adjusted to 4, 5, or 6 using concentrated trace metal grade HCl and NaOH, since the pH of the field soil solution varied from 4.8 to 6.7 among the three forest nutrient richness levels. The samples were shaken for two-week intervals for a total of 10 weeks. After shaking, the solutions were centrifuged at 2600 rpm for 1 hr, supernatant was decanted, and a new solution of the same pH was added. A new solution was added after every two weeks to avoid precipitation and oversaturation of elements in solution, to provide discretized replication for the time series and to provide adequate sample mass for elemental analyses. The pH of the supernatant was measured to determine changes in pH following the 2 weeks of weathering. The supernatant was then acidified with HNO_3 for stability and a subsample aliquot was diluted for elemental analyses using the same ICP-OES procedure as the soil and rock nutrients.

To calculate release rates of the elements, surface area was measured. Soil surface area for two depths from each forest nutrient richness was analyzed using the Brunauer-Emmett-Teller method by the particle technology labs (https://particletechlabs.com/).

3.2.5 Data processing

3.2.5.1 Parent material mineral abundance

Three areas were mapped on each prepared sample using decreasing beam sizes of 20, 10 and 5 um. The resulting data were plotted for graphical representation and multivariate analysis at all resolutions. At the finest resolution (5 um), single pixel data were subjected to hierarchical clustering analysis using JMP® Pro. Characteristic groupings of elemental relative intensity ratios were used to identify specific minerals within the various clusters, including pixels representing void space. A large portion of each sample consisted of pixels characteristic of phase overlaps or ‘edges’, where two or more minerals contributed to the signal and could not be definitively identified. Following mineral identification, we calculated mineral coverage of the map area (um^2) based on the size of the pixel (25 um^2), excluding void space. Quantification error for individual mineral groups was determined to be linearly correlated to the area covered by “edges” so that the total error was distributed with equal weight across the various mineral area fractions.

3.2.5.2 Field: Soil nutrients and base saturation

Exchangeable and total soil nutrient concentrations were standardized to elemental mass per mass of soil using the amount of soil used for each sample. The cation exchange capacity

(CEC) was estimated by summing the milliequivalents (meq) of exchangeable cations including Al, Fe, Ca, Mg, K, and Na. Base saturation (%) was then calculated by taking the sum of the base cation (Ca, Mg, K, Na) concentration divided by each elements charge and dividing by the CEC.

3.2.5.3 Field: Soil to solution nutrient release rates calculation

Elemental concentrations of the soil solution were used to estimate the in-field nutrient release rates of soil among the nutrient-richness gradient. Estimates of soil nutrient release rates ($g/cm^2/yr$) were calculated using the following formula:

$$\text{Soil nutrient release} = \frac{SS}{Bd * Depth * LA * SA} \tag{1}$$

where *SS* is the elemental concentration leaching rate (g/yr), *Bd* is the bulk density of the soil from the profile (g/cm^3), *Depth* is the depth (cm) of soil from the top of the mineral soil to the top of the lysimeter, *LA* is the area of the lysimeter that is collecting soil water (cm^2), *SA* is the average surface area of the soil (cm^2/g). Soil nutrient release rates were calculated for each plot within each soil nutrient richness (n =45).

3.2.5.4 Soil chemical index of alteration

Since feldspars are a major component of rocks and soil, determining the changes in chemical composition associated with feldspar weathering provides insight to the extent of weathering the soil has undergone. The chemical index of alteration was used to determine the relative degree of weathering throughout the soil profile (Nesbitt and Young, 1982):

$$\text{Chemical Index of Alteration} = \frac{Al_2O_3}{(Al_2O_3+Na_2O+CaO+K_2O)} \quad (2)$$

where molar values for each oxide were calculated from total digest cation concentrations. The assumption in this calculation is that all the Ca at these sites is in CaO.

3.2.5.5 Soil base depletion index

In addition to the chemical index of alteration, we calculated the base depletion index to determine the ratio of oxides of base cations compared to oxides that comprise clay and secondary minerals in soils. We used the following equation to calculate the base depletion index (Anda et al., 2023; Jien et al., 2016):

$$\text{Base Depletion Index} = \frac{(CaO+MgO+Na_2O+K_2O)}{(Fe_2O_3+Al_2O_3+TiO_{2)}} \quad (3)$$

where molar values for each oxide were calculated from total digest cation concentrations. The assumption in this calculation is that all the Ca at these sites is in CaO.

3.2.5.6 Soil tau profile plots

A mass transfer coefficient (τ) was calculated throughout the soil profile for each inorganic element to determine the depletion or enrichment of elements relative to the parent material (Brimhall and Dietrich, 1986) using the following equation adapted from Wackett et al. (2018):

$$\tau_{\text{j,soil}}=\frac{Cj,soil * CTi,pm}{Cj,pm * CTi,soil}-1 \tag{4}$$

where the element of interest (*j*) in the weathered soil (*soil*) or parent material (*pm*) were normalized to Ti (*Ti*), an immobile element. Concentrations (C) for the *soil* were used for each depth within each plot among nutrient richness. Concentrations for the *pm* were the *j* and *Ti* concentration of the deepest depth horizon sampled for each plot among the nutrient richness gradient. Tau was calculated for each depth within each plot among the nutrient richness gradient. A positive τ value represents an enrichment of a target element in the soil compared to the parent material, whereas a negative τ value represents a depletion (e.g. Bonar et al., 2023; Brantley and Lebedeva, 2011; Richardson and King, 2018)

3.2.6 Statistical analyses

To address the assumption of normality, the physicochemical variable, and all exchangeable nutrient and total Ca, K, and Mg concentrations were log-transformed prior to analysis. A multivariate mixed-effects ANOVA (MANOVA) was used to investigate the influence of soil physicochemical characteristics (i.e. clay content, organic matter, pH) on exchangeable and total nutrient concentrations.

To assess the impact of nutrient richness and depth on soil nutrient concentrations and physical characteristics, we used two-way mixed-effects analysis of variance (ANOVA). Nutrient richness and depth were treated as categorical fixed effects, while nutrient concentrations served as the response variable. To ensure independence, each plot (n=15) within each nutrient richness was considered an independent sampling unit and modeled as a random effect.

Weathering indices (i.e. soil nutrient release rates, chemical index of alteration, base depletion index), tau plots, and soil solution elements were analyzed using mixed-effects ANOVAs to determine differences among forest nutrient richness and depth. Nutrient richness and depth were treated as categorical fixed effects while solution concentration, weathering indices and tau values served as response variables. Again, each plot was modeled as a random effect to ensure independence. No transformation was needed for these analyses to meet the assumption of normality.

Elemental concentrations in soil solutions were analyzed using ANOVA to determine differences among forest nutrient richness. All elements were log-transformed to meet the assumption of normality prior to analyses. Also, soil nutrient release rates were analyzed using ANOVAs to determine differences among forest nutrient richness and the influence of soil physicochemical characteristics. Tukey's Honest Significant Difference (HSD) tests were used to identify pairwise differences within factors exhibiting statistically significant overall effects.

For the soil weathering experiment, an ANOVA was conducted to determine the influence of forest nutrient richness, pH, and depth on nutrient release rates. A logarithmic transformation was used on Al, Ca, Mg, and P concentrations to meet the normality of residuals assumption.

All statistical analyses were performed using *R* version 4.2.3 (R Core Team, 2023).

3.3 Results and Discussion

3.3.1 Soil properties across nutrient richness gradient

Forest soil characteristics including clay content, soil organic matter, pH, and base saturation play critical roles in nutrient sorption and retention within the ecosystem. Examining the physicochemical properties along the nutrient richness gradient as part of our first objective, we observed significant differences in soil organic matter, pH, and base saturation, but not clay content (Figure 3.1; Supplemental Table 3.2). We found that clay content was not influenced by nutrient richness (p =0.71) even though the moderate sites had a higher clay content (15.3%), than the rich (7.34%) and poor (9.06%). Although not significant, this observation agrees with previous studies on young granitic soils having low clay content such as at the poor site and young micaceous and schists having high clay content such as at the rich site (Righi and Meunier, 1991). Clay content did not change with depth across the nutrient gradient (p =0.15), indicating that pedogenesis has not formed strongly contrasting horizons across the varying soil materials.

Soil organic matter content decreased significantly with depth, which was expected due to diminished biological inputs in deeper soil horizons (p <0.01; Figure 3.1). Overall, soil organic matter differed among forest nutrient richness (p <0.01). Moderate sites exhibited the highest organic matter content (6.73%), followed by poor sites (6.66%), and rich sites having the lowest (6.02%). This pattern aligns with expectations, as higher clay content, although not significantly different between sites, can enhance organic matter retention through increased mineral protection and surface area sorption (Paul, 2016). This trend was consistent across all nutrient richness levels, with rich sites consistently displaying lower clay and organic matter content.

Despite pH being significantly higher at the rich sites (*p* <0.01; Figure 3.1) than the poor and moderate sites, the measured pH values of 4.92 would be considered strongly acidic, which decreases even further at the moderate site with pH 4.27 and poor site with pH 4.11. This range in pH values are similar to other studies in the region that report pH ranging from about 3 to 7 (Armfield et al., 2019; Hazlett et al., 2020; Schattman et al., 2023). The acidity of the soil is likely attributed to a combination of soil mineralogy and calcium content. The weathering of aluminosilicate minerals increases the acidity (decreases pH) of the soil while the parent material containing calcium (i.e limestone) is a buffering agent, resisting changes in pH. The calcium content of the soil over time many have been affected by factors such as acid rain, diminishing the buffering capacity of the soil and allowing the mineral weathering and organic matter decomposition to have a greater impact on soil pH. Additionally, the observed increase in pH with depth (*p* <0.01) is likely attributed to the input of organic acids from decomposition of organic matter in the surface horizons, which can contribute to acidification.

Similar to pH, base saturation varied significantly along the forest nutrient richness gradient (*p* <0.01), with rich sites exhibiting the highest values (54.4%), followed by moderate (19.6%) and poor (4.79%). At the rich site, base saturation increased with depth (*p* <0.01), mirroring the depth-dependent pattern observed in pH. Soil pH and mineralogy directly influence base saturation by affecting the availability of cation exchange sites and the types and abundance of clay minerals. The observed base saturation values in these forests are comparable to those reported in other regional studies (5-25%; Hazlett et al., 2020). Base saturation levels below 15% has been linked to inhibited tree growth (Cronan and Grigal, 1995; Walthert et al., 2013), suggesting potential growth restrictions in nutrient poor and moderate sites. These results support our initial hypothesis and objective, indicating that despite similar climate and vegetation, the soil parent material has generated lasting effects on the soil acidity and nutrient status. This underscores the importance of considering site-specific nutrient conditions for sustainable management.

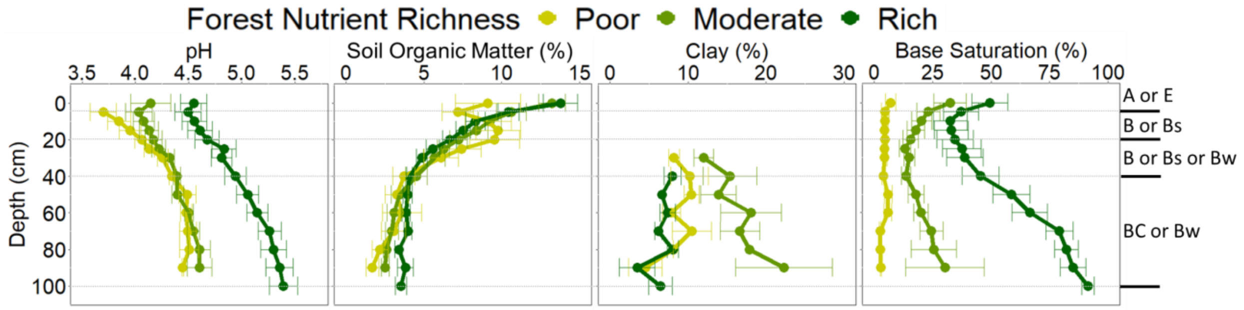

Figure 3.1. The average soil clay content, soil organic matter, pH, and base saturation through the soil profile spanning a nutrient richness gradient. The estimated soil horizons for the sites are delineated by a dashed gray line on the right. Each point represents the mean with error bars indicating the standard error.

3.3.2 Soil nutrients across nutrient richness gradient

3.3.2.1 Parent material mineral abundance

Mapping by EPMA of the major soil elements revealed differences in the texture and general mineral composition of the soils across sites. The soil of the poor site appeared to be dominated by sand-size Si, Na, and Al rich phases embedded in a matrix of fine sand (Figure 3.2; Supplemental Figure 3.2 and 3.3). The moderate site was dominated by aggregates of Al-rich elongated minerals (i.e. micas) with small Si-rich and Na rich phases (Figure 3.2). The presence of a typical garnet porphyroblast in the sample is notable, and points to the metamorphic nature of the parent material at the moderate site. The rich site was dominated by micrometric Si-rich minerals with smaller Na, Al and Mg rich phases and few submicrometric minerals (Figure 3.2).

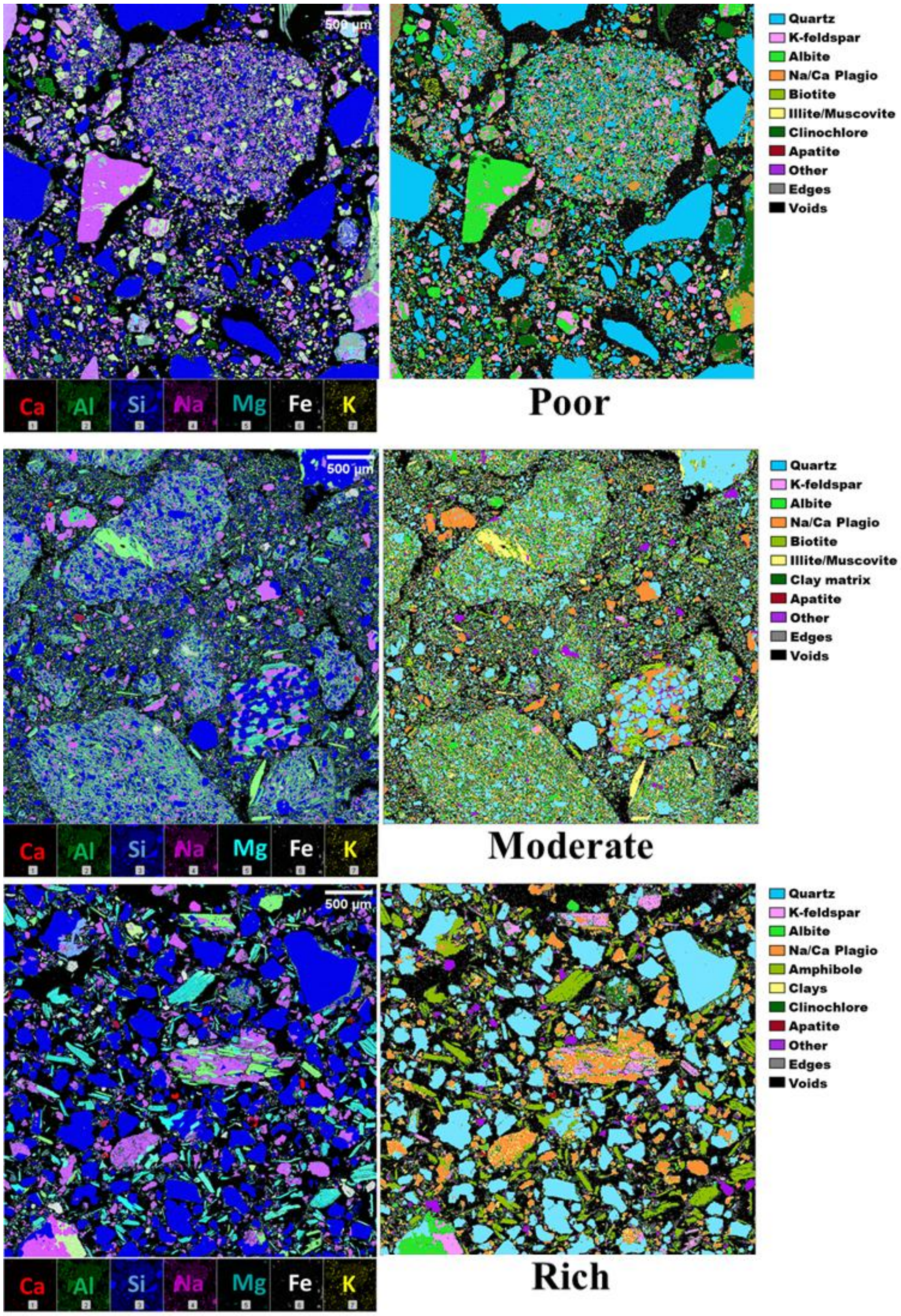

Figure 3.2. Electron microprobe elemental maps of representative soils from each site and results of the clustering characterization of the maps using hierarchical agglomerative clustering. Clustering characterizations identify minerals based on relative elemental compositions.

To further characterize the parent material mineralogy, we identified and quantified the mineral phases in the parent material from each forest to provide a baseline for future nutrient availability (Table 3.2). Quantitative analysis by EPMA confirms that the soils from all sites were dominated by quartz and plagioclase. For Ca-bearing minerals in all sites, Ca was principally present in plagioclase and apatite with the poor site exhibiting the lowest total abundance in these minerals (4.8%). Interestingly, there was no clear mineralogical trend that follows the site nutrient richness index. However, it appears that the nutrient bearing minerals varied across the gradient, with Na and K in feldspars in the poor site, fine clay minerals in the moderate site, and large amphiboles in the rich site. These results partially support our hypothesis for objective 1, as we did not observe a clear difference in the total amount of nutrient bearing minerals across the site. However, each site showed specific characteristics such as different grain sizes and different dominant nutrient-bearing mineral types.

Table 3.2. Parent material mineral abundance for each forest nutrient richness. Mineral phases were identified using electron probe microanalysis. Micas refers to the combination of muscovite, biotite, and chlorite.

Mineral Phases	***Bulk Mineral Abundance of Parent Material (%)***		
	Poor	**Moderate**	**Rich**
Quartz	41.1 (4.8)	33.4 (7.6)	45.9 (8.0)
Ca-Plagioclase*	4.6 (0.5)	7.2 (1.6)	6.6 (1.1)
Na-Plagioclase	24.0 (2.8)	13.4 (3.0)	10.1 (1.8)
K-feldspar	13.0 (1.5)	0.2 (0.1)	4.5 (0.8)
Amphibole	6.9 (0.8)	-	14.8 (2.6)
Micas	8.5 (1.0)	18.9 (4.3)	8.3 (1.4)
Clay Minerals	1.7 (0.2)	23.3 (5.3)	6.1 (1.1)
Apatite	0.2 (0.1)	0.1 (0.1)	0.3 (0.1)
Other	0.3 (0.1)	3.4 (0.8)	3.4 (0.6)

* Ca-plagioclase comprise all plagioclase with a Ca:Na ratio over 1:4

3.3.2.2 Total concentrations of soil elements

We investigated if the total nutrient concentrations of soil provide information on the overall edaphic nature of a site and is a strong indicator of the long-term sustainability of the soil fertility for multiple harvests as part of our first objective. Overall, total elemental concentrations aside from P varied significantly along the forest Ca-Mg nutrient richness gradient (p <0.01;

Figure 3.3; Supplemental Table 3.3). Total Ca concentrations were highest (p <0.01) at rich sites (13.0 mg/g) compared to the moderate (5.73 mg/g) and poor (5.89 mg/g) sites and concentrations increased with depth (p <0.01). The soil total Ca concentrations in these forests were similar to other studies in the region, that ranged from 2.5 to 24 mg/g (Dijkstra and Smits, 2002; Finzi et al., 1998; Richardson and Friedland, 2016). This large range is attributed to differences in parent material compositions. The total soil Ca concentrations across the nutrient richness gradient is attributed to plagioclase mineral abundance in the parent material, also found by other studies in the region (Bower et al., 2023; Likens et al., 1998; Table 3.2). Total Mg followed a similar trend where the rich site was significantly (p <0.01) higher (27.3 mg/g) than the moderate (9.47 mg/g) and poor (3.07 mg/g) and increased with depth (p < 0.01). These sites fall within the natural total Mg concentration range in this region (2 mg/g to 168 mg/g; Woodruff et al., 2015), and the Mg concentrations correspond to amphibole abundance (Eberl and Smith, 2009; Figure 3.2; Table 3.2). The total Ca and Mg concentrations highlight the natural nutrient richness gradient of the studied forests, supporting that parent material mineralogy does control nutrient soil nutrient concentrations.

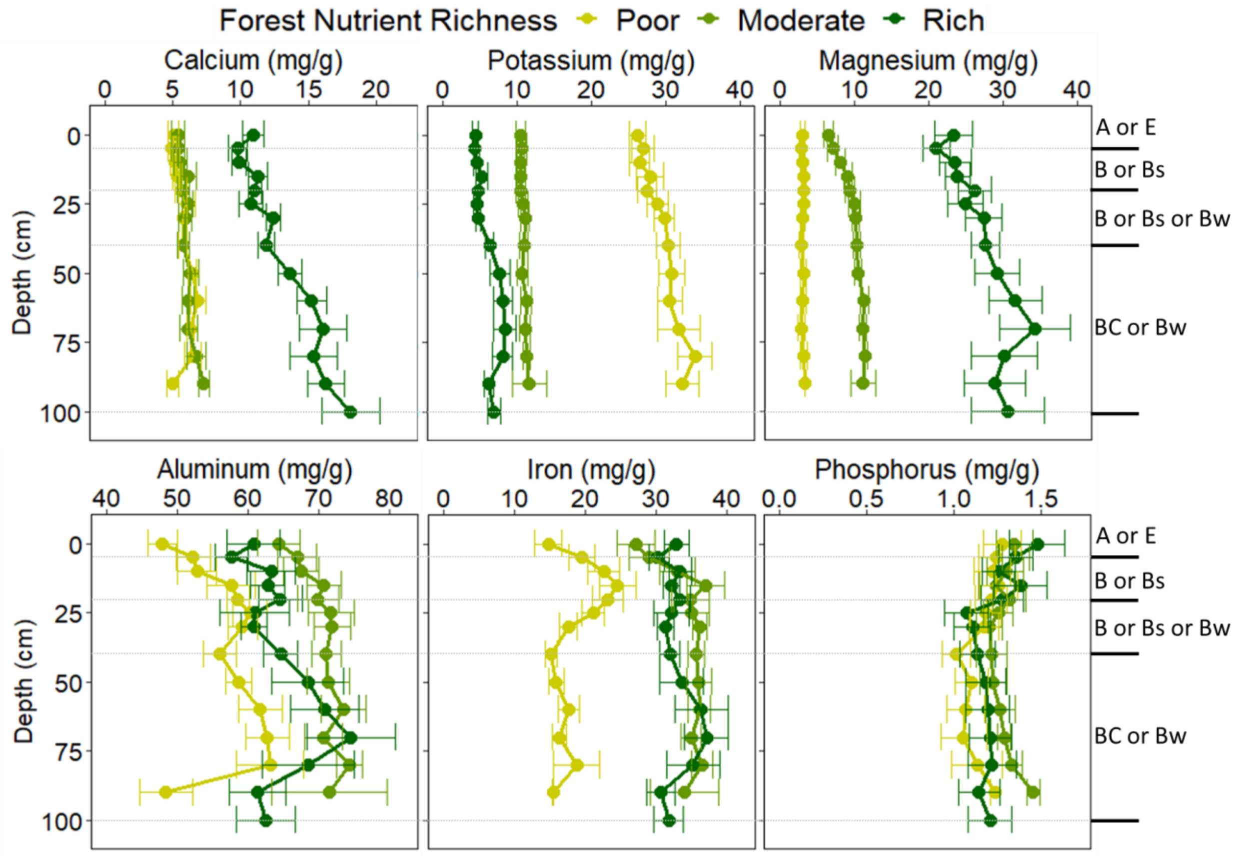

Figure 3.3. Total nutrient profiles (Ca, K, Mg, Al, Fe, P) across forest nutrient richness. The y-axis corresponds to the depth below the top of the mineral soil. The estimated soil horizons for the sites are delineated by a dashed gray line on the right. Each point represents the mean with error bars indicating the standard error.

We expected the total soil K concentrations to be inverse to the Ca and Mg concentration trends as their host aluminosilicate minerals (e.g. K- feldspar, and micas) vary with lithologic formation (Safonov et al., 2011) and our results support this hypothesis. We found that total K concentrations were significantly higher (*p* <0.01) at the poor site (28.8 mg/g) and lower at the moderate (10.8 mg/g) and rich (6.05 mg/g) sites. There were no significant differences in K concentrations with depth (*p* = 0.32). These total K concentrations fall within the observed range (4.2 mg/g to 51 mg/g; Woodruff et al., 2015) for this region. Total soil K concentrations strongly corresponded to parent material K-feldspar, and mica abundance (Figure 3.3; Table 3.2; Eberl and Smith, 2009). Unlike Ca and Mg, which are more mobile due to their presence in weathering susceptible minerals like plagioclase and amphiboles, K is less likely to be mobilized due to the greater resistance of micas to weathering.

Total P concentrations did not significantly vary among forest nutrient richness levels (*p* =0.75), with moderate (1.29 mg/g) and rich sites (1.23 mg/g) exhibiting slightly higher P concentrations than poor sites (1.17 mg/g). Although these values are lower than those reported in other regional studies (5-27 mg/g; Woodruff et al., 2015), they are comparable. While apatite was detected in trace amounts across all sites using EPMA, they were detected in trace amounts, contributing to the overall lower P content of these soils compared to previous studies.

Total Al concentrations varied significantly among the forest nutrient richness gradient (*p* <0.01). The highest concentrations were observed at the moderate sites (70.1 mg/g), followed by the rich sites (64.5 mg/g) and the poor sites (56.7 mg/g). These concentrations were strongly correlated with clay content, which in these sites, is directly linked to the abundance of Al-rich minerals in the parent material (Table 3.2). Also, the elevated Al concentrations contribute to the acidic nature of the soils at these sites. This suggests that the weathering of aluminosilicate minerals in the soil is a primary driver of soil acidity. Total Al concentrations did not vary significantly with depth (*p* =0.48), indicating that Al is primarily bound in recalcitrant minerals, such as clays, rather than being readily exchangeable.

Additionally, we examined the potential sorption of inorganic nutrients to secondary Fe oxyhydroxides, which we approximate with total Fe concentrations. We found that Fe varied significantly with forest nutrient richness (*p* <0.01) with rich (33.2 mg/kg) and moderate (34.3 mg/kg) sites having higher total Fe compared to poor (19.1 mg/kg). Soil total Fe concentrations are attributed to amphibole, mica, and clay mineral abundances in the soil (Figure 3.3; Table 3.2; Eberl and Smith, 2009). Total Fe was also significantly increased with depth (*p* <0.01) where concentrations were depleted in the E horizons and significantly increased with depth into a diagnostic Bs horizon (spodic horizon) for the poor site. This highlights that the formation of secondary Fe oxides in the spodic horizon either did not increase sorption capacity for nutrients or that chemical weathering and sourcing of nutrients throughout the rest of the soil profile is a more dominant controlling factor (Fink et al., 2016).

3.3.2.3 Exchangeable soil elements

Exchangeable nutrients are the most readily available for tree uptake and were investigated to assess how parent material mineralogy influences their availability from parent material mineralogy. We observed significant effects that followed the forest nutrient richness gradient (*p* <0.01) with the highest average Ca concentration of at the rich site (758 mg/kg) and the lowest at the poor site (51.3 mg/kg; Figure 3.4; Supplemental Table 3.3). The moderate sites fell in between (194 mg/kg) the other two sites. These soil concentrations are similar to other studies, where the typical range for exchangeable Ca is between 30 and 200 mg/kg, with the exception of the rich site, which was more than three times higher than the range extent observed in non-calcareous literature (Asmare et al., 2023; Bowden et al., 2019; Dijkstra and Smits, 2002; Oursin et al., 2023). According to the NRCS and other studies, exchangeable soil Ca concentrations within this range are unlikely to be detrimental to non-woody and woody plants (Ericsson, 1994; Soil Survey Staff, 2014). However, studies have noted reduced basal area growth in sugar maple (Schaberg et al., 2006) and diminished tree height in various species (Li et al., 2023) growing on soils with exchangeable Ca values at the lower end of this range. Therefore, we expect forest productivity should not be significantly hindered in our studied forests even though they are on a natural nutrient gradient.

.

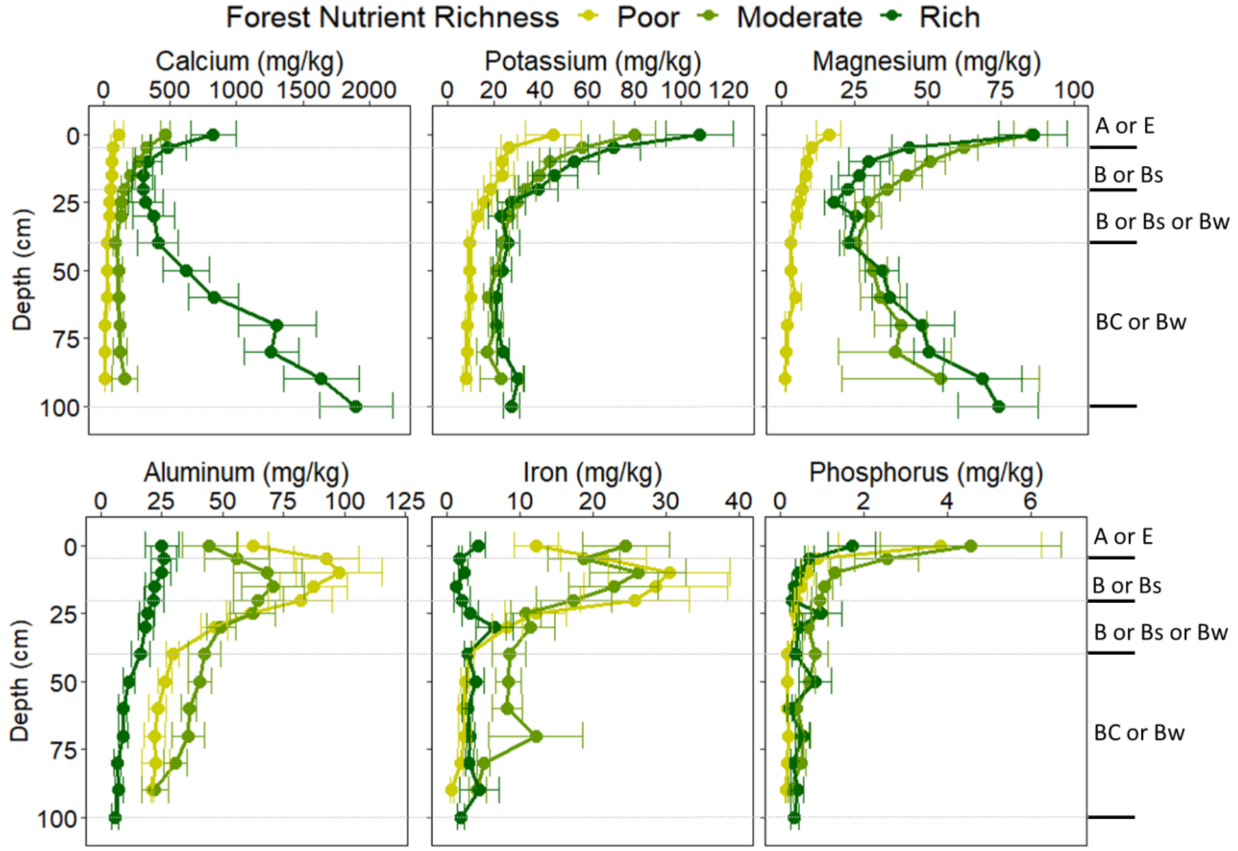

Figure 3.4. Exchangeable elemental profiles (Ca, K, Mg, Al, Fe, P) across a nutrient richness gradient. The y-axis corresponds to the depth below the top of the mineral soil. The estimated soil horizons for the sites are delineated by a dashed gray line on the right. Each point represents the mean with error bars indicating the standard error.

Similarly, exchangeable soil Mg concentrations were significantly higher in the rich (41.5 mg/kg) and moderate (42.9 mg/kg) sites compared to the poor sites (7.04 mg/kg; $p < 0.01$; Figure 3.3). Mica and amphibole minerals are the main source of Mg in these soils and the exchangeable Mg concentrations correspond to the abundance of these minerals at each forest (Figure 3.4; Table 3.2). Exchangeable Mg concentrations along the nutrient richness gradient were below the typical range (60 to 300 mg/kg) for adequate nutrient availability to support growth (Hornbeck et al., 2019). Other studies have reported Mg concentrations ranging from 11 to 266 mg/kg in forest soils which fall within this range (Oh et al., 2007; Olorunfemi et al., 2018; Schaberg et al., 2006). The study with the lowest values saw varying growth rates but these rates were attributed to the Ca and P availability since Mg availability was relatively similar among the stands they examined (Schaberg et al., 2006).

We expected that exchange K concentrations would not directly correspond with the Ca-Mg gradient, as K-bearing aluminosilicate minerals are distinct from Ca-Mg bearing ones. However, we found the exchangeable K concentrations were significantly higher in the rich (38.8 mg/kg) and moderate (35.6 mg/kg) sites compared to the nutrient poor site (18.9 mg/kg; $p < 0.01$; Figure 3.3). This observed range falls within the range reported in other studies of forest soil exchangeable K (50 to 429 mg/kg; Boerner et al., 2003; Bowden et al., 2019; Olorunfemi et al., 2018). According to previous studies, exchangeable K concentrations exceeding 150 mg/kg should support productivity of both non-woody and woody plants (Ericsson 1994; Horneck et al., 2019).

Exchangeable P concentrations did not significantly vary among forest nutrient richness ($p = 0.07$). Although not significant, a trend was observed, with the moderate nutrient richness sites exhibited the highest concentrations (1.31 mg/kg), followed by the poor (0.735 mg/kg) and rich sites (0.570 mg/kg; Figure 3.4). Despite variations in soil extraction procedures used to evaluate exchangeable P (e.g. Mehlich-3 vs Olsen vs Bray-P1), our measured concentrations are consistent with other studies that ranged from 0.8 to 4.0 mg/kg (Liu et al., 2014). Notably, Gradowski and Thomas (2006) found that forest productivity may be P-limited when exchangeable P falls below 5 mg/kg, suggesting that P availability could be a tree productivity constraint across the forest nutrient gradient. Additionally, exchangeable P concentrations can be influenced by clay content and Al concentrations. Given that total Al concentrations followed a similar pattern to exchangeable P concentrations, it is likely that clay content plays a more dominant role in controlling exchangeable P availability than P mineral abundance in these forests.

Exchangeable Al concentrations varied significantly among the forest nutrient richness gradient (p <0.01; Figure 3.4). The highest concentrations were observed at the poor sites (59.1 mg/kg), followed by the moderate sites (51.4 mg/kg) and the rich sites (16.1 mg/kg). While our measured values fall within the typical range of 10-300 mg/kg for exchangeable Al, the concentrations varied substantially among sites, likely reflecting the clay mineral abundances and their control on Al concentrations in the soil (Dragum 1988; Álvarez et al., 2005). In contrast, exchangeable Fe did not significantly vary across the forest nutrient richness gradient (p = 0.54). While moderate sites had slightly higher Fe concentrations (15.1 mg/kg) compared to poor (14.1 mg/kg), the rich sites had the lowest concentrations (3.17 mg/kg). However, exchangeable Fe concentrations decreased significantly with depth (p <0.01), likely due to the weathering of Fe-bearing minerals such as amphiboles and micas. As weathering progresses, Fe may be released from these minerals and transported downwards in the soil profile, leading to higher concentrations in deeper horizons and lower towards the surface

3.3.2.4 Weathering indices throughout the soil profile

The chemical index of alteration varied significantly among forest nutrient richness levels (*p* <0.01) and decreased significantly with depth (*p* <0.01; Figure 3.5; Supplemental Table 3.4). Moderate sites displayed the highest chemical index of alteration (72.7%), followed by rich sites (68.0%), while poor sites had the lowest (52.7%). The higher chemical index of alteration percentages indicates more advanced silicate weathering, suggesting that poor sites have undergone the least silicate weathering. However, this is likely attributed to the higher abundance of Na plagioclase and K feldspar in these soils which are most present in this value range (Nesbitt and Young, 1989). The observed decrease in chemical index of alteration with depth is consistent with the expectations that upper horizons experience more weathering than deeper horizons, which are close to the parent material. The percentages in our study align with previous reports, which typically indicate lower percentages (50-60) in recently formed soils (e.g. from glaciation; Nesbitt and Young, 1982). Given the climate of these sites, moderate precipitation and temperature conditions are likely to have contributed to some degree of silicate weathering, resulting in chemical indexes of alteration slightly exceeding the typical range for recently formed soils (Fedo et al., 1995).

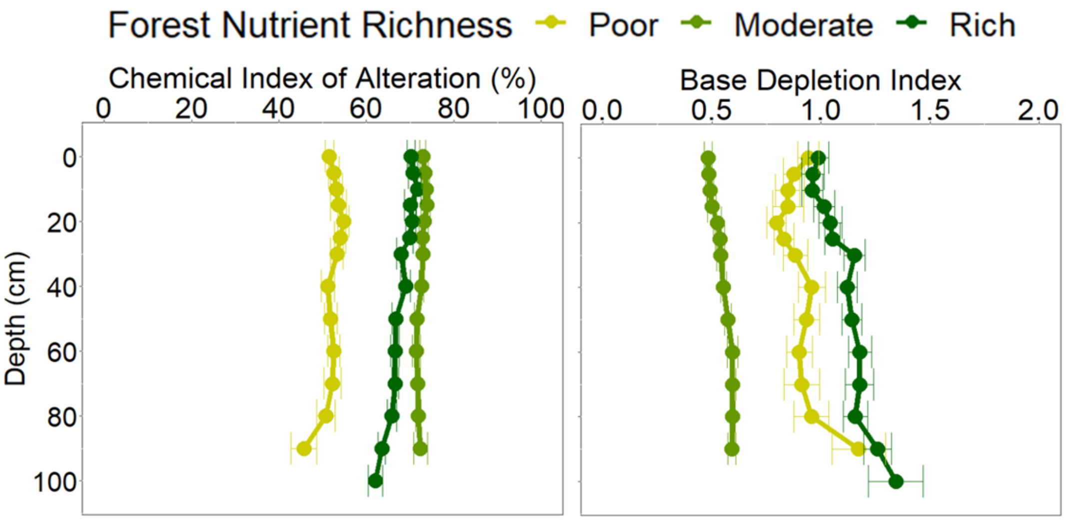

Figure 3.5. Weathering indices throughout the soil profile showing the chemical index of alteration by percentage in the first panel and the base depletion index which is a unitless number in the second panel. For each index, the three nutrient richness gradient levels are shown in differing colors. Each point represents the average with standard error bars.

Similarly, the base depletion index varied significantly among forest nutrient richness levels ($p < 0.01$) and increased significantly with depth ($p < 0.01$; Figure 3.5). Base depletion index values, which are unitless ratios of base cation bearing to transition metal oxides, indicate the relative abundance of base-bearing minerals compared to the recalcitrant minerals. Rich sites exhibited the highest base depletion index (1.11), followed by poor sites (0.887), and moderate sites had the lowest (0.535). These values align with those reported in a study of volcanic soils, where base depletion indexes ranged from 0.83 to 1.53 (Anda et al., 2023). The higher base depletion index at rich sites reflects a greater abundance of base cations, likely due to the presence of Ca-plagioclase, apatite, and K feldspar minerals. Conversely, the lower base depletion index at nutrient poor sites can be attributed to the predominance of recalcitrant aluminosilicate minerals. The increase in base depletion index with depth suggests that base cations have been preferentially depleted from the upper soil horizons, possibly due to biological uptake and weathering processes.

3.3.2.5 Enrichment-depletion of elements throughout the soil profile

Understanding nutrient resupply to soil is important for ensuring sustainable forest harvesting and management practices. To investigate the influence of parent material mineralogy on nutrient depletion, mass transfer (τ) plots were created. These plots evaluate the enrichment or depletion of elements relative to their concentrations in uniform parent material, leveraging Ti as the reference element (Figure 3.6; Supplemental Table 3.5). As previously noted, the uniformity of the parent material was determined using Zr/Ti ratios. Calcium τ values were all negative, indicating depletion compared to parent material, with the most depletion observed at the nutrient rich sites ($p < 0.01$). Soil Mg τ values were depleted in moderate sites but enriched in rich and poor sites compared to the parent material ($p < 0.01$). Soil K τ values were all positive, indicating enrichment relative to the parent material with a significant difference among forest nutrient richness ($p < 0.01$).

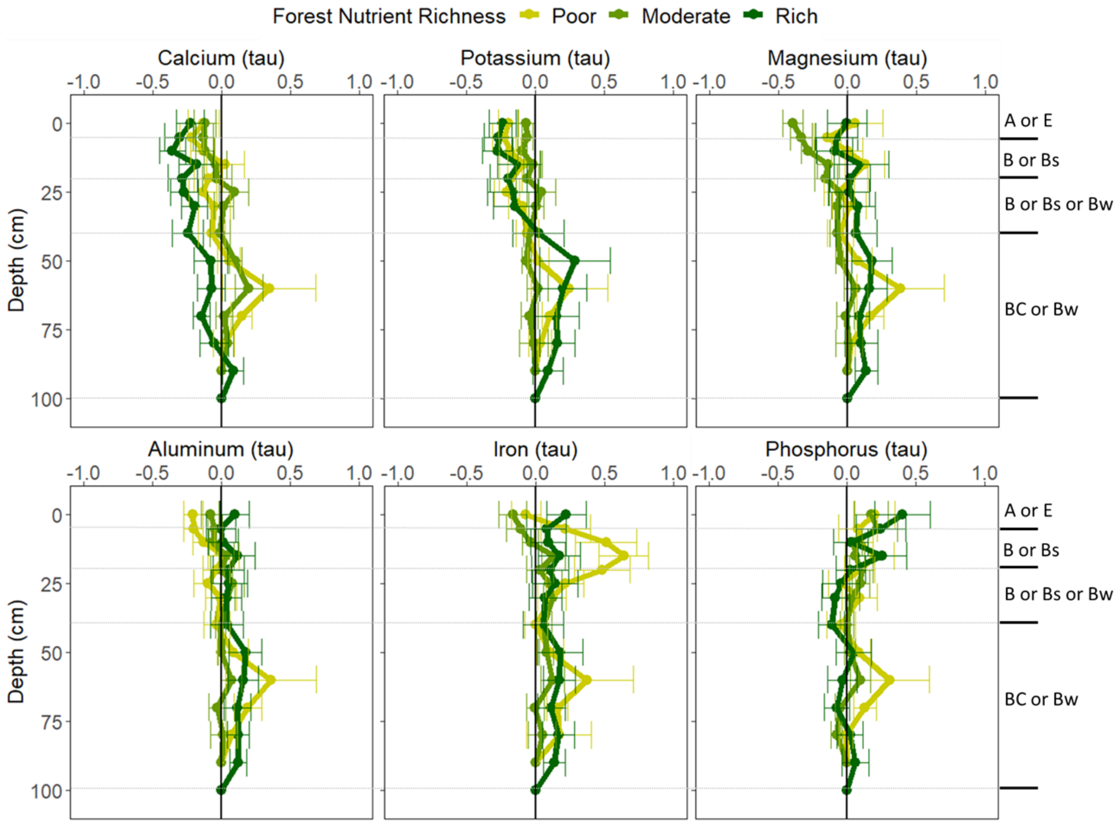

Figure 3.6. Tau plots of total nutrients (via hydrofluoric digestion) standardized by the total nutrients of the parent material throughout the soil profile and across a nutrient richness gradient. The estimated soil horizons for the sites are delineated by a dashed gray line on the right. Each point represents the mean with error bars indicating the standard error.

We expected to observe either a greater depletion of Ca, Mg, and K in the nutrient rich site due to the presence of more soluble minerals (e.g. Ca-plagioclase) or for the nutrient poor site to show greater depletion due to the low abundance and potential loss of minor nutrient-bearing minerals (e.g. apatite). Remarkably, the observed enrichment or depletion patterns for these elements were consistent across all forest nutrient richness levels throughout the soil profile (Figure 3.4). We propose that the lack of significant Ca, Mg, and K depletion in nutrient rich sites can be attributed to the buffering effect of Ca-plagioclase weathering, as evidenced by the absence of strongly developed soil horizons like K and Spodic horizons, significantly higher pH, and significantly higher exchangeable Ca compared to the other richness levels. The base depletion index further supports this hypothesis, indicating a high abundance of base cations associated with cation-bearing minerals. Additionally, we hypothesize that the nutrient poor sites did not experience greater base cation depletion due to their predominance of recalcitrant aluminosilicate minerals. The lower chemical index of alteration in these soils suggests a less severe degree of weathering, but biological cycling may also be replenishing lost nutrient from the deeper horizons or through more efficient internal cycling.

Soil P τ values were also enriched across the nutrient richness gradient, but there were no significant differences among nutrient richness levels (p =0.80). The enrichment of P in surface soils is very common in forested ecosystems due to biological uplift by trees, where this limited nutrient is tightly cycled compared to other nutrients. Within the northeastern United States, similar P enrichment was observed in Pennsylvania ranging from -0.25 to 1 in the A horizon (Kraepiel et al., 2015). Much of the A horizon was enriched in P which was contributed to from biological uplift or atmospheric inputs.

Overall, τ plot profiles for soil nutrients, except for P, did not follow soil organic matter or clay mineral content (Figure 3.1; Figure 3.6). Tau values for P were highest in the upper 20 cm of the mineral soil, which corresponds with higher soil organic matter. The enrichment of P and high organic matter suggests biological inputs, such as litterfall, are influencing the P in the upper mineral soil horizons. This is not surprising as the more organic matter in soil, the higher the sorption capacity for nutrients (Kang et al., 2009). This process involves active uptake by roots and recycling to the surface via litterfall, which contributes to an elevated nutrient abundance in the upper mineral soil horizons (Dijkstra and Smits, 2002; Xia et al., 2023). The significant interaction between nutrient richness and depth indicated that the effect of nutrient richness on nutrient concentrations varied depending on depth, with the exception of Al.

Total soil Al concentrations throughout the profile were enriched compared to parent material with the rich sites having the highest enrichment ($p < 0.01$). Overall, there were no extreme depletions or enrichments in total soil nutrients. Tau Fe was mostly depleted compared to the parent material; however, nutrient moderate sites were the most depleted ($p < 0.01$). In the Bs horizon, Fe τ values were positive, indicating enrichment in comparison to the parent material. The enrichment is due to the accumulation of Fe oxides that are illuviated from the above A/E horizon at the poor and moderate sites.

3.3.3 Field soil weathering rates and batch reactor

3.3.3.1 Field soil solution

Dissolved organic carbon (DOC) and solution pH are critical factors influencing mineral weathering and adsorption processes in soil. To investigate the impact of parent material on elemental availability, we analyzed in-field soil solution chemistry. We found that DOC concentrations were significantly higher at the poor (8.66 mg/L) and moderate sites (7.35 mg/L) compared to the rich sites (3.57 mg/L; $p < 0.01$). These values fall within the range of similar studies reporting DOC concentrations (1.0 to 16.8 mg/L; Kerr and Eimers, 2012; Wilson et al., 2022). Conversely, soil solution pH was significantly higher at the rich sites (6.53) compared to the moderate (5.45) and poor sites (5.38; $p < 0.01$). These pH values fall within reported values that range from 3.5 to 6.9 (Armfield et al., 2019; Gruba and Mulder, 2008). We observed a negative correlation between DOC and soil solutions pH, suggesting that higher DOC concentrations may contribute to lower pH values in the soil solutions. This relationship is likely due to the formation of organic acids from the decomposition of organic matter, which can increase the acidity of the soil solution.

Elemental concentrations in soil solution are an important source of mineral nutrition for trees because they are easily drawn up via mass flow by tree roots. Overall, elemental concentrations were significantly influenced by forest nutrient richness ($p < 0.01$), except for K ($p = 0.365$), and P ($p = 0.71$; Figure 3.7). Soil solution Ca concentrations were significantly higher at the rich site (16.0 mg/L) than both moderate (1.42 mg/L) and poor (0.852 mg/L; $p = 0.03$). Other studies have found Ca concentration in soil water ranging from 1.2 to 1.72 mg/L in the region (Armfield et al., 2019; McHale et al., 2002; Minocha et al., 2000; Porter et al., 2022). Magnesium concentrations were significantly higher at the rich (0.668 mg/L) and moderate (0.600 mg/L) sites than poor sites (0.217 mg/L; $p < 0.01$). Other studies have found Mg concentrations in soil water ranging from 0.2 to 0.51 mg/L in the region (McHale et al., 2002; Minocha et al., 2000; Porter et al., 2022). The rich sites are more than 10 times the upper extent of this range, most likely due to the high abundance of easily weathered Ca bearing minerals. These results are not surprising since the pH is buffered by Ca minerals in the soil. As pH decreases, Ca minerals are weathered and the hydrogen ions from organic acids are adsorbed, resulting in an increased or stable soil solution pH (Cincotta et al., 2019; Kerr and Eimers, 2012). Soil solution Ca and Mg concentrations were inversely correlated to dissolved organic carbon concentrations in the soil solution.

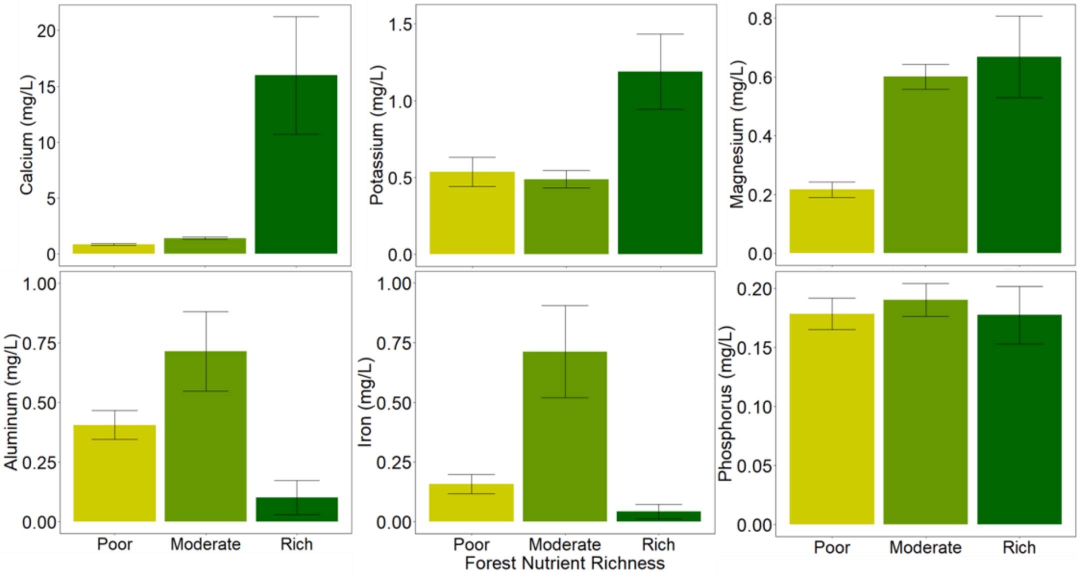

Figure 3.7. Elemental concentrations in soil water collected from lysimeters. These averages with standard error bars are categorized by forest nutrient richness. Values used are from spring and fall 2022.

Soil solution K concentrations did not significantly differ across the forest nutrient richness gradient (*p* =0.36). These results align with the soil exchangeable fraction and base cation saturation data, which were all higher for the nutrient rich site than the poor site. Other studies have found K concentration in soil water ranging from 0.1 to 2.35 mg/L in the region (McHale et al., 2002; Minocha et al., 2000; Porter et al., 2022). All nutrient concentrations were highest at the rich sites, which correlated to higher pH and negatively correlated with clay content (Figure 3.1; Figure 3.4). The low clay content and clay and mica minerals present in these soils suggests a reduced capacity to hold onto nutrients, potentially leading to higher concentrations of nutrients in the soil solutions. This effect may be exacerbated by the higher pH, which can indicate soil buffering and the reduced tendency of nutrients to be retained by clay minerals.

Soil solution P concentrations remain relatively consistent across the forest nutrient gradient, with no significant differences observed (*p* =0.71). Concentrations ranged from 0.177 to 0.190 mg/L which are comparable to previous findings in the same region (Minocha et al., 2000). The lack of variation in soil solution P concentrations is consistent with the insignificant differences in exchangeable P and total P concentrations across the nutrient richness gradient. This suggests that the limited abundance of P-bearing minerals, such as apatite, throughout the nutrient richness gradient exerts minimal influence on P availability in the soil solution; however it is possible that the apatite content in these soils is too low to detect a significant effect. Furthermore, soil solution P concentrations did not strongly correlate with soil solution pH or dissolved organic carbon concentrations, indicating that these factors have minimal influence on P availability at these sites.

Considering Al and Fe as a proxy for the combined effect of primary mineral dissolution and solubility of ions, our results highlight greater weathering and soluble ion transport at the poor and moderate site than the rich site. Moderate sites had significantly higher soil solution Al concentrations (0.714 mg/L) than poor (0.405 mg/L) and rich sites (0.101 mg/L; *p* <0.01). Solution Al concentrations were greatest at the moderate site, despite lower soil pH at the poor site. Moreover, soil solution Al was significantly different between poor and moderate sites despite not being significantly different for the exchangeable Al soil profile. Other studies have found Al concentration in soil water ranging from 0.40 to 0.61 mg/L to in the region (Minocha et al., 2000; Porter et al., 2022). Soil solution Fe concentrations were significantly higher at the moderate sites (71.3 mg/mL) compared to the rich (0.043 mg/L) and poor sites (0.158 mg/mL; *p*

<0.01). Another study found Fe concentration in the region much lower at 0.0089 mg/L (Porter et al., 2022). We hypothesize the higher pH at the rich site decreased soluble Fe while the lower abundance of Fe bearing aluminosilicate minerals at the poor site limited soluble Fe at the poor site.

3.3.3.2 Estimated field nutrient release rates

Quantifying the field elemental release rates is important for understanding the loss of soil nutrients depending on parent material and our experimental design allows for an approximation. We estimated elemental release rates by scaling the soil water concentrations with soil volume, bulk density, surface area and yearly water fluxes. Our estimates (Figure 3.8) suggest that elemental release rates did not differ among forest nutrient richness ($p > 0.05$) since there were no significant differences in nutrient release rates across the forest nutrient richness for Ca ($p = 0.27$), Mg ($p = 0.33$), K ($p = 0.74$), and P ($p = 0.28$). Although not significant, rates for Ca were higher for rich sites (6.12 mg/m^2/yr) than moderate (0.92 mg/m^2/yr) and poor (0.89 mg/m^2/yr), which follows the same trend observed for soil water concentrations (Figure 3.7). Release rates of Mg and K had comparable values across the nutrient richness gradient, which is a different result compared to soil water Mg and K concentrations (Figure 3.7; Figure 3.8). Estimated P release rates were inverse to the soil nutrient richness gradient and do not follow similar trends as the soil waters. These differences across the nutrient richness gradient were not significant because the variability was large within each forest nutrient richness, oftentimes greater than 50% of the mean. The large variability was due to the upscaling of compounding errors from nutrient concentration, quantity of soil water collected, and bulk density heterogeneity among plots within a forest nutrient richness.

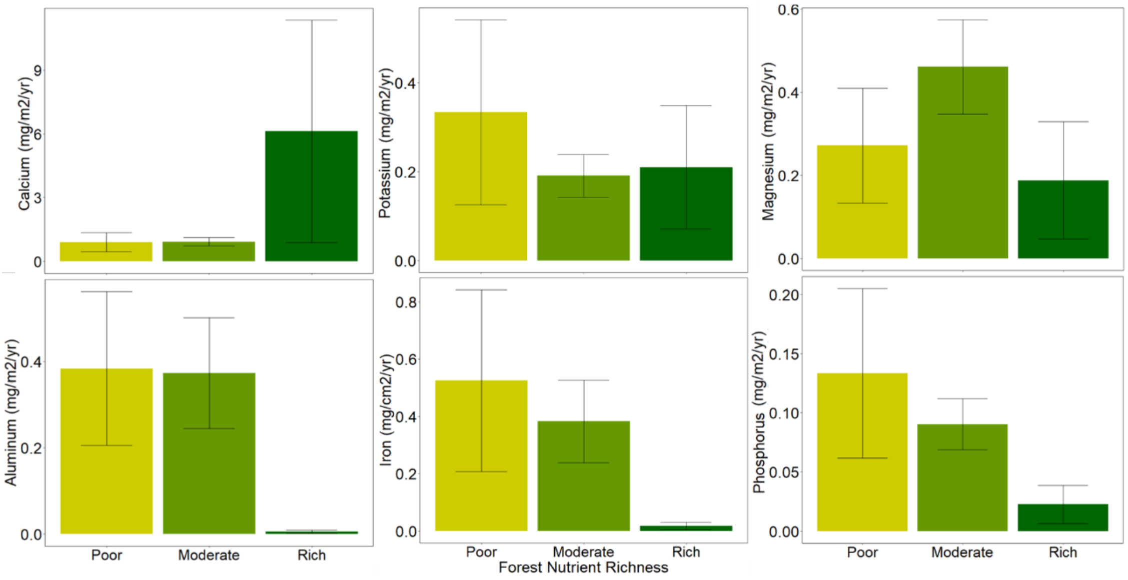

Figure 3.8. In field soil weathering rates that were calculated from soil water solutions among forest nutrient richness. Error bars represent standard error.

Field weathering rates for Al (*p* =0.13) and Fe (*p* =0.28) were also not statistically different across the forest nutrient richness gradient. Estimated Al release rates were highest at the poor site (0.38 mg/m^2/yr) with moderate sites in the middle (0.37 mg/m^2/yr) and the rich sites having the lowest (0.0055 mg/m^2/yr). Estimated Fe release rates followed the same trajectory with rates the highest at the poor sites (0.52 mg/m^2/yr) and lowest at the rich sites (0.018 mg/m^2/yr). These rates were higher for poor and moderate sites than rich, which matches observations for soil water concentrations and is inverse to DOC concentrations. Overall, the estimated rates were highest where the soil pH was the lowest.

This is one of the first studies to estimate in-field release rates for inorganic nutrients by scaling annual soil water concentrations to soil volume. The majority of published "field" estimated weathering rates come from biogeochemical and Monte Carlo models (Futter et al., 2012), and laboratory experiments (Kolka et al., 1996) whereas ours uses field measurements to calculate the release rates. An assumption that our calculation makes is that all the released elements in the soil above the lysimeter are being collected, although that is not completely true because we do not account for tree uptake or lateral movement of soil water.

3.3.3.3 Batch reactor chemistry

While field-based weathering rate calculations can offer a valuable baseline for understanding weathering processes and nutrient availability in an ecosystem, laboratory experiments using batch reactors can provide a more controlled environment to assess nutrient release rates specifically from soil minerals without the complexities of forest floor dynamics and aboveground inputs. We found that nutrient release rates were significantly different across the forest nutrient richness gradient among soil materials and different depths ($p < 0.01$; Table 3.3; Supplementary Table 3.3). The Ca and Mg release rates were significantly different among the three forests with rich sites having higher rates than moderate, and poor sites ($p < 0.01$). Soil K release rates were significantly higher at rich sites (0.778 mg/m^2/day) than poor (0.550 mg/m^2/day), and moderate sites (0.462 mg/m^2/day; $p < 0.01$). The release rates of Ca, Mg, and K correspond to the exchangeable elemental concentrations of each in the soil, exhibiting the highest concentrations and release rates in the rich sites, a trend consistent with findings in a similar study (Street et al., 2023).

Contrary to the other elements, P release rates did not follow the nutrient gradient. Soil P release rates were highest at poor sites (10.1 mg/m^2/day) compared to rich (6.16 mg/m^2/day) and moderate sites (4.96 mg/m^2/day: $p < 0.01$). Since P bearing minerals were in low abundance in the parent material, our results suggest that P adsorption to soil surfaces is more pronounced at the poor sites than the rich and moderate, which is supported by another study in the area (Street et al., 2023). Additionally, the higher Ca concentrations in the moderate and rich sites may induce Ca-P bearing mineral precipitation since this reaction is primarily governed by the Ca concentration and pH in the soil (Tunesi et al., 1999).

Using Al and Fe as a proxy for aluminosilicate and ferrosilicate weathering, we expected higher release rates at the poor site due to lower base cation buffering and match our field observations. However, we found release rates of Al were significantly higher at rich (6.3 $mg/m^2/day$) and poor (5.9 $mg/m^2/day$) sites than moderate (4.3 $mg/m^2/day$; $p < 0.01$). Similarly, the Fe release rates were significantly higher in poor (13.4 $mg/m^2/day$) and rich (10.3 $mg/m^2/day$) sites compared to the moderate sites (7.2 $mg/m^2/day$; $p < 0.01$). Higher Al release rates at the rich site indicated higher aluminosilicate weathering rates, supporting the idea of Ca-plagioclase weathering buffering pH and supporting the idea that base cation saturation and pH promote nutrient adsorption. Higher Fe release rates at the poor site contributed to secondary Fe oxide dissolution due to the low pH.

Overall, we saw greater release rates at the surface rather than with depth (Table 3.3; Supplemental Table 3.3). Greater release rates at the surface may be attributed to the increased exposure and easier weathering of already weathered mineral surfaces, despite the deeper soils undergoing weathering of more soluble minerals typically hypothesized as important elemental sources.

Solution acidity had significant effects on elemental release rates from soil. There were no effects of pH on Ca ($p = 0.05$) or P ($p = 0.38$) release rates from soil. Soil Mg release rates were significantly affected by solution acidity, with pH 4 releasing an average of 2.19

mg/m^2/day, pH 5 at 1.27 mg/m^2/day, and pH 6 at 0.888 mg/m^2/day ($p < 0.01$). Similarly, K release rates were significantly higher at pH 4 (0.711 mg/m^2/day) than at pH 6 (0.510 mg/m^2/day), but not at pH 5 (0.568 mg/m^2/day; $p < 0.01$). Soil acidity and Ca concentrations in soils affect the precipitation of Ca-P bearing minerals, which might affect the measurable P in solution (Tunesi et al., 1999), or because of the small ionic radius P may be adsorbed to soil surfaces after being released into solution (Street et al., 2023). Soil Al release rates were also affected by solution acidity, with pH 4 (7.96 mg/m^2/day) significantly increasing rates compared to pH 5 (4.62 mg/m^2/day) and pH 6 (4.02 mg/m^2/day; $p < 0.01$). Soil Fe release rates were highest with pH 4 (14.5 mg/m^2/day) compared to pH 5 (8.89 mg/m^2/day) and pH 6 (7.46 mg/m^2/day; $p < 0.01$).

From our batch reactor experiments, we found a correspondence of parent material and solution chemistry to nutrient release rates from soil. Parent materials with high total Ca, and Mg concentrations exhibited higher release rates, typically corresponding to rich sites. Additionally, soil acidity influenced release rates, with more acidic solutions releasing more elements from minerals in the soil. Understanding the controls and influences of weathering rates is crucial for accurate nutrient budget calculation. Therefore, our finding that nutrient release rates were controlled by both soil solution acidity and parent material mineralogy is important and is supported by other studies that found effects of both pH and mineralogy on elemental release rates (Casetou-Gustafson et al., 2019; Richardson and Zuñiga, 2021; Zhang et al., 2019). Additionally, the batch reactor release rates were one to five orders of magnitude larger than the estimate in field rates, most likely due to ecosystem dynamics such as plant uptake and lateral flow that are not present in the laboratory. Unfortunately, our batch reactor experiment highlighted that the in-field weathering estimates were only useful when soil nutrients were high, in the case of Ca from Ca-plagioclase or very low, in the case of P from apatite; although this does provide a useful, cost-effective tool for estimating relative release rates across sites.

Table 3.3. Batch reactor average release rates of inorganic nutrients from soils with varying pH among three depth ranges. These averages were calculated from the last 28-days of the 70-day total experiment because once steady state had been achieved. Each treatment average consists of six replicates with reported standard error (±).

Soil Nutrient Richness	**Depth Range (cm)**	**Initial pH**	***Soil Nutrients Release Rate (mg/m^2/d)***					
			Al	**Fe**	**Ca**	**K**	**Mg**	**P**
Rich	5-10	4	10.9 (±2.3)	36.6 (±9.4)	0.196 (±0.030)	0.894 (±0.074)	0.785 (±0.19)	11.05 (±4.8)
		5	4.95 (±0.66)	19.3 (±4.9)	0.180 (±0.026)	0.658 (±0.13)	0.286 (±0.055)	10.53 (±4.7)
		6	3.99 (±0.61)	17.4 (±4.7)	0.152 (±0.026)	0.566 (±0.081)	0.192 (±0.033)	10.2 (±4.5)
	30-40	4	9.15 (±1.2)	13.6 (±0.92)	0.158 (±0.014)	0.565 (±0.072)	0.560 (±0.067)	11.0 (±4.8)
		5	5.62 (±1.1)	8.65 (±1.3)	0.155 (±0.023)	0.500 (±0.050)	0.236 (±0.023)	11.4 (±5.1)
		6	6.46 (±1.5)	7.26 (±1.1)	0.164 (±0.041)	0.587 (±0.081)	0.184 (±0.023)	10.7 (±4.8)
	80-90	4	5.78 (±0.85)	8.70 (±0.85)	0.163 (±0.037)	0.433 (±0.042)	0.700 (±0.095)	8.58 (±3.8)
		5	3.28 (±0.55)	4.91 (±0.92)	0.213 (±0.079)	0.356 (±0.048)	0.280 (±0.063)	9.26 (±4.1)
		6	3.55 (±0.6)	3.79 (±0.65)	0.242 (±0.10)	0.388 (±0.053)	0.177 (±0.038)	8.33 (±3.8)
Moderate	5-10	4	8.55 (±1.2)	13.8 (±2.1)	0.985 (±0.11)	0.381 (±0.076)	2.43 (±0.42)	6.56 (±2.8)
		5	6.42 (±0.96)	11.5 (±2.2)	0.824 (±0.068)	0.316 (±0.070)	1.72 (±0.33)	6.63 (±2.8)
		6	6.16 (±0.85)	10.8 (±1.7)	0.918 (±0.19)	0.238 (±0.033)	1.22 (±0.26)	5.97 (±2.5)
	30-40	4	6.05 (±0.75)	9.39 (±1.2)	1.365 (±0.19)	0.660 (±0.12)	2.967 (±0.27)	6.64 (±2.8)

		5	3.51 (±0.43)	6.51 (±0.65)	1.122 (±0.14)	0.551 (±0.075)	1.88 (±0.19)	5.99 (±2.6)
		6	3.53 (±0.64)	6.88 (±1.1)	0.870 (±0.076)	0.54 (±0.081)	1.60 (±0.18)	6.11 (±2.6)
	80-90	4	10.9 (±1.51)	15.2 (±2.0)	1.721 (±0.26)	1.75 (±0.66)	6.28 (±1.29)	5.76 (±2.4)
		5	6.74 (±1.6)	10.4 (±2.1)	1.18 (±0.14)	1.43 (±0.63)	4.41 (±1.26)	6.12 (±2.6)
		6	4.95 (±1.0)	8.04 (±1.4)	0.751 (±0.030)	1.14 (±0.46)	3.19 (±0.80)	5.63 (±2.4)
Poor	5-10	4	5.16 (±1.3)	9.82 (±2.7)	0.315 (±0.047)	0.404 (±0.084)	1.26 (±0.31)	5.21 (±2.3)
		5	2.77 (±0.41)	5.54 (±1.0)	0.361 (±0.036)	0.319 (±0.062)	0.54 (±0.094)	5.74 (±2.5)
		6	2.20 (±0.35)	4.65 (±1.2)	0.246 (±0.023)	0.323 (±0.050)	0.332 (±0.049)	6.12 (±2.7)
	30-40	4	9.53 (±1.2)	14.3 (±1.1)	0.318 (±0.11)	0.701 (±0.15)	2.81 (±0.23)	5.87 (±2.6)
		5	5.49 (±1.1)	8.43 (±0.81)	0.473 (±0.13)	0.561 (±0.13)	1.25 (±0.10)	5.98 (±2.6)
		6	3.57 (±0.67)	5.66 (±0.71)	0.455 (±0.088)	0.458 (±0.088)	0.653 (±0.068)	5.82 (±2.5)
	70-80	4	5.58 (±0.70)	8.74 (±0.98)	0.735 (±0.11)	0.613 (±0.15)	1.95 (±0.15)	3.43 (±1.4)
		5	2.80 (±0.30)	4.78 (±0.37)	0.694 (±0.044)	0.424 (±0.079)	0.853 (±0.038)	3.401 (±1.4)
		6	1.81 (±0.20)	2.67 (±0.23)	0.494 (±0.022)	0.358 (±0.060)	0.433 (±0.040)	3.09 (±1.3)

3.4 Synthesis and Conclusions

Our study explored the influence of parent material on soil nutrient concentrations and their release rates in northern hardwood forests of New England, U.S. We found a strong link between the abundance of Ca and Mg- bearing minerals in the parent material and their total and exchangeable fraction in the soil and led to higher soil pH and base cation saturation. All of these factors promote the growth of northern hardwood trees. Our EPMA data revealed that the Ca and Mg gradient is generated from an abundance of Ca-plagioclase, mica, and amphibole minerals, rather than carbonates as typically hypothesized. Despite the differences in Ca and Mg bearing minerals and total and exchangeable concentrations, we did not detect significant differences in soil water Ca and Mg concentrations along the nutrient gradient. The Ca and Mg rich sites were about six times greater than those at the poor and moderate sites but were not significantly different due to spatial heterogeneity. The high soil water concentrations Ca might indicate enhanced acid buffering capacity, even though carbonates were not detected using EPMA. This suggests greater Ca availability to trees at the rich sites in solution and in solid phase, which likely contributes to higher overall site productivity, especially through tree growth.

Soil total K and P followed a different pattern than Ca and Mg. Total K concentrations were highest at the Ca-Mg poor site, indicating the importance of K feldspar in controlling soil K concentrations. However, exchangeable K concentrations positively corresponded with increased site nutrient richness. This likely reflects the combined effects of increasing CEC and soil pH, which promote the availability of K for plant uptake. Even though nutrient rich sites have lower abundance of K-bearing minerals, the increased availability due to higher CEC and pH make them less likely to be K limited for tree growth. Total P was lowest at the poor sites across sites but had comparable abundances of apatite therefore other P bearing aluminosilicate minerals are the major source of P in these soils. Exchangeable P concentrations were highest at the moderate site, likely due to the combined effects of clay content and Fe concentrations, which are known to influence P adsorption. Despite these differences in exchangeable P, no significant differences were observed in soil water P concentrations. This finding suggests that P sorption with Fe and Al is occurring at the nutrient rich site, evident from the pH, and low Fe and Al concentrations in the soil water. These results highlight the importance of considering soil properties like pH, CEC, Fe, and Al concentrations since these factors influence K and P availability, which impacts the accessibility by plants.

Assessing the impact of weathering on nutrient release was an important goal of this work. We expected that greater acidity and lower Ca and Mg abundance may lead to overall faster depletion rates at the nutrient poor site compared to the rich site. Interestingly, soil profile τ values revealed similar levels of depletion and enrichment for all elements (Ca, Mg, K, and P) across the nutrient richness gradient, suggesting that both the soil buffering capacity and the resistance of minerals to weathering influence release rates. We compared field weathering rates obtained from lysimeter water with laboratory batch reactor experiments. While the calculated field nutrient release rates were one to two orders of magnitude lower (Ca, Mg, K) or five orders of magnitude lower (P) than in the laboratory experiment, the relative trend in nutrient richness among sites was consistent across both methods. The estimated field nutrient release rates were much lower than the laboratory experiment because of ecosystem dynamics such as plant uptake and lateral flow that remove elements from solution before leaching through the soil profile. The laboratory-based batch reactor study indicated that Ca and Mg nutrient release rates corresponded to their total soil abundance but, P was significantly higher at the poor sites, suggesting a greater influence of mineral phases. These trends were amplified by increased soil water acidity. While total elemental concentrations provide a basic understanding, soil characteristics like mineralogy and pH play a crucial role in mineral weathering, sorption and ultimately the accessibility of nutrients for tree growth.

Our study highlights the critical role of parent material mineralogy, particularly minerals rich in Ca and Mg, in controlling nutrient release rates and influencing long-term forest productivity. These minerals promote higher base saturation in the soil, making essential nutrients like Ca and Mg readily available for tree uptake, thus enhancing site productivity. Interestingly, we initially anticipated carbonate minerals to be the primary Ca source in these forests, however, no carbonate minerals were detected through EPMA. Therefore, their role in release rates appears less significant than expected. Consequently, sites with parent material rich in Ca-plagioclase, mica, and amphibole minerals may be suitable for supporting shorter timber harvesting rotations while maintaining soil health and nutrient supply over extended time frames. However, further research on aboveground productivity is warranted to fully understand these implications for sustainable forest management practices.

3.5 Acknowledgements

We thank the 2021 soil pit crew for all their efforts helping dig soil pits and sampling soils. Thank you to Marissa Hanley, Rhea Negron, Bren Cable, Eve Foran, and Christopher Marshall, for their assistance collecting and processing soil waters. A special thank you to John Sweeney for building essential equipment and items for this project and Kevin Evans for assistance in locating field sites. This study was funded by the USDA National Institute of Food and Agriculture Grant 2021-67019-34250 with long-term silviculture studies at the Bartlett Experimental Forest supporting this project funded by the USDA Forest Service Northern Research Station.

Supplemental Tables and Figures

Supplemental Table 3.1. The average and coefficients of variation for the titanium to zirconium ratio within each nutrient richness.

Nutrient Richness	Plot Average	CV (%)
Poor	3.94	29.5
Moderate	18.4	17.8
Rich	23.5	23.0

Supplemental Table 3.2. Soil physical characteristics *p* values for ANOVA table Type II Sum of Squares with no adjustment.

Factor	pH	Loss on Ignition	Clay	Base Saturation
Richness	<0.001	<0.001	0.712	<0.001
Depth	<0.001	<0.001	0.145	<0.001
Richness*Depth	0.027	0.003	0.219	0.116

Supplemental Table 3.3. Soil chemical characteristics *p* values for ANOVA table Type II Sum of Squares with no adjustment for soil exchangeable, total, and weathering nutrients.

	Nutrients					
Factor	**Al**	**Fe**	**Ca**	**K**	**Mg**	**P**
			Soil Exchangeable			
Richness	<0.001	0.0536	<0.001	<0.001	<0.001	0.0683
Depth	<0.001	<0.001	<0.001	<0.001	<0.001	<0.001
Richness*Depth	0.020	0.0034	<0.001	0.252	<0.001	0.181
			Soil Total			
Richness	<0.001	<0.001	<0.001	<0.001	<0.001	0.749
Depth	0.477	0.0021	0.0146	0.323	<0.001	0.959
Richness*Depth	0.943	0.0133	0.998	0.0115	0.479	1.00
			Soil Weathering			
Richness	<0.001	0.0023	<0.001	0.0069	<0.001	<0.001
Depth	0.00072	0.0069	<0.001	0.0015	0.021	<0.001
pH	<0.001	<0.001	0.048	<0.001	<0.001	0.383

Supplemental Table 3.4. The *p* values for the influence of each nutrient richness and depth on the chemical index of alteration and base depletion index.

Factor	**Chemical Index of Alteration**	**Base Depletion Index**
Richness	<0.001	<0.001
Depth	<0.001	<0.001

Supplemental Table 3.5. The *p* values for the influence of each nutrient richness and depth on the tau (τ) value for each element.

Factor	**Al**	**Fe**	**Ca**	**K**	**Mg**	**P**
Richness	<0.001	<0.001	<0.001	<0.001	<0.001	0.798
Depth	<0.001	0.190	<0.001	<0.001	0.328	0.564
Richness* Depth	0.0879	0.144	0.00151	<0.001	0.206	0.591

Supplemental Figure 3.1. Representative soil pits for each nutrient richness: **a)** Low richness: moderate granular structure with abundant fine roots and 20-30% rock fragments. Color ranges from gray to yellowish-red to olive brown and olive gray in deeper horizons. **b)** Moderate richness: weak subangular structure with common fine roots and 15-20% rock fragments. Color transitions from dark brown to dark yellowish brown to olive brown. **c)** Rich richness: weakly granular structure with few roots and 5-10% rock fragments in the A and B horizons. Color transitions from dark yellowish brown to olive brown to dark grayish brown.

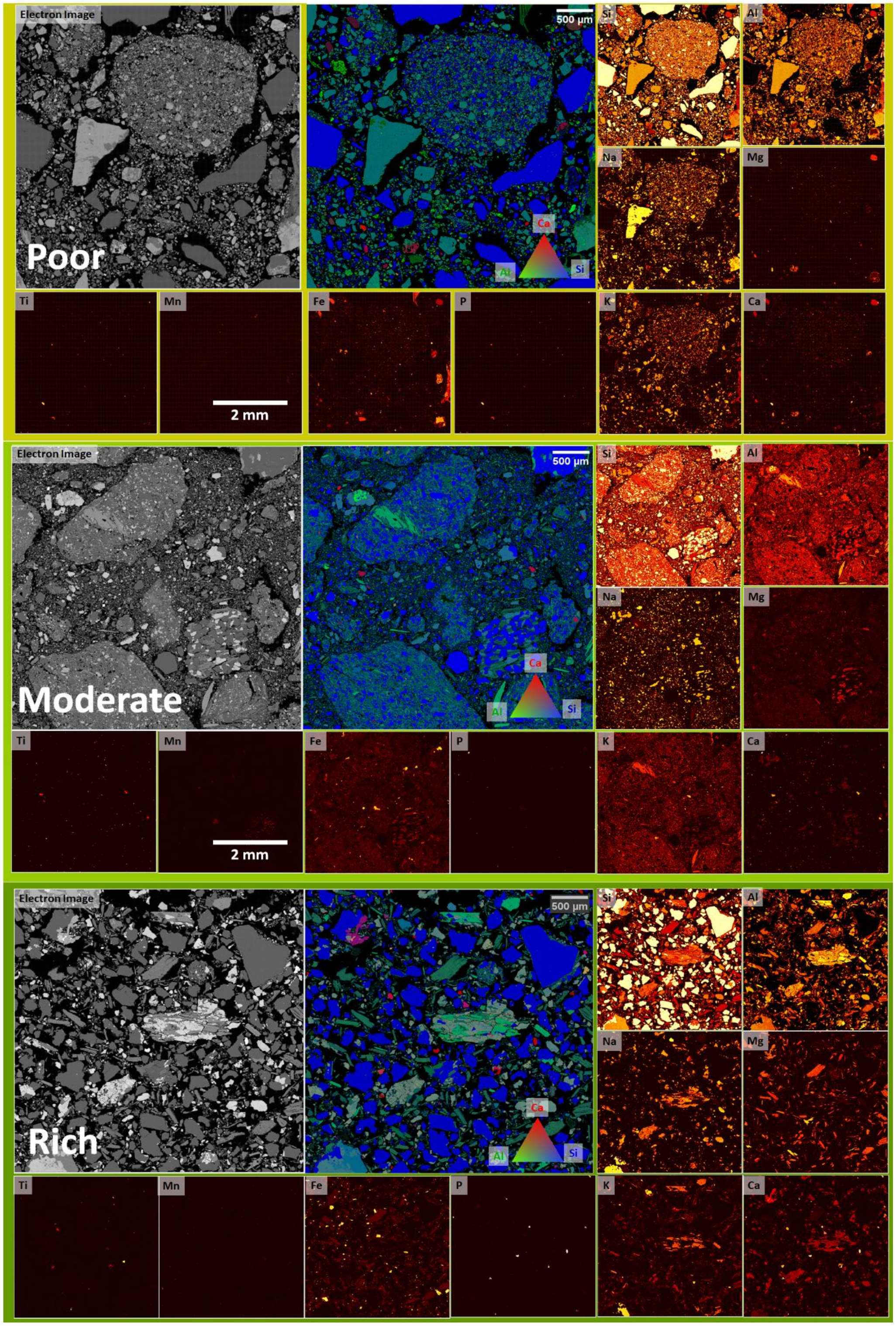

Supplemental Figure 3.2. Electron microprobe maps for each forest nutrient richness with accompanying elemental maps. Each site shows an electron image (the sum of all counts), a tri-color image in RGB (red: Ca counts, green: Al counts, blue: Si counts) and individual maps for all analyzed elements.

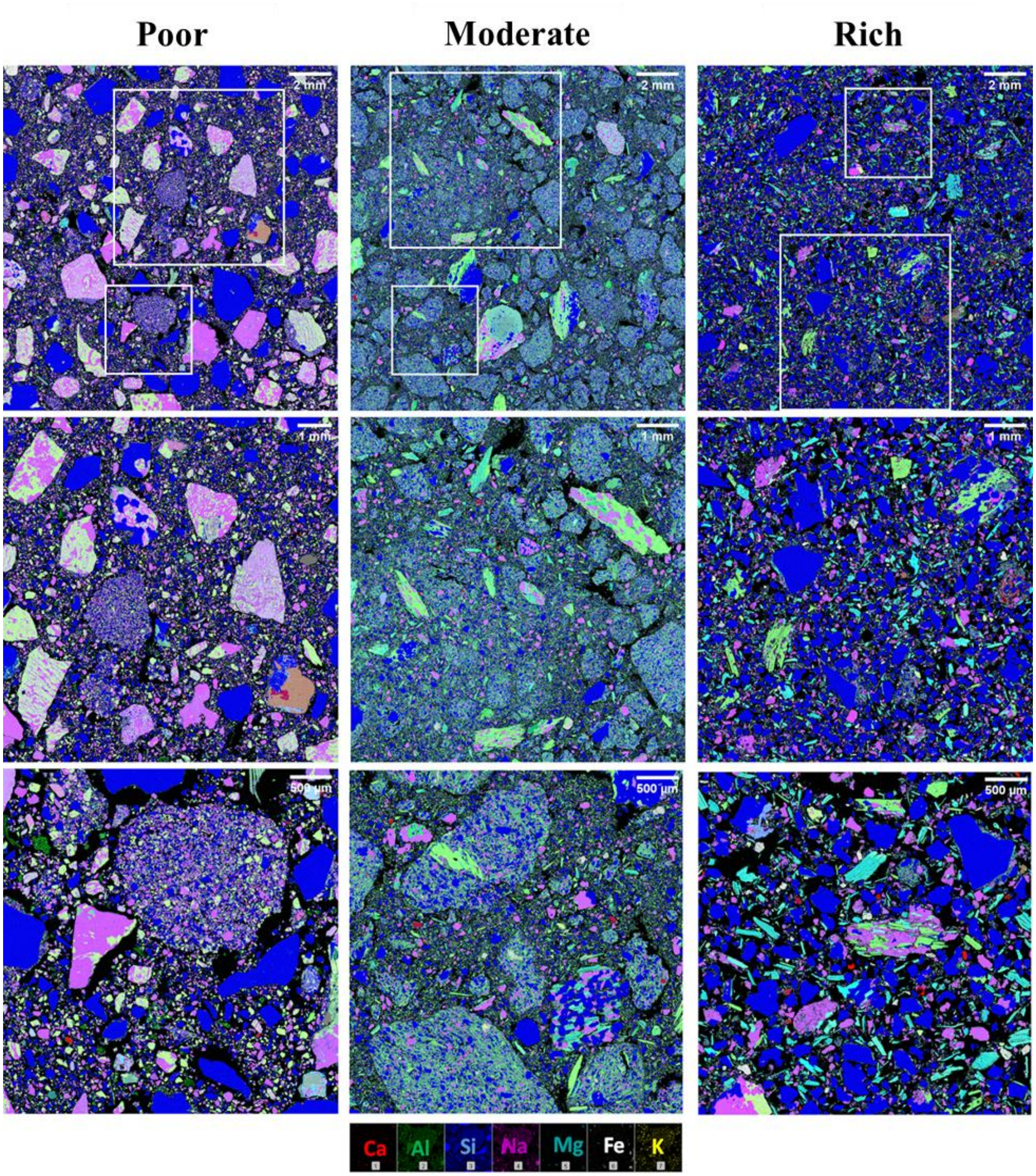

Supplemental Figure 3.3. Elemental maps for a representative soil sample per site at three different resolutions. Maps in the top row have a resolution of 20 um/pixel, middle row maps a resolution of 10um/pixel, and the bottom row a resolution of 5um/pixel. Images correspond to a seven-color band combination with resulting colors reflecting the cumulative composition in all analyzed elements. As a result, black pixels correspond to void spaces in the sample. Squares in the top maps indicate the location of the higher resolution maps.

References

Achat, D. L., Deleuze, C., Landmann, G., Pousse, N., Ranger, J., and Augusto, L. (2015). Quantifying consequences of removing harvesting residues on forest soils and tree growth - A meta-analysis. Forest Ecology and Management, 348, 124–141. https://doi.org/10.1016/j.foreco.2015.03.042

Achat, D. L., Martel, S., Picart, D., Moisy, C., Augusto, L., Bakker, M. R., and Loustau, D. (2018). Modelling the nutrient cost of biomass harvesting under different silvicultural and climate scenarios in production forests. Forest Ecology and Management, 429, 642–653. https://doi.org/10.1016/j.foreco.2018.06.047

Adams, M. B., Kelly, C., Kabrick, J., and Schuler, J. (2019). Temperate forests and soils (pp. 83–108). https://doi.org/10.1016/b978-0-444-63998-1.00006-9

Álvarez, E., Fernández-Marcos, M. L., Monterroso, C., and Fernández-Sanjurjo, M. J. (2005). Application of aluminium toxicity indices to soils under various forest species. In Forest Ecology and Management (Vol. 211, Issue 3, pp. 227–239). https://doi.org/10.1016/j.foreco.2005.02.044

Anda, M., Purwanto, S., Dariah, A., Watanabe, T., and Dahlgren, R. A. (2023). A 200-year snapshot of soil development in pyroclastic deposits derived from the 1815 super explosive eruption of Mount Tambora in Indonesia. Geoderma, 433. https://doi.org/10.1016/j.geoderma.2023.116454

April, R., and Newton, R. (1992). Mineralogy and Mineral Weathering. In Atmospheric Deposition and Forest Nutrient Cycling (pp. 378–425). Springer.

Armfield, J. R., Perdrial, J. N., Gagnon, A., Ehrenkranz, J., Perdrial, N., Cincotta, M., Ross, D., Shanley, J. B., Underwood, K. L., and Ryan, P. (2019a). Does stream water composition at sleepers river in vermont reflect dynamic changes in soils during recovery from acidification? Frontiers in Earth Science, 6. https://doi.org/10.3389/feart.2018.00246

Asmare, T. K., Abayneh, B., Yigzaw, M., and Birhan, T. A. (2023). The effect of land use type on selected soil physicochemical properties in Shihatig watershed, Dabat district, Northwest Ethiopia. Heliyon, 9(5). https://doi.org/10.1016/j.heliyon.2023.e16038

Augusto, L., Achat, D. L., Bakker, M. R., Bernier, F., Bert, D., Danjon, F., Khlifa, R., Meredieu, C., and Trichet, P. (2015). Biomass and nutrients in tree root systems-sustainable harvesting of an intensively managed Pinus pinaster (Ait.) planted forest. GCB Bioenergy, 7(2), 231–243. https://doi.org/10.1111/gcbb.12127

Barnes, W. A., Quideau, S. A., and Swallow, M. J. B. (2018). Nutrient distribution in sandy soils along a forest productivity gradient in the athabasca oil sands region of Alberta, Canada. Canadian Journal of Soil Science, 98(2), 277–291. https://doi.org/10.1139/cjss-2017-0074

Bennett, D. S, Wittkop, C.A., and Dicken, C.L. (2006). Bedrock Geologic Map of New Hampshire - A Digital Representation of the Lyons and others 1997 map and ancillary files: U.S. Geological Survey Data Series 215, scale 1:250,000

Boerner, R. E. J., Morris, S. J., Decker, K. L. M., and Hutchinson, T. F. (2003). Soil and Forest Floor Characteristics.

Bojórquez-Quintal, E., Escalante-Magaña, C., Echevarría-Machado, I., and Martínez-Estévez, M. (2017). Aluminum, a friend or foe of higher plants in acid soils. In Frontiers in Plant Science (Vol. 8). Frontiers Media S.A. https://doi.org/10.3389/fpls.2017.01767

Bonar, A. L., Soreghan, G. S., and Elwood Madden, M. E. (2023). Assessing Weathering, Pedogenesis, and Silt Generation in Granitoid-Hosted Soils from Contrasting Hydroclimates. Journal of Geophysical Research: Earth Surface, 128(7). https://doi.org/10.1029/2023JF007095

Bowden, R. D., Wurzbacher, S. J., Washko, S. E., Wind, L., Rice, A. M., Coble, A. E., Baldauf, N., Johnson, B., Wang, J., Simpson, M., and Lajtha, K. (2019). Long-term Nitrogen Addition Decreases Organic Matter Decomposition and Increases Forest Soil Carbon. Soil Science Society of America Journal, 83(S1). https://doi.org/10.2136/sssaj2018.08.0293

Bower, J. A., Ross, D. S., Bailey, S. W., Pennino, A. M., Jercinovic, M. J., McGuire, K. J., Strahm, B. D., and Schreiber, M. E. (2023). Development of a lateral topographic weathering gradient in temperate forested podzols. Geoderma, 439. https://doi.org/10.1016/j.geoderma.2023.116677

Brantley, S. L., and Lebedeva, M. (2011). Learning to read the chemistry of regolith to understand the critical zone. Annual Review of Earth and Planetary Sciences, 39, 387–416. https://doi.org/10.1146/annurev-earth-040809-152321

Brimhall, G. H., and Dietrich, W. E. (1986). Constitutive mass balance relations between chemical composition, volume, density, porosity, and strain in metasomatic hydrochemkai systems: Results on weathering and pedogenesis. Geochimica et Cosmochimica Acta, 51, 567–587.

Casetou-Gustafson, S., Akselsson, C., Hillier, S., and Olsson, B. A. (2019a). The importance of mineral determinations to PROFILE base cation weathering release rates: A case study. Biogeosciences, 16(9), 1903–1920. https://doi.org/10.5194/bg-16-1903-2019

Casetou-Gustafson, S., Akselsson, C., Hillier, S., and Olsson, B. A. (2019b). The importance of mineral determinations to PROFILE base cation weathering release rates: A case study. Biogeosciences, 16(9), 1903–1920. https://doi.org/10.5194/bg-16-1903-2019

Cincotta, M. M., Perdrial, J. N., Shavitz, A., Libenson, A., Landsman-Gerjoi, M., Perdrial, N., Armfield, J., Adler, T., and Shanley, J. B. (2019). Soil Aggregates as a Source of Dissolved Organic Carbon to Streams: An Experimental Study on the Effect of Solution Chemistry on Water Extractable Carbon. Frontiers in Environmental Science, 7. https://doi.org/10.3389/fenvs.2019.00172

Cleavitt, N. L., Battles, J. J., Johnson, C. E., and Fahey, T. J. (2018). Long-term decline of sugar maple following forest harvest, Hubbard Brook Experimental Forest, New Hampshire. Canadian Journal of Forest Research, 48(1), 23–31. https://doi.org/10.1139/cjfr-2017-0233

Coile, T. S. (1952). Soil and the Growth of Forests. Advances in Agronomy, 4, 329–398.

Cronan, C. S., and Grigal, D. F. (1995). Use of Calcium/Aluminum Ratios as Indicators of Stress in Forest Ecosystems. Journal of Environmental Quality, 24(2), 209–226. https://doi.org/10.2134/jeq1995.00472425002400020002x

Dijkstra, F. A., and Smits, M. M. (2002). Tree species effects on calcium cycling: The role of calcium uptake in deep soils. Ecosystems, 5(4), 385–398. https://doi.org/10.1007/s10021-001-0082-4

Dijkstra, F. A., Van Breemen, N., Jongmans, A. G., Davies, G. R., and Likens, G. E. (2003). Calcium weathering in forested soils and the effect of different tree species. Biogeochemistry, 62, 253–275.

Eberl, D. D., and Smith, D. B. (2009). Mineralogy of soils from two continental-scale transects across the United States and Canada and its relation to soil geochemistry and climate. Applied Geochemistry, 24(8), 1394–1404. https://doi.org/10.1016/j.apgeochem.2009.04.010

Ericsson, T. (1994). Nutrient Dynamics and Requirements of Forest Crops. New Zealand Journal of Forest Science, 24(2/3), 133–168.

Federer, C.A., and Hornbeck, J.W. 1985. The buffer capacity of forest soils in New England. Water Air Soil Pollut. 26: 163–173.

Fedo, C. M., Wayne Nesbitt, H., and Young, G. M. (1995). Unraveling the effects of potassium metasomatism in sedimentary rocks and paleosols, with implications for paleoweathering conditions and provenance. Geology, 23(10), 921–924. https://doi.org/10.1130/0091-7613(1995)023<0921:uteopm>2.3.co;2

Fink, J. R., Inda, A. V., Tiecher, T., and Barrón, V. (2016). Iron oxides and organic matter on soil phosphorus availability. In Ciencia e Agrotecnologia (Vol. 40, Issue 4, pp. 369–379). Federal University of Lavras. https://doi.org/10.1590/1413-70542016404023016

Finzi, A. C., Canham, C. D., and van Breemen, N. (1998). Canopy Tree-Soil Interactions within Temperate Forests: Species Effects on pH and Cations. Ecological Applications, 8(2), 447. https://doi.org/10.2307/2641084

Futter, M. N., Klaminder, J., Lucas, R. W., Laudon, H., and Köhler, S. J. (2012). Uncertainty in silicate mineral weathering rate estimates: Source partitioning and policy implications. Environmental Research Letters, 7(2). https://doi.org/10.1088/1748-9326/7/2/024025

Garrett, L. G., Smaill, S. J., Beets, P. N., Kimberley, M. O., and Clinton, P. W. (2021). Impacts of forest harvest removal and fertiliser additions on end of rotation biomass, carbon and nutrient stocks of Pinus radiata. Forest Ecology and Management, 493. https://doi.org/10.1016/j.foreco.2021.119161

Gee, G.W. and Bauder, J.W. (1986) Particle-Size Analysis. In: Klute, A., Ed., Methods of Soil Analysis, Part 1. Physical and Mineralogical Methods, Agronomy Monograph No. 9, 2nd Edition, American Society of Agronomy/Soil Science Society of America, Madison, WI, 383-411.

Goldich S.S. (1938) A study in rock-weathering. Journal of Geology, 46, 17–58.

Goyne, K. W., Brantley, S. L., and Chorover, J. (2006). Effects of organic acids and dissolved oxygen on apatite and chalcopyrite dissolution: Implications for using elements as organomarkers and oxymarkers. Chemical Geology, 234(1–2), 28–45. https://doi.org/10.1016/j.chemgeo.2006.04.003

Gradowski, T., and Thomas, S. C. (2006). Phosphorus limitation of sugar maple growth in central Ontario. Forest Ecology and Management, 226(1–3), 104–109. https://doi.org/10.1016/j.foreco.2005.12.062

Gruba, P., and Mulder, J. (2008). Relationship between Aluminum in Soils and Soil Water in Mineral Horizons of a Range of Acid Forest Soils. Soil Science Society of America Journal, 72(4), 1150–1157. https://doi.org/10.2136/sssaj2007.0041

Hazlett, P., Emilson, C., Lawrence, G., Fernandez, I., Ouimet, R., and Bailey, S. (2020). Reversal of forest soil acidification in the Northeastern United States and Eastern Canada: Site and soil factors contributing to recovery. Soil Systems, 4(3), 1–22. https://doi.org/10.3390/soilsystems4030054

Heřmanská, M., Voigt, M. J., Marieni, C., Declercq, J., and Oelkers, E. H. (2022). A comprehensive and internally consistent mineral dissolution rate database: Part I: Primary silicate minerals and glasses. Chemical Geology, 597.

Hornbeck, D.A., Sullivan, D.M., Owen, J., and Hart, J.M. (2019). Soil Test Interpretation Guide. EC 1478. Corvallis, OR: Oregon State University Extension Service.

Hornbeck, J. W., Smith, C. T., Martin, C. W., Tritton, L. M., and Pierce, R. S. (1990). Effects of Intensive Harvesting on Nutrient Capitals of Three Forest Types in New England. 30, 55–64.

Jackson, K., and Thomas Meetei, T. (2018). Influence of soil pH on nutrient availability: A Review. Journal of Emerging Technologies and Innovative Research, 5(12), 707–713. www.jetir.org

Jenny, H. (1941) Factors of Soil Formation: A System of Quantitative Pedology. Dover Publications, New York, 281 p.

Jien, S. H., Baillie, I., Huang, W. S., Chen, Y. Y., and Chiu, C. Y. (2016). Incipient ferralization and weathering indices along a soil chronosequence in Taiwan. European Journal of Soil Science, 67(5), 583–596. https://doi.org/10.1111/ejss.12363

JMP®, Version 17. SAS Institute Inc., Cary, NC, 1989–2023

Jordan, C. F. (1968). A simple, tension free lysimeter. Soil Science, 105(2), 81–86. https://doi.org/10.1097/00010694-196802000-00003.

Kang, J., Hesterberg, D., and Osmond, D. L. (2009). Soil Organic Matter Effects on Phosphorus Sorption: A Path Analysis. Soil Science Society of America Journal, 73(2), 360–366. https://doi.org/10.2136/sssaj2008.0113

Kaupenjohann, M., Zech, W., Hantschel, R., Horn, R., and Schneider, B. U. (1989). Mineral Nutrition of Forest Trees: A Regional Survey. In E.-D. Schulze, O. L. Lange, and R. Oren (Eds.), Forest Decline and Air Pollution (Vol. 77, pp. 282–294). Springer Berlin Heidelberg. https://doi.org/10.1007/978-3-642-61332-6

Kelly, E. F., Chadwick, O. A., and Hilinski, T. E. (1998). The effect of plants on mineral weathering. Biogeochemistry, 42, 21–53.

Kerr, J. G., and Eimers, M. C. (2012). Decreasing soil water Ca 2+ reduces DOC adsorption in mineral soils: Implications for long-term DOC trends in an upland forested catchment in southern Ontario, Canada. Science of the Total Environment, 427–428, 298–307. https://doi.org/10.1016/j.scitotenv.2012.04.016

Kolka, R. K., Grigal, D. F., and Nater, E. A. (1996). Forest soil mineral weathering rates: use of multiple approaches. In Geoderma (Vol. 73). ELSEVIER.

Koteff, C., and Pessl, F. (1981). Systematic Ice Retreat in New England. In Geological Survey Professional Paper 1179.

Kraepiel, A. M. L., Dere, A. L., Herndon, E. M., and Brantley, S. L. (2015). Natural and anthropogenic processes contributing to metal enrichment in surface soils of central Pennsylvania. Biogeochemistry, 123(1–2), 265–283. https://doi.org/10.1007/s10533-015-0068-5

Li, H., Zhao, Y., Weng, X., Zhou, Y., Zhang, S., Liu, L., and Pei, J. (2023). The Most Suitable Calcium Concentration for Growth Varies among Different Tree Species—Taking Pinus tabuliformis, Pinus sylvestris var. mongolica, Populus, and Morus alba as Examples. Forests, 14(7). https://doi.org/10.3390/f14071437

Liese, H. C. (1973). Mineral Composition of the Conway Granite in New Hampshire. GSA Bulletin, 84, 331–334.

Likens, G. E., Driscoll, C. T., Buso, D. C., Siccama, T. G., Johnson, C. E., Lovett, G. M., Fahey, T. J., Reiners, W. A., Ryan, D. F., Martin, C. W., and Bailey, S. W. (1998). The biogeochemistry of calcium at Hubbard Brook. In Biogeochemistry (Vol. 41).

Liu, X., Meng, W., Liang, G., Li, K., Xu, W., Huang, L., and Yan, J. (2014). Available phosphorus in forest soil increases with soil nitrogen but not total phosphorus: Evidence from subtropical forests and a pot experiment. PLoS ONE, 9(2). https://doi.org/10.1371/journal.pone.0088070

Lyons, J.B., Bothner, W.A., Moench, R.H., and Thompson Jr., J.B. (1997) Bedrock geologic map of New Hampshire. U.S. Geological Survey. https://doi.org/10.3133/70211051

Manning, D. A. C. (2022). Mineral stabilities in soils: how minerals can feed the world and mitigate climate change. Clay Minerals, 57(1), 31–40. https://doi.org/10.1180/clm.2022.17

McHale, M. R., McDonnell, J. J., Mitchell, M. J., and Cirmo, C. P. (2002). A field-based study of soil water and groundwater nitrate release in an Adirondack forested watershed. Water Resources Research, 38(4), 2-1-2–16. https://doi.org/10.1029/2000wr000102

McKenzie, N. N., Jacquier, D. D., Isbell, R. R., and Brown, K. K. (2004). Austrailian Soils and Landscapes (pp. 1-433). CSIRO Publishing.

Minocha, R., Long, S., Magill, A. H., Aber, J., and Mcdowell, W. H. (2000). Foliar free polyamine and inorganic ion content in relation to soil and soil solution chemistry in two fertilized forest stands at the Harvard Forest, Massachusetts. In Plant and Soil (Vol. 222).

Morris, D. M., Kwiaton, M. M., and Duckert, D. R. (2014). Black spruce growth response to varying levels of biomass harvest intensity across a range of soil types: 15-year results. Canadian Journal of Forest Research, 44(4), 313–325. https://doi.org/10.1139/cjfr-2013-0359

Nesbitt, H. W., and Young, G. M. (1982). Early Proterozoic climates and plate motions inferred from major element chemistry of Intites. Nature, 299, 715–717.

Nesbitt, H. W., and Young, G. M. (1989). Formation and Diagenesis of Weathering Profiles. The Journal of Geology, 97(2), 129–147. http://www.journals.uchicago.edu/t-and-c

Nezat, C. A., Blum, J. D., Klaue, A., Johnson, C. E., and Siccama, T. G. (2004). Influence of landscape position and vegetation on long-term weathering rates at the Hubbard Brook Experimental Forest, New Hampshire, USA. Geochimica et Cosmochimica Acta, 68(14), 3065–3078. https://doi.org/10.1016/j.gca.2004.01.021

Nezat, C. A., Blum, J. D., Yanai, R. D., Hamburg, S. P., and Filippelli, G. (2007). A sequential extraction to determine the distribution of apatite in granitoid soil mineral pools with application to weathering at the Hubbard Brook Experimental Forest, NH, USA. Applied Geochemistry, 22, 2406–2421. https://doi.org/10.1016/j.apgeochem.2007.06.012

Oh, N. H., Hofmockel, M., Lavine, M. L., and Richter, D. D. (2007). Did elevated atmospheric CO2 alter soil mineral weathering?: An analysis of 5-year soil water chemistry data at Duke FACE study. Global Change Biology, 13(12), 2626–2641. https://doi.org/10.1111/j.1365-2486.2007.01452.x

Olorunfemi, I. E., Fasinmirin, J. T., and Akinola, F. F. (2018). Soil physico-chemical properties and fertility status of long-term land use and cover changes: A case study in forest vegetative zone of Nigeria. Eurasian Journal of Soil Science, 7(2), 133–150. https://doi.org/10.18393/ejss.366168

Orton, T.G., Pringle, M.J., and Bishop, T.F.A. (2016). A one-step approach for modelling and mapping soil properties based on profile data sampled over varying depth intervals. Geoderma, 262, 174-186. https://doi.org/10.1016/j.geoderma.2015.08.013

Oursin, M., Pierret, M. C., Beaulieu, É., Daval, D., and Legout, A. (2023). Is there still something to eat for trees in the soils of the Strengbach catchment? Forest Ecology and Management, 527. https://doi.org/10.1016/j.foreco.2022.120583

Paul, E. A. (2016). The nature and dynamics of soil organic matter: Plant inputs, microbial transformations, and organic matter stabilization. In Soil Biology and Biochemistry (Vol. 98, pp. 109–126). Elsevier Ltd. https://doi.org/10.1016/j.soilbio.2016.04.001

Pichler, V., Gömöryová, E., Leuschner, C., Homolák, M., Abrudan, I. V., Pichlerová, M., Střelcová, K., Di Filippo, A., and Sitko, R. (2021). Parent material effects on soil organic carbon concentration under primeval european beech forests at a regional scale. Forests, 12(4). https://doi.org/10.3390/f12040405

Porter, V. M., Shanley, J. B., Sebestyen, S. D., and Liu, F. (2022). Controls on decadal, annual, and seasonal concentration-discharge relationships in the Sleepers River Research Watershed, Vermont, northeastern United States. Hydrological Processes, 36(3). https://doi.org/10.1002/hyp.14559

Ratcliffe, N.M., Stanley, R.S., Gale, M.H., Thompson, P.J., and Walsh, G.J. (2011). Bedrock geologic map of Vermont: U.S. Geological Survey Scientific Investigations Map 3184, 3 sheets, scale 1:100,000.

Richard, R., Kane, E., Bronson, D., and Kolka, R. (2022). Whole-Tree Harvest Effects on Macronutrients in an Oak-Dominated System after Seven Years. Forests, 13(10). https://doi.org/10.3390/f13101532

Richardson, J. B., and Friedland, A. J. (2016). Influence of coniferous and deciduous vegetation on major and trace metals in forests of northern New England, USA. Plant and Soil, 402(1–2), 363–378. https://doi.org/10.1007/s11104-016-2805-5

Richardson, J. B., and King, E. K. (2018). Regolith weathering and sorption influences molybdenum, vanadium, and chromium export via stream water at four granitoid Critical Zone Observatories. Frontiers in Earth Science, 6. https://doi.org/10.3389/feart.2018.00193

Richardson, J. B., Petrenko, C. L., and Friedland, A. J. (2017). Base cations and micronutrients in forest soils along three clear-cut chronosequences in the northeastern United States. Nutrient Cycling in Agroecosystems, 109(2), 161–179. https://doi.org/10.1007/s10705-017-9876-4

Richardson, J. B., and Zuñiga, L. X. (2021). Quantifying aluminosilicate manganese release and dissolution rates across organic ligand treatments for rocks, minerals, and soils. Acta Geochim. https://doi.org/10.1007/s11631

Righi, D. and Meunier, A., 1991. Characterization and genetic interpretation of clays in an acid brown soil (Dystrochrept) developed in a granitic saprolite. Clays and Clay Minerals, 39, pp.519-530.

Rogers, N. S., D’amato, A. W., and Leak, W. B. (2021). Long-term evolution of composition and structure after repeated group selection over eight decades. Canadian Journal of Forest Research, 51(7), 1080–1091. https://doi.org/10.1139/cjfr-2020-0339

Rout, G. R., and Sahoo, S. (2015). Role of Iron in Plant Growth and Metabolism. Reviews in Agricultural Science, 3(0), 1–24. https://doi.org/10.7831/ras.3.1

Roy, M. È., Surget-Groba, Y., Delagrange, S., and Rivest, D. (2021). Legacies of forest harvesting on soil properties along a chronosequence in a hardwood temperate forest. Forest Ecology and Management, 496. https://doi.org/10.1016/j.foreco.2021.119437

Safonov, O. G., Bindi, L., and Vinograd, V. L. (2011). Potassium-bearing clinopyroxene: a review of experimental, crystal chemical and thermodynamic data with petrological applications. Mineralogical Magazine, 75(4), 2467–2484. https://doi.org/10.1180/minmag.2011.075.4.2467

Schaberg, P. G., Tilley, J. W., Hawley, G. J., DeHayes, D. H., and Bailey, S. W. (2006). Associations of calcium and aluminum with the growth and health of sugar maple trees in Vermont. Forest Ecology and Management, 223(1–3), 159–169. https://doi.org/10.1016/J.FORECO.2005.10.067

Schachtman, D. P., Reid, R. J., and Ayling, S. M. (1998). Update on Phosphorus Uptake Phosphorus Uptake by Plants: From Soil to Cell. Plant Physiology, 116, 447–453. https://academic.oup.com/plphys/article/116/2/447/6085629

Schattman, R. E., Jean, H., Faulkner, J. W., Maden, R., McKeag, L., Nelson, K. C., Grubinger, V., Burnett, S., Erich, M. S., and Ohno, T. (2023). Effects of irrigation scheduling approaches on soil moisture and vegetable production in the Northeastern U.S.A. Agricultural Water Management, 287. https://doi.org/10.1016/j.agwat.2023.108428

Soil Survey Staff, Natural Resources Conservation Service, United States Department of Agriculture. Web Soil Survey. Available online. Accessed September 4, 2023.

St. Clair, S. B., Sharpe, W. E., and Lynch, J. P. (2008). Key interactions between nutrient limitation and climatic factors in temperate forests: A synthesis of the sugar maple literature. Canadian Journal of Forest Research, 38(3), 401–414. https://doi.org/10.1139/X07-161

Street, B. B., Rice, A. M., and Richardson, J. B. (2023). Forest floor and Na azide effect on elements in leachate from contrasting New Hampshire and Virginia forest soils. Soil Science Society of America Journal, 87(6), 1444–1457. https://doi.org/10.1002/saj2.20580

Sulieman, M., Saeed, I., Hassaballa, A., and Rodrigo-Comino, J. (2018). Modeling cation exchange capacity in multi geochronological-derived alluvium soils: An approach based on soil depth intervals. Catena, 167, 327-339. https://doi.org/10.1016/j.catena.2018.05.001

Tessier, A., C Campbell, P. G., and Bisson, M. (1979). Sequential Extraction Procedure for the Speciation of Particulate Trace Metals. Analytical Chemistry, 51(7), 844–851. https://pubs.acs.org/sharingguidelines

Tunesi, S., Poggi, V., and Gessa, C. (1999). Phosphate adsorption and precipitation in calcareous soils: the role of calcium ions in solution and carbonate minerals. In Nutrient Cycling in Agroecosystems (Vol. 53).

U.S. Geological Survey, Aziscohos Formation, Lower unnamed member at https://mrdata.usgs.gov/geology/state/sgmc-unit.php?unit=NHOCAzl%3B0. (Accessed September 7, 2023)

U.S. Geological Survey, Waits River Formation- Carbonaceous phyllite and limestone member at https://mrdata.usgs.gov/geology/state/sgmc-unit.php?unit=VTDSw%3B0. (Accessed September 7, 2023)

Vadeboncoeur, M. A., Hamburg, S. P., Yanai, R. D., and Blum, J. D. (2014). Rates of sustainable forest harvest depend on rotation length and weathering of soil minerals. Forest Ecology and Management, 318, 194–205. https://doi.org/10.1016/j.foreco.2014.01.012

Van Breemen, N., Finzi, A. C., and Canham, C. D. (1997). Canopy tree-soil interactions within temperate forests: effects of soil elemental composition and texture on species distributions 1.

Velbel, M. A. (1993). Constancy of silicate-mineral weathering-rate ratios between natural and experimental weathering: implications for hydrologic control of differences in absolute rates. Chemical Geology, 105, 89–99.

Wacket, A.A., Yoo, K., Amundson, R., Heimsath, A.M., and Jelinski, N.A. (2018). Climate controls on coupled processes of chemical weathering, bioturbation, and sediment transport across hillslopes. Earth Surface Processes and Landforms 43 (8), 1575-1590.

Walmsley, J. D., Jones, D. L., Reynolds, B., Price, M. H., and Healey, J. R. (2009). Whole tree harvesting can reduce second rotation forest productivity. Forest Ecology and Management, 257(3), 1104–1111. https://doi.org/10.1016/j.foreco.2008.11.015

Walthert, L., Graf Pannatier, E., and Meier, E. S. (2013). Shortage of nutrients and excess of toxic elements in soils limit the distribution of soil-sensitive tree species in temperate forests. Forest Ecology and Management, 297, 94–107. https://doi.org/10.1016/j.foreco.2013.02.008

Wang, Z., Hassan, M. U., Nadeem, F., Wu, L., Zhang, F., and Li, X. (2020). Magnesium Fertilization Improves Crop Yield in Most Production Systems: A Meta-Analysis. Frontiers in Plant Science, 10(January), 1–10. https://doi.org/10.3389/fpls.2019.01727

White, A. F., and Brantley, S. L. (2003). The effect of time on the weathering of silicate minerals: Why do weathering rates differ in the laboratory and field? Chemical Geology, 202(3–4), 479–506. https://doi.org/10.1016/j.chemgeo.2003.03.001

White, P. J., and Broadley, M. R. (2003). Calcium in plants. In Annals of Botany (Vol. 92, Issue 4, pp. 487–511). https://doi.org/10.1093/aob/mcg164

Wilson, S. G., Dahlgren, R. A., Margenot, A. J., Rasmussen, C., and O’Geen, A. T. (2022). Expanding the Paradigm: The influence of climate and lithology on soil phosphorus. Geoderma, 421. https://doi.org/10.1016/j.geoderma.2022.115809

Woodruff, L., Cannon, W. F., Smith, D. B., and Solano, F. (2015). The distribution of selected elements and minerals in soil of the conterminous United States. Journal of Geochemical Exploration, 154, 49–60. https://doi.org/10.1016/j.gexplo.2015.01.006

Xia, R., Zhang, S. Q., Li, J., Li, H., Ge, L. S., and Yuan, G. L. (2023). Spatial distribution and quantitative identification of contributions for nutrient and beneficial elements in top- and sub-soil of Huairou District of Beijing, China. Ecological Indicators, 154. https://doi.org/10.1016/j.ecolind.2023.110853

Zhang, Y., Rimstidt, D. J., Huang, Y., and Zhu, C. (2019). Kyanite far from equilibrium dissolution rate at 0–22 °C and pH of 3.5–7.5. Acta Geochimica, 38(4), 472–480. https://doi.org/10.1007/s11631-019-00347-9

Chapter 4

The influence of soil calcium and magnesium on forest biomass, nutrient dynamics, and timber value in actively managed New England forests

---

Submission in preparation for ***Forest Ecology and Management***

Authors

Alexandrea M. Rice[1,4*], Anthony W. D’Amato[3], Grace A. Smith[3], Nicolas Perdrial[2,3], Justin B. Richardson[1,4]

[1]Department of Environmental, Geographic, and Climates Sciences, University of Massachusetts Amherst, Amherst, MA, USA

[2]Department of Geography and Geosciences, University of Vermont, Burlington, VT, USA

[3]Rubenstein School of Environment and Natural Resources, University of Vermont, Burlington, VT, USA

[4]Present address: Department of Environmental Sciences, University of Virginia, VA, USA

*Corresponding Author: utw7wd@virignia.edu

4.0 Abstract

The availability of soil nutrients plays a fundamental role in shaping forest structure, productivity, and nutrient cycling. However, the influence of soil nutrient richness on merchantable wood volume and value remains poorly understood in glaciated landscapes. In this study, we investigated how soil calcium and magnesium availability influence tree biomass, nutrient concentrations and pools, and the economic value of merchantable trees across a natural soil fertility gradient. Forests were categorized as Poor, Moderate, or Rich based on soil Ca and Mg content. We quantified aboveground woody and foliar nutrient concentrations and pools across tree size classifications and genera to assess how nutrient richness influences forest productivity. We also used Monte Carlo simulations for wood quality to determine the value of merchantable wood along the nutrient richness gradient. We found that wood Ca, K, and P concentrations increased with increasing soil nutrient richness, whereas Mg concentrations were highest at the Moderate nutrient forest. Wood nutrient pools did not follow the expected pattern, as the Poor nutrient forest had the greatest total biomass, offsetting differences in nutrient concentrations when scaled to pools. Green leaf nutrient concentrations and pools had genera-specific trends, with green leaf Ca having the strongest relationship to soil nutrient richness, with more available soil Ca and Mg increasing green leaf Ca but not Mg concentrations. Surprisingly, merchantable wood volume did not differ across the soil nutrient richness gradient, suggesting that site-specific factors such as the nutrient availability of other elements, and the fact that these are young, recently glaciated soils may have a strong influence. Merchantable wood value was highest at the Moderate nutrient richness forest, suggesting that wood quality, rather than total volume were primary drivers of economic value. Our findings suggest that in young, recently glaciated soils, forests can be managed to produce comparable biomass and value even on Ca

and Mg poor soils. However, the sustainability of these practices is unknown and requires further investigation to inform best management practices.

4.1 Introduction

Intensive timber harvesting methods in the northeastern United States (U.S.), such as whole-tree harvesting and clearcutting, may accelerate nutrient depletion by removing essential elements from the ecosystem and lead to diminished tree regeneration and growth over time (Achat et al., 2015; Richardson et al., 2017; Ouimet et al., 2021). Whole-tree harvesting removes nutrient-rich components like branches, foliage, and in some cases stumps. This can lead to long-term reductions in soil nutrient availability and stocks (Thiffault et al., 2010). Studies across the northeastern United States have found that harvesting can decrease key nutrients, such as calcium (Ca), magnesium (Mg), potassium (K) and phosphorus (P), which raises concerns about long-term soil nutrient depletion and its effects on forest productivity (Carpenter et al., 2021; Richard et al., 2022). While some research suggests that removing harvest residues may have minimal impact on the composition of tree species or understory communities, other studies highlight that nutrient losses can hinder the survival and growth of regenerating trees, particularly high-value species like sugar maple (*Acer saccharum*; Achat et al., 2015; Marlow and Peart, 2014; Moore et al., 2012). Since tree harvesting depletes essential soil nutrients, understanding their role in tree physiology is crucial for assessing how nutrient losses may affect forest regeneration and long-term productivity.

Inorganic nutrients like Ca, Mg, K, and P serve key functions for tree growth and development. Phosphorus is essential for photosynthesis, nutrient uptake, and plant growth (Schachtman et al., 1998). Calcium is vital for plant structure, function, and overall development (White and Broadley, 2003). Magnesium plays an important role in plant energy as a component of chlorophyll (Dukic et al., 2023; Wang et al., 2020). Potassium is crucial for plant growth and function, regulating respiration and stomatal control (Kaiser, 1982). Much focus across the New

England region of the U.S. has examined nitrogen (N) because of historical N pollution and its greater demand by forests (Finzi and Canham, 2000; Lovett and Mitchell, 2004; Magill et al., 2004), and inorganic nutrients remain poorly characterized.

New England soils vary in nutrient availability and total abundance due to differences in parent material, weathering and historical disturbances (Nezat et al., 2008; Rice et al., 2024). In soil, there are two nutrient pools of particular interest, the total and plant available pools. Plant available nutrients are readily accessible for uptake by plants, while total nutrients are bound in minerals and released through weathering (Schlesinger and Bernhardt, 2013). Among the plant essential nutrients, P and Ca are often the most limiting, followed by K, with Mg the most abundant of the four (Vadeboncoeur et al., 2010). Phosphorus is often the first element to become depleted due to the low abundance of P-bearing minerals such as apatite and slow weathering rates (Gress et al., 2007; Nazet et al., 2008). Calcium is frequently the second most depleted element, partly due to historical acid rain impacts (Lawrence and Huntington, 1999; Vadebonceour et al., 2014). In these soils, Ca is most readily available when weathered from carbonate rich glacial till, otherwise, Ca exists in low bioavailable forms in more weathering resistant aluminosilicate minerals (Rice et al., 2024). Total soil K concentrations are generally higher in soils than P and Ca, however K can be depleted in particularly sandy soils with low cation exchange capacity (Tripler et al., 2006; Cornut et al., 2021). Of the four elements, Mg is typically the least limiting in New England soils due to its relative abundance in many parent materials. Inadequate soil nutrients may limit woody biomass production, impacting both economic and ecological resources. Nutrient limitations can hinder forest growth and health, potentially restricting species regeneration and diversity (Leak et al., 2014). Losses in soil nutrient fertility have been shown to reduce tree growth by 3-7% in the short term (Carpenter et al., 2021; Richard et al., 2022).

Soil nutrient richness plays a critical role in shaping forest ecosystems by influencing tree growth, species composition, and overall forest productivity (Lucash et al., 2012; Achat et al., 2018; St, Claire et al., 2008). Soil nutrient richness, a measure of the availability of essential elements, is influenced by several factors, including soil type, bedrock geology, and atmospheric deposition (Federer et al., 1989). In New England, bedrock geology is dominated by igneous and metamorphic rocks that range from nutrient-rich metamorphosed rocks such as marble, schist and shale, to nutrient-poor granites and quartzite. Soils in the region are largely derived from glacial till and glaciofluvial deposits with varying rock and mineralogical composition, which contributes to high variability and complexity in determining soil nutrient richness for a forest (Rice et al., 2024). The heterogeneity in glacial till and glaciofluvial mineralogy contributes to variations in soil nutrient richness, which is often manifested in differences in forest composition and productivity among forests, such as sugar maple-dominated forests on calcareous derived soils and greater American beech (*Fagus grandifolia*) abundance on acidic granite-derived soils (Juice et al., 2006; Leak and Sendak, 2002; Long et al., 2009; Siccama et al., 2007).

Understanding nutrient allocation and storage requires the consideration of tree size and species-specific characteristics (Otto and Watmough, 2021). Nutrient concentrations in foliage and woody biomass of trees vary with size, with smaller trees typically having higher concentrations than larger trees (Achat et al., 2018). Nutrient concentrations also vary among tree species, especially those that are sensitive to soil acidity and the nutrient richness of the soil. *Acer saccharum* is known to require higher concentrations of Ca in the soil and is sensitive to changes in Ca availability and acidity (Gauthier et al., 2015; Hallett et al., 2006; Hong et al., 2022; Long et al., 2009; Phillips and Watmough, 2012). In addition to *Acer saccharum*, *Fagus grandifolia* and *Betula alleghaniensis* (yellow birch) are also common hardwood species found within northeastern forests. In many areas, *Fagus grandifolia* often dominates the understory following harvests, or any partial canopy disturbance, by producing dense thickets of highly shade-tolerant root suckers which in return out compete more commercially desirable and less tolerant species like *Acer saccharum* and *Betula alleghaniensis* (Rogers et al., 2021). *Fagus* has also been found to dominate in forests with nutrient poor soil, whereas *Acer*, and *Fraxinus* are dominant on nutrient rich forests (Bakken and Cook, 1998; Kobe et al., 1995). Studies evaluating the effects of Ca and Mg on *Acer saccharum* found elevated concentrations of Ca, Mg, and P in tree foliage (Moore et al., 2000; Schaberg et al., 2006). Although these studies have been instrumental in determining the role of genera and tree size classification in forest nutrient dynamics, not much is known about how the nutrient content of young, previously glaciated, soils affect the efficacy and sustainability of harvests, especially potential impacts on merchantable wood volumes and their economic values.

Despite extensive research on forest dynamics, key knowledge gaps remain on how site nutrient richness influences aboveground nutrient storage and merchantable wood volume, particularly on young, glaciated soils. In this study, we utilized a natural soil Ca-Mg nutrient richness gradient across three Vermont and New Hampshire forests with similar management histories. Our primary objective was to investigate how site nutrient richness influences aboveground nutrient pools and merchantable wood volume. To achieve this objective, we addressed three specific research questions: (1) Does site nutrient richness affect aboveground nutrient concentrations and pools?, (2) Does tree size classification, and/or tree genera significantly affect aboveground foliar and woody nutrient pools?, (3) Does site nutrient richness, forest maturation stage, and/or tree genera significantly affect merchantable wood volume and overall forest value?

For the first research question, we hypothesized that the forest with high nutrient richness would exhibit greater aboveground nutrient (Ca, Mg, K, P) concentrations and pools, suggesting that belowground availability controls aboveground uptake. For the second question, we hypothesized that certain tree genera, particularly *Acer* and *Betula*, would exhibit increased nutrient uptake with greater belowground availability and during maturation from sapling to merchantable size due to luxury uptake. Lastly, for the third question, we hypothesized that total and genera-specific merchantable wood volume would be greatest at the nutrient-rich forest, leading to the highest overall economic value among forests. Overall, this study aims to quantify the influence of soil nutrients on aboveground woody, foliar, and merchantable wood biomass, providing valuable insights for sustainable forest management practices in the New England region.

4.2 Methods

4.2.1 Study area and soil physicochemical characteristics

This study investigated three managed U.S. New England forests with documented harvest histories: Bartlett Experimental Forest in central New Hampshire, Second College Grant in northern New Hampshire, and Clement Woodlot in eastern Vermont (Table 4.1). All three forests are located on mountainous landscapes and are dominated in varying proportions by American beech (*Fagus grandifolia*), sugar maple (*Acer saccharum*), yellow birch (*Betula alleghaniensis*), red maple (*Acer rubrum*), and white ash (*Fraxinus americana*) as the primary canopy species. Smaller components of pin cherry (*Prunus pensylvanica*) and striped maple (*Acer pensylvanicum*) were present in more recently harvested areas. All three forests have been managed with similar silvicultural approaches to establish uneven-aged forest structures which provide a unique set of forests for this study. In Bartlett Experimental Forests, specifically in the sampled compartments (5 and 6), harvesting has occurred through group selection. Historically, harvests initiated in the 1930s, followed by subsequent cuts in 1951, 1960, and the early to mid-1990s (Rogers et al., 2021; Yamasaki et al., 2014). In Second College Grant, within the management area that we sampled, harvesting has primarily utilized single-tree and group selection harvests over the past several decades. Prior to this period, harvests were largely characterized as targeted removal of conifers in the late 1800 and early 1900s and diameter-limit harvests of hardwood sawlogs in the 1950s (Jevon et al., 2019). Clement Woodlot is the only site that was historically cleared for agricultural uses (sheep pasture) with the forests developing following agricultural abandonment managed primarily with single-tree and group selection harvests beginning in the 1980s. All three forests were naturally regenerated.

Table 4.1. Site characteristics for each of the three forests used in this study including the location of each forest, bedrock geology and soil chemical traits. Error is standard error for the mean. Nutrient values were extracted from Rice et al., (2024). MAT = mean annual temperature, MAP = Mean annual precipitation

Forest	**Nutrient Richness‡**	**Lat.**	**Long.**	**MAT§**	**MAP§**	**Soil pH**	**Base Sat.**	**Total Soil Ca**	**Total Soil Mg**	**Total Soil K**	**Total Soil P**
		dd	dd	°C	mm		%	mg/g	mg/g	mg/g	mg/g
Bartlett Experimental Forest	Poor	44.048	-71.272	5.9	1406	4.11	5.04 ± 0.99	5.91 ± 0.41	3.09 ± 0.29	28.94 ± 1.2	1.18 ± 0.08
Second College Grant	Moderate	44.887	-71.130	4.1	1196	4.27	19.09 ± 3.0	5.69 ± 0.31	9.49 ± 0.42	10.83 ± 0.49	1.27 ± 0.07
Clement Woodlot	Rich	44.049	-72.311	5.5	1163	4.92	54.2 ±5.8	12.96 ± 0.54	27.3 ± 2.2	6.08 ± 0.58	1.24 ± 0.10

‡ *Nutrient richness is based upon Ca and Mg concentrations within parent material.*

§*PRISM Climate Group, Oregon State University, https://prism.oregonstate.edu, data created 4 Feb 2014, accessed 16 Dec 2020.*

Soils across the three forests range from poorly to somewhat excessively drained Spodosols and Inceptisols developed from glacial till and glaciofluvial deposits. The three forests studied exhibit a natural soil Ca-Mg gradient, with Bartlett Experimental Forest classified as the nutrient “Poor”, Second College Grant as the nutrient “Moderate”, and Clement Woodlot as the nutrient “Rich” forest. This gradient is due to the range in parent material composition (Ratcliffe et al., 2011; Rice et al., 2024) and is attributed to the variations in parent material compositions.

The Rich forest has a high abundance of amphiboles and sodium feldspar, the Moderate forest is dominated by clay and mica minerals, and the Poor forest is abundant in potassium and sodium feldspar (Rice et al., 2024). The Poor forest is predominantly mapped as Marlow Series which is a Coarse-loamy, isotic, frigid Oxyaquic Haplorthod (Soil Survey Staff, 2022). The Moderate forest is mainly mapped as the Peru Series which is a coarse-loamy, isotic, frigid Aquic Haplorthod. The Rich forest is mapped as predominantly the Colrain Series, a coarse-loamy, mixed, active, frigid Humic Dystrudept although our observations suggest the soil may be an Oxyaquic Eutrudept.

4.2.2 Tree mensuration and sampling

In each forest, we established fifteen circular, 400-m^2 plots. This standardized plot size ensured compatibility with long-term studies in the region, facilitating data comparison and synthesis (Rogers et al., 2021). To ensure a representative sample within each forest, plots were categorized into three developmental stages (young, intermediate, mature) based on species composition, tree diameter at breast height (DBH), and time since the last record harvest, with five plots per stage.

Within each plot, all trees with a DBH $\geq$ 10.1 cm were identified to species. Trees were further classified into five size classes based on DBH: sapling (2.5 - 12.6 cm), poletimber (softwoods: 12.6 - 23 cm; hardwoods: 12.6 - 28 cm), small sawtimber (28 - 33 cm), medium sawtimber (33 - 40.5 cm) and large sawtimber (> 40.5 cm). This size classification was defined by Luppold and Pug (2016). Only poletimber and sawtimber trees were considered for merchantable wood volume calculations.

Green leaves and small branches were collected from at least one individual of each of the three most abundant tree species (*Acer, Betula,* and *Fagus*) within each of the 15 plots within each forest. If a target species was absent from a plot, samples were collected from the two most frequent tree species present. Sampling occurred in mid-July 2022 from the mid-canopy of healthy trees with full canopies using a Notch Big Shot slingshot with a tethered throw weight. Mid July was chosen because by this time of the year tree leaves have fully expanded and their nutrient concentrations are stable. A minimum of ten leaves and two branches were collected from each sampled tree. Healthy trees were defined as those with vibrant green foliage, a full canopy, strong branches free from excessive cracks or breaks, and bark free from excessive cracks, peeling or signs of disease and insect infestation.

4.2.3 Sample Processing and inorganic nutrient analyses

4.2.3.1 Leaf and Branch Processing

Each branch and green leaf sample was ground to < 2 mm using a Model 4 Thomas Wiley Mill, and a 0.50 g homogenized subsample was ashed at 500 °C for 8 hrs to remove organic matter, which can reduce the efficiency of the subsequent acid digestion. The ash was then digested with 5 mL of reverse aqua regia (9 HNO_3 : 1 HCl) at 90º C for 45 min, a procedure recognized as a pseudototal digestion (Quevauviller, 1998). For quality control and assurance, every 20 samples were accompanied by a preparation blank, a duplicate sample, and two certified reference materials (NIST 1547a Peach leaves and NIST 1537a Tomato leaves). Digests were then diluted to 50 mL with deionized water, followed by a further dilution of a 3 mL subsample to 15 mL for elemental analysis. Concentrations of inorganic nutrients (Ca, Mg, K, P) were measured using an Agilent 5110 Inductively Coupled Plasma Optical Emission Spectrometer (ICP-OES; Agilent Technology, Santa Clara, California, USA). Recoveries for pseudototal digests of Ca, K, Mg, and P in the certified reference materials ranged from 81 – 112 % of their certified values. The coefficient of variation for duplicate samples was < 7 % for all elements analyzed. Metal concentrations in the preparation blanks were < 0.1 % of their analyte concentrations.

4.2.4 Calculations and assumptions

4.2.4.1 Woody and foliar biomass concentrations and pools

Our analysis focused on six dominant tree genera (*Acer*, *Betula*, *Fagus*, *Fraxinus*, *Prunus*, *Tsuga*). Tree genera that accounted for less than 3 % of the total basal area across each forest were not analyzed individually but instead were grouped into a single category labeled "Other". The only exception was *Picea,* which comprised 12 % of the basal area at the Rich forest and was therefore retained as a distinct genus in the analysis. These genera included in the "Other" category were *Abies*, *Amelanchier*, *Malus*, *Ostrya*, *Picea*, *Pinus*, *Populus,* and *Quercus*. Stand age affected composition, with early-successional species such as *Prunus pensylvanica*, and *Acer pensylvanicum* present in younger plots. Basal area was calculated using only live trees. Although standing dead trees were not explicitly excluded, there were rarely present in the plots. Of the 972 trees measured, only one was a snag and no additional standing dead trees were encountered during sampling.

Woody and foliar biomass were estimated for each tree using the allometric equation utilized by Ter-Mikaelian and Korzukhin (1997) with regional and state-specific data for tree species (Eq 1).

$$M= a\,(D)^b \qquad (1)$$

Where M is the oven dried mass (kg) of the biomass component of the tree (stem, branch or foliage), D is diameter at breast height (cm), and *a* and *b* are regional species-specific parameters that vary depending on the tree component. If *a* and *b* parameters were not published for a specific species, the parameters were used from the most closely related species within the same genus or family.

Branches and green leaf concentrations of Ca, Mg, K, and P were scaled from the digest to a per dry weight concentration prior to statistical analyses and calculation of nutrient pools. If elemental concentrations for a specific species were missing within a plot, values were used from the tree species within the plot that were most closely related based on genera, family, function, and DBH similarities. Further, woody (kg m^{-2}; Eq. 2) and foliar (g m^{-2}; Eq. 3) nutrient pools were calculated for each element (Ca, Mg, K, P) using the following equations:

$$\text{Wood Nutrient Pool} = \sum (M_{wood,i} * C_{wood,i}) \qquad (2)$$

$$\text{Foliar Nutrient Pool} = \sum (M_{foliar,i} * C_{foliar,i}) \qquad (3)$$

where $M_{wood,i}$ represents the wood (stem + branches) biomass of the *i*th species, and $C_{wood,i}$ represents the total wood nutrient concentration of the i^{th} species. Similarly, $M_{foliar,i}$ represent the foliar biomass of the *i*th species and $C_{foliar,i}$ represent the foliar nutrient concentration of the *i*th species. The sums were calculated for each genus within each of the 15 plots within each forest.

4.2.4.2 Merchantable wood volume

Total merchantable wood volume and value were calculated for each of the 45 forest plots and summarized by forest nutrient richness. Merchantable wood refers to the estimated volume of usable stem wood suitable for commercial timber products which typically exclude branches and leaves. Only trees with sufficient DBH (>12.5 cm) were considered merchantable. This threshold reflects the minimum size generally accepted for commercial harvesting. In total, 761 trees met this criterion and were included in the analysis. To calculate merchantable wood volume, first the merchantable height of each tree was calculated using an equation published by Ek et al. (1984). This equation utilizes species-specific coefficients within the northeastern U.S. region. Next, merchantable wood volume was calculated using Honer's equation (Honer et al., 1983), which uses merchantable tree height, DBH, and species-specific regression coefficients. For species without reported coefficients, the coefficients of the most closely related genus were used first, followed by those of the same family.

To estimate the economic value of each merchantable tree, we first calculated the number of 4.88 m (commonly, 16-foot) saw logs that could be cut based on merchantable stem height. Board foot was then estimated using the International ¼ Inch Rule which calculated usable lumber volume based on DBH and log count while accounting for material lost during milling (e.g. a ¼ inch saw kerf). This rule is widely used in our study region and is considered the most accurate for regional timber assessments.

4.2.4.3 Monte Carlo simulation of wood value

To estimate the variability in total merchantable wood value across the forest nutrient richness gradient, we conducted Monte Carlo simulations with 10,000 iterations. These simulations were designed to account for uncertainty in wood quality which was not directly assessed in the field (e.g. stem straightness, defects, or rot).

Tree timber value for each tree was calculated by multiplying the estimated board foot by species-specific stumpage prices that were dependent on wood quality. Timber values were obtained from the New Hampshire Department of Revenue Administration using average prices reported for the Northern Region for the period of October 1, 2024 to March 31, 2025 (revenue.nh.gov/taxes-glance/timber-tax; Table 4.2). For each species, stumpage prices were published as “low” and “high” which we interpreted as proxies for low- and high-quality wood, respectively. To represent mid-quality timber, we used the midpoint between the published low and high values.

We modeled four scenarios to capture a range of plausible wood quality distributions: 1) all wood classifies as pulpwood with value randomized within the reported low and high price range; 2) a fixed distribution of low (23%), mid (36%), and high (41%) quality timber; 3) a fixed distribution including pulpwood (17%), low (25%), mid (35%), and high (23%) quality wood based on harvest observation reported by Luppold and Pugh (2016); and 4) a randomized distribution of pulpwood and sawtimber quality classes with proportions drawn from a uniform distribution (0-1) and normalized to sum to one in each iteration. This simulation framework provides a robust estimation of both the mean and range of total merchantable wood values across the forest nutrient richness gradient by explicitly incorporating price uncertainty and variation in wood quality.

Table 4.2. Estimated monetary value for tree species by wood quality for northern New Hampshire, including pulpwood and sawlog values. Pulpwood values are reported per metric ton, while sawlog values are reported per thousand board feet (MBF). The values for each species and wood quality were derived from the New Hampshire Department of Revenue Administration's Average Stumpage Value Information for October 1, 2024 to March 31, 2025.

Species	Pulpwood Low Value ($ ton^{-1})	Pulpwood High Value ($ ton^{-1})	Sawlog Low Value ($ MBF^{-1})	Sawlog High Value ($ MBF^{-1})
Abies balsamea	$0	$4.41	$120	$175
Acer rubrum	$3.31	$11.02	$100	$225
Acer saccharum	$3.31	$11.02	$225	$450
Betula alleghaniensis	$3.31	$11.02	$150	$300
Betula papyrifera	$3.31	$11.02	$100	$220
Fagus grandifolia	$3.31	$11.02	$30	$120
Fraxinus americana	$3.31	$11.02	$130	$250
Picea glauca	$0	$4.41	$120	$175
Pinus strobus	$0	$3.31	$120	$200
Populus tremuloides	$3.31	$11.02	$30	$120
Quercus rubra	$3.31	$11.02	$200	$425
Tsuga canadensis	$0.55	$5.51	$30	$70

4.2.5 Statistics

All statistical analyses were performed using R software (Developmental Core Team, 2024). To meet the assumption of normality required for analysis of variance (ANOVA), woody and foliar concentrations of Ca, Mg, K, and P as well as woody and foliar nutrient pools, were log-transformed prior to analyses. Linear mixed-effects models were used to analyze woody and foliar nutrient concentrations and pools, accounting for the random variation within plots nested within developmental stages. A Type III ANOVA, implemented using the ‘car’ package, was performed to assess the effects of forest nutrient richness, tree size classification, tree genera, and the interaction of forest nutrient richness with tree size classification as well as with tree genera. Post-hoc Tukey Honest Significant Difference tests were conducted to determine significant differences between group means when main effects and interactions were found to be significant. The normality of residuals was checked using the Shapiro-Wilk test.

4.3 Results

4.3.1 Forest genera composition and biomass across nutrient gradient

Forest genera varied along the nutrient richness gradient, with a higher proportion of *Fagus* and lower proportion of *Acer* at the Poor forest than the other two forests. *Acer* had the highest overall abundance across all forests, with the Moderate forest having the greatest abundance across all tree size classes. The Poor forest was characterized by a relative abundance of *Fagus* (27.3 %), *Acer* (21.0 %), and *Betula* (18.1%). Within our sampling plots, *Tsuga* was only present at the Poor forest. Conversely, the Moderate forest was dominated by *Acer* (62.5 %), followed by *Betula* (18.6 %), and *Fagus* (15.1%). The Rich forest had a different composition, with *Acer* (49.3 %) and *Fraxinus* (18.6 %) as the most abundant genera, followed by *Fagus* (10.9 %). For our analyses, we focused on six common hardwood genera most abundant across the three forests: *Acer*, *Betula*, *Fagus*, *Fraxinus*, *Prunus*, and *Tsuga* (Figure 4.1). All other tree genera were categorized as “Other”.

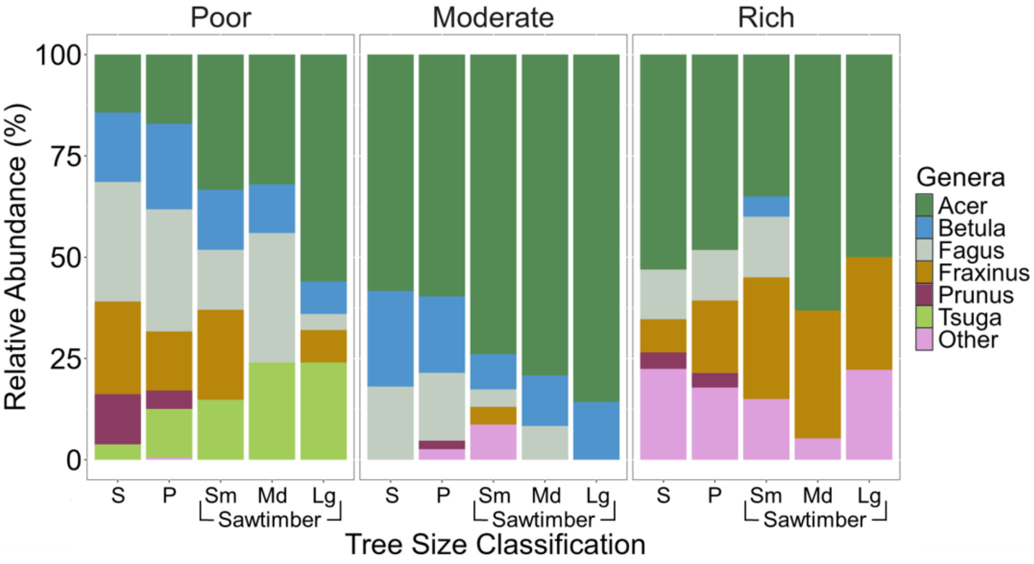

Figure 4.1. Relative abundance for each genus and tree size classification across the nutrient richness gradient. The six most abundant genera are shown, with less abundant genera categorized as “Other”. On the x-axis, tree size classifications are represented as follows: “S” for sapling, “P” for poletimber, “Sm” for small sawtimber, “Md” for medium sawtimber, and “Lg” for large sawtimber.

Stem density decreased across forest nutrient richness, with the Poor forest (0.0634 stems m^{-2}) exhibiting the highest stem density followed by the Moderate (0.0527 stems m^{-2}) and the lowest in the Rich forest (0.0455 stems m^{-2}; Table 4.3). This trend was also observed across all genera. Poletimber consistently had the highest stem density, while large sawtimber had the lowest among all tree size classes. Similarly, basal area followed this pattern with higher values observed in the Poor forest (26.89 cm^2 m^{-2}) and the lowest generally at the Moderate forest (19.2 cm^2 m^{-2}; Table 4.3). For all genera and genera-specific values, basal area was highest in poletimber and lowest in saplings.

Table 4.3. Stem density (stems m^{-2}) and basal area (cm m^{-2}) across forest nutrient richness and tree size classifications. Data are presented for all genera as well as the most common tree genera (*Acer*, *Betula*, *Fagus*). Basal area units (cm^2 m^{-2}) are equivalent to the commonly reported units in forestry (m^2 ha^{-1}).

	Forest Nutrient Richness	**Tree Size Classification**				
		Sapling	Poletimber	Small Sawtimber	Medium Sawtimber	Large Sawtimber
Stem Density (stems m^{-2})	Poor	0.0174	0.0331	0.0045	0.0042	0.0042
	Moderate	0.0120	0.0317	0.0038	0.0040	0.0012
	Rich	0.0081	0.0279	0.0033	0.0032	0.0030
All Genera Basal Area (cm^2 m^{-2})	Poor	1.75	8.87	3.26	4.34	8.67
	Moderate	1.21	8.99	2.79	4.13	2.12
	Rich	0.84	7.64	2.49	3.45	7.06
Acer Basal Area (cm^2 m^{-2})	Poor	0.25	1.65	1.13	1.38	5.09
	Moderate	0.71	5.47	2.08	3.28	1.81
	Rich	0.46	3.78	0.78	2.13	2.83
Betula Basal Area (cm^2 m^{-2})	Poor	0.31	1.74	0.44	0.49	0.54
	Moderate	0.28	1.53	0.24	0.50	0.31
	Rich	-	-	0.14	-	-
Fagus Basal Area (cm m^{-2})	Poor	0.50	2.69	0.51	1.42	0.53
	Moderate	0.22	1.50	0.13	0.35	-
	Rich	0.10	1.03	0.35	-	-

The general distribution of DBH was similar across the forest nutrient richness gradient, with the highest stem counts occurring in the smallest diameter classes and a steep decline as DBH increased (Figure 4.2). The majority of stems fell within the 5 - 20 cm DBH range, with relatively few exceeding 50 cm. However, differences were observed among nutrient richness categories within specific DBH classes. The Poor forest had slightly higher stem counts in the smaller DBH classes compared to the Moderate and Rich forests. A similar trend was observed for DBH classes greater than 50 cm, although the differences were less pronounced.

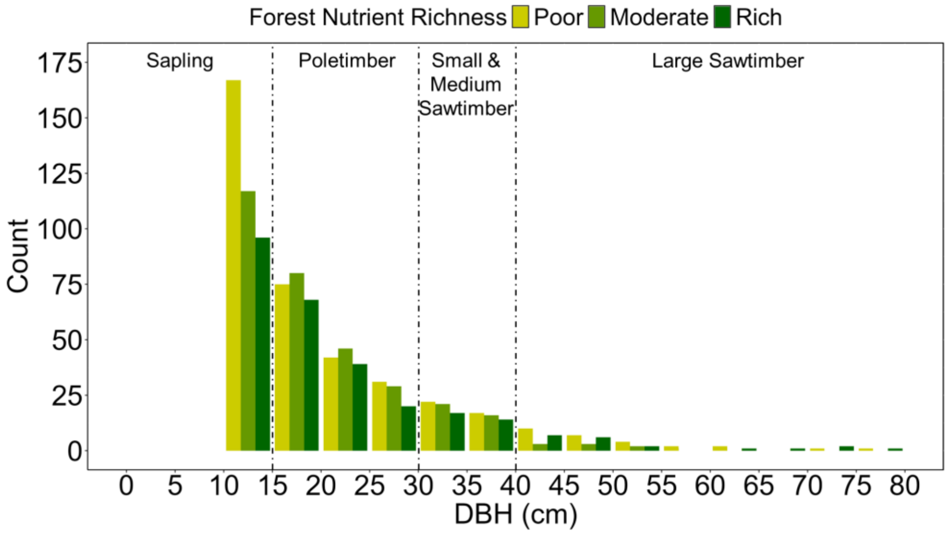

Figure 4.2. Diameter distribution of trees across the forest nutrient richness gradient. Bars represent the total number of trees measured across the 15 plots within each forest, grouped into 5 cm DBH increments. Bar colors indicate different forest nutrient richness categories.

Woody biomass generally exhibited the highest values in the Poor forest (15.2 kg m^{-2}) and lowest at the Moderate forest (11.4 kg m^{-2}; Table 4.4). This trend was observed across “all genera” and was mostly consistent across *Acer*, *Betula*, and *Fagus*. Summing across all genera and comparing them among each genus, poletimber had the highest woody biomass.

Foliar biomass followed similar trends to woody biomass (Table 4.4). The Poor forest (660 g m^{-2}) had overall the highest foliar biomass values, while the Rich forest had the lowest (493 g m^{-2}). All genera had decreasing foliar biomass from Poor forest to Rich forest (Table 4.4). Overall, the poletimber tree size had the highest foliar biomass out of the five classifications. Across all size classes, saplings consistently had the lowest foliar biomass (Table 4.4).

Table 4.4. Woody (kg m^{-2}) and foliar (g m^{-2}) biomass across forest nutrient richness and tree size classifications. Data are presented for all genera as well as the most common tree genera (*Acer*, *Betula*, *Fagus*).

	Forest Nutrient Richness	**Tree Size Classification**				
		Sapling	Poletimber	Small Sawtimber	Medium Sawtimber	Large Sawtimber
All Genera Woody Biomass (kg m^{-2})	Poor	0.65	4.23	1.76	2.54	6.04
	Moderate	0.48	4.61	1.72	2.87	1.73
	Rich	0.34	3.82	1.48	2.27	4.07
Acer Woody Biomass (kg m^{-2})	Poor	0.07	0.80	0.62	0.76	3.93
	Moderate	0.27	2.79	1.35	2.27	1.50
	Rich	0.17	1.93	0.57	1.52	2.39
Betula Woody Biomass (kg m^{-2})	Poor	0.12	0.81	0.25	0.30	0.41
	Moderate	0.11	0.75	0.15	0.33	0.24
	Rich	-	-	0.09	-	-
Fagus Woody Biomass (kg m^{-2})	Poor	0.23	1.59	0.37	1.12	0.53
	Moderate	0.10	0.90	0.09	0.27	-
	Rich	0.05	0.61	0.25	-	-
All Genera Foliar Biomass (g m^{-2})	Poor	41.3	197	69.6	99.3	253
	Moderate	27.5	229	86.8	132	81.0
	Rich	17.7	166	58.8	91.3	159
Acer Foliar Biomass (g m^{-2})	Poor	10.9	45.6	29.9	33.4	181
	Moderate	17.7	154	71.6	117	75.4
	Rich	9.87	105	30.1	79.0	120
Betula Foliar Biomass (g m^{-2})	Poor	6.23	36.7	8.64	9.56	9.83
	Moderate	5.16	28.1	4.36	9.15	5.60
	Rich	-	-	2.57	-	-
Fagus Foliar Biomass (g m^{-2})	Poor	10.6	51.6	9.09	24.5	8.32
	Moderate	4.59	28.6	2.28	5.97	-
	Rich	2.12	19.6	6.21	-	-

4.3.2 Effects of soil nutrient richness on aboveground nutrients

4.3.2.1 Wood nutrient concentrations and pools

Forest nutrient richness significantly influenced wood Ca, Mg, K, and P concentrations (all $p<0.01$; Figure 4.3). Wood Ca concentrations generally followed the nutrient richness gradient with the Rich (8.18 g kg^{-1}) and Moderate (8.17 g kg^{-1}) forest having the highest concentrations, and the lowest at the poor (5.65 g kg^{-1}; $p < 0.01$). Wood Mg concentrations did not follow the nutrient richness gradient. The Moderate forest had significantly higher wood Mg concentrations (0.93 g kg^{-1}) than the Rich forest (0.77 g kg^{-1}; $p < 0.01$) and the Poor forest (0.64 g kg^{-1}; $p < 0.01$). The Rich forest had significantly higher wood Mg concentrations than the Poor forest ($p < 0.01$). Wood K concentrations were highest at the Rich forest (2.75 g kg^{-1}) and lowest at the Poor (1.64 g kg^{-1}; $p < 0.01$) and Moderate (1.60 g kg^{-1}; $p < 0.01$) forests. Wood K concentrations were not significantly different between the Poor and Moderate forests ($p = 0.15$). Wood P concentrations were significantly different among the forest nutrient richness gradient ($p < 0.01$). Wood P concentrations at the Rich (0.72 g kg^{-1}) and Moderate (0.59 g kg^{-1}) forests were significantly higher than the Poor (0.54 g kg^{-1}; $p < 0.01$) forest. Wood P concentrations at the Rich and Moderate forests were similar ($p = 0.51$).

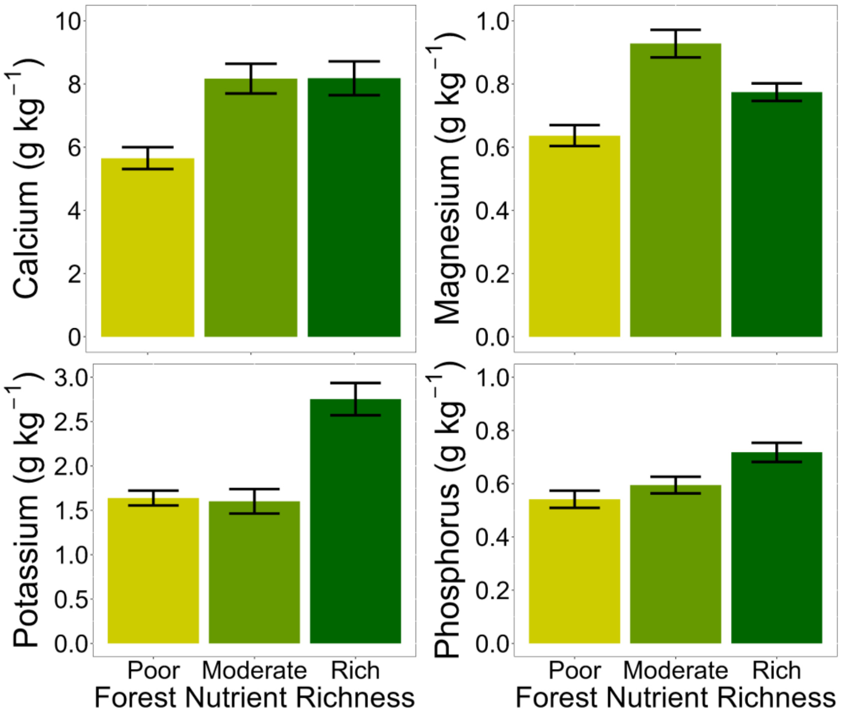

Figure 4.3. Wood nutrient concentrations (Ca, Mg, K, P) across the forest nutrient richness gradient. Values were calculated from elemental concentrations of branch samples. Each bar presents the average across plots (n = 15) within each forest, and error bars indicate standard errors.

Additionally, the concentrations of wood nutrients varied across forest nutrient richness and tree genera for all four elements ($p < 0.01$) but not between forest nutrient richness and tree size classification ($p > 0.80$). The forest nutrient richness influenced wood Ca, Mg, K, and P concentrations differently depending on the tree genera (Figure 4.4). Wood nutrient concentrations were significantly influenced by forest nutrient richness in *Acer*, *Betula,* and *Fagus* but rarely *Fraxinus*, *Prunus*, and *Tsuga.* Specifically, *Acer* had significantly higher wood Ca, Mg, and K at the Moderate and Rich forests compared to the Poor forest (p <0.01), while P concentrations remained the same across the nutrient richness gradient ($p > 0.82$). Similarly, *Betula* wood Ca, Mg, and P concentrations were higher in Moderate and Rich forests compared to the Poor forest ($p < 0.01$), although K concentrations did not differ significantly ($p = 0.07$). *Fagus* displayed a contrasting trend, with wood Ca, and Mg concentrations significantly higher at the Poor and Moderate forests compared to the Rich forest ($p < 0.01$), and higher wood K concentrations in the Poor and Moderate forests compared to the Rich forest ($p < 0.01$). Forest nutrient richness did not influence *Fagus* wood P concentrations ($p > 0.98$). *Prunus* had significant differences in only wood Mg concentrations, with higher concentrations at the Moderate and Rich forests compared to the Poor forest ($p = 0.04$), and in wood K concentrations with higher concentrations at the Rich forest compared to the Poor and Moderate forests ($p < 0.01$). Forest nutrient richness did not influence *Prunus* wood P concentrations ($p > 0.98$).

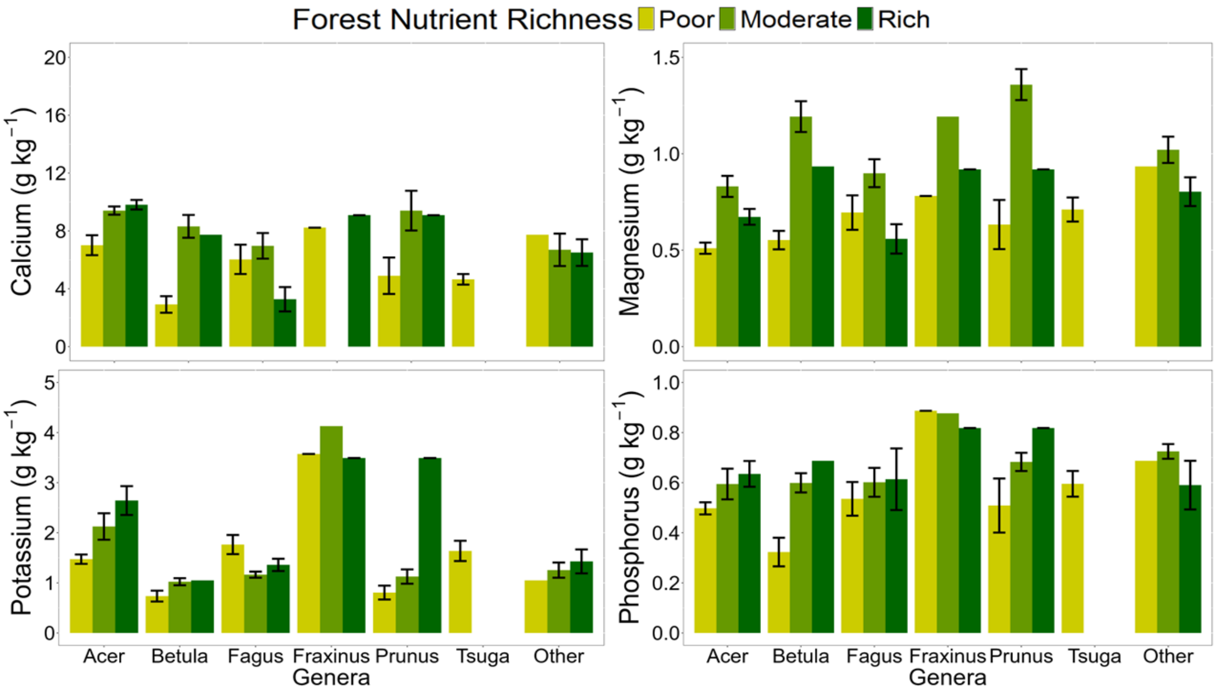

Figure 4.4. Wood nutrient concentrations (Ca, Mg, K, P) forest nutrient richness and genera. Values were calculated from elemental concentrations of branch samples. Each bar represents the average across plots within each forest (n = 15) with error bars as standard error.

Forest nutrient richness also significantly influenced woody Ca, Mg, and P pools (all $p < 0.01$), but not K ($p = 0.11$; Figure 4.5). The Moderate forest had significantly higher wood Ca pools (81.4 g m^{-2}) than both the Rich (62.7 g m^{-2}; $p = 0.01$) and Poor forests (62.6 g m^{-2}; $p < 0.01$). Similarly, the Moderate forest also exhibited significantly higher wood Mg pools (7.96 g m^{-2}) compared to both Poor (6.66 g m^{-2}; $p < 0.01$) and Rich forests (5.83 g m^{-2}; $p = 0.01$). Wood Mg pools in Poor and Rich forests did not differ significantly ($p = 0.72$). Unlike Ca and Mg, forest nutrient richness did not significantly affect wood K pools ($p = 0.11$), with mean values ranging from 14.8 g m^{-2} (Rich) to 15.9 (Moderate). For wood P pools, the Rich (5.68 g m^{-2}; $p < 0.01$) and Moderate forest (5.42 g m^{-2}; $p < 0.01$) had significantly higher pools than the Poor forest (4.94 g m^{-2}). There were no significant differences between the Rich and Moderate forests ($p = 0.92$).

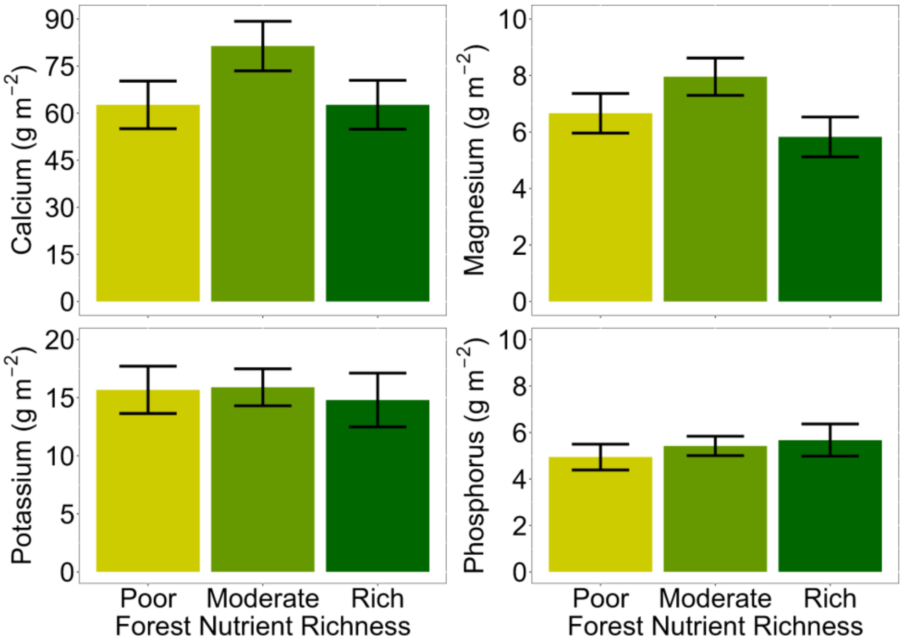

Figure 4.5. Wood nutrient pools (Ca, Mg, K, P) across the forest nutrient richness gradient. Values were calculated from elemental concentrations of branch samples and allometric equations for estimating tree wood (kg) from diameter at breast height. Each bar represents the average across plots within each forest (n = 15) with error bars as standard error.

Wood nutrient pools varied significantly across forest nutrient richness and tree genera for all four elements (Ca, Mg, K, P; $p < 0.01$; Figure 4.6), but not with tree size classification ($p > 0.49$). Specifically, *Acer* had higher wood Ca, Mg, and K pools in Moderate and Rich forests compared to the Poor forest ($p < 0.01$), with no significant difference in wood P pools ($p = 0.06$). *Betula* had significantly higher Ca pools at the Moderate and Rich forests compared to the Poor forest ($p < 0.01$), while wood Mg ($p = 0.76$), K ($p = 1.0$), and P ($p = 0.57$) pools did not differ. *Fagus* had a different pattern, with no significant difference in wood Ca pools ($p = 0.08$), wood Mg pools ($p = 0.41$) or wood P pools ($p = 0.68$), but wood K pool differed significantly with the Poor forest having higher K pools than the Moderate and Poor forests ($p < 0.01$). Neither

Fraxinus nor *Prunus* wood nutrient pools differed across the forest nutrient richness gradient (p =1.0 for all elements).

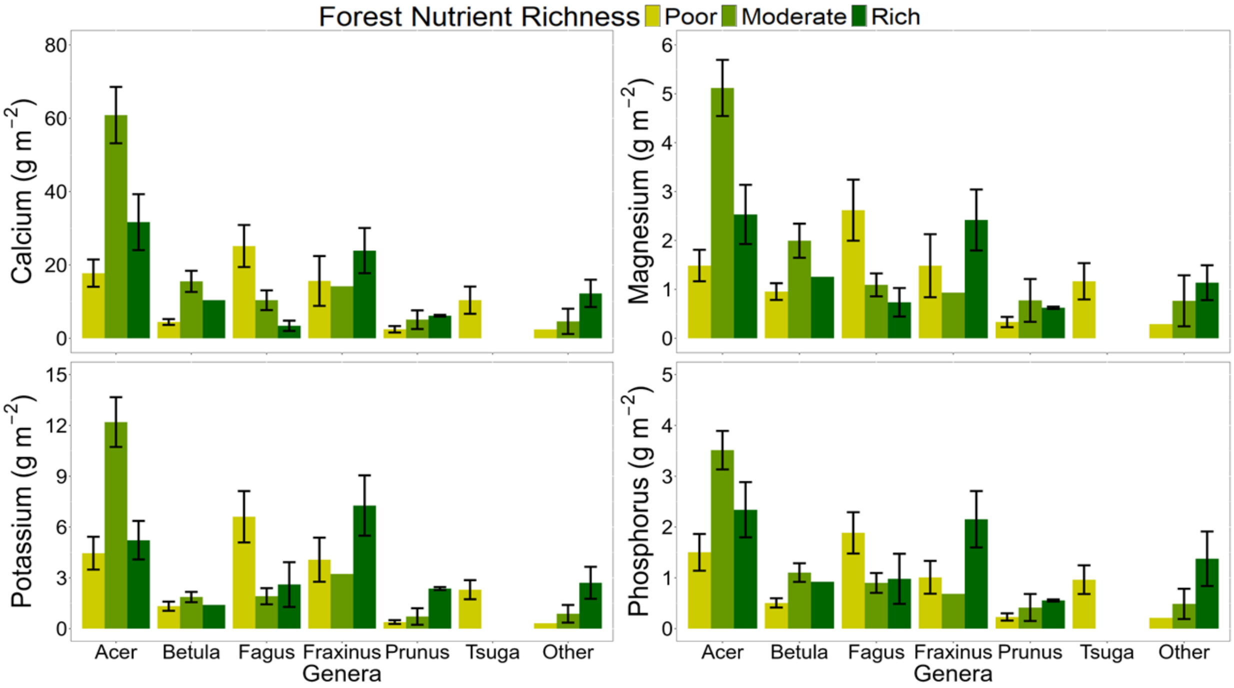

Figure 4.6. Wood nutrient pools (Ca, Mg, K, P) across tree size classifications and forest nutrient richness. Values were calculated from elemental concentrations of branch samples and allometric equations for estimating tree wood (kg) from diameter at breast height. Each bar represents the average across plots within each forest (n = 15) with error bars as standard error.

4.3.2.2 Green leaf nutrient concentrations and pools

Green leaf nutrient concentrations varied across the forest nutrient richness gradient (all $p < 0.01$; Figure 4.7). Calcium concentrations increased significantly with nutrient richness, with the Rich forest having the highest concentrations (9.67 g kg^{-1}), followed by the Moderate (7.84 g kg^{-1}), and the lowest at Poor forest (6.98 g kg^{-1}; $p < 0.01$). Green leaf Mg concentrations were highest at the Moderate forest (2.32 g kg^{-1}), significantly greater than the Rich forest (1.69 g kg^{-1}; $p = 0.036$), which in turn has significantly greater Mg concentrations than the Poor forest (1.57 g kg^{-1}; $p < 0.01$). Conversely, green leaf K concentrations were highest at the Poor forest (8.00 g kg^{-1}), followed by the Rich forest (7.03 g kg^{-1}), and the lowest at the Moderate forest (6.18 g kg^{-1}; $p < 0.01$). Green leaf P concentrations were significantly higher in the Moderate (1.33 g kg^{-1}) and Rich (1.31 g kg^{-1}) forests compared to the Poor forest (1.02 g kg^{-1}; $p < 0.01$). However, there were no significant differences in green leaf P concentrations between the Moderate and Rich forests ($p = 0.89$).

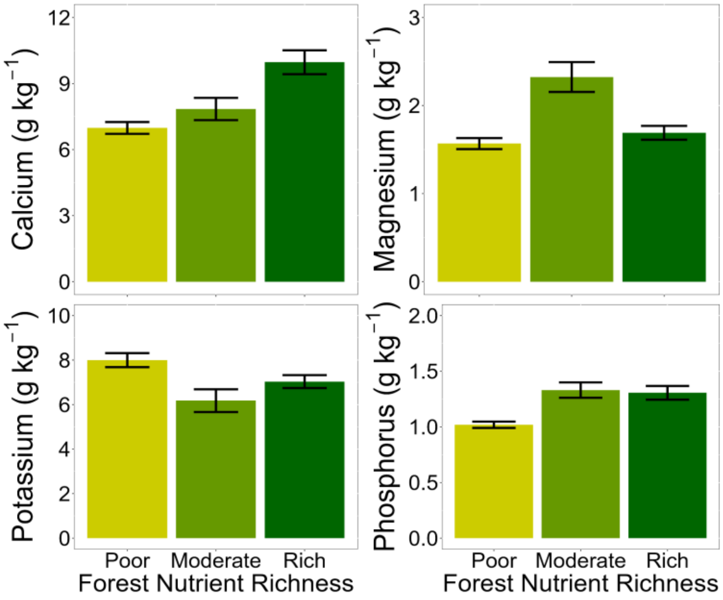

Figure 4.7. Green leaf nutrient concentrations (Ca, Mg, K, P) forest nutrient richness and genera. Values were calculated from elemental concentrations of green leaf samples. Each bar represents the average across plots within each forest (n = 15) with error bars as standard error.

Green leaf nutrient concentrations also varied across forest nutrient richness and tree genera ($p < 0.01$), except for P ($p = 0.16$; Figure 4.8). In *Acer*, green leaf Ca and Mg concentrations were higher at the Rich forest compared to the Poor and Moderate forests ($p < 0.01$), while green leaf K concentrations were higher at the Rich forests compared to the Poor and Moderate forests ($p < 0.01$). *Betula* green leaf Mg concentrations were higher at the Moderate and Rich forests compared to the Poor forest ($p < 0.01$), but green leaf Ca ($p = 0.90$) and Mg ($p = 0.89$) concentrations did not differ. *Fagus* green leaf K concentrations were higher at the Poor and Rich forests compared to the Moderate forest ($p < 0.01$), while there were no differences in green leaf Ca ($p = 1.0$) and Mg ($p = 0.84$) concentrations. *Fraxinus* green lead Ca ($p = 1.0$), Mg ($p = 0.78$), and K ($p = 1.0$) did not differ across the nutrient richness gradient. Similarly, *Prunus* green leaf Ca ($p = 1.0$), Mg ($p = 0.37$), and K ($p = 0.86$) did not differ across the nutrient richness gradient.

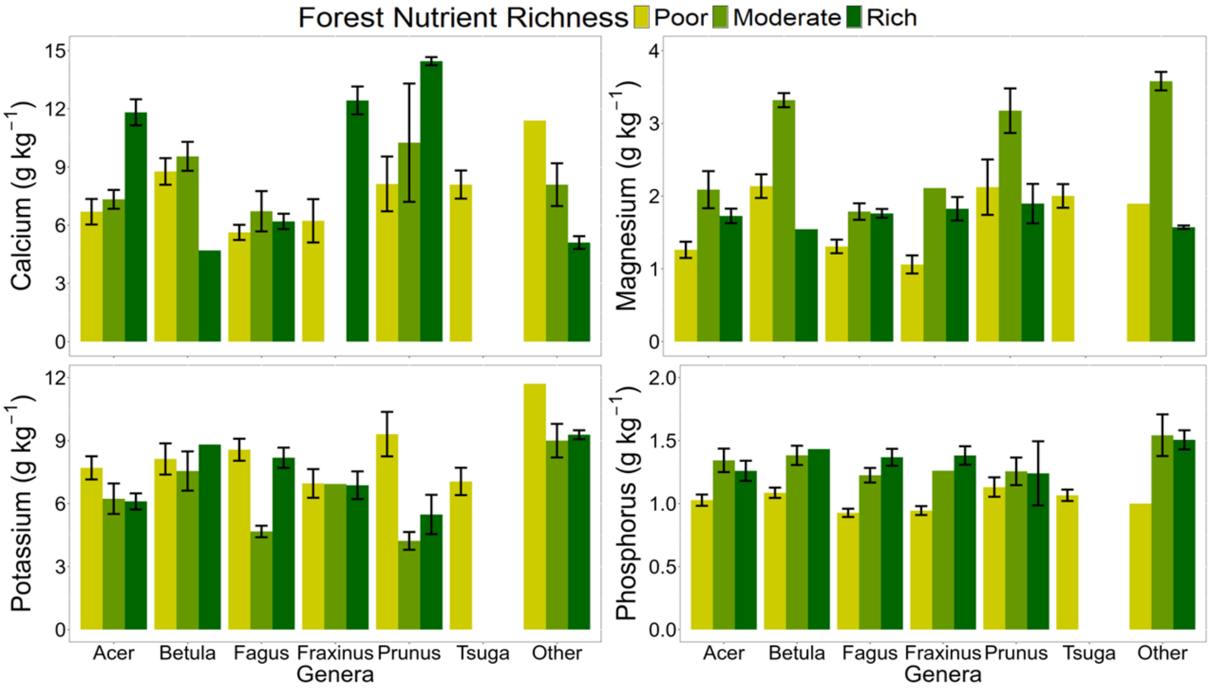

Figure 4.8. Green leaf nutrient concentrations (Ca, Mg, K, P) forest nutrient richness and genera. Values were calculated from elemental concentrations of green leaf samples. Each bar represents the average across plots within each forest (n = 15) with error bars as standard error.

Unlike green leaf nutrient concentrations, forest nutrient richness only significantly affected Mg ($p = 0.01$), and K ($p < 0.01$) pools (Figure 4.9). Green leaf Ca pools were not affected by forest nutrient richness ($p = 0.13$) where the Poor forest (3.22 g m^{-2}) had the highest average followed by the Moderate forest (2.97 g m^{-2}), and the lowest but insignificant average at the Rich forest (2.12 g m^{-2}). Green leaf Mg pools followed the same trend, however there were significant differences with forest nutrient richness ($p = 0.01$). For Mg pools, the Moderate forest (0.684 g m^{-2}; $p < 0.01$) and Poor forest (0.684 g m^{-2}; $p < 0.01$) was significantly higher than the Rich forest (0.538 g m^{-2}). Conversely, green leaf K pools were significantly affected by forest nutrient richness ($p < 0.01$), with the Poor forest (3.39 g m^{-2}) having significantly higher K pools than both the Rich (2.20 g m^{-2}; $p = 0.03$) and Moderate (2.20 g m^{-2}; $p < 0.01$) forests. Green leaf P pools were not significantly different among forest nutrient richness ($p = 0.25$).

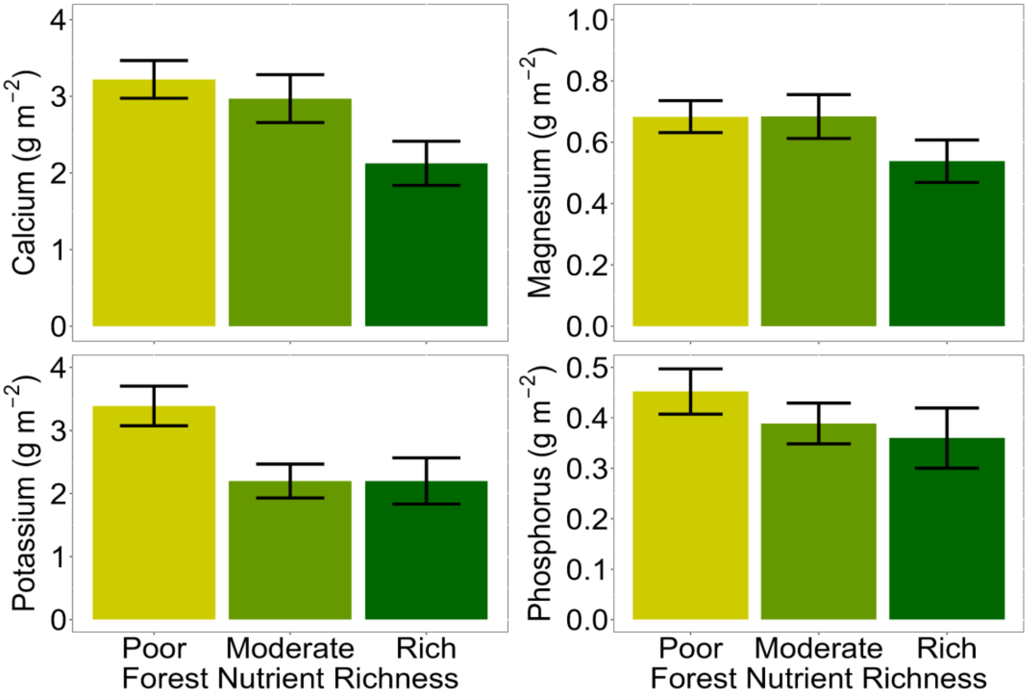

Figure 4.9. Green leaf nutrient pools (Ca, Mg, K, P) across the forest nutrient richness gradient. Values were calculated from elemental concentrations of green leaf samples and allometric equations for estimating tree foliage (kg) from diameter at breast height. Each bar represents the average across plots within each forest (n = 15) with error bars as standard error.

Unlike green leaf nutrient concentrations, green nutrient pools varied only in Ca ($p < 0.05$), and K ($p < 0.01$) pools, but not Mg ($p = 0.06$) or P ($p = 0.09$) pools (Figure 4.10). Although green leaf Ca and Mg pools had significant differences, these differences were not observed within genera. Specifically, green leaf Ca pools did not differ across the forest nutrient richness gradient in *Acer* ($p > 0.45$), *Betula* ($p = 1.0$), *Fagus* ($p > 0.89$), *Fraxinus* ($p = 1.0$), or

Prunus (p = 1.0). Similarly, green leaf K pools did not differ across the forest nutrient richness gradient *Acer* (p = 1.0), *Betula* (p = 0.93), *Fagus* (p = 0.23), *Fraxinus* (p = 1.0), or *Prunus* (p = 0.99).

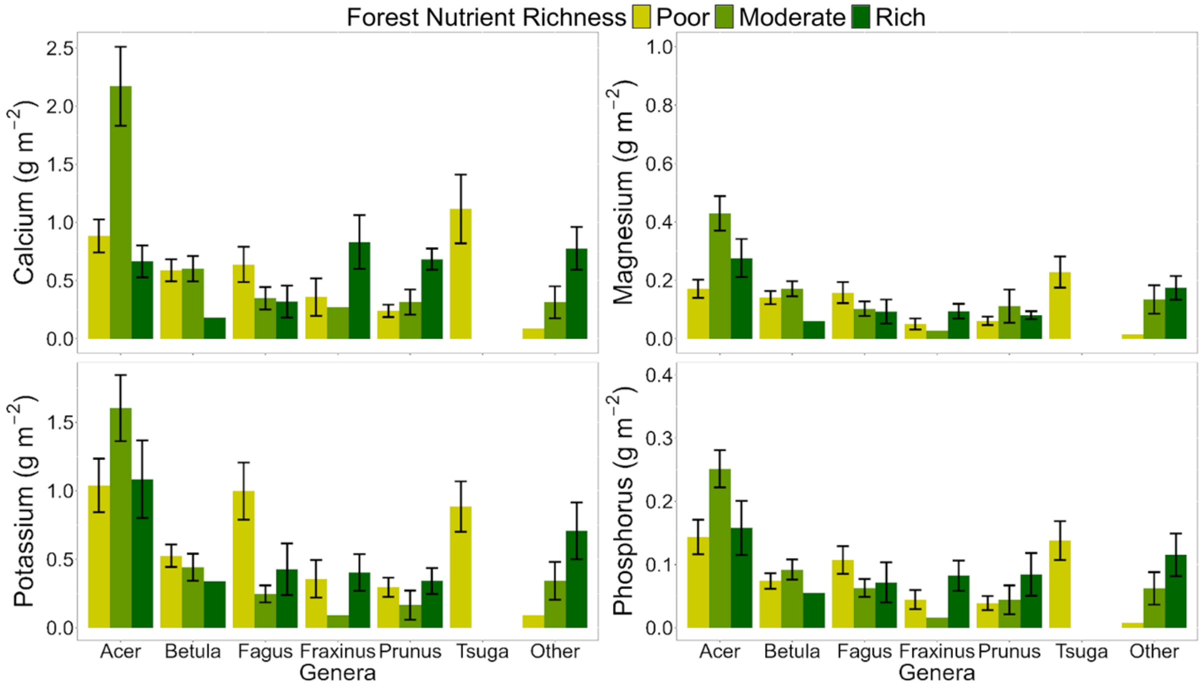

Figure 4.10. Green leaf nutrient pools (Ca, Mg, K, P) across tree size classifications and forest nutrient richness. Values were calculated from elemental concentrations of green leaf samples and allometric equations for estimating tree foliage (kg) from diameter at breast height. Each bar represents the average across plots within each forest (n = 15) with error bars as standard error.

4.3.3 Effects of genus and developmental stage on aboveground nutrients

4.3.3.1 Wood nutrient concentrations by tree size classes and genera

Wood nutrient concentrations varied significantly among some of the tree genera (all $p < 0.01$; Figure 4.11) but were not significantly influenced by tree size class for Ca (p = 0.54), Mg

(p = 1.00), K (p = 0.49), or P (p = 0.64; Supplemental Figure 4.1). *Fraxinus* exhibited the highest concentration of Ca, Mg, K, and P out of all the genera. Specifically, Wood Ca concentrations were highest in *Fraxinus* (8.79 g kg^{-1}) and *Acer* (8.73 g kg^{-1}) out of all genera. *Acer*, the most abundant genus across the three forests, had significantly higher Ca concentrations than *Prunus* (7.01 g kg^{-1}; p = 0.035), *Fagus* (5.98 g kg^{-1}; $p < 0.01$), *Betula* (5.40 g kg^{-1}; $p < 0.01$), and *Tsuga* (4.65 g kg^{-1}; $p < 0.01$). Additionally, *Prunus*, *Fagus*, *Betula*, and *Tsuga* did not differ significantly in Ca concentrations (all p > 0.64). For wood Mg concentrations, *Fraxinus* (0.88 g kg^{-1}; $p < 0.01$), and *Prunus* (0.87 g kg^{-1}; p = 0.03), and *Tsuga* (0.71 g kg^{-1}; $p < 0.01$) had significantly higher concentrations than *Acer* (0.68 g kg^{-1}). *Prunus*, *Betula* (0.83 g kg^{-1}), and *Fagus* (0.74 g kg^{-1}) exhibited similar Mg concentrations (all $p > 0.07$). *Fraxinus* (3.53 g kg^{-1}) had significantly higher wood K concentrations than all other genera ($p > 0.01$). *Acer* (2.17 g kg^{-1}) had the second-highest K concentration, significantly greater than *Prunus* (1.69 g kg^{-1}; $p < 0.01$), *Fagus* (1.52 g kg^{-1}; $p < 0.01$), and *Betula* (0.82 g kg^{-1}; $p < 0.01$). As for wood P concentrations, *Fraxinus* (0.84 g kg^{-1}) had the highest concentration, similar to *Prunus* (0.65 g kg^{-1}; p = 0.068) and *Tsuga* (0.60 g kg^{-1}; p = 0.28). *Betula* had the lowest P concentration (0.44 g kg^{-1}). *Fagus* P concentrations were similar to *Prunus* (p = 1.00), *Tsuga* (p = 0.65), and *Acer* (0.59 g kg^{-1}; p = 0.93).

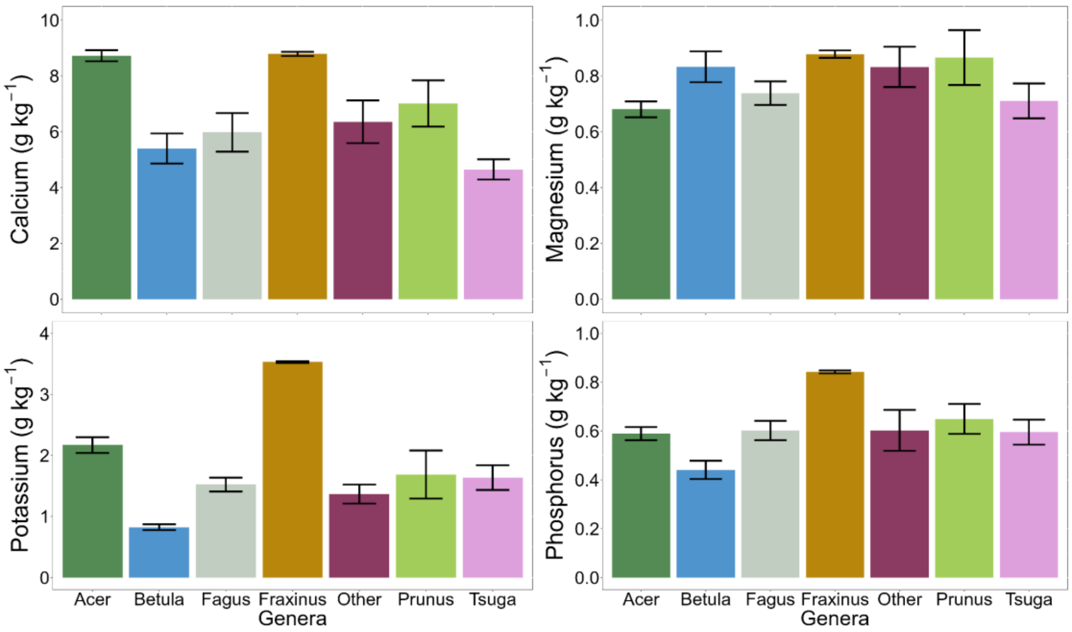

Figure 4.11. Wood nutrient concentrations (Ca, Mg, K, P) across tree genera. Values are calculated from elemental concentrations of branch samples. Each bar represents the average with error bars as standard error.

4.3.3.2 Wood nutrient pools by tree size classes and genera

Unlike concentrations, wood nutrient pools varied significantly among tree size class (all $p < 0.01$; Figure 4.12), as the more numerous pole-sized trees had greater biomass than fewer large sawtimber trees. Poletimber consistently exhibited the highest pools of Ca, Mg, K, and P compared to the smaller size classes. Poletimber exhibited the highest average wood Ca content (86.6 g m^{-2}), followed by medium sawtimber (43.1 g m^{-2}), small sawtimber (40.8 g m^{-2}), large sawtimber (34.0 g m^{-2}), and saplings (11.8 g m^{-2}). There were no significant differences between small and medium sawtimber ($p = 0.70$) or between small sawtimber and poletimber ($p = 0.06$). Similarly, wood Mg pools were significantly higher in poletimber (8.63 g m^{-2}) than small sawtimber (4.30 g m^{-2}; $p < 0.01$), medium sawtimber (3.94 g m^{-2}; $p < 0.01$), large sawtimber (3.60 g m^{-2}; $p < 0.01$), and saplings (1.23 g m^{-2}; $p < 0.01$). Poletimber (19.6 g m^{-2}) also, had significantly higher K pools than large sawtimber (6.09 g m^{-2}; $p < 0.01$), medium sawtimber (11.0 g m^{-2}; $p < 0.01$), small sawtimber (9.58 g m^{-2}; $p = 0.01$), and saplings (2.76 g m^{-2}; $p < 0.01$). There were no significant differences among small sawtimber, medium sawtimber, and saplings ($p > 0.11$). Additionally, poletimber (6.61 g m^{-2}) had significantly higher P pools than large sawtimber (2.92 g m^{-2}; $p < 0.01$), medium sawtimber (3.15 g m^{-2}; $p < 0.01$), and saplings (0.88 g m^{-2}; $p < 0.01$). Large and medium sawtimber had similar P pools (both $p > 0.068$).

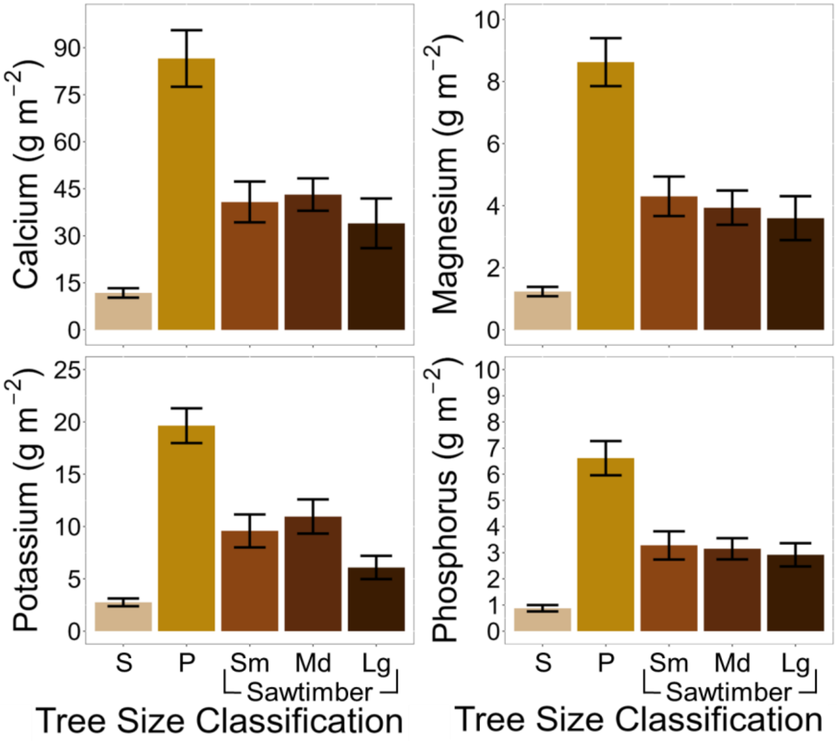

Figure 4.12. Wood nutrient pools (Ca, Mg, K, P) across tree size classifications. Values were calculated from elemental concentrations of branch samples and allometric equations for estimating tree wood (kg) from diameter at breast height. Each bar presents the average across plots (n = 15) within each forest, and error bars indicate standard errors. On the x-axis, tree size

classifications are represented as follows: “S” for sapling, “P” for poletimber, “Sm” for small sawtimber, “Md” for medium sawtimber, and “Lg” for large sawtimber.

Wood Ca, Mg, K, and P pools varied significantly among tree genera (all $p < 0.01$), generally following species abundance for each forest (Figure 4.13). *Acer* consistently exhibited the highest pools of all four nutrients and was most abundant. Specifically, *Acer* (106.2 g m^{-2}) had the highest Ca pools, significantly greater than *Fagus* (31.9 g m^{-2}; $p < 0.01$), *Betula* (18.6 g m^{-2}; $p < 0.01$), *Tsuga* (10.4 g m^{-2}; $p < 0.01$), and *Prunus* (5.83 g m^{-2}; $p = 0.017$). However, *Acer* did not differ significantly from *Fraxinus* (34.0 g m^{-2}; $p = 0.98$), which was also common at the Poor and Rich forests and comparable wood Ca concentrations. *Fagus* and *Betula* had similar Ca pools to all other genera except *Acer* (all $p > 0.05$). For wood Mg pools, Tsuga (1.54 g m^{-2}) had significantly lower pools than *Acer* (8.83 g m^{-2}; $p < 0.01$), *Fagus* (4.16 g m^{-2}; $p = 0.05$), and *Fraxinus* (3.33 g m^{-2}; $p = 0.01$). No significant differences were observed among the remaining genera (all $p > 0.01$). Additionally, *Acer* (21.9 g m^{-2}) had significantly higher K pools than *Tsuga* (2.30 g m^{-2}; $p < 0.01$) and *Betula* (3.04 g m^{-2}; $p < 0.01$). *Ace*r had similar K pools to *Fagus* (8.64 g m^{-2}; $p = 0.40$), *Fraxinus* (10.3 g m^{-2}; $p = 0.83$), and *Prunus* (1.50 g m^{-2}; $p = 0.078$). For P pools, *Acer* had significantly higher concentrations than *Betula* ($p = 0.01$) and *Tsuga* ($p = 0.02$). There were no significant differences among the remaining genera ($p > 0.05$).

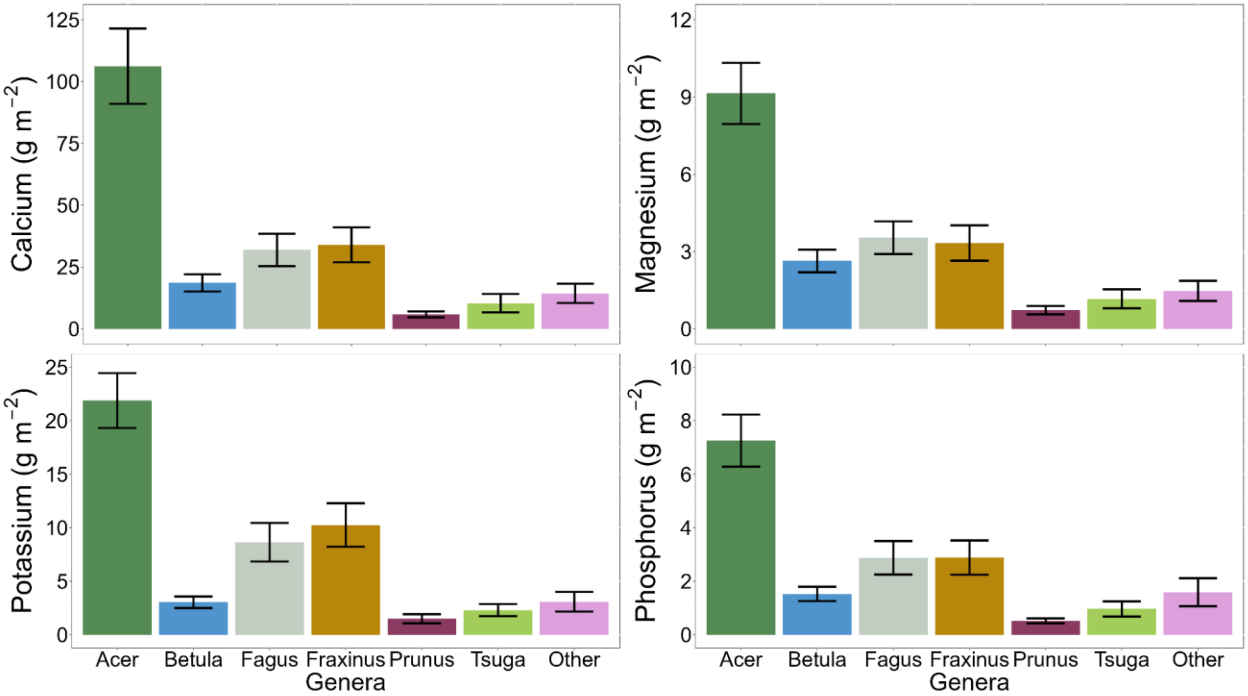

Figure 4.13. Wood nutrient pools (Ca, Mg, K, P) across tree genera. Values are calculated from elemental concentrations of branch samples and allometric equations for estimating tree wood (kg) from diameter at breast height. Each bar represents the average with error bars as standard error.

4.3.3.3 Green leaf nutrient concentrations by tree size class and genera

Green leaf nutrient concentrations did not differ among tree size classes ($p > 0.77$; Supplemental Figure 4.2). However, green leaf nutrient concentrations varied significantly among tree genera ($p < 0.01$; Figure 4.14). *Fagus* consistently exhibited the lowest concentrations of Ca, Mg, K, and P. *Betula* (9.16 g kg^{-1}) had the highest green leaf Ca concentrations, significantly higher than *Acer* (8.48 g kg^{-1}; $p = 0.01$) and *Fagus* (6.37 g kg^{-1}; $p < 0.01$) Ca concentrations. The lowest green leaf Ca concentrations were found in *Fagus*. Leaf Mg concentrations were also significantly different among genera ($p < 0.01$). *Betula* (2.64 g kg^{-1}), and *Tsuga* (2.00 g kg^{-1}) had the highest green leaf Mg concentrations and had significantly higher concentrations than *Acer* (1.82 g kg^{-1}; $p < 0.01$). *Acer* had similar Mg concentrations to *Prunus* (2.21 g kg^{-1}; $p = 0.08$), *Fraxinus* (1.56 g kg^{-1}; $p = 0.93$), and *Fagus* (1.52 g kg^{-1}; $p = 1.0$). *Fagus* had the lowest green leaf Mg concentrations out of all of the genera. *Betula* (7.75 g kg^{-1}) and *Prunus* (7.75 g kg^{-1}) had the highest green leaf K concentrations. *Betula* had significantly higher K concentrations than *Acer* (6.73 g kg^{-1}; $p < 0.01$) green leaves. *Acer* and *Fagus* (6.81 g kg^{-1}) had the lowest K concentrations in green leaves. No other significant differences in K concentrations were observed among genera ($p > 0.15$). For green leaf P concentrations, *Acer* (1.25 g kg^{-1}) had the highest concentrations. Only *Betula* (1.20 g kg^{-1}) had significantly higher P concentrations than *Fagus* (1.11 g kg^{-1}; $p = 0.02$), which in turn had significantly higher P concentrations than *Tsuga* (1.07 g kg^{-1}; $p = 0.02$). The lowest P concentrations were in *Fagus* green leaves out of all the genera.

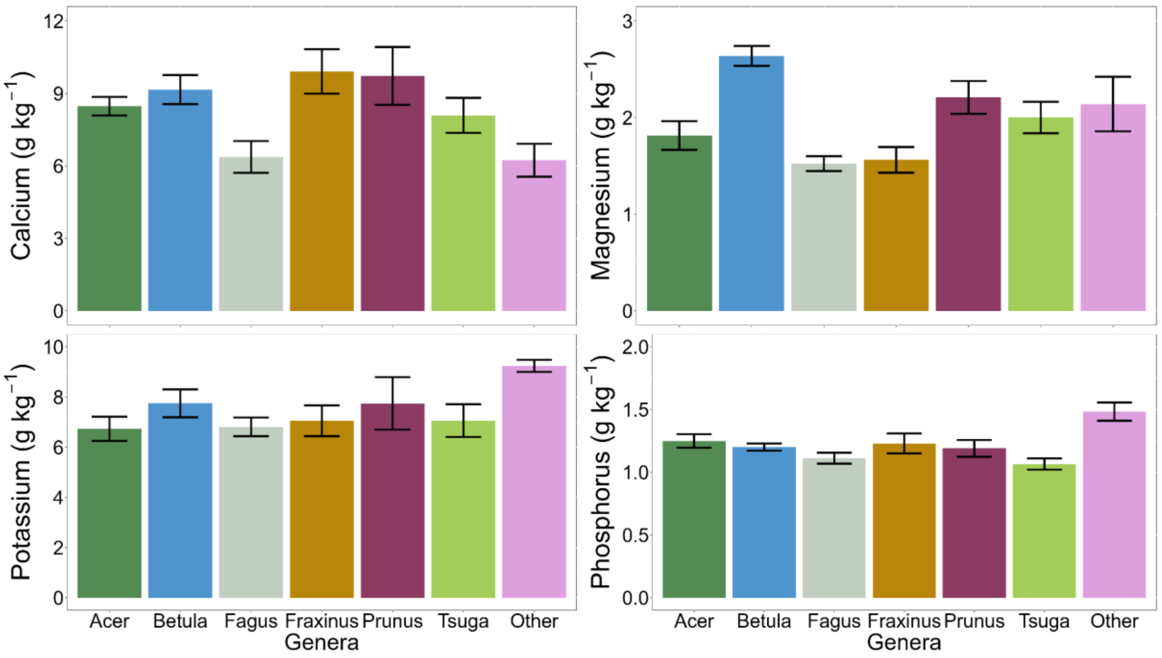

Figure 4.14. Green leaf nutrient concentrations (Ca, Mg, K, P) across tree genera. Values are calculated from elemental concentrations of green leaf samples. Each bar represents the average with error bars as standard error.

4.3.3.4 Green leaf nutrient pools by tree size class and genera

Unlike nutrient concentrations, green leaf nutrient pools varied significantly among tree size classifications ($p < 0.01$; Figure 4.15) and genera ($p < 0.01$; Figure 4.16). Across all nutrients, pools were highest in poletimber and lowest in saplings. Poletimber (3.28 g m^{-2}) had the highest green leaf Ca pools, significantly higher than medium (1.66 g m^{-2}; $p < 0.01$), large (1.45 g m^{-2}; $p < 0.01$), and sapling (0.79 g m^{-2}; $p < 0.01$) trees. Sapling had the lowest Ca pool out of tree size classifications and was significantly lower than all other classes ($p < 0.01$). Green leaf Mg and K pools followed a similar pattern, with poletimber having the highest pools for both nutrients. Poletimber (0.828 g m^{-2}) having the highest ($p < 0.01$) green leaf Mg pools and saplings (0.171 g m^{-2}) had the lowest ($p < 0.01$) out of all tree size classifications. Green leaf K pools differed significantly among tree size classifications, with poletimber (3.50 g m^{-2}) having the highest K pool. Additionally, saplings (0.694 g m^{-2}: $p < 0.01$) had the lowest green leaf K pools. Green leaf P pools were also highest in poletimber (0.506 g m^{-2}), significantly higher than all other size classifications ($p < 0.04$). The lowest green leaf P pools were in saplings (0.115 g m^{-2}), significantly lower than all other tree classifications ($p < 0.01$). Only small (0.237 g m^{-2}) and medium (0.237 g m^{-2}) sawtimber were similar to each other ($p = 0.99$).

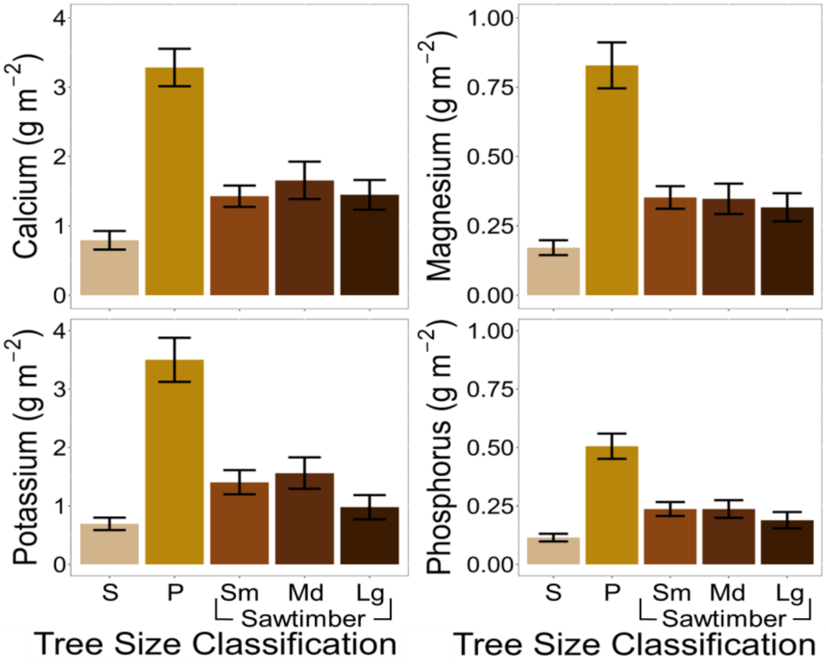

Figure 4.15. Green leaf nutrient pools (Ca, Mg, K, P) across tree size classifications. Values were calculated from elemental concentrations of green leaves and allometric equations for estimating tree foliage (kg) from diameter at breast height. Each bar presents the average across plots (n = 15) within each forest, and error bars indicate standard errors. On the x-axis, tree size classifications are represented as follows: “S” for sapling, “P” for poletimber, “Sm” for small sawtimber, “Md” for medium sawtimber, and “Lg” for large sawtimber.

Among genera, *Acer* consistently exhibited the highest pools of Ca, Mg, K, and P (Figure 4.16). Conversely, *Prunus* had the lowest pools of Ca, Mg, K, and P. Again, *Acer* (3.53 g m^{-2}) had the highest pools of Ca among all the genera. *Prunus* (0.55 g m^{-2}) had the lowest pool of Ca among all the genera. *Acer* had significantly higher green leaf Ca pools than Fraxinus (1.04 g m^{-2}; $p < 0.01$) and *Fagus* (1.00 g m^{-2}; $p < 0.01$). Genera differed significantly in green leaf Mg pools ($p < 0.01$). *Acer* (0.848 g m^{-2}) had the highest Mg pool in green leaves out of the genera. *Prunus* (0.110 g m^{-2}) had the lowest green leaf Mg pools out of the genera. However, due to large variability in Mg pools, *Prunus* was similar to *Acer* ($p = 0.99$), *Betula* (0.294 g m^{-2}; $p = 1.00$), *Fagus* (0.269 g m^{-2}; $p = 0.63$) and *Tsuga* (0.229 g m^{-2}; $p = 0.66$). Green leaf K pools were highest in *Acer* (3.55 g m^{-2}) compared to the other five genera. Contrarily, *Prunus* (0.406 g m^{-2}) had the lowest K pools. *Fagus* (1.29 g m^{-2}), *Betula* (0.932 g m^{-2}), and *Tsuga* (0.885 g m^{-2}) all had similar green leaf K pools ($p > 0.21$). Green leaf P pools were highest in *Acer* (0.527 g m^{-2}) out of the other genera and significantly higher than *Fagus* (0.182 g m^{-2}; $p = 0.03$), *Betula* (0.158 g m^{-2}; $p < 0.01$) and *Fraxinus* (0.108 g m^{-2}; $p < 0.01$). The lowest P pools were lowest in *Prunus* (0.0769 g m^{-2}) out of the other genera.

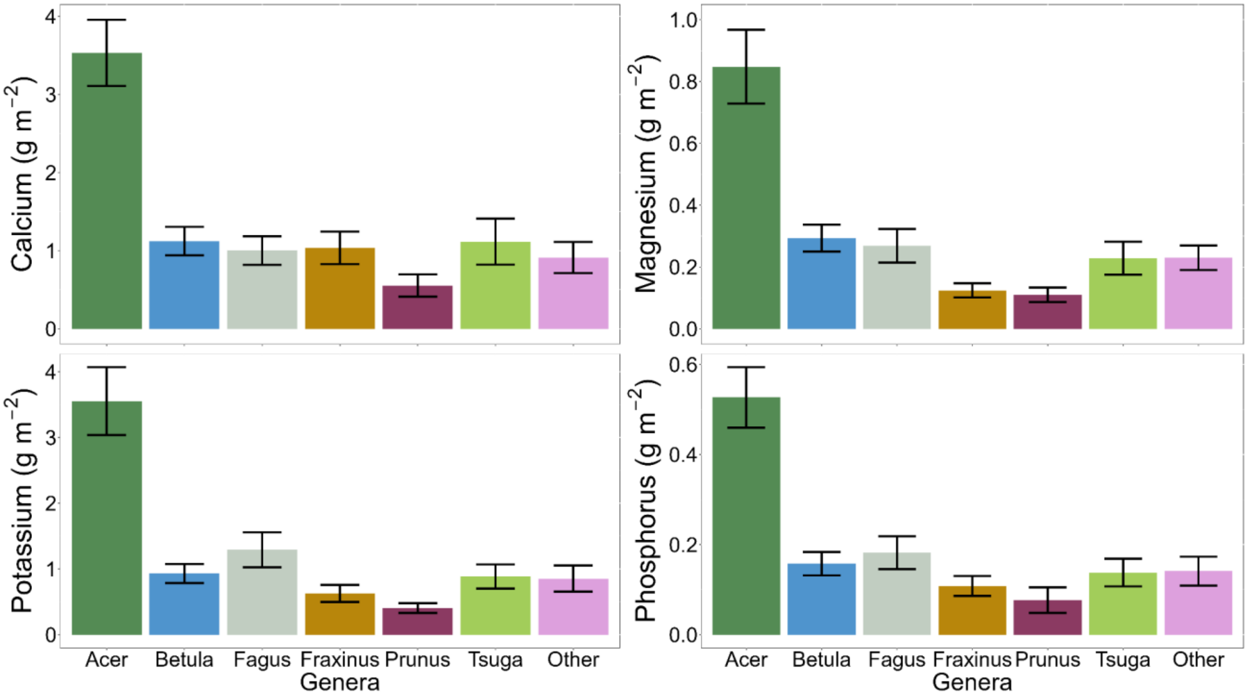

Figure 4.16. Green leaf nutrient pools (Ca, Mg, K, P) across tree genera. Values are calculated from elemental concentrations of green leaf samples and allometric equations for estimating tree foliage (kg) from diameter at breast height. Each bar represents the average with error bars as standard error.

4.3.4 Merchantable wood volumes and values

4.3.4.1 Merchantable wood volumes

Merchantable wood volumes were calculated and compared across forest nutrient richness, tree size classification, or tree genera to determine significant effects. Surprisingly, forest nutrient richness did not influence merchantable wood volumes ($p = 0.88$), nor did tree genera ($p = 0.06$). However, merchantable tree volumes did vary significantly among tree size classifications ($p < 0.01$; Figure 4.17). Poletimber trees had the highest merchantable wood volumes per area (9, 290 $\mathrm{cm}^3\ \mathrm{m}^{-2}$; $p < 0.01$). Small, mid, and large sawtimber all had comparable merchantable wood volumes to each other ($p > 0.07$).

Additionally, we examined the three most abundant tree genera (*Acer*, *Betula*, *Fagus*) separately to determine if forest nutrient richness or tree size classification significantly affected their total merchantable wood. Forest nutrient richness significantly influenced merchantable wood volumes for *Acer* ($p = 0.03$), but not for *Betula* ($p = 0.98$), or *Fagus* ($p = 0.16$). For *Acer* the Moderate forest had significantly higher merchantable wood volume than the Poor forest ($p = 0.02$) but was similar to the Rich forest ($p = 0.44$). Also, tree size classification did significantly influence total merchantable wood volume for the combination of all genera ($p < 0.31$), but not *Acer* ($p =0.31$), *Betula* ($p = 0.05$), or *Fagus* ($p = 0.10$; Figure 3.17). When all genera were combined, total merchantable wood volume was highest for the poletimber (9,290 $\mathrm{cm}^3\ \mathrm{m}^{-2}$; $p < 0.01$) compared to all other size classes. There were no significant differences among the other size classes ($p > 0.05$).

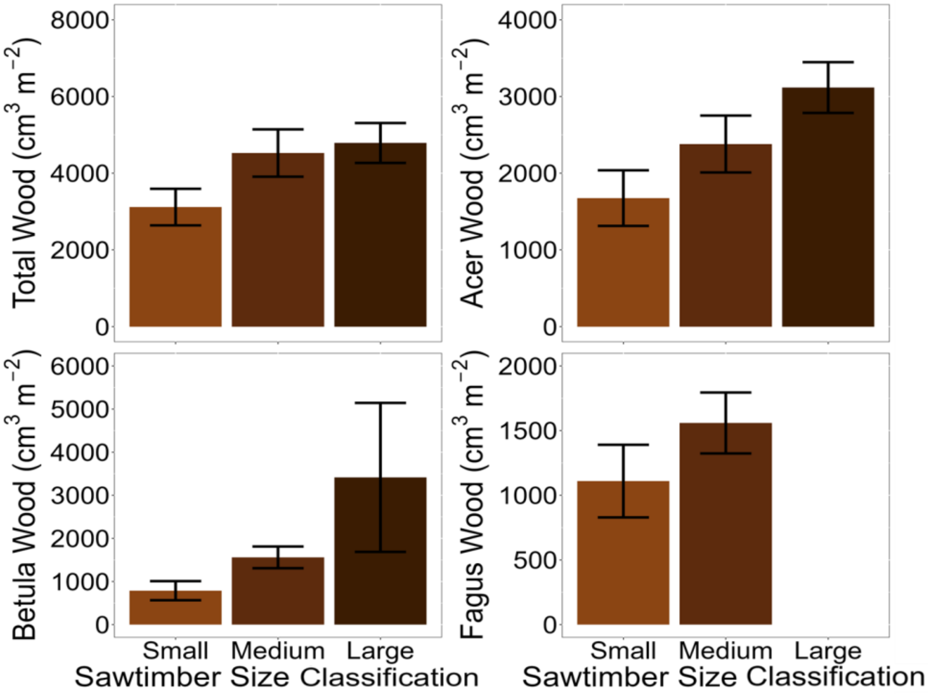

Figure 4.17. Merchantable wood volume (cm^3 m^{-2}) across three sawtimber size classifications (Small, Medium, Large. The top-left panel represents total wood volume across all genera, while the other panels show wood volume for specific genera: *Acer* (top-right), *Betula* (bottom-left), and *Fagus* (bottom-right). Error bars indicate standard error.

The relationship between merchantable wood volume and soil nutrient availability was examined for Ca, Mg and a combination of nutrients to determine if and what soil nutrients influence merchantable wood (Supplemental Figure 4.3). There were no significant relationships between merchantable wood volume and available soil nutrients. A weak positive correlation was found between merchantable wood volume and soil available Ca ($R^2 = 0.14$, $p = 0.41$), although this relationship was not significant. In contrast, a non-significant weak negative correlation was found between merchantable wood volume and soil available Mg ($R^2 = - 0.27$, $p = 0.1$). When soil available Ca and Mg were added together, the relationship with merchantable wood volume remained positive and non-significant ($R^2 = 0.12$, $p = 0.48$). Similarly, the relationship between merchantable wood volume and the combined availability of Ca, Mg, K, and P was also positive and non-significant ($R^2 = 0.15$, $p = 0.39$).

4.3.4.2 Merchantable wood values

We simulated the value of each forest based on four scenarios (Figure 4.18). When all wood was assumed to be pulpwood, the value per area of forest was roughly the same for each forest with the Moderate forest (\$0.06 m^{-2}) having the highest value, followed by the Poor forest (\$0.06 m^{-2}) and the lowest value was at the Rich forest (\$0.05 m^{-2}; $p < 0.01$). Conversely, when only non-pulpwood qualities (low, mid, high) were considered, the Moderate forest had the highest value (\$1.26 m^{-2}; $p < 0.01$) followed by the Rich forest (\$1.13 m^{-2}; $p < 0.01$) and then the Poor forest (\$1.03 m^{-2}; $p < 0.01$). In the scenario incorporating a mixture of pulpwood, low, mid, and high quality wood, the Moderate forest (\$1.09 m^{-2}; $p < 0.01$) again had the highest value, followed by the Rich forest (\$0.97 m^{-2}; $p < 0.01$) and the lowest at the Poor forest (\$0.89 m^{-2}; $p < 0.01$). The third scenario, including all wood qualities, generally resulted in lower total values compared to the scenario excluding pulpwood, likely due to the lower values associated with pulpwood. We ran a fourth scenario because we were interested in exploring if the value of the forest was more driven by the price due to wood quality or if the volume of the wood in a forest can overcome that. We found that when the distribution of wood quality (pulp, low, mid, high) was randomized, the Moderate forest (\$0.91 m^{-2}; $p < 0.01$) was still the highest valued forest, followed by the Rich forest (\$0.81 m^{-2}; $p < 0.01$), and the lowest value was at the Poor forest (\$0.74 m^{-2}; $p < 0.01$).

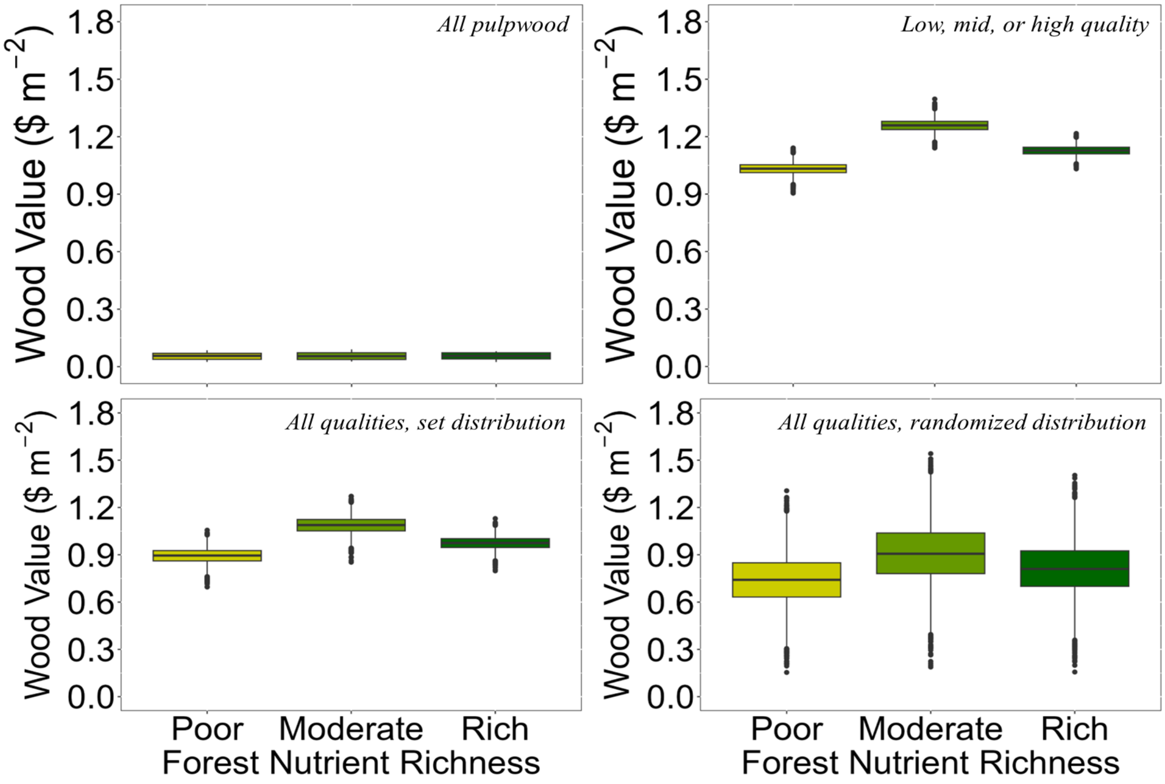

Figure 4.18. Box plots of merchantable wood value ($ m^{-2}) across forest nutrient richness. The four panels represent different scenarios where merchantable wood quality is varied: All merchantable wood is pulpwood (top-left), all wood is classified as low, mid, or high quality wood (top-right), all wood classified as pulpwood, low, mid or high quality and the ratio of these is based on published values (bottom-left), and all wood is classified as pulpwood, low, mid, or high quality and the distribution of these is randomized for each simulation (bottom-right).

4.4 Discussion

4.4.1 Effects of soil nutrient richness on aboveground concentrations and pools

We hypothesized that wood nutrient concentrations and pools would increase as forest nutrient richness increased. As expected, our findings suggest that soil nutrient richness influences wood nutrient concentrations, with Ca, K, and P concentrations lowest at the Poor forest and highest at the Rich forest. However, wood Mg concentrations did not follow this trend. The relationship between soil nutrient richness and wood Ca, K, and P likely reflects the direct uptake and incorporation of these nutrients into woody tissues. However, the lack of a clear trend for Mg suggests other factors may influence Mg assimilation such as differences in mechanisms of Mg uptake compared to the other nutrients (van der Heijden et al., 2014), internal allocation strategies (Dalling et al., 2024; Xu et al., 2022), or possible interactions with other nutrients (Chen et al., 2018). Further, the uptake of Mg has been found to decrease if there is high availability of Ca, K and manganese (Mn) in the soil due to competitive interactions at the root level (Gransee and Fuhrs, 2013). A study comparing the nutrient concentrations of sapwood and heartwood along a soil nutrient gradient found similar results, where wood Ca, Mg, K, and P concentrations were lowest at the nutrient poor site and highest at the nutrient rich site (Roy et al., 2021). While regional studies quantifying wood nutrient concentrations are limited, similar wood nutrient concentrations have been reported in the White Mountains of New Hampshire (Arthur et al., 1999; Yang et al., 2016). Another study reported slightly lower concentrations in similar species at the Hubbard Brook Experimental Forest in New Hampshire (Johnson et al., 2014). However, this discrepancy is likely due to the differences in sampling methods, as our study focused on branches rather than bole wood, which typically contains lower nutrient concentrations (Choi et al., 2016; Oelmann et al., 2010; Yang et al., 2016). Our results suggest that soil nutrient availability strongly influences wood nutrient concentrations, although the degree of influence varies by element. This relationship is important for forest productivity as these nutrients (Ca, Mg, K, P) play a key role in forest health and productivity. Additionally, each of these nutrients affect wood properties, which directly impact wood quality and, in turn, the economic value of the forest (dos Santos Angelico et al., 2021).

The high wood Mg concentrations at the Moderate site warrant further explanation. Interestingly, all genera measured had higher wood Mg concentrations at the Moderate forest compared to the other two forests despite exchangeable Mg levels being similar between the Moderate and Rich forests (Rice et al., 2024). The concentrations of Mg in the soil leachate also did not differ substantially between the Moderate and Rich forest. One reason for the high Mg despite differences in soil Mg is the difference in texture. The Moderate forest had loam soil with the highest clay content among the three forests, while the Poor and Rich forests had coarser sandy loam textures. Soils with greater clay content generally have higher cation exchange capacity which can increase the availability and retention of cations like Mg (Brady and Weil, 2016; Jobbagy and Jackson, 2001). If the higher cation exchange capacity at the Moderate forest may have buffered Mg availability and improved the efficiency of Mg uptake even without great exchangeable Mg concentrations or lower leachate concentrations. Additionally, finer textured soils can maintain more stable soil moisture conditions which could create more consistent Mg uptake across growing seasons (Kozlowski and Pallardy, 1997). The potential influence of soil physical properties on wood nutrient concentrations highlights their importance when interpreting patterns of nutrient uptake. In particular, the trend in wood Mg concentrations suggests that the accumulation of Mg in wood may be more sensitive to soil clay content and species-specific physiological traits than to bulk soil availability. This decoupling emphasizes the need for an integrated approach when assessing forest nutrient dynamics and their implications for forest health, productivity, and resilience.

Green leaf nutrient concentrations had a more complex relationship with soil nutrient richness compared to woody tissues. Only green leaf Ca concentrations followed the expected nutrient richness gradient, with the highest Ca concentrations observed in the Rich forest. In contrast, Mg concentrations were highest in the Moderate forest, likely reflecting its relatively high soil Mg availability (Rice et al., 2024). Green leaf K and P concentrations did not align with soil nutrient availability, suggesting that additional factors influence their concentrations. The strong relationship between green leaf Ca and soil available Ca indicated a direct link between nutrient availability and foliar nutrient assimilation. However, the decoupling of green leaf K and P from soil nutrient availability suggests processes such as the leaching of soluble elements through atmospheric precipitation and internal nutrient cycling play a stronger role in regulating foliar nutrient concentrations (Staelens et al., 2007; Turpault et al., 2021). Green leaf nutrient concentrations observed in this study were consistent with those reported for hardwood forests in other portions of our study region (Hong et al., 2022; Yang et al., 2016). While some studies report a strong relationship between soil P availability and foliar P concentrations (Cross and Perakis, 2010), our findings did not support this relationship, reinforcing the influence of atmospheric deposition on foliar K and P dynamics. Our findings suggest that luxury uptake of K and P was limited in the managed temperate forests, implying that trees on nutrient-poor sites may rely more on internal cycling rather than direct uptake from the soil. However, we did not measure nutrient resorption or efficiency, further research is needed to better understand how trees regulate nutrient use under varying soil nutrient conditions. From a forest management perspective, the leaching of these elements from foliage is likely not an issue, as these leached elements are presumed to return to the forest floor and remain available for plant uptake. In fact, this process may be beneficial by contributing to soil nutrient pools before whole-tree harvests.

Despite differences in wood and green leaf nutrient concentrations, neither wood nor green leaf nutrient pools (Ca, Mg, K, P) followed the expected soil nutrient richness gradient. The lack of correlation between soil nutrient richness and nutrient pools suggests that other factors, particularly differences in total wood and foliar biomass, play a more dominant role in nutrient storage than concentrations. For example, although wood nutrient concentrations were higher in the nutrient Rich forest, differences in total woody biomass offset these trends. Similarly, the Poor forest had the highest total woody biomass, thereby eliminating the expected relationship between soil nutrient richness and nutrient pools (Table 4.4). Additionally, green leaf nutrient pools did not follow the expected nutrient richness gradient, with forest nutrient richness only affecting Mg and K pools, which were lowest at the Rich forest. Green leaf Ca pools displayed an inverse relationship with forest nutrient richness, due to the Poor forest having the highest foliar biomass and the Rich forest the lowest. Similar trends have been observed in other temperate hardwood forests, where biomass accumulation can overshadow or emphasize trends in nutrient concentrations (Dalling et al., 2024; Rutkowski and Stottlemyer, 1993). These findings suggest that nutrient exports in woody and foliar biomass may be influenced more by forest structure and total biomass accumulation rather than soil nutrient availability which is important to consider when managing timber harvesting regimes.

The unexpected finding that the nutrient Poor forest had the highest total biomass suggests that factors beyond soil Ca and Mg availability are influencing forest productivity. One possibility is that nitrogen, which is a commonly limiting nutrient in temperate forests and may be higher at the Poor site due to differences in mineralization rates, historical atmospheric deposition, or species-driven nutrient cycling (Carter et al., 2017). Additionally, the Poor forest had a higher abundance of *Tsuga canadensis* and *Fagus grandifolia* which both are shade-tolerant, late-successional species known for their ability to form dense canopies and accumulate substantial biomass even on nutrient poor soils (Halman et al., 2015; Nolet and Kneeshaw, 2018; Rogers, 1978). Disturbance history may also play a since the Poor forest is the oldest of the three forests and it has had a longer period without major harvesting (approximately 40 additional years) likely contributed to the greater biomass accumulation. These interacting factors (i.e. species composition, nutrient use efficiency, and stand age) may explain how the nutrient Poor forest supported the highest biomass. Understanding the mechanisms that decouple biomass from base cation availability is important for predicting long-term forest productivity and resilience, particularly under changing climate and harvesting regimes.

4.4.2 Effects of tree size and genera on aboveground concentrations and pools

Tree size classification did not influence wood or green leaf nutrient concentrations, but concentrations varied among genera. *Fraxinus* had the highest wood Ca, Mg, K, and P concentrations, while *Betula* and *Fagus* had some of the lowest. In contrast, *Betula* had the highest green leaf Ca, Mg, and K concentrations, whereas *Fagus* had the lowest. These results align with regional studies that found *Betula* generally have higher wood and green leaf nutrient concentrations than *Fagus* (Hong et al., 2022; Park and Yanai, 2009; Yang et al., 2016). The lack of influence of tree size classification on wood nutrient concentrations suggests that nutrient allocation is primarily driven by species or genera specific traits rather than size. These differences may be attributed to species-specific nutrient uptake efficiencies (Gonzales et al., 2023; Hong et al., 2022), potential plasticity in nutrient acquisition strategies (Mao et al., 2019), mycorrhizal associations (Pena and Tibett, 2024) and interspecies competition (Fahey et al., 1998). Further meaning that trees on nutrient-poor soils may increase nutrient use efficiency by the resorption of more nutrients (Schmidt et al., 2015), may alter their root structures to access more nutrients (Mao et al., 2019), or enhance mycorrhizal relationship to optimize nutrient acquisition and to maintain tree productivity (Pena and Tibbet, 2024).

While wood and green leaf nutrient concentrations did not differ by tree size, nutrient pools were highest in poletimber trees due to their greater biomass within each forest. This occurred because nutrient pools are a function of both concentration and biomass, meaning that even if nutrient concentrations remain constant across size classes, trees with more biomass will store higher total amounts of nutrients. Poletimber having the highest biomass among all three forests is most likely a function of natural succession with the ability of an area to hold a large quantity of small trees compared to large trees (Leak and Yamasaki, 2010; Schroeder et al., 1997). Similarly, *Acer* had consistently higher wood and green leaf nutrient pools than all other genera, primarily due to its high biomass within each forest rather than inherently higher nutrient concentrations. This pattern has been established in previous studies showing that species with greater biomass accumulation contribute disproportionately to total nutrient pools, and tree size classifications influence total nutrient storage more than nutrient concentrations alone (Dalling et al., 2024; Palvianinen et al., 2007; Rutkowski and Stottlemyer, 1993). These findings suggest that nutrient export through harvesting will be more strongly influenced by tree size class and species of the removed tree, rather than by differences in wood or green leaf nutrient concentrations. Managing for species with high biomass, such as *Acer* in these forests, could enhance forest nutrient retention, while excessive removal may accelerate soil nutrient depletion.

4.4.3 Effects of soil nutrient richness on merchantable wood volumes and values

Our findings indicate that forest nutrient richness does not significantly affect merchantable wood volumes, contrary to our initial hypothesis. Instead, tree size classification emerged as the primary driver of merchantable wood volume, with poletimber trees contributing the most volume across the three forests. Additionally, while tree genera did not significantly affect total merchantable volume, *Acer* showed differences in merchantable wood volume depending on tree size classification (Figure 4.17), whereas *Betula* and *Fagus* did not. The economic value of merchantable wood was more complex, as tree genera played a crucial role in determining the overall value of the forest.

Despite expectations that the nutrient Rich forest would yield greater merchantable wood volumes due to improved tree growth, our results indicated no significant relationship between nutrient richness and total merchantable wood. One possible explanation is that factors such as tree age, stand history, and species composition overshadow the influence of soil nutrients. For example, the trees at the Poor forest are approximately 40 years older than those in the other two forests due to differences in historical management of each forest. Additionally, the presence of *Tsuga* at the Poor site allows for increased stem density leading to higher overall biomass. Over time, the cumulative biomass compensated for its lower nutrient availability, reducing the expected difference in merchantable wood volume. Additionally, factors such as species or genera competition (Rozendaal et al., 2020), light availability (Beauchamp et al., 2025), and past disturbances (Depres et al., 2017) may have influenced growth patterns, potentially masking any direct effects of soil nutrient richness on merchantable wood volume.

Tree size classification, however, only significantly affected merchantable wood volumes in *Acer*. Poletimber total merchantable wood volumes were significantly higher than the other size classifications. The higher woody biomass in poletimber is the driver for the high total merchantable wood volumes (Table 4.4). When considering tree genera, *Acer* had differing total volumes of merchantable wood yield. The differences in merchantable wood volume among tree genera further suggests that species or genera specific growth rates and ecological traits influence forest productivity more than soil nutrient richness, if adequate soil nutrients are available. Such differences could potentially be due to moisture availability (Stern et al., 2023), species growth rates (Levesque et al., 2015), shade tolerance (Walters and Reich, 1996), and species or genera specific competitive strategies (Coates et al., 2008; Hartmann and Messier, 2011).

Our findings aligned with previous research which found that tree size is a dominant factor influencing timber production, whereas soil nutrient availability may play a more indirect role (e.g., through species composition and stand dynamics). Other studies have found that in relatively young stands, that the majority of the biomass is stored in smaller trees (Piponiot et al., 2022; Searle and Chen, 2017; Taylor et al., 2014). The lower overall biomass in larger trees is attributed to the higher stocking densities in smaller trees as well as faster growth rates.

Unlike merchantable wood volumes, forest nutrient richness did have an impact on the economic value of the forest when wood quality was considered. Monte Carlo simulations revealed that wood value varied depending on the assumed distribution of pulpwood, low-, mid-, and high- quality sawtimber. The Moderate forest had the highest value of wood per area in three out of the four simulations. The Moderate forest was valued significantly higher no matter the distribution of wood quality because of the high abundance of *Acer* which is one of the highest economically valued out of the genera present. Other studies have also found that the total valuation of a forest or region is skewed by the abundance of high valued species (Luppold and Bumgardner, 2021). These findings suggest that species composition and abundances play a critical role in the economic value of a forest and that slight differences in harvesting techniques or management practices can affect the overall economic value of a forest. When wood quality was randomized, the Moderate forest remained the highest valued, suggesting that either moderate soil fertility supports an optimized balance of wood volume or that forests on relatively young soils can be actively managed to be productive, with effects on the soil not immediately reflected in the merchantable wood. However, this does not imply that such production is sustainable in the long-term.

4.4.4 Limitations of study and future research directions

While our study provides valuable insights into the relationship between soil nutrient richness, aboveground biomass, and merchantable wood values, our results may have been influenced by several variable that were unaccounted for. Nitrogen dynamics were not examined in our study but likely play a critical role since N is often the most limiting nutrient in temperate forest (Aber et al., 1998). This means that tree growth can be limited even in nutrient rich soils if N availability is insufficient (Aber et al., 1998). In our study, the lack of a relationship between soil nutrient richness and merchantable wood volumes may be explained by variations in N availability rather than Ca and Mg in the soil. Additionally, historical land use and past harvesting intensities could have affected the soil nutrient stocks and species composition (Compton and Boone, 2000). The age discrepancy between the Poor forest (about 40 years) and the other two forests further complicates direct comparisons, as biomass accumulation over time may have offset expected differences in nutrient pools and wood volume due to soil nutrient richness.

Phosphorus limitation also presents a critical and underexplored pathway for future research particularly in relation to wood quality and forest productivity. Although wood quality was not directly measured in this study, P plays an essential role in plant energy metabolism, cell division, and lignification which influence wood formation and structure (Fang et al., 2024; Liu et al., 2024). Across all three forests in this study, exchangeable P concentrations were consistently below 5 mg/kg which suggests that productivity or wood quality may be limited based on this published threshold (Gradowski and Thomas, 2006; Rice et al., 2024). Notably, P release rates were lowest at the Poor forest and highest at the Rich which suggests reduced mineral weathering inputs could further constrain P availability and forest productivity. Prio work has shown that P deficiency can impair vascular development, reduce photosynthetic efficiency, and lower lignin content in wood tissues (Graciano et al., 2006), all of which may contribute to reductions in wood density, strength, and merchantable quality. Despite previous research, the direct relationship between soil P availability and wood fiber quality remains poorly quantified particularly across glaciated landscapes with varying parent material. Given the importance of P in wood structure and overall tree vigor, future research should explicitly evaluate how P availability affects species-specific wood formation traits and their implications for timber value. Such studies would provide critical insights for developing adaptive forest management strategies that sustain wood quality and forest productivity under P limited conditions.

Beyond soil fertility, species composition, hydrology, and species plasticity likely contributed to the observed patterns in biomass and wood volume. Competition between species affects growth rates and influences nutrient acquisition strategies, where nutrient efficient species such as *Fagus* may outcompete more nutrient demanding species such as *Fraxinus* (Rust and Savill, 2000). Hydrological factors, such as soil moisture and nutrient leaching also play a critical role in the retention and availability of nutrients in forest soils. These factors influence the pool of nutrients that are directly available to the trees, further influencing tree growth and wood chemistry across the forests. Furthermore, much remains unknown about the extent to which species exhibit plasticity in nutrient uptake and allocation. Some species may adjust their foliar or wood nutrient concentrations in response to soil nutrient availability, while others may be more rigid in their uptake strategies (Tobner et al., 2013). Understanding how these additional factors influence the aboveground nutrient concentrations would further provide insight for developing more sustainable forestry practices.

To further refine our understanding of how soil nutrient richness affects forest productivity and timber quality, future research should focus on several key areas. Investigating historical land use effects on soil nutrient stocks and tree productivity through dendrochronology, soil carbon dating, and historical records would help clarify how past management practices not only influenced the past but continue to shape the present-day forest composition and nutrients. Understanding species-specific growth responses and the interactions caused by competition under varying soil nutrient conditions will be essential for predicting how forest compositions may change over successive harvests. This will be particularly important for nutrient demanding species that compete with more nutrient efficient species. Furthermore, developing predictive models that integrate soil nutrient richness, tree species composition, and economic factors will help optimize sustainable harvesting strategies, for both economic and ecological sustainability. Finally, assessing long term changes in wood and green leaf nutrient concentrations following harvests will be critical for determining the effect that repeated harvesting has on different tree species and will further provide insight of plasticity in nutrient uptake. By addressing these knowledge gaps, future research can further improve our understanding in long term sustainability of nutrients which will inform forest managers on strategies that maintain soil fertility while ensuring economic returns.

4.4.5 Implications for Forest Management

Sustainable forest management requires a balance between maximizing economic returns and maintaining soil fertility long-term. Whole tree harvesting often includes harvesting branches and foliage, which are commonly used for wood pellet production and bioenergy feedstocks (Latterini et al., 2022). However, not leaving behind residues will quickly deplete the soils of essential nutrients, therefore selectively leaving nutrient rich residues on site could mitigate nutrient depletion from the soil, particularly in nutrient-poor forests (Rothstein and Gadoth-Goodman, 2023). Given the high nutrient concentrations of *Acer* and *Fraxinus* in their biomass, leaving these species as residue may help mitigate nutrient depletion and support the long-term soil fertility of the site, particularly on nutrient poor soils. Conversely, forests with inherently nutrient-rich soils may be able to sustain more intensive harvests without immediate detrimental effects on fertility, although long-term monitoring remains critical.

Species selection also plays an important role in sustaining soil nutrients long term. *Acer* should be harvested conservatively in nutrient poor forests to support long term sustainability since the leaves and branches have high Ca content. Similarly, *Betula* have high foliar nutrient concentrations, so leaving a portion of unharvested trees behind could help maintain soil fertility over successional harvests. Additionally, *Fagus* often dominates forests on nutrient-poor soils, therefore an increase in abundance may indicate a decline in soil fertility. Even though there is an economic incentive to harvest species with high merchantable wood volume and value, leaving a portion of key species unharvested could sustain forest productivity long-term.

Furthermore, while maximizing timber volume is economically desirable, prioritizing the slow-growing, nutrient efficient species can contribute to long-term forest health and sustainability. Fast-growing species, while initially producing high merchantable wood volumes, may deplete the soil nutrients at a fast rate, compromising the productivity of the forest long-term.

To proactively manage forests for long term productivity, routine monitoring of soil and green leaf concentrations should be incorporated into management plans. Early detection of nutrient depletion, especially on sites undergoing intensive harvests, would allow managers to adjust harvesting intensities, strategize residue left behind, and identify select species to mitigate losses in productivity long term. By considering and incorporating nutrient dynamics into management plans, forest managers can ensure the economic viability of timber production while preserving essential ecosystem functions.

Despite the lower soil nutrient concentrations both in exchangeable and total, the high biomass at the Poor forests indicated that forests on nutrient poor soils may still maintain high biomass and economic returns through adaptive management strategies that account for site limitations. Practices such as species selection favoring nutrient efficient or stress tolerant species such as *Tsuga canadensis* and *Fagus grandifolia*, longer rotation lengths, and reducing harvesting intensity can help sustain productivity over time. In particular, Long et al. (2019) emphasize that recognizing and working within the inherent constraints of site quality if critical which can be applied to the glaciated northeastern forests. In forests with nutrient poor soils, forest managers should focus on maintaining species that can thrive under limited base cation availability and consider interventions such as soil amendments or modified harvesting regimes only when justified by long-term monitoring. However, key uncertainties remain especially regarding how repeats harvests will impact soil nutrient pools, whether biomass recovery can keep pace with nutrient loss and how the alteration of climate may interact with existing nutrient limitations. Long-term experiments and monitoring are essential to resolve these uncertainties and ensure that adaptive management strategies are both ecologically sustainable and economically viable.

4.5 Conclusion

We found that while wood and green leaf nutrient concentrations responded to soil Ca and Mg availability, wood and green leaf nutrient pools were driven more by biomass accumulation than by soil nutrients. Additionally, the lack of a significant relationship between the nutrient richness of the soil and merchantable wood volume suggests that other factors such as stand genera composition, and site history, including management, play a stronger role in determining timber production in recently glaciated forests. Economic analyses revealed that wood value is not solely a function of wood volume but that there is an influence by genera composition and wood quality which varied across the nutrient gradient. Our findings challenge the expectation that greater soil nutrient richness directly translates to higher merchantable wood production. These findings highlight the need for site specific considerations in forest management and the importance of integrating soil nutrient management into forest management decisions, especially when harvesting. Although we found no direct impacts of soil nutrient richness on merchantable wood volumes on these rather young soils, maintaining this productivity requires strategic planning. These plans should involve leaving behind nutrient rich harvesting residues, species-specific harvesting decisions, and periodic soil assessments to ensure the longevity of the forest. By incorporating these strategies, forest managers can ensure continued timber production while supporting the function of the ecosystem.

4.6 Acknowledgements

We thank several University of Massachusetts Amherst, and University of Vermont staff, faculty, and students that contributed to the collection of soils and green leaves for this study. A special thank you William Leak, Mariko Yamasaki and Christine Costello for implementing and overseeing several of the long-term experiments used in this study. Thank you to Kevin Evans for guidance in locating and accessing field sites. This study was funded by the Grant 2021-67019-34250 of the USDA National Institute of Food and Agriculture with additional support by the USDA Forest Service Northern Research Station through long-term silviculture studies at the Bartlett Experimental Forest.

Supplemental Figures and Tables

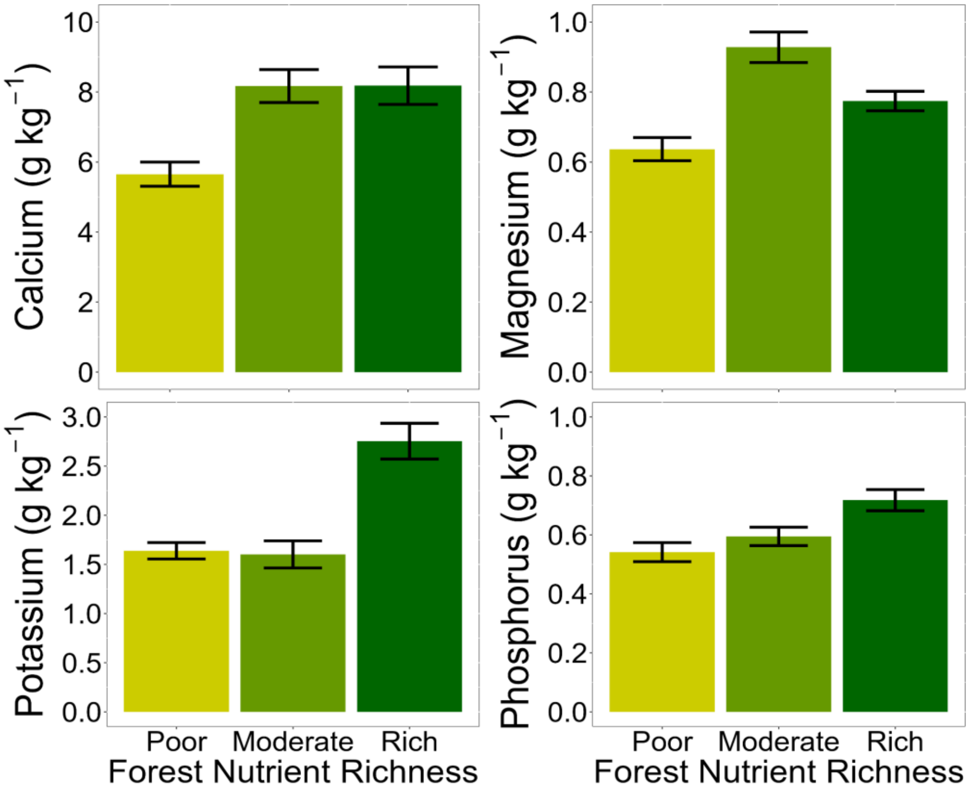

Supplemental Figure 4.1. Wood nutrient concentrations (Ca, Mg, K, P) across tree size classifications. Values were calculated from elemental concentrations of branch samples. Each bar presents the average across plots (n = 15) within each forest, and error bars indicate standard errors. On the x-axis, tree size classifications are represented as follows: “S” for sapling, “P” for poletimber, “Sm” for small sawtimber, “Md” for medium sawtimber, and “Lg” for large sawtimber.

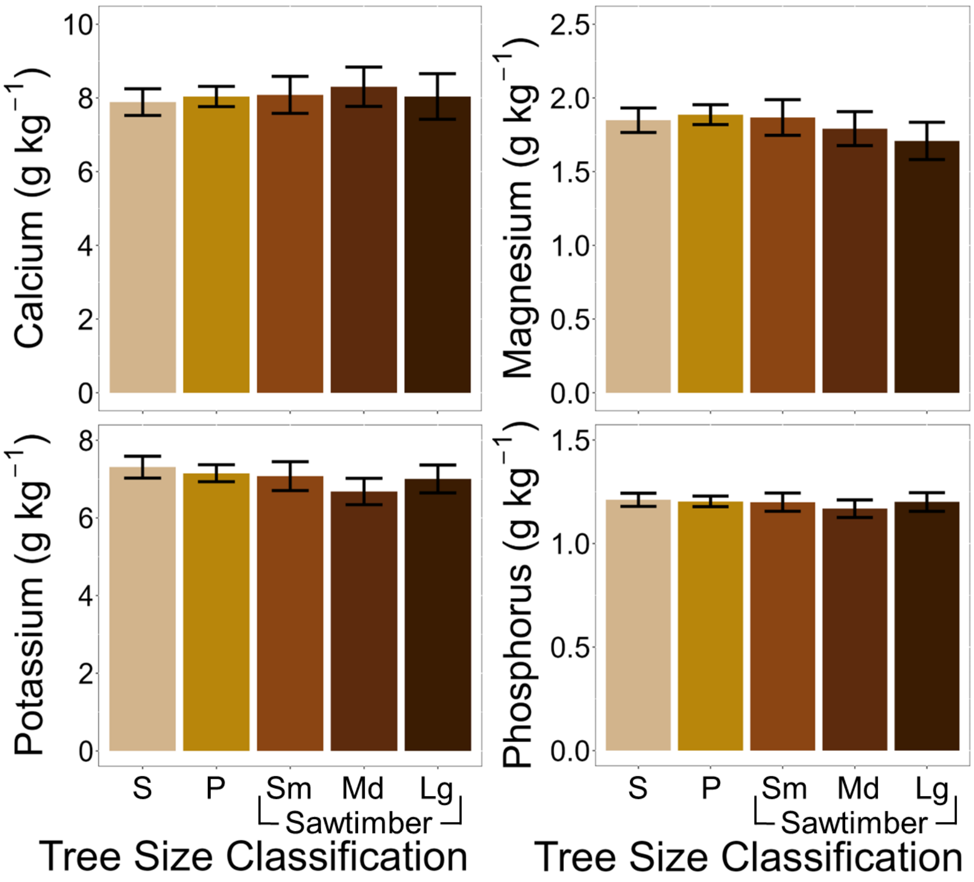

Supplemental Figure 4.2. Green leaf nutrient concentrations (Ca, Mg, K, P) across tree size classifications. Values were calculated from elemental concentrations of green leaves. Each bar presents the average across plots (n = 15) within each forest, and error bars indicate standard errors. On the x-axis, tree size classifications are represented as follows: “S” for sapling, “P” for poletimber, “Sm” for small sawtimber, “Md” for medium sawtimber, and “Lg” for large sawtimber.

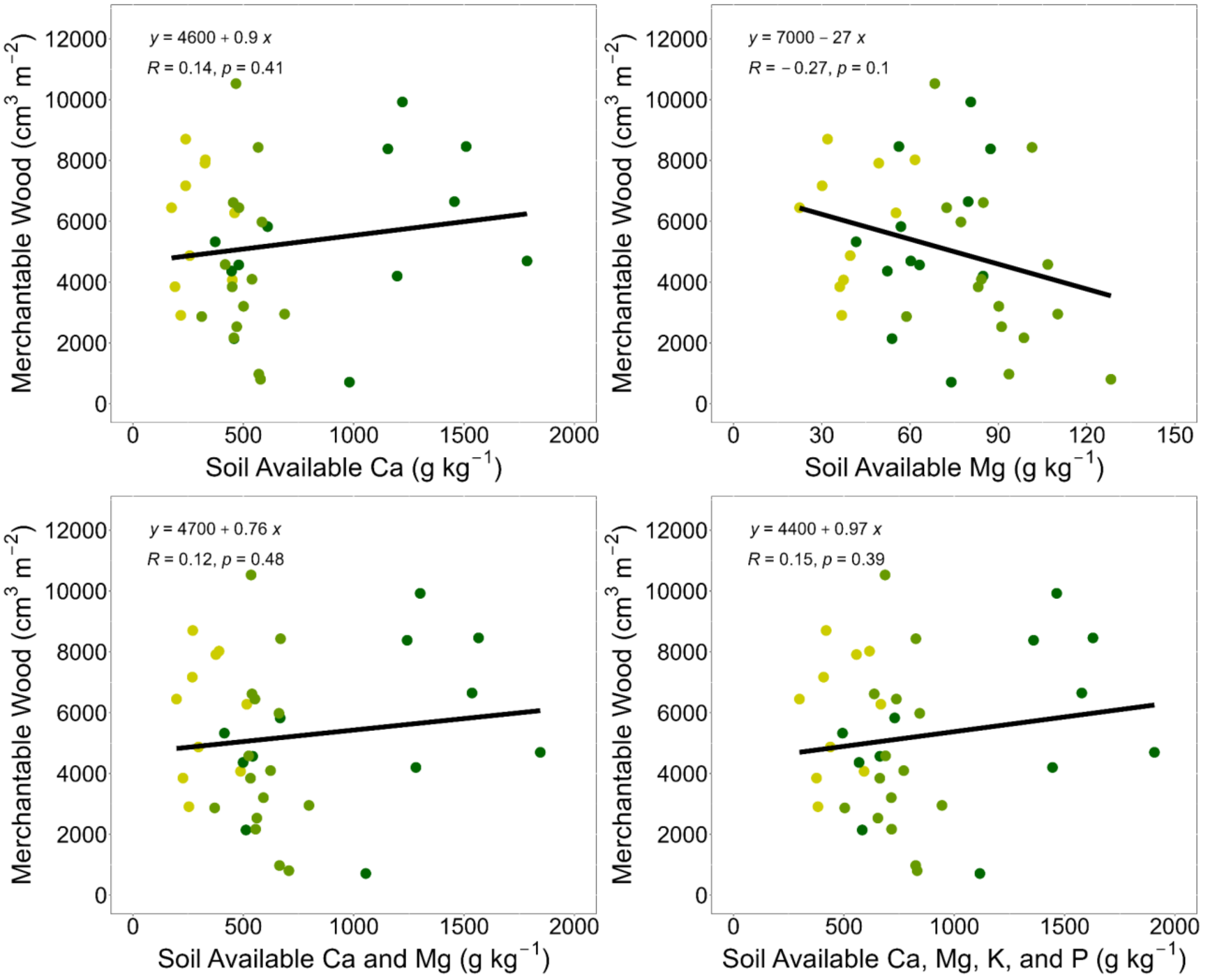

Supplemental Figure 4.3. Scatter plots illustrate the relationship between merchantable wood volume (cm^3 m^{-2}) and soil available Ca (g kg^{-1}), Mg (g kg^{-1}), Ca and Mg (g kg^{-1}), and Ca, Mg, K, and P (g kg^{-1}). Each point is a plot and colored by forest nutrient richness. Regression equations, R^2, and p-values are shown for each relationship.

References

Aber, J., McDowell, W., Nadelhoffer, K., Magill, A., Berntson, G., Kamakea, M., McNulty, S., Currie, W., Rustad, L., and Fernandez, I. (1998). Nitrogen saturation in temperate forest ecosystems: Hypotheses revisited. *BioScience, 48*(11), 921-934.

Achat, D. L., Deleuze, C., Landmann, G., Pousse, N., Ranger, J., & Augusto, L. (2015). Quantifying consequences of removing harvesting residues on forest soils and tree growth - A meta-analysis. Forest Ecology and Management, 348, 124–141. https://doi.org/10.1016/j.foreco.2015.03.042

Achat, D. L., Martel, S., Picart, D., Moisy, C., Augusto, L., Bakker, M. R., & Loustau, D. (2018). Modelling the nutrient cost of biomass harvesting under different silvicultural and climate scenarios in production forests. Forest Ecology and Management, 429, 642–653. https://doi.org/10.1016/j.foreco.2018.06.047

Arthur, M.A., Siccama, T.G., and Yanai, R.D. (1999). Calcium and magnesium in wood of northern hardwood forest species: Relations to site characteristics. *Canadian Journal of Forest Research, 29*(3), 339-346. https://doi.org/10.1139/x98-210

Bakken, P.N and Cook, J.E. (1998). Regeneration potential of six habitat types common to north-central Wisconsin. N. J. Appl. For 15:116–123

Beauchamp, N., Kunstler, G., Touzot, L., Ruiz Benito, P., Cienciala, E., Dahlgren, J., Hawryło, P., Klopčič, M., Lehtonen, A., Šebeň, V., Socha, J., Zavala, M. A., and Courbaud, B. (2025). Light competition affects how tree growth and survival respond to climate. *Journal of Ecology*, 113(2), 1–17. https://doi.org/10.1111/1365-2745.14489

Brady, N.C., and Weil, R.R. (2016). *The nature and properties of soils* (15th ed.). Pearson.

Carpenter, R., Ward, E.B., Wikle, J., Duguid, M.C., Bradford, M.A., and Ashton, M.S. (2021). Soil nutrient recovery after shelterwood timber harvesting in a temperate oak hardwood forest: Insights using a twenty-five -year chronosequence. *Forest Ecology and Management, 499.*

Carter, T.S., Clark, C.M., Fenn, M.E., Jovan, S., Perakis, S.S., Riddell, J., Schaberg, P.G., Greaver, T.L., and Hastings, M.G. (2017). Mechanisms of nitrogen deposition effects on temperate forest lichens and trees. *Ecosphere, 8*(3). https://doi.org/10.1002/ecs2.1717

Chen, Z.C., Peng, W.T., Li, J., and Liao, H. (2018). Functional dissection and transport mechanism of magnesium in plants. *Seminars in Cell and Developmental Biology*, 74, 142-152. https://doi.org/10.1016/j.semcdb.2017.08.005

Choi, B.J., Baek, G., Jo, C.G, Park, S.W., Yoo, B.O., Jeong, S.Y., Lee, K.S., and Kim, C. (2016). Biomass and nutrient stocks of tree components by stand density in a *Quercus glauca* plantation. *Journal of Korean Forest Science*, *105*(3), 294-302.

Coates, K.D., Canham, C.D., LePage, P.T. (2008). Above- versus below-ground competitive effects and responses of a guild of temperate tree species. *Journal of Ecology*, 97, 118-130. https://doi.org/10.1111/j.1365-2745.2008.01458.x

Compton, J.E., and Boone, R.D. (2000). Long-term impacts of agriculture on soil carbon and nitrogen in New England forests. *Ecology, 81*(8), 2314-2330.

Cornut, I., Le Maire, G., Laclau, J.-P., Guillemot, J., Mareschal, L., Nouvellon, Y., and Delpierre, N. (2021). Potassium limitation of wood productivity: A review of elementary processes and ways forward to modelling illustrated by Eucalyptus plantations, *Forest Ecology and Management, 318*, 119275, https://doi.org/10.1016/j.foreco.2021.119275.

Cross, A., and Perakis, S.S. (2010). Tree species and soil nutrient profiles in old-growth forests of the Oregon Coast range. *Canadian Journal of Forest Research*, *41*, 195-210.

Dalling, J.W., Flores III, M.R., and Heineman, K.D. (2024). Wood nutrients: Underexplored traits with functional and biogeochemical consequences. *New Phytologist*, 244(5), 1694-1708. https://doi.org/10.1111/nph.20193

Despres, T., Vitkova, L., Bace, R., Cada, V., Janda, P., Mikolas, M., Schurman, J.S., Trotsiuk, V., and Svoboda, M. (2017). Past disturbances and interspecific competition as drivers of spatial pattern in primary spruce forests. *Ecosphere*, 8(12), https://doi.org/10.1002/ecs2.2037

dos Santos Angelico, T., Marcati, C.R., Rossi, S., da Silva, M.R., and Sonsin-Oliveira, J. (2021). Soil effects on stem growth and woody anatomy of tamboril are mediated by tree age. *Forests*, 12(8), 1058. https://doi.org/10.3390/f12081058

Dukic, E., van Maldegem, K.A., Shaikh, K.M., Fukuda, K., Topel, M., Solymosi, K., Hellsten, J., Hansen, T.H., Husted, S., Higgins, J., Sano, S., Ishijima, S., and Spetea, C. (2023). Chloroplast magnesium transporters play essential but differential roles in maintaining magnesium homeostasis. *Frontiers in Plant Science* 14. https://doi.org/10.3389/fpls.2023.1221436

Ek, A. R., Birdsall, E. T., and Spears, R. J. (1984). A simple model for estimating total and merchantable tree heights (Research Note NC-309). U.S. Dept. of Agriculture, Forest Service, North Central Forest Experiment Station.

Fahey, T.J., Battles, J.J. and Wilson, G.F. (1998). Responses of early successional northern hardwood forests to changes in nutrient. *Ecological Monographs*, 68(2), 183-212. https://doi.org/10.1890/0012-9615(1998)068[0183:ROESNH]2.0.CO;2

Fang, X., Yang, D., Deng, L., Zhang, Y., Lin, Z., Zhou, J., Chen, Z., Ma, X., Guo, M., Lu, Z., and Ma, L. (2024). Phosphorus uptake, transport, and signaling in woody and model plants. *Forest Research, 4*. https://doi.org/10.48130/forres-0024-0014

Federer, C.A., Hornbeck, J.W., Tritton, L.M., Martin, C.W., Pierce, R.S., and Smith, C.T. (1989). Long-term depletion of calcium and other nutrients in eastern US forests. *Environmental Management*, 13, 593-601. https://doi.org/10.1007/BF01874965d

Finzi, A.C., and Canham, C.D. (2000). Sapling growth in response to light and nitrogen availability in a southern New England forest. *Forest Ecology and Management*, 131, 153-165. https://doi.org/10.1016/S0378-1127(99)00206-6

Gauthier, M.M., Guillemette, F., and Bedard, S. (2015). On the relationship between saplings and ingrowth in northern hardwood stands. Forest ecology and management, 358, 261-271. https://doi.org/10.1016/j.foreco.2015.09.020

Gonzales, K., Yanai, R.D., Fahey, T.J., and Fisk, M.C. (2023). Evidence for P limitation in eight northern hardwood stands: Foliar concentrations and resorption by three tree species in a factorial N by P addition experiment. *Forest Ecology and Management, 529*.

Gradowski, T., and Thomas, S. C. (2006). Phosphorus limitation of sugar maple growth in central Ontario. Forest Ecology and Management, 226(1–3), 104–109. https://doi.org/10.1016/j.foreco.2005.12.062

Gransee, A., and Fuhrs, H. (2013). Magnesium mobility in soils as a challenge for oil and plant analysis, magnesium fertilization and root uptake under adverse growth conditions. *Plant Soil, 368*, 5-21.

Gress, S.E., Nichols, T.D., Northcraft, C.C. and Peterjohn, W.T. (2007). Nutrient limitation in soils exhibiting differing nitrogen availabilities: What lies beyond nitrogen saturation? *Ecology ,88*, 119-130. https://doi.org/10.1890/0012-9658(2007)88[119:NLISED]2.0.CO;2

Hallett, R. A., Bailey, S. W., Horsley, S. B., and Long, R. P. (2006). Influence of nutrition and stress on sugar maple at a regional scale. Canadian Journal of Forest Research, 36(9), 2235-2246. https://doi.org/10.1139/x06-120

Halman, J.M., Schaberg, P.G., Hawley, G.J., Hansen, C.F., and Fahey, T.J. (2015). Differential impacts of calcium and aluminum treatments on sugar maple and American beech growth dynamics. *Canadian Journal of Forest Research, 45*(1), 52-59. https://doi.org/10.1139/cjfr-2014-0250

Hartmann, H., and Messier, C. (2011). Interannual variation in competitive interactions from natural and anthropogenic disturbances in a temperate forest tree species: Implications for ecological interpretation. *Forest Ecology and Management*, 261(11), 1936-1944. https://doi.org/10.1016/j.foreco.2011.02.018

Honer, T. G., Ker, M. F., and Alemdag, I. S. (1983). Metric timber tables for the commercial species of Central and Eastern Canada (Info. Rept. M-X-140). Maritimes Forest Research Centre, Canadian Forest Service, Fredericton, New Brunswick.

Hong, D.S., Gonzales, K.E., Fahey, T.J., and Yanai, R.D. (2022). Foliar nutrient concentrations of six northern hardwood species responded to nitrogen and phosphorus fertilization but did not predict tree growth. Peer J, https://doi.org/10.7717/peerj.13193.

Ishfaq, M., Wang, Y., Yan, M., Wang., Z., Wu, L., Li, C., and Li, X. (2022). Physiological essence of magnesium in plants and its widespread deficiency in the farming system of China. *Frontiers in Plant Science, 13*. https://doi.org/10.3389/fpls.2022.802274

Jobbágy, E. G., and Jackson, R. B. (2001). The distribution of soil nutrients with depth: Global patterns and the imprint of plants. *Biogeochemistry*, 53(1), 51–77.

Jevon, F.V., D'Amato, A.W., Woodall, C.W., Evans, K., Ayres, M.P., and Matthes, J.H. (2019). Tree basal area and conifer abundance predict soil carbon stocks and concentrations in an actively managed forest of northern New Hampshire, USA. *Forest Ecology and Management, 451.*

Johnson, C.E., Petras, R.J., April, R.H.,and Siccama, T.G. (2004). Post-glacial lead dynamics in a forest foil. *Water, Air, and Soil Pollutions, 4,* 579-590.

Juice, S.M., Fahey, T.J., Driscoll, C.T., Denny, E.G., Eager, C., Cleavitt, N.L., Minocha, R., and Richardson, A.D. (2006). Response of sugar maple to calcium addition to northern hardwood forest. *Ecology,* 87 (5), 1267-1280. 10.1890/0012-9658(2006)87[1267:rosmtc]2.0.co;2

Kaiser, W. M. (1982). Correlation between changes in photosynthetic activity and changes in total protoplast volume in leaf tissue from hygro-, meso- and xerophytes under osmotic stress. Planta, 154, 538-545. https://doi.org/10.1007/BF00402997

Kobe, R.K, Pacala, S.W., Silander Jr, J.A. and Canham, C.D. (1995). Juvenile tree survivorship as a component of shade tolerance. Ecol. Appl 5:517–532.

Kozlowski, T.T., and Pallardy, S.G. (1997). *Growth control in woody plants.* Academic Press.

Latterini, F., Civitarese, V., Walkowiak, M., Picchio, R., Karaszewski, Z., Venanzi, R., Bembenek, M., & Mederski, P. S. (2022). Quality of pellets obtained from whole trees harvested from plantations, coppice forests, and regular thinnings. *Forests, 13.*

Lawrence, G.B., and Huntington, T.G. (1999). Soil-calcium depletion linked to acid rain and forest growth in the eastern United States. U.S. Geological Survey Water-Resources Investigations Report 98-4267. https://doi.org/10.3133/wri984267

Leak, W.B., and Yamasaki, M. (2010). Seventy-year record of changes in the composition of overstory species by elevation on the Bartlett Experimental Forest (Res. Pap. NRS-13). U.S. Department of Agriculture, Forest Service, Northern Research Station.

Leak, W.B., Sendak, P.E. (2002). Field Note- Changes in Species, Grade, and Structure Over 48 Years in a Managed New England Northern Hardwood Stand. *Northern Journal of Applied Forestry*, 19, 25-28. https://doi.org/10.1093/njaf/19.1.25

Leak, W.B., Yamasaki, M., & Holleran, R. (2014). Silvicultural guide for northern hardwoods in the northeast. *USFS General Technical Report NRS-132*.

Levesque, M., Walthert, L., and Weber, P. (2015). Soil nutrients influence growth response of temperate tree species to drought. *Journal of Ecology*, 104(2), 377-387.https://doi.org/10.1111/1365-2745.12519

Liu, G., Zhang, G., Wu, Z., Lu, W., Lin, Y., Wang, C., Shang, X., Huang, A., and Luo, J. (2024). Comparative proteomic analysis provides insights into wood formation in immature xylem at different ages in *Eucalyptus urophylla* x *Eucalyptus grandis*. *Frontiers in Plant Science*, 15. https://doi.org/10.3389/fpls.2024.1431164

Long, R.P., Horsley, S.B., Bailey, S.W., Hallet, R.A., and Hall, T.J. (2019). Sugar maple decline and lessons learned about Allegheny Plateau soils and landscapes. In: S.L. Stout (Ed.), *SILVAH: 50 years of science-management cooperation. Proceedings of the Allegheny Society of American Foresters training session; 2017 Sept. 20-22; Clarion, PA.* (*Gen. Tech. Rep. NRS-P*-186, pp. 80-97). U.S Department of Agriculture, Forest Service, Northern Research Stations.

Long, R.P., Horsley, S.B., Hallett, R.A., and Bailey, S.W. (2009). Sugar maple growth in relation to nutrition and stress in the northeastern United States. *Ecological Applications,* 19 (6), 1454-1466. 10.1890/08-1535.1

Lovett, G.M., and Mitchell, M.J. (2004). Sugar maple and nitrogen cycling in the forests of eastern North America. Frontiers in ecology and the Environment, 2 (2), 81-88. https://doi.org/10.1890/1540-9295(2004)002[0081:SMANCI]2.0.CO;2

Lucash, M.S., Yanai, R.D., Blum, J.D., and Park, B.B. (2012). Foliar nutrient concentrations related to soil sources across a range of sites in the northeastern United States. *Soil Science Society of American Journal, 76*(2), 674-683.

Luppold, W.G., and Bumgardner, M.S. (2021). Regional analysis of U.S. sawn hardwood product prices from 2000 to 2020. *BioProducts Business, 6,* 1-12.

Luppold, W., and Pugh, S. (2016). Diversity of the eastern hardwood resource and how this diversity influences timber utilization. *Forest Product Journal, 66,* 58-65.

Magill, A.H., Aber, J.D., Currie, W.S., Nadelhoffer, K.J., Martin, M.E., McDowell, W.H., Melillo, J.M., and Steudler, P. (2004). Ecosystem response to 15 years of chronic nitrogen additions at the Harvard Forest LTER, Massachusetts, USA. Forest Ecology and Management, 196, 7-28. https://doi.org/10.1016/j.foreco.2004.03.033

Mao, Z., Corrales, A., Zhu, K., Yuan, Z., Lin, F., Ye, J., Hao, Z., and Wang, X. (2019). Tree mycorrhizal associations mediate soil fertility effects on forest community structure in a temperate forest. *New Phytologist, 223,* 475-486.

Marlow, J., and Peart, D.R. (2014). Experimental reversal of soil acidification in a deciduous forest: Implications for seedling performance and changes in dominance of shade-tolerant species. Forest Ecology and Management, 313, 63-68. https://doi.org/10.1016/j.foreco.2013.10.036

Marschner, H. (2012). *Mineral nutrition of higher plants* (3rd ed.). Academic Press.

Moore, J.D., Camite, C., and Ouimet, R., (2000). Effects of liming on the nutrition, vigor, and growth of sugar maple at the Lake Clair Watershed, Quebec, Canada. *Canadian Journal of Forest Research, 30*, 725-735.

Moore, J.D., Ouiment, R., and Duchesne, L. (2012). Soil and sugar maple response 15 years after dolomitic lime application. Forest Ecology and Management, 281, 130-139. https://doi.org/10.1016/j.foreco.2012.06.026

Nezat, C.A., Blum, J.D., Yanai, R.D., and Park, B.B. (2008). Mineral sources of calcium and phosphorus in soils of the Northeastern United States. *Soil Science Society of America Journal, 72*(6), 1786-1794. https://doi.org/10.2136/sssaj2007.0344

Nolet, P., and Kneeshaw, D. (2018). Extreme events and subtle ecological effects: Lessons from a long-term sugar maple-American beech comparison. *Ecosphere, 9*(7). https://doi.org/10.1002/ecs2.2336

Oelmann, Y., Potvin, C., Mark, T., Werther, L., Tapernon, S., and Wilcke, W. (2010). Tree mixture effects on aboveground nutrient pools of trees in an experimental plantation in Panama. *Plant Soil, 326,* 199-212.

Otto, N.F.J., and Watmough, S.A. (2021). Does forest tree species composition impact modelled soil recovery from acidic deposition? *Canadian Journal of Forest Research, 5*(3), 372-384.https://doi.org/10.1139/cjfr-2021-0170

Ouimet, R., Duchesne, L., and Tremblay, S. (2021). Long-term soil fertility and site productivity in stem-only and whole-tree harvested stands in boreal forest of Quebec (Canada). Forests, 12, 583.

Palvianinen, M., Finer, L., Lauren, A., Mannerkoski, H., Piirainen, S., and Starr, M. (2007). Development of ground vegetation biomass and nutrient pools in a clear-cut disc-plowed boreal forest. *Plant and Soil*, 297, 43-52. https://doi.org/10.1007/s11104-007-9317-2

Park, B.B., and Yanai, R.D. (2009). Nutrient concentrations in roots, leaves and wood of seedling and mature sugar maple and American beech at two contrasting sites. Forest Ecology and Management, 258 (7), 1153-1160. https://doi.org/10.1016/j.foreco.2009.06.003

Pena, R., and Tibbett, M. (2024). Mycorrhizal symbiosis and the nitrogen nutrition of forest trees. *Applied Microbiology and Biotechnology, 108.*

Phillips, T., and Watmough, S.A. (2012). A nutrient budget for a selection harvest: implications for long-term sustainability. *Canadian Journal of Forest Research, 42*(12), 2064-2077.

Piponiot, C., Anderson-Teixeira, K. J., Davies, S. J., Allen, D., Bourg, N. A., Burslem, D. F. R. P., Cárdenas, D., Chang-Yang, C.-H., Chuyong, G., Cordell, S., Dattaraja, H. S., Duque, Á., Ediriweera, S., Ewango, C., Ezedin, Z., Filip, J., Giardina, C. P., Howe, R., Hsieh, C.-F., ... Muller-Landau, H. C. (2022). Distribution of biomass dynamics in relation to tree size in forests across the world. *New Phytologist, 234*(5), 1664–1677. https://doi.org/10.1111/nph.17995

Quevauviller, P. (1998). Operationally defined extraction procedures for soils and sediment analysis I. Standardization. *TrAC Trends in Analytical Chemistry, 17*(5), 289-298. https://doi.org/10.1016/S0165-9936(97)00119-2

Ratcliffe, N. M., Stanley, R. S., Gale, M. H., Thompson, P. J., and Walsh, G. J. (2011). Bedrock geologic map of Vermont (Vol. 3184). U.S. Geological Survey.

Rice, A. R., Perdrial, N., Treto, V., D'Amato, A. W., Smith, G. A., and Richardson, J. B. (2024). Influence of parent material mineralogy on forest soil nutrient release rates across a nutrient richness gradient. Geoderma, 451.

Richard, R., Kane, E., Bronson, D., and Kolka, R. (2022). Whole-tree harvest effects on macronutrients in an oak-dominated system after seven years. *Forests, 13*.

Richardson, J.B., Petrenko, C.L., and Friedland, A.J. (2017). Base cations and micronutrients in forest soils along three clear-cut chronosequences in the northeastern United States. *Nutrient Cycling in Agroecosystems*, 109, 161-179. https://doi.org/10.1007/s10705-017-9876-4

Rogers, N. S., D'Amato, A. W., and Leak, W. B. (2021). Long-term evolution of composition and structure after repeated group selection over eight decades. Canadian Journal of Forest Research, 51, 1080-1091.

Rogers, R.S. (1978). Forests dominated by hemlock (*Tsuga canadensis*): distribution as related to site and postsettlement history. *Canadian Journal of Botany, 56*(7), 843-854. https://doi.org/10.1139/b78-096

Rothstein, D.E., and Gadoth-Goodman, D. (2023). Changes in ecosystem nutrient pools through stand development following whole-tree harvesting of jack pine (*Pinus banksiana*) on sandy, nutrient poor soils in northern Lower Michigan. *Forest Ecology and Management, 529*. https://doi.org/10.1016/j.foreco.2022.120648

Roy, M. È., Surget-Groba, Y., Delagrange, S., & Rivest, D. (2021). Legacies of forest harvesting on soil properties along a chronosequence in a hardwood temperate forest. Forest Ecology and Management, 496. https://doi.org/10.1016/j.foreco.2021.119437

Rozendaal, D. M. A., Phillips, O. L., Lewis, S. L., Affum-Baffoe, K., Alvarez-Davila, E., Andrade, A., Aragão, L. E. O. C., Araujo-Murakami, A., Baker, T. R., Bánki, O., Brienen, R. J. W., Camargo, J. L. C., Comiskey, J. A., Djuikouo Kamdem, M. N., Fauset, S., Feldpausch, T. R., Killeen, T. J., Laurance, W. F., Laurance, S. G. W., ... Vanderwel, M. C. (2020). Competition influences tree growth, but not mortality, across environmental gradients in Amazonia and tropical Africa. *Ecology, 101*(7), e03052. https://doi.org/10.1002/ecy.3052

Rust, S., and Savill, P.S. (2000). The root systems of *Fraxinus excelsior* and *Fagus sylvatica* and their competitive relationships. *Forestry, 73*(5), 499-508.

Rutkowski, D.R., and Stottlemyer, R. (1993). Composition, biomass and nutrient distribution in mature northern hardwood and boreal forest stands, Michigan. *The American Midland Naturalist, 130,* 13-30.

Schaberg, P. G., Tilley, J. W., Hawley, G. J., DeHayes, D. H., & Bailey, S. W. (2006). Associations of calcium and aluminum with the growth and health of sugar maple trees in Vermont. Forest Ecology and Management, 223(1–3), 159–169. https://doi.org/10.1016/J.FORECO.2005.10.067

Schachtman, D. P., Reid, R. J., and Ayling, S. M. (1998). Update on phosphorus uptake by plants: From soil to cell. Plant Physiology, 116(2), 447-453. https://doi.org/10.1104/pp.116.2.447

Schmidt, M., Veldkamp, E., and Corre, M.D. (2015). Tree species diversity effects on productivity, soil nutrient availability and nutrient response efficiency in a temperate deciduous forest. *Forest Ecology and Management, 338*, 114-123.

Schroeder, P., Brown, S., Mo, J., Birdsey, R., and Cieszewski, C. (1997). Biomass estimation for temperate broadleaf forests of the United States using inventory data. *Forest Science, 43*(3), 424-434. https://doi.org/10.1093/forestscience/43.3.424

Searle, E.B., and Chen, H.Y.H. (2017). Tree size thresholds produce biased estimates of forest biomass dynamics. *Forest Ecology and Management, 400,* 468-474. https://doi.org/10.1016/j.foreco.2017.06.042

Siccama, T.G., Fahey, T.J., Johnson, C.E., Sherry, T.W., Denny, E.G., Girdler, E.B., Likens, G.E., and Schwarz, P.A. (2007). Population and biomass dynamics of trees in a northern hardwood forest at Hubbard Brook. *Canadian Journal of Forest Research,* 37 (4), 737-749. https://doi.org/10.1139/X06-261

Schlesinger, W.H., and Bernhardt, E.S. (2013). Biogeochemistry: An analysis of global change. Academic Press.

Soil Survey Staff, 2022. Keys to Soil Taxonomy, 13th edition. USDA Natural Resources Conservation Service.

Staelens, J., Schrijver, A.D., and Verheyen, K. (2007). Seasonal variation in throughfall and stemflow chemistry beneath a European beech (*Fagus sylvatica*) tree in relation to canopy phenology. *Canadian Journal of Forest Research,* 37(8), 1359-1372. https://doi.org/10.1139/X07-003

St. Clair, S. B., Sharpe, W. E., & Lynch, J. P. (2008). Key interactions between nutrient limitation and climatic factors in temperate forests: A synthesis of the sugar maple literature. Canadian Journal of Forest Research, 38(3), 401–414. https://doi.org/10.1139/X07-161

Stern, R.L., Schaberg, P.G., Rayback, S.A., Hansen, C.F., Murakami, P.F., and Hawley, G.J. (2023). Growth trends and environmental drivers of major tree species of the northern hardwood forest of eastern North America. *Journal of Forestry Research*, 34, 37-50. https://doi.org/10.1007/s11676-022-01553-7

Taylor, A.R., Seedre, M., Brassard, B.W., and Chen, H.Y.H. (2014). Decline in net ecosystem productivity following canopy transition to late-succession forests. *Ecosystems, 17*, 778-791. https://doi.org/10.1007/s10021-014-9759-3

Ter-Mikaelian, M.T., and Korzukhin, M.D. (1997). Biomass equations for sixty-five North American tree species. *Forest Ecology and Management, 97*, 1-24.

Thiffault, E., Paré, D., Brais, S., and Titus, B. D. (2010). Intensive biomass removals and site productivity in Canada: A review of relevant issues. The Forestry Chronicle, 86(1), 36-42.

Tobner, C.M., Paquette, A., and Messier, C. (2013). Interspecific coordination and intraspecific plasticity of fine root traits in North American temperate tree species. *Frontiers in Plant Science, 4*, 1-11.

Tripler, C. E., Kaushal, S. S., Likens, G. E., and Walter, M. T. (2006). Patterns in potassium dynamics in forest ecosystems, Ecology Letters, 9, 451–466. https://doi.org/10.1111/j.1461-0248.2006.00891.x

Turpault, M.P., Kirchen, G., Calvaruso, C., Redon, P.O., and Dincher, M. (2021). Exchanges of major elements in a deciduous forest canopy. *Biogeochemistry*, 152, 51-71. https://doi.org/10.1007/s10533-020-00732-0

Vadeboncoeur, M.A. (2010). Meta-analysis of fertilization experiments indicates multiple limiting nutrients in northeastern deciduous forests. *Canadian Journal of Forest Research, 40*, 1766-1780.

Vadeboncoeur, M. A., Hamburg, S. P., Yanai, R. D., & Blum, J. D. (2014). Rates of sustainable forest harvest depend on rotation length and weathering of soil minerals. Forest Ecology and Management, 318, 194–205. https://doi.org/10.1016/j.foreco.2014.01.012

van der Heijden, G., Dambrine, E., Pollier, B., Zeller, B., Ranger, J., and Legout, A. (2014). Mg and Ca uptake by roots in relation to depth and allocation to aboveground tissues: results from an isotopic labeling study in a beech forest on base-poor soil. *Biogeochemistry*, 122, 375-393. http://dx.doi.org/10.1007/s10533-014-0047-2

Walters, M.B., and Reich, P.B. (1996). Are shade tolerance, survival, and growth linked? Low light and nitrogen effects on hardwood seedlings. *Ecology*, 77(3), 841-853. https://doi.org/10.2307/2265505

Wang, Z., Hassan, M. U., Nadeem, F., Wu, L., Zhang, F., and Li, X. (2020). Magnesium fertilization improves crop yield in most production systems: A meta-analysis. Frontiers in Plant Science, 10, 1-10. https://doi.org/10.3389/fpls.2019.01727

White, P. J., and Broadley, M. R. (2003). Calcium in plants. Annals of Botany, 92(4), 487-511. https://doi.org/10.1093/aob/mcg164

Xu, H., Luo, Z., Hu, W., Jia, Y., Wang, Y., Ye, X., Li, Y., Chen, L.S., and Guo, J. (2022). Magnesium absorption, translocation, subcellular distribution and chemical forms in citrus seedlings. *Tree Physiology*, 42(4), 862-876. https://doi.org/10.1093/treephys/tpab148

Yamasaki, M., Costello, C.A., and Leak, W.B. (2014). Effects of clearcutting, patch cutting, and low-density shelterwoods on breeding birds and tree regeneration in New Hampshire northern hardwoods. Research paper NRS-26. U.S. Department of Agriculture, Forest Service, Northern Research Station.

Yang Yang, Ruth D. Yanai, Farrah R. Fatemi, Carrie R. Levine, Paul J. Lilly, and Russell D. Briggs. (2016). Sources of variability in tissue chemistry in northern hardwood species. *Canadian Journal of Forest Research*. 46(3): 285-296. https://doi.org/10.1139/cjfr-2015-0302

Chapter 5

Integrative Synthesis and Implications

My dissertation provides a comprehensive assessment of how parent material mineralogy influences nutrient availability, weathering rates, and forest productivity across a nutrient richness gradient in glaciated forests of Vermont and New Hampshire. By integrating mineralogical, geochemical, isotopic, and ecological data this research advances our understanding of nutrient cycling processes and offers insights for sustainable forest management in formerly glaciated forests.

5.1 Chapter Summaries

In Chapter 2, I demonstrated that nutrient release rates in glacial soils are predominantly controlled by the mineralogical composition of local bedrock. Isotopic analyses of Ca and Mg revealed distinct nutrient sourcing patterns across the gradient. At the Poor forest, soil Ca and Mg were derived primarily from local granite while at the Moderate forest these nutrients originated mostly from schist. In contrast, isotopic signatures at the Rich forest indicate additional nutrient inputs beyond local bedrock and are likely from colluvial transport, biological recycling, or atmospheric deposition. Although rock fragments had higher weathering rates per unit surface area, soils released substantially more nutrients overall due to their greater reactive surface area. These findings emphasize that both bedrock mineralogy and soil physical properties play critical roles in regulating nutrient mobilization and long-term availability.

In Chapter 3, I built on this framework by linking mineralogical controls to soil chemical properties and nutrient availability. Soils at the Rich forest were abundant in silicate minerals such as Ca-plagioclase, micas, and amphiboles and had higher pH and base cation saturation which support the growth of northern hardwood species. Contrary to expectations, carbonate minerals did not significantly contribute to Ca availability which highlights the importance of silicate minerals in sustaining nutrient supply in these forests. Phosphorus dynamics emerged as a potential limitation across all three forests as the exchangeable P concentrations were consistently below 5 mg/kg, a threshold associated with reduced plant productivity (Gradowski and Thomas, 2006). At the Poor forest, the combination of low exchangeable P and high P release rates suggests biological mechanisms such as mycorrhizal associations or root exudation which may be driving mineral P mobilization. These results highlight the need to integrate biological and mineralogical perspectives when evaluating forest nutrient dynamics.

In Chapter 4, I examined how soil nutrient richness influence forest productivity, merchantable wood volume, and economic value. Contrary to my initial hypothesis, the nutrient Poor forest had the highest total biomass which suggests that recently glaciated soils may support substantial growth despite limited nutrient availability. The Poor forest may have more efficient internal nutrient cycling, high microbial activity, or species adaptations to nutrient stress compared to the other two forests. Economic analyses showed that the Moderate forest had the highest merchantable wood value which was driven by species composition and total wood volume rather than quality. These findings challenge the assumption that higher nutrient richness directly translates to greater productivity or economic return (Vadeboncoeur et al., 2010). Instead, these results point to the importance of stand history, species composition, and ecological adaptations which reinforces the need for species specific forest management strategies that balance both ecological and economic goals.

Together these chapters demonstrate that while parent material sets the foundational constraints on nutrient availability that forest productivity emerges from the interactions of geological, biological, and management factors. The isotopic analyses in particular complement the mineralogical and ecological findings by identifying nutrient sources that cannot be inferred from concentration alone. These data clarify how soils mobilize and retain Ca and Mg along a nutrient richness gradient and how these dynamics shape forest growth and resilience over time.

The findings from this research are broadly relevant to other formerly glaciated regions with similar terrain to Vermont and New Hampshire. However, differences in local bedrock composition and glacial history limit the generalizability of these results. Expanding future studies to include a wider variety of parent materials, soil types, and climate regimes will enhance our ability to apply these conclusions more broadly.

5.2 Management implications

Importantly, the lasting influence of soil parent material on acidity and nutrient richness suggests that these underlying geologic differences could play an important role in how forests respond to ongoing environmental change. Forests on more nutrient rich parent material may be better buffered against acidification and more capable of sustaining nutrient supply under changing conditions like altered precipitation patterns or atmospheric deposition. In contrast, forests on acidic, nutrient poor parent materials may be more vulnerable to nutrient losses or slower to recover following disturbance and harvesting. These results highlight how parent material not only influences current soil and forest conditions but also shapes future ecosystem resilience.

5.3 Study limitations

Due to resource limitations, there were several types of observations that could only be made in a limited manner. First, only nine rock samples and nine parent material soil samples were analyzed for mineral abundances using EPMA and XRD, with three rocks and three soils from each forest. This small sample size did not account for changes with depth or spatial variability among plots, which is particularly relevant given the high spatial heterogeneity of glacial soils. As a result, important soil and rock minerals may not have been identified. To increase confidence in identifying nutrient bearing minerals, future studies should aim to analyze at least one major rock type from every plot to better capture the mineral presence and abundance. Another limitation is the relatively short duration of laboratory weathering measurements which does not account for long-term trends or seasonal variability. Long-term monitoring would improve our understanding of nutrient sustainability over time by capturing temporal fluctuations in weathering rates. Additionally, I did not directly measure biological factors such as root exudation and microbial activity which play critical roles in nutrient mobilization, especially for elements like P. Without direct measurements, nutrient weathering rates are possibly underestimated in this study as root exudates and mycorrhizal fungi can significantly enhance P availability. Another study using the same three forests further supports the influence of mycorrhizal fungi, reporting more severe and diverse surface modifications on Ca-bearing minerals by hyphae at the Poor forest than the less intense modifications at the Rich forest (Treto, 2023). These findings suggest that hyphae enhance mineral weathering of Ca-bearing minerals which would increase nutrient release rates at the Poor forest in comparison to what we reported. Future research should focus on directly assessing microbial activity, root exudate composition, and mycorrhizal associations to better constrain nutrient weathering rates and availability to trees, ultimately improving predictions of long-term nutrient sustainability. During my field work, we attempted to collect root water to capture the concentration and uptake rate of nutrients from the rooting zone. However, the quantity of water was small (< 5 mL) and the contamination from the outside of the root was high. For these reasons, we abandoned this approach despite its novel and important value in illuminating tree uptake rates of nutrients. Finally, estimating the economic value of merchantable wood posed a challenge as wood quality information could not be collected for each tree within the forests. Instead, I modeled wood quality distributions to estimate economic value, but this approach introduces several uncertainties including assumptions about the proportion of high versus low quality wood and the use of stumpage prices as proxies for actual grade. Additionally, the model did not account for the potential influences of soil nutrient richness on wood quality, which may be an important but underexplored relationship. Collecting detailed wood quality data such as stem straightness, branching structure, and presence of defects would have allowed for a more direct assessment of how soil mineralogy and nutrient availability affect both the physical characteristics and economic value of timber. Future studies should directly measure these parameters to better understand how underlying soil parent material properties influence wood quality and forest economic potential across different site conditions.

5.4 Future directions

Future research should focus on addressing key knowledge gaps in nutrient cycling by leveraging isotopic tracing and predictive modeling to enhance our understanding of nutrient acquisition of trees. One promising avenue is the use of Ca and Mg isotopes not only to trace nutrient origins from rocks to soil but also to trace nutrient acquisition pathways within trees. Specifically, studies should explore whether soil nutrient richness influences the source of nutrient uptake in trees using Ca and Mg isotopes as tracers. This approach would provide insights into how trees preferentially acquire nutrients from specific mineral pools or soils horizons under varying nutrient availability conditions. Additionally, expanding isotopic analyses to other essential nutrients like K would provide insight into how trees acquire and cycle essential nutrients across different soil nutrient regimes. Future research could even evaluate if different harvesting techniques influence the acquisition of nutrients by trees. This integrated isotopic approach would not only clarify the contributions of mineral weathering versus biological cycling but also help predict how nutrient limitations might shift under changing environmental conditions. Furthermore, future studies should develop predictive models that integrate soil nutrient richness, tree composition, and forest management practices to optimize long-term nutrient sustainability for a first. By incorporating data on the nutrient demand of certain tree species, soil mineralogy, and isotopic tracing, models could estimate the optimal percentage of branches and leaves to leave behind at a harvest site to maintain soil fertility.

Additionally, the observed differences in total elemental concentrations, particularly Ca and Mg along the nutrient richness gradient suggest the nutrient rich forests may better withstand nutrient depletion from harvesting. In contrast, forests with lower total nutrient pools may be more susceptible to long-term nutrient declines under repeated or intensive harvesting regimes. These imbalances could lead to slower recovery following harvesting, shifts in species composition, or changes in ecosystem function. A study documented successional shifts from nutrient demanding species such as white oak to more mesophytic hardwood following disturbance and this pattern may be more pronounced in nutrient limited forests such as the Poor forest (Abrams and Downs, 1990). Future predictive models should account for total nutrient pool size combined with mineral weathering rates and nutrient demand of dominant tree species to more accurately estimate the long-term sustainability of forest productivity under various management practices.

Such models would help forest managers make decisions regarding the retention of biomass after logging to sustain long-term ecosystem productivity and soil health. These models can provide more accurate site-based recommendations by incorporating data on total nutrient pools, weathering rates, species-specific nutrient demands, and harvest residue levels which are particularly important in glaciated forests where parent material controls both the size and replenishment rate of nutrient pools. Models that ignore these geologic and mineralogical constraints may overestimate the ability for a forest to recover nutrients lost during harvesting which will lead to long-term declines in forest productivity and compositional shifts.

This work improves our understanding of how geological and biological processes interact to shape forest nutrient dynamics, productivity, and economic value. This dissertation highlights the critical role of parent material in regulating long-term ecosystem function by linking mineralogy, isotopic tracers, and ecological outcomes across a nutrient richness gradient. These findings offer practical implications for adaptive forest management, particularly in nutrient poor forests vulnerable to acidification, harvesting, or climate change. Sustaining productivity in these forests will require site-specific strategies that consider not only nutrient pools but also the mechanisms that govern nutrient mobilization, retention, and plant availability over time.

5.5 The call for a new paradigm in forest management

As forest management intensifies to meet growing demands for timber, biomass, and carbon sequestration the long-term resilience of temperate northern hardwood forests in the northeastern United States will depend on our ability to sustain soil nutrient reserves. My dissertation highlights that the depletion of soil parent material minerals in young glaciated soils represent a major and underrecognized threat to forest productivity. True sustainability will require a paradigm shift that moves beyond the short-rotation, maximizing yield models towards management strategies grounded in soil mineralogy, nutrient cycling dynamics, and species specific nutrient demands. If this shift does not occur northeasters forests risk entering a slow, predictable decline that is driven by cumulative nutrient exhaustion.

At the time as the depletion of soil nutrients, biotic disturbances are accelerating changes in forest composition. The decline of *Fraxinus* species due to the emerald ash borer is opening nutrient rich soils to recolonization by *Acer* species, particularly *Acer saccharum* which shared similar preferences to *Fraxinus* for fertile, well-drained soils. However, *Acer saccharum* has even higher demands for Ca, Mg, K, and P which may intensify nutrient depletion over time, particularly if harvesting practices do not prioritize residue retention.

Simultaneously, the downfall of *Fagus grandifolia* from beech bark and beech leaf disease will reshape species dynamics on poorer soils. The likely expansion of *Acer rubrum* which is a generalist species that is tolerant of a wide range of conditions, could further shift nutrient cycling processes and soil nutrient exhaustion. *Acer rubrum* requires more Ca and K than *Fagus* which suggests that this replacement may expedite the exhaustion of soil nutrients if intervention is not taken.

In the short term, *Fraxinus* mortality will cause a pulse of base cations (Ca, Mg, K) if left to decompose as the wood and leaves have high concentrations of these elements. However, without species capable of maintaining nutrient cycling and without active soil conservation efforts, northeastern forests could experience gradual declines in productivity with a slow but predictable shift towards nutrient exhaustion, altered species composition, and diminished ecosystem services.

The future of these forests is not yet in ink and sealed. By integrating mineralogical understandings, adaptive management, and long-term nutrient monitoring, we can create a future where soil fertility and forest productivity are sustained for future generations. However, ignoring these mineralogical constraints may guarantee the decline in forests that we right now have the opportunity to prevent.

References

Abrams, M.D. and Downs, J.A. (1990). Successional replacement of old-growth white oak by mixed mesophytic hardwoods in southwestern Pennsylvania. *Canadian Journal of Forest Research*, *20*(12), pp.1864-1870.

MacFarlane, D. W., and Meyer, S. P. (2005). Characteristics and distribution of potential ash tree hosts for emerald ash borer." *Forest Ecology and Management*, 213(1–3), 15–24.

Schlesinger, W. H., and Bernhardt, E. S. (2020). *Biogeochemistry: An Analysis of Global Change* (4th ed.).

Treto, Victoria, "In-Situ Weathering of Calcium Bearing Minerals In Forested Ecosystems" (2023). Graduate College Dissertations and Theses. 1711. https://scholarworks.uvm.edu/graddis/1711

Vadeboncoeur, M.A. (2010). Meta-analysis of fertilization experiments indicates multiple limiting nutrients in northeastern deciduous forests. *Canadian Journal of Forest Research*, *40*, 1766-1780.